PHOTOPHYSICS AND PHOTOCHEMISTRY OF 1,3-DIKETONATOBORON DIFLUORIDES

by

Xianen Cheng

B.Sc., University of Science and Technology of China, 1964.

THESIS SUBMITTED IN PARTIAL FULFILLMENT OF THE REQUIREMENTS FOR
THE DEGREE OF DOCTOR OF PHILOSOPHY
in the Department
of
Chemistry

© Xianen Cheng 1990
Simon Fraser University
April 1990

All right reserved. This thesis may not be reproduced
in whole or part, by photocopy or other means,
without permission of the author.

APPROVAL

Name: Xianen Cheng

Degree: DOCTOR OF PHILOSOPHY

Title of Thesis: Photophysics and Photochemistry of 1,3-Diketonatoboron Diflorides

Examining Committee:

Chairman: Dr. R. K. Pomeroy

Dr. Y. L. Chow
Senior Supervisor

Dr. B. M. Pinto

Dr. T. J. Bor[illegible]d

Dr. A. Tracey
Internal Examiner

Dr. Peter Wan
External Examiner
Department of Chemistry
University of Victoria
Victoria, B.C.

Date Approved:

PARTIAL COPYRIGHT LICENSE

I hereby grant to Simon Fraser University the right to lend my thesis, project or extended essay (the title of which is shown below) to users of the Simon Fraser University Library, and to make partial or single copies only for such users or in response to a request from the library of any other university, or other educational institution, on its own behalf or for one of its users. I further agree that permission for multiple copying of this work for scholarly purposes may be granted by me or the Dean of Graduate Studies. It is understood that copying or publication of this work for financial gain shall not be allowed without my written permission.

Title of Thesis/Project/Extended Essay

THE PHOTOPHYSICS AND PHOTOCHEMISTRY OF 1,3-DIKETONATOBORON DIFLUORIDES

Author: _____
(signature)

Xianen Cheng
(name)

April 19, 1990
(date)

ABSTRACT

Dibenzoylmethanatoboron difluoride ($DBMBF_2$) has been used as a model compound to study the photophysics and photochemistry of β-diketonatoboron difluorides. $DBMBF_2$ has the lowest singlet excited state energy (Es = 73.0 Kcal/mol) and triplet state energy (62 Kcal/mol) as estimated from the 0-0 bands of the emission spectra. The fluorescence of $DBMBF_2$ is quenched by various types of olefins. The quenching rate constants are correlated to ionization potentials (IP) of the quenchers and free energy changes (ΔG^o) of the corresponding photoinduced electron transfer (PET) processes. $DBMBF_2$ in CH_3CN fluoresces at 398 and 416 nm at low [$DBMBF_2$] (10^{-7}-10^{-2} M) and gives a new structureless band centered at 522 nm at [$DBMBF_2$] > 0.05 M, indicating the formation of $DBMBF_2$ excimer. The excimer emission is quenched by cycloheptene ($k_q\tau$ = 6.77 M^{-1}) and 3,3-dimethyl-1-butene ($k_q\tau$ = 0.4 M^{-1}). $DBMBF_2$ can form ground state complexes (GSC) with a number of electron donors. Fluorescence emissions from two GSC (with 2,4-dimethyl-1,3-pentadiene and 1,3-cyclohexadiene) are recorded and assigned.

The chemical consequences of the interaction of singlet excited state $DBMBF_2$ with donor olefins are determined by the energetics of the donor-acceptor (D-A) pairs. For donor olefins with IP < 8.4 eV, corresponding to ΔG^o < -0.4 eV, the cation radical reactions of the donor prevail, for which an intermolecular electron transfer within encounter complexes leading to the direct formation of solvent separated radical

ion pairs is suggested to be the major initiation step. For donor olefins with IP > 8.4 eV, the donor-acceptor cycloadditions occur. The $k_q\tau$ values obtained from the fluorescence quenching monitored at 398 nm agree reasonably well with those obtained from the quantum yield measurements of the cycloadducts. The cycloaddition of $DBMBF_2$ with olefins are demonstrated to proceed via both the exciplex and triplex pathways; the relative importance of either pathway is decided by the concentration of $DBMBF_2$. The stereoselectivities and regiospecificities of the cycloaddition reactions are discussed.

Several related photoreactions of acetylacetone are studied. Acetylacetone undergoes photodimerization in non-polar solvents to give a single furanoid compound out of many possibilities. Its stereochemistry is controlled by the stereoelectronic effects in the transition state. Acetylacetone photocycloadds to norbornene in competition with a reversible energy transfer between the reactants. Acetylacetone is shown to sensitize the radical addition reactions of various solvents to norbornene with quantum yields greater than unity.

To my father, a great chemist

ACKNOWLEDGEMENT

The author wishes to express his gratitude to
Dr. Y. L. Chow for his continual encouragement, guidance, and financial support during the course of this study;
Dr. B. M. Pinto, Dr. W. R. Richards, Dr. R. Hill, and Dr. T. J. Borgford for their valuable advice,
Dr. A. S. Tracey for his genuine guidance and helpful discussion in explanation of NMR spectra,
Mrs. M. Tracey for running hundreds of 400 MHz NMR spectra,
Mr. G. Owen for running MS spectra,
Mr. P. Saunders for his instrumentation service,
members of Dr Chow's group for their cooperation.

The financial support from Simon Fraser University, the Department of Chemistry is acknowledged.

CONTENTS

LIST OF TABLES

LIST OF FIGURES

SYMBOLS AND ABBREVIATIONS

A*	excited state acceptor
$AABF_2$	acetylacetonatoboron difluoride
A_{GSC}	absorbance of a ground state complex
BA	benzoylacetone
$BABF_2$	benzoylacetonatoboron difluoride
BAHA	*tris*-(*p*-bromophenyl)aminium hexachloroantimonate
CI	chemical ionization (in MS spectra)
CIDNP	chemically induced dynamic nuclear polarization
CIP	contact ion radical pair
CT	charge transfer
1-CN-Np	1-cyanonaphthalene
9-CN-An	9-cyanoanthracene
9-CN-Ph	9-cyanophenanthrene
COSY	two-dimentional correlation NMR spectroscopy
D*	excited state donor
DBM	dibenzoylmethane
$DBMBF_2$	dibenzoylmethanatoboron difluoride
DCN-An	9,10-dicyanoanthracene
m-DCNB	m-dicyanobenzene
p-DCNB	1,4-dicyanobenzene
DCN-Np	1,4-dicyanonaphthalene
DDB	2,4-dicyano-5,6-dichloro-1,4-benzoquinone

E^*	Excited state energy
$E^{ox}_{1/2}$	oxidation potential
EI	electron impact ionization (in MS spectra)
E_s	singlet excited state energy
E_T	triplet excited state energy
$E_T(30)$	an empirical parameter of solvent polarity
FID	flame ionization detector (for GC)
FIS	free ion radical species
GSC	ground state complex
HH	head-to-head
HT	head-to-tail
I	intensity of fluorescence
IP	ionization potential
K	formation constant of GSC
k_q	quenching rate constant
MCH	methylcyclohexane
1-MeO-Np	1-methoxynaphthalene
NBD	norbornadiene
NOE	Neuclear Overhauser Effect
NOESY	two-dimentional NOE correlation NMR spectroscopy
PET	photoinduced electron transfer
QC	quadricyclane
RT	retention time (on GC spectroscopy)
SCE	saturated calomel electrode

SSIP	solvent separated ion radical pair
TCB	tetrachloro-1,4-benzoquinone
TCN-An	2,6,9,10-tetracyanoanthracene
TCNB	1,2,4,5-tetracyanobenzene
THF	tetrahydrofuran
$TMHBF_2$	2,6-Tetramethyl-3,5-Heptanedionatoboron Difluoride
ΔE_{coul}	solvent stabilization energy for ion separation
ε_{GSC}	extinction coefficient of GSC
ΔG°	free enthalpy change
Φ	quantum yield
λ_{ex}	wavelength of excitation light beam
λ_f^{max}	wavelength of maximum fluorescence emission
λ_{ph}^{max}	wavelength of maximum phosphorescence emission
λ_{moni}	wavelength of monitoring (for excitation spectra)
τ	lifetime

COMPOUND CATALOG

(also see "SYMBOLS AND ABBREVIATIONS")

1 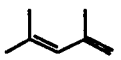

2 

3 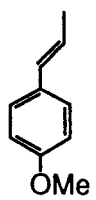

4 

5 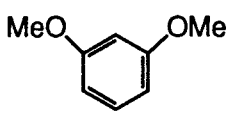

6 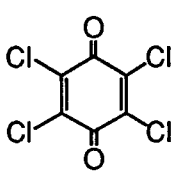

7 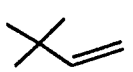

8 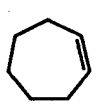

9 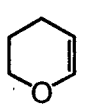

10 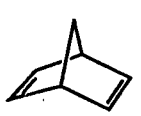

11 

12 

13 

14 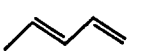

15 

16 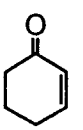

17 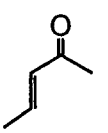

18 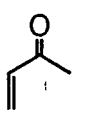

19 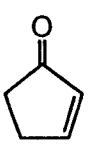

20 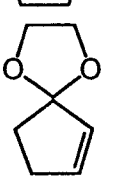

21

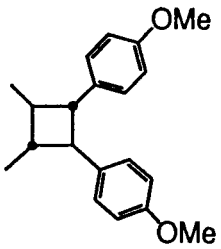

22

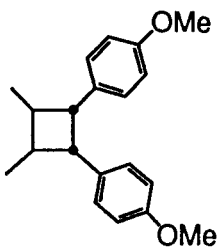

23

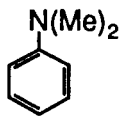

24

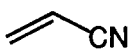

25

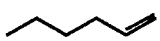

26

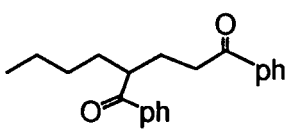

27

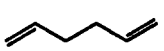

28

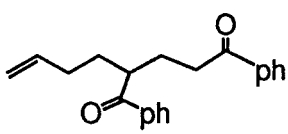

29

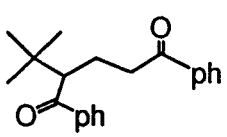

30

31a

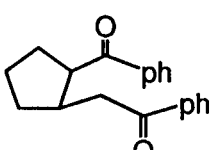

31b

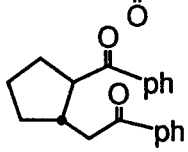

32

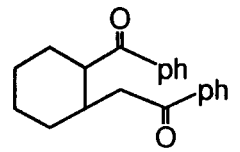

33

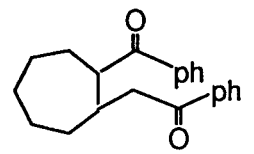

34

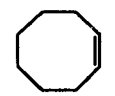

35

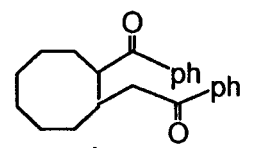

36a

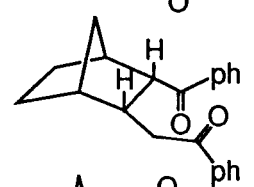

36b

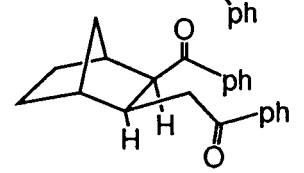

37

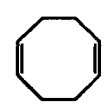

38

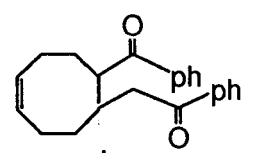

39

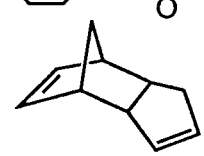

40a
40b

adduct of DBM with **39**

41a

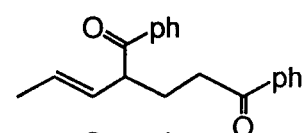

41b

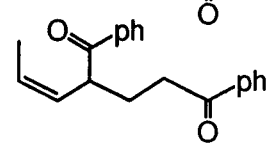

42

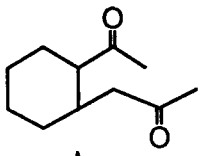

43a

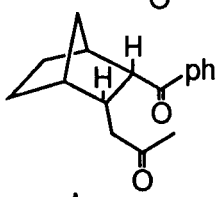

43b

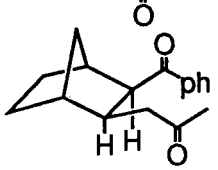

43c

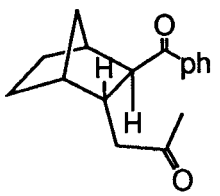

44

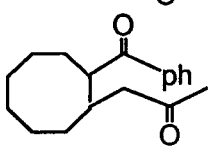

45

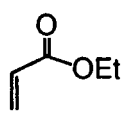

46

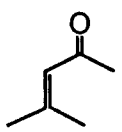

47a

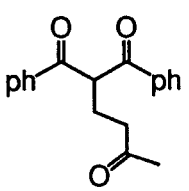

47b

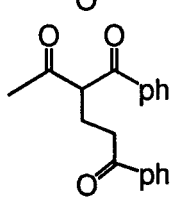

48a

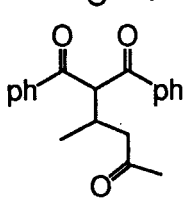

48b

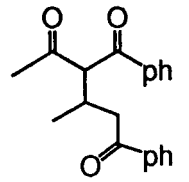

48c a diasteriomer of **48b**

49a

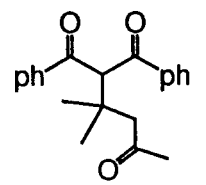

49b

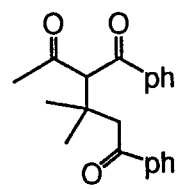

50b

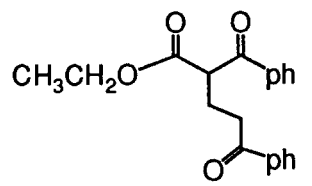

51

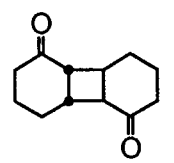

52

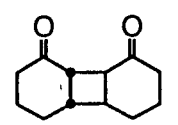

53

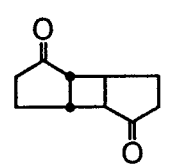

54

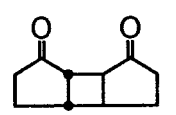

55 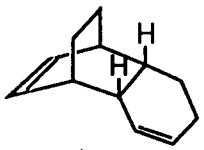

56 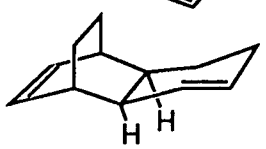

57 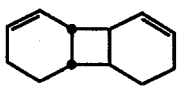

58 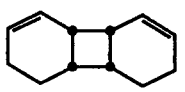

59 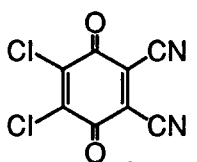

60 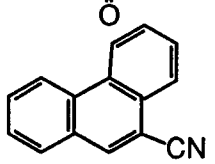

61 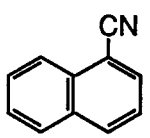

62 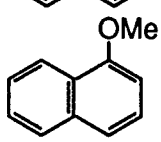

63 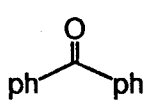

64 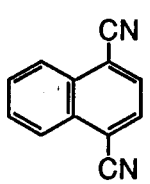

65 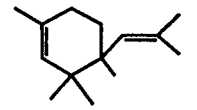

66 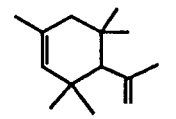

67 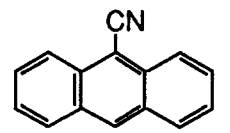

68 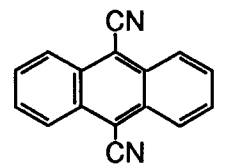

69 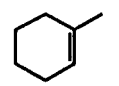

70 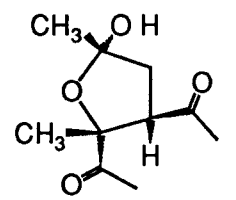

71 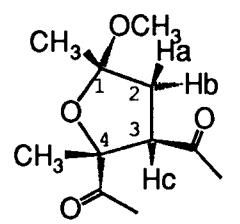

72 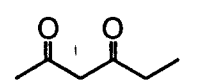

73 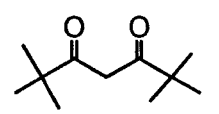

74 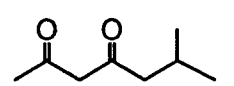

75 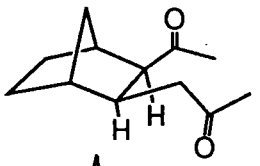

76 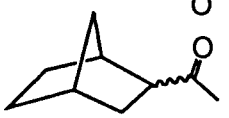

77 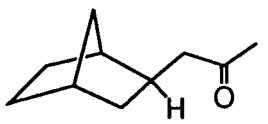

78 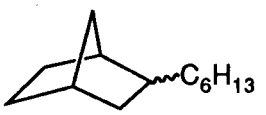

79 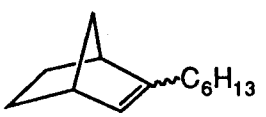

80 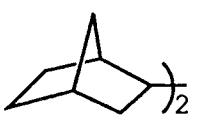

81 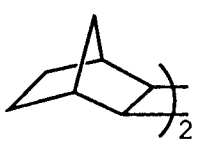

82a-d 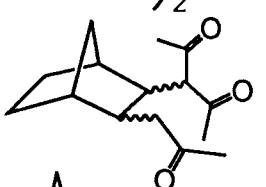

83 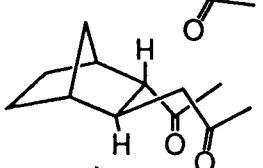

84a 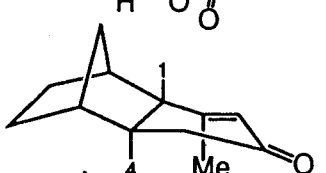

84b 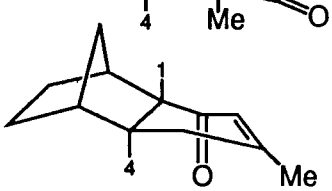

85 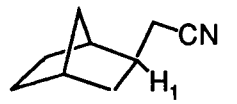

86a,b 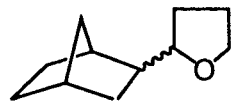

87a,b 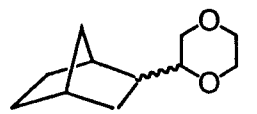

88a 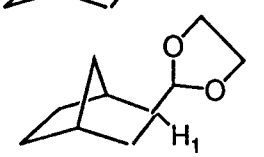

88b,c 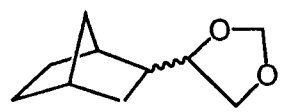

89 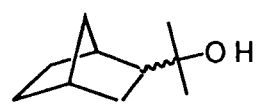

90 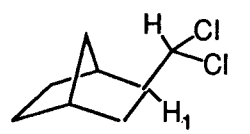

91a,b 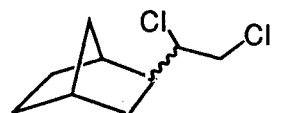

92 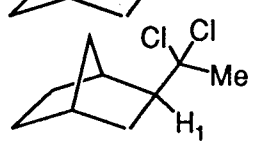

93 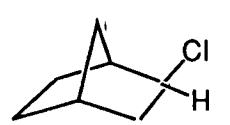

94 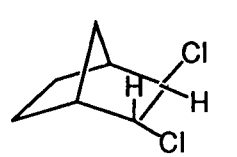

95a 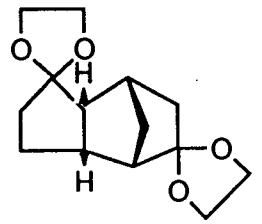

95b 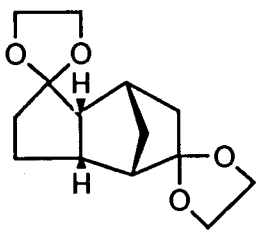

96a 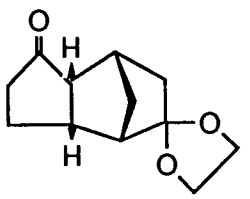

96b 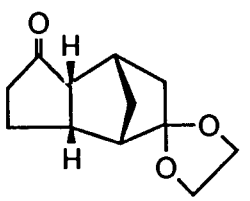

97 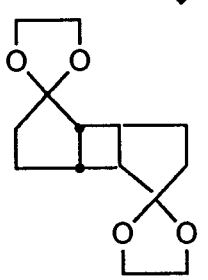

98a 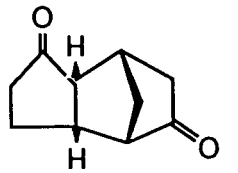

98b 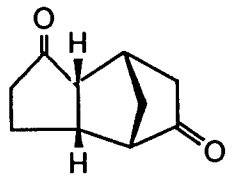

99a 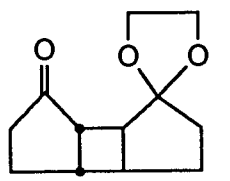

99b 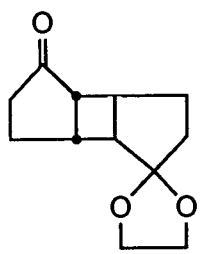

100 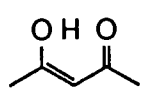

CHAPTER 1 INTRODUCTION

1-1 Electron Acceptor-Sensitizer in Photoinduced Electron Transfer (PET) Reactions

In a PET reaction either an excited state donor (D*) or an excited state acceptor (A*) can be involved (Eq.1-1) depending on the nature of reaction. If there are no other chemical interactions than single electron transfer between

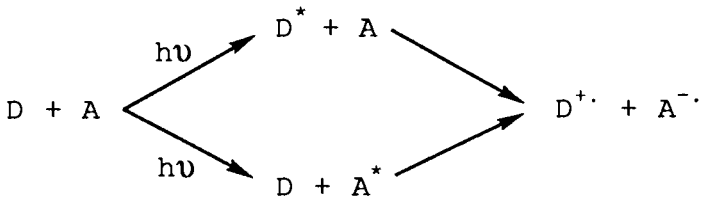

(1-1)

donor and acceptor and the excited state species is not consumed during the course of reaction, the species being excited is a sensitizer. In this case, subsequent reactions of the radical ion of a substrate, the counterpart of sensitizer in Eq.1-1, is the aim of investigation. Because of the ubiquity of cation radical reactions especially in organic chemistry, more attention has been paid to the PET reactions in which the sensitizer acts as an electron acceptor (electron acceptor-sensitizer).[1]

According to the statistics updated to 1988, PET reactions involving electron acceptor-sensitizers are at least twice as

many as those involving electron donor-sensitizers. Electron acceptor-sensitizers most commonly seen in literature, which cover three quarters of this type of PET reactions published,[2] are mainly cyanoaromatics given in Table 1-1. A variety of cation radical mediated reactions, e.g. *cis-trans* isomerization,[3,4] rearrangement,[5] "2+2" cycloaddition,[6-8] "Diels-Alder" dimerization,[9-11] nucleophilic addition,[12] and oxidation,[13,14] can be induced by these sensitizers.

However, not always feasible is a complete electron transfer shown in Eq.1-1 for all donor-cyanoaromatic systems while a partial electron transfer may occur, usually characterized by the formation of "stable" exciplexes that do not further collapse to ionic species.[15-19] In this case, cycloaddition and/or coupling reactions between the donor and acceptor may result as the chemical consequence of exciplex formation.[20-22] Of course, the cyanoaromatics are no longer sensitizers when they are involved in bimolecular chemical reactions. However, studies on this type of donor-acceptor interaction constitute another important part of the PET theme.

Among less frequently used electron acceptor-sensitizers, carbonyl compounds, especially quinones, are relatively popular. One of them, tetrachloro-1,4-benzoquinone (TCB), is of great importance in PET due to its strong tendency to act as a single electron acceptor, and is therefore also listed in Table 1-1.

Since only limited types of electron acceptor-sensitizer have been employed so far, searching for new members of the family and related new reactions is one of the challenges in current PET studies.

Table 1-1 Parameters of Most Commonly Used Electron Acceptor-Sensitizer[a]

sensitizer	$E_{1/2}^{red}$ (V)[b]	$\Delta E_{0,0}$ (eV)[c]
1-cyanonaphthalene(1-CN-Np)	-1.98	3.75
9-cyanophenanthrene(9-CN-Ph)	-1.88	3.42
m-dicyanobenzene(m-DCNB)	-1.86[b]	4.31[d]
9-cyanoanthracene(9-CN-An)	-1.70[e]	2.96
1,4-dicyanobenzene(p-DCNB)	-1.60	4.27
1,4-dicyanonaphthalene(DCN-Np)	-1.28	3.45
9,10-dicyanoanthracene(DCN-An)	-0.89	2.88
1,2,4,5-tetracyanobenzene(TCNB)	-0.65	3.83
2,6,9,10-tetracyanoanthracene(TCN-An)	-0.45	2.82
tetrachloro-1,4-benzoquinone(TCB)	+0.02	2.70(T)[f]

a. Data are cited from ref. 13 unless otherwise specified.
b. Reduction potential in CH_3CN *vs.* SCE.
c. Lowest singlet excitation energy except for TCB.
d. Cited from ref. 2.
e. Cited from ref. 23.
f. The triplet excitation energy cited from ref. 24.

1-2. Excited State Ketones and β-Diketones as Electron Acceptor

Over the last two decades, widespread studies have attempted to elucidate if photoexcited ketones can act as electron acceptors. Direct observations of resulting radical ions are achieved by means of transient absorption spectroscopy, ESR, and CIDNP in donor-ketone systems in the presence of very strong electron donors such as amines,[25-28] anisols,[29] or 1,4-dioxene.[30] For other weaker donors, one of commonly used experimental methods to provide evidence for PET is to correlate the rate constants of emission quenching or quantum yields of products formation with redox potentials of reactants involved.[24] Mattay and coworkers have demonstrated that the fluorescence and phosphorescence quenching of biacetyl, benzophenone, and benzil by electron rich olefins correlated nicely to the oxidation potentials of the quenchers.[31] Similar results for other emissive ketones were also observed earlier.[32] On the other hand, studies on two major bimolecular reactions of excited ketones, namely, oxetane formation and hydrogen abstraction, have shown that PET may be involved in competition with the "conventional" diradical mechanisms, and that it may become the major pathway when the counterparts constitute a favorable donor-acceptor pair.[33,34]

Obviously, ketones have some disadvantages for being electron acceptor-sensitizers. (1) They tend to form "stable"

exciplexes with donors rather than go all the way to produce solvent separated free ionic species.[31] (2) Excited state ketones (usually in their triplet state), being diradical in nature, may undergo fast chemical reactions (e.g. hydrogen abstraction) with the donor or solvents in competition with PET processes. (3) The ketyl radical anion resulting from a complete PET is a highly reactive species. The first difficulty may be overcome by addition of lithium salts to excharge the cation radical out of the exciplex formed between the excited state ketone and a donor (e.g. 1,3-cyclohexadiene, Scheme 1-1).[35,36]

Scheme 1-1:

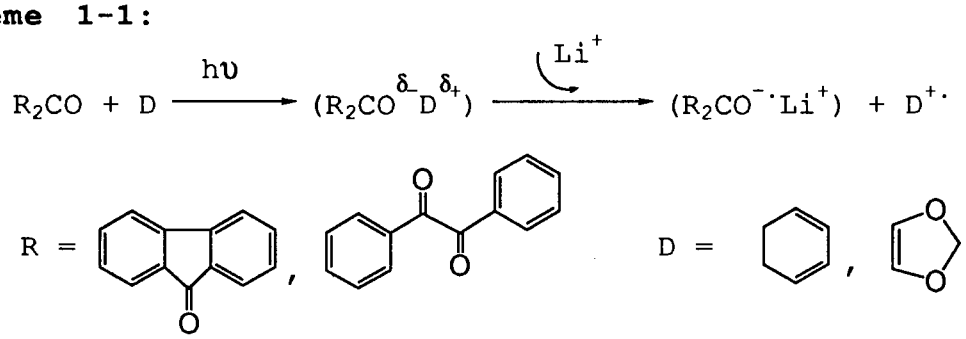

In contrast to monoketones and α-diketones, β-diketones have received little attention as being PET reagents. This is because most diketones exist mainly in their enol form which can no longer be regarded as electron deficient compounds. For example, acetylacetone has a reduction potential[37] of -2.68 V (*vs.* SCE), 0.82 V lower than that of benzophenone;[30] but has an ionization potential[38] of 8.85 eV, 0.86 eV lower than that of acetone.[39] From these redox parameters, we may

regard acetylacetone as a moderate electron-rich species like simple cyclic olefins.* Indeed, no hint of PET was depicted in mechanistic studies[40-42] on the well known de Mayo reaction (Scheme 1-2) with one exception, in which the diketone is modified by attaching a strong electron withdrawing group to the methine carbon.[43] It was claimed that 3-cyano-2,4-pentanedione added to cyclohexene *via* an exciplex formed from the singlet excited state ketone and ground state cyclohexene (Scheme 1-3). Though there are no systematic experimental data to support the PET mechanism proposed in the scheme, the reaction does show a significant difference in mechanism compared with the conventional de Mayo reactions, and provide an example for the reactivity modifications of a β-diketone.

Scheme 1-2: The de Mayo reaction

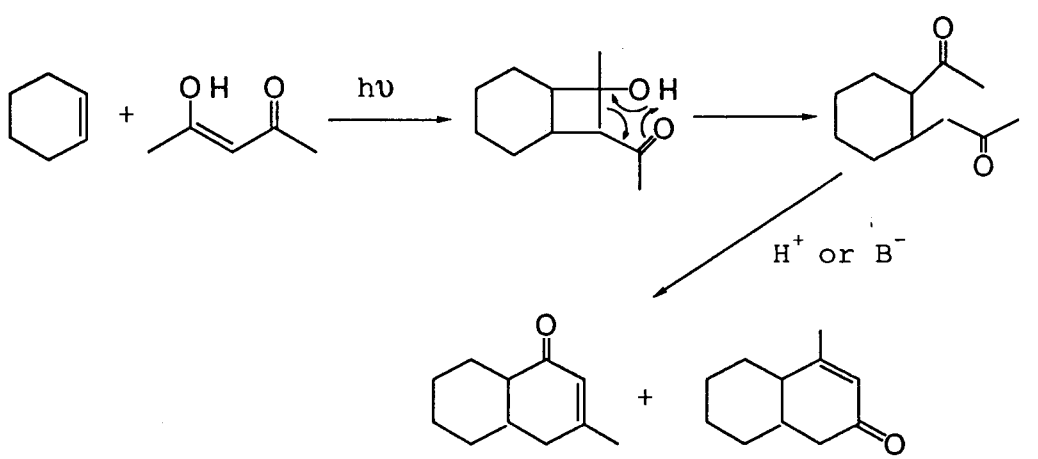

* Compare the IP values (eV): cyclohexene (8.94), cycloheptene (8.87), cyclooctene (8.82), and norbornene (8.95).

Scheme 1-3:

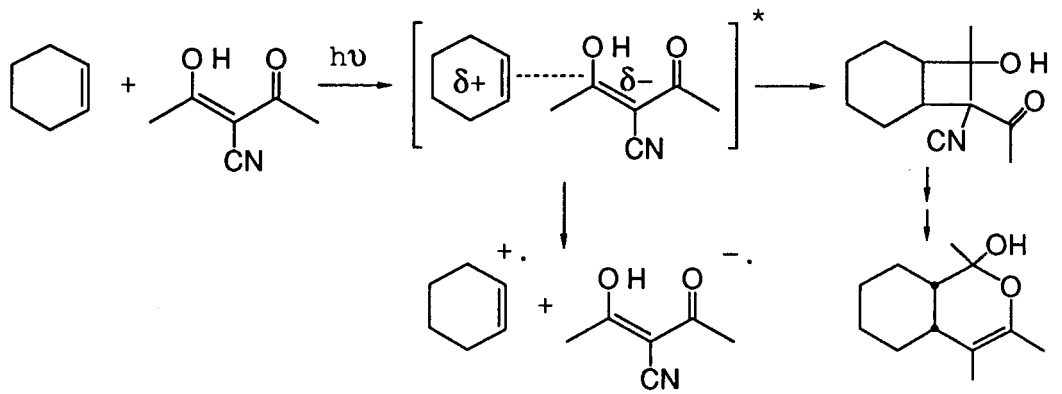

1-3. β-Diketonatoboron Difluorides

In chelate compounds of β-diketones, alkaline metal and transition metal complexes are the best investigated. In general, the polarization of electron density in the chelate ring is assigned with the positive end at the metal and the negative end at the ligand.[43,44] Retrieving the reactions of β-diketone-metal complexes, one can therefore hardly find an example in which such a chelate compound acts as an electron acceptor unless it encounters an extremely strong electron donor, e.g., Grignard reagents.[45] In contrast, some metal chelates of acetylacetone do act as electron donors leading to the net reduction of the metal and oxidation of the ketone,[46-50] which has been plausibly supported by the observation of acetylacetone radical[51] generated in a triplet sensitization process described in Eq.1-2.

$$Cu(acac)_2 + {}^3Ph_2CO \longrightarrow Cu(acac)^+ + acac^{\cdot} + Ph_2CO^{-\cdot} \quad (1\text{-}2)$$

However, another group of chelate compounds, the complexes of β-diketones with pseudo-metal elements, e.g. P,[52,53] Si,[54-58] and B,[59,60] may bear an electron density distribution in the chelate ring opposite to that in metal chelates as implicated by the deshielding effects on the diketone moiety commonly observed in their ^1H NMR spectra. Of particular interest are β-diketonatoboron difluorides because of their good accessibility and unique properties with regard to the candidacy of potential electron acceptor-sensitizers.

The first report of the synthesis of β-diketonatoboron difluorides was published in 1924.[61] Since then more than 20 stable analogues have been isolated from boron trifluoride catalyzed acylation and related reactions of carbonyl compounds or purposely synthesized.[62-69] The chelate structures of these difluorides (Eq.1-3) are clearly

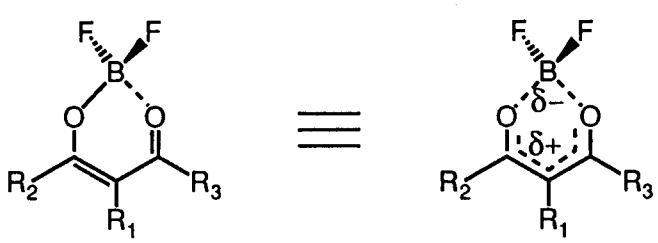

(1-3)

R_1	R_2	R_3	
H	CH_3	CH_3	$AABF_2$
H	CH_3	C_6H_5	$BABF_2$
H	C_6H_5	C_6H_5	$DBMBF_2$
H	$t\text{-}C_4H_9$	$t\text{-}C_4H_9$	$HMPBF_2$

indicated by the spectroscopic data. In a systematic IR study of 18 difluorides,[62] all the compounds showed pronounced shifts to lower frequencies in the absorption positions of carbon-carbon and carbon-oxygen double bond stretching frequencies. None of them gave any indication of the existence of free carbonyl groups. The UV/VIS absorption spectra of these difluorides, consistent with other dialkyl boron-β-diketone complexes, have a marked bathochromic shift[70,71] in the principal absorption maximum, accompanied by an enhancement in the extinction coefficient, when compared with those of the parent enols. A $\pi-\pi^*$ transition in the delocalized π-electron system in the chelating ligand is, therefore, assigned for the principal absorption.[62] Both the ^1H or ^{13}C NMR spectra of acetylacetonatoboron difluoride ($AABF_2$) show an identical chemical shift for the two methyl groups, in agreement with magnetic equivalency of groups in the symmetrical chelate structure.[72] The lack of coupling between the fluorine and boron nuclei is also attributed to the fact that the boron atom is in a highly symmetrical environment.[62] The X-ray crystallography study[73] of benzoylacetonatoboron difluoride ($BABF_2$), demonstrating that the two B-O bonds (1.488Å) and the two C-O bonds (1.304Å) have an identical bond length, added a firm proof for the chelate structure.

The charge separation shown in Eq.1-3 is concluded from the fact that these chelate compounds have large dipole moments (see Table 1-2) and that in the NMR studies the

methine proton signals are shifted to lower field with respect to the corresponding parent enols of diketones.[61] Furthermore, an NMR study[37] on several acetylacetone-BR_2 (R = F, aryls, alkyls) complexes shows that the "red" shift of the methine proton is accompanied by a "blue" shift of the ^{11}B signals, giving a linear Taft correlation with the σ^* values of R group. This is interpreted in terms of that as R is made more electron-withdrawing, donation to the boron atom by the chelate ring is increased so that electron shielding at the diketone moiety is decreased whereas at the boron atom is increased.

The four difluorides quoted in Eq.1-3, especially dibenzoylmethanatoboron difluoride ($DBMBF_2$), have been photophysically and photochemically studied throughout the work presented in this thesis. We chose them as candidates for electron acceptor-sensitizer on the basis of a survey of their properties. As shown in Table 1-2, the difluorides have fairly high reduction potentials which are comparable with those of cyanoaromatics (Table 1-1). The significant increase (0.90 V) in the reduction potential for $AABF_2$ compared with that of acetylacetone indicates a drastic improvement in electron acceptability resulting from chelating with BF_2 group. Nevertheless, the chelate ring structure is expected to be able to gain some stabilization for the anion radical species resulting from an electron transfer interaction, an important factor among those which determine the feasibility

Table 1-2. Some Properties of Selected β-diketonatoboron Difluorides Cited from Literature.[37,62,74]

compd	m.p. (°C)	absorption spectra λmax (nm)	log ε	$E_{1/2}^{red}$ (V)[a]	dipole moment (D)	Δδ (ppM)[b]
$DBMBF_2$	197	270 365 378	3.69 4.62 4.57	-1.30	6.7	0.42
$AABF_2$	43	283	4.23	-1.78 (-2.68)[c]	7.6	0.65
$BABF_2$	157	265 330 342	3.69 4.51 4.29	-1.71	/	0.42
$TMHBF_2$	83	293	4.35	/	/	0.52

a. Reported *vs.* SCE.

b. The down field shift of the methine proton NMR signal with respect to that of the corresponding parent diketone (enol form).

c. Of acetylacetone, listed for comparison.

of such processes.[75] Indeed, the dark colored anion radical of $DBMBF_2$ was observed in the electrolysis,[37] that can be sustained for "several months under an inert atmosphere in a drybox".[76] These BF_2 compounds have been used as electron acceptors in the fabrication of photoconducting materials.[74,77]

From the photophysical and photochemical point of view, however, these β-diketonatoboron difluorides have received little attention. Despite the publications of some studies on

their emission properties,[78-80] more detailed investigation is apparently needed, for example, the concentration dependence. The thermal stability of these compounds are known: they are stable in water but are subject to alkaline hydrolysis[81] under reflux and acid catalyzed hydrolysis[63] at room temperature. According to our work, they are also stable towards UV light (> 300 nm) in CH_3CN but decompose slowly upon irradiation in nonpolar solvents such as hexane, giving tarry materials. To our knowledge, there have been no publications dealing with photochemistry of β-diketonatoboron difluorides. However, photoinduced alkyl migration reactions (Scheme 1-4) of dialkylboryl acetylacetone complexes have been reported[82,83] as the sole example of the photochemistry of β-diketonatoboron compounds.

Scheme 1-4:

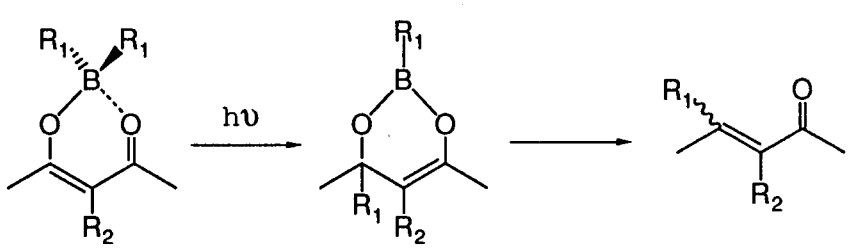

1-4. Research Proposal

$AABF_2$ was isolated and identified in our lab as a thermal by-product in an attempted study of the de Mayo reaction of acetylacetone with cyclohexene in the presence of boron trifluoride. After learning its properties documented in the literature, we realized that it might act as electron acceptor-sensitizers in PET reactions. We have decided to examine photophysical and photochemical behaviors of selected β-diketonatoboron difluorides as a result of the folowing considerations.

(1) There is a certain need for discovery of a new type of electron acceptor-sensitizer.

(2) The chelating with BF_2 group may furnish reactivity modifications of β-diketones with regard to their electron acceptability.

(3) β-diketonatoboron difluorides are fairly stable either thermally or towards the light.

(4) They have extinction coefficients as high as ~40,000, and therefore would absorb light very efficiently.

(5) They bear high reduction potentials which are comparable with those of cyanoaromatics, a proven class of good electron acceptor-sensitizer.

(6) They structurally favor the stabilization of anion radical species.

(7) They are easy to synthesize and purify.

The aims of my research can be outlined as follows.

(1) To examine the fluorescence and phosphorescence emissions of β-diketonatoboron difluorides.

(2) To conduct $DBMBF_2$ fluorescence intensity quenching with a series of quenchers over a wide range of electron donating abilities.

(3) To search for possible ground state complexes and/or exciplexes formed with electron donors.

(4) To check the possibility for the β-diketonatoboron difluorides to induce cation radical reactions of electron-rich substrates.

(5) To investigate if there is any donor-acceptor addition reaction using β-diketonatoboron difluorides as electron acceptors.

(6) To investigate the synthetic and mechanistic features of the reactions.

(7) To compare the advantages and disadvantages of the β-diketonatoboron difluorides as electron acceptor-sensitizers.

(8) To examine related reactions of acetylacetone either being a sensitizer or acting as a reactant.

CHAPTER 2 RESULT

2-1. Spectroscopic Studies of β-Diketonatoboron Difluorides

2-1-1. Absorption and Fluorescence Spectra

The fluorescence data of $AABF_2$ and $DBMBF_2$ in $CHCl_3$ were first published in 1986.[78] We were puzzled by the high concentration (5×10^{-2} M) employed in the measurements and hence embarked on the reinvestigation. The fluorescence and phosphorescence spectra of $AABF_2$ in $CHCl_3$ (fluorescence only), CH_3CN, and methylcyclohexane (MCH) were taken and the data are listed in Table 2-1. A broad and structureless fluorescence emission was observed in samples with high concentration of $AABF_2$ ($> 10^{-2}$ M) in all the solvents. The emission intensities dropped sharply as the concentration went down, obviously faster than a proportional decrease as we did not find any emission when the concentration was reduced to or below 1×10^{-3} M even with both the slits and sensitivity of spectrophotometer turned to maxima. Moreover, excitation beams at wavelengths (349 nm in $CHCl_3$ and CH_3CN, 320 nm in MCH) far beyond the absorption region of $AABF_2$ (Fig.2-1) had to be used to obtain the strongest emissions.

The phosphorescence spectra of $AABF_2$ in MCH and CH_3CN were recorded at 77K though the sample in the latter solvent was

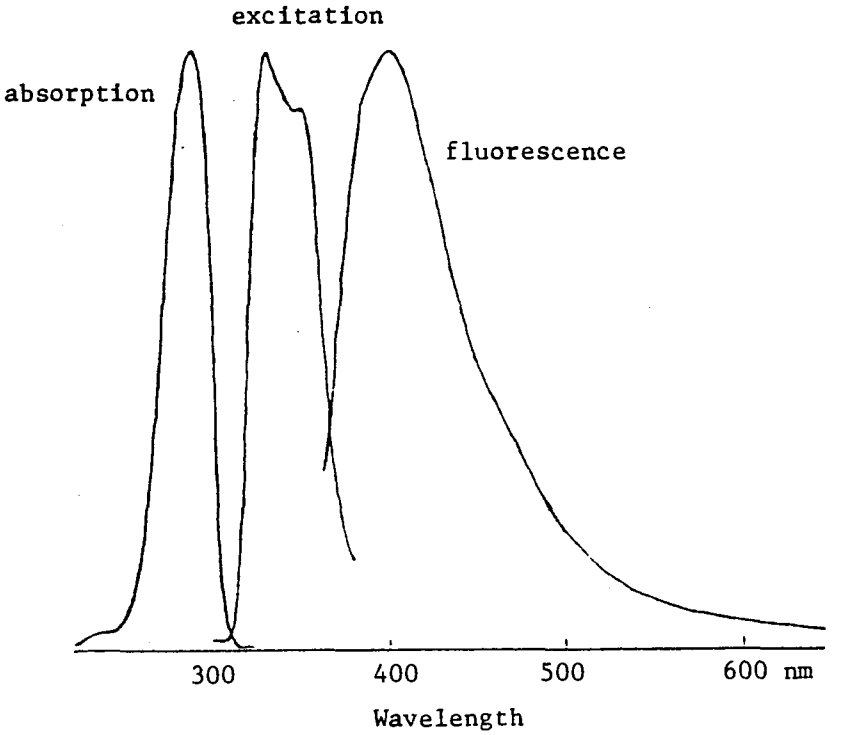

Figure 2-1. The fluorescence emission (λ_{ex} = 349 nm) and excitation (λ_{moni} = 398 nm) spectra of $AABF_2$ (0.05 M) in CH_3CN measured in right angle cell. The absorption spectrum was recorded in CH_3CN with [$AABF_2$] = 2.0 X 10^{-4} M (1 cm cell).

Table 2-1. The Emission Data of $AABF_2$ in Various Solvents[a].

solvent	[$AABF_2$] (10^{-2} M)	fluorescence λ_{ex}(nm)	fluorescence λ_f^{max} (nm)	phosphorescence λ_{ex}(nm)	phosphorescence λ_{ph}^{max} (nm)
$CHCl_3$	5.30	349	395	/[b]	/[b]
CH_3CN	5.03	349	398[c]	315	442
MCH	1.0[d]	320	391	315	459

a. The fluorescence spectra were recorded at room temperature and the phosphorescence spectra at 77K with accuracies of ± 0.5nm for λ_f^{max} and ± 2nm for λ_{ph}^{max}. b. Not measured.

c. Obtained by the spectrum corrected for the Raman band of the solvent. d. Saturated solution.

a glassy solution. The data are also listed in Table 2-1. Again, high concentration had to be used and no phosphorescence emission was found from dilute samples ($[AABF_2] < 1 \times 10^{-3}$ M).

$DBMBF_2$ emits strongly both in solutions and in the solid state. In a dilute CH_3CN solution of $DBMBF_2$ (e.g. 5×10^{-6} M) the fluorescence spectrum showed two emission maxima, λ_f^{max}, at

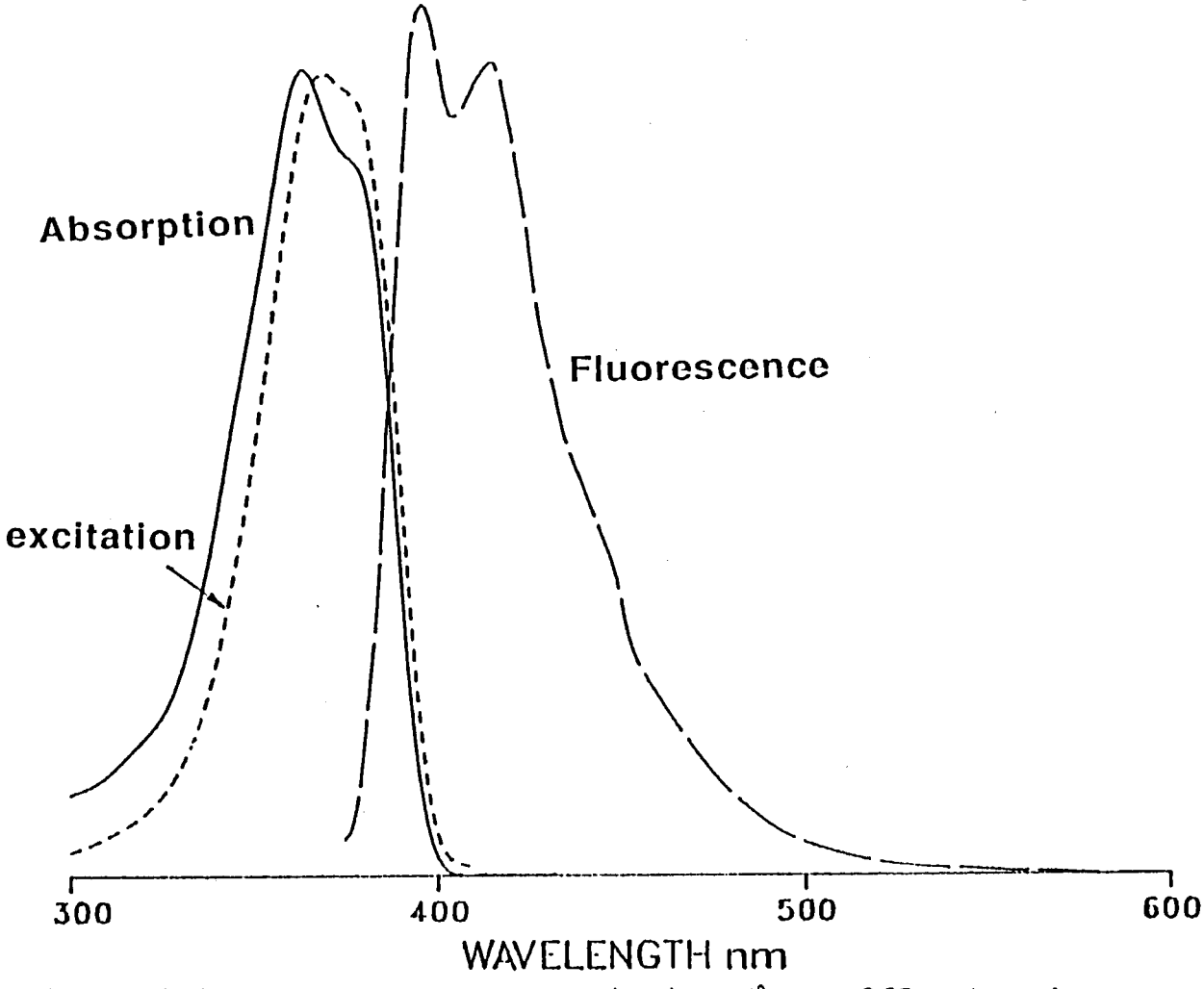

Figure 2-2. The fluorescence emission (λ_{ex} = 365 nm) and excitation (λ_{moni} = 416 nm) spectra of $DBMBF_2$ (5×10^{-6} M) in CH_3CN. The absorption spectrum was recorded in CH_3CN with $[DBMBF_2] = 2.0 \times 10^{-4}$ M (0.1 cm cell).

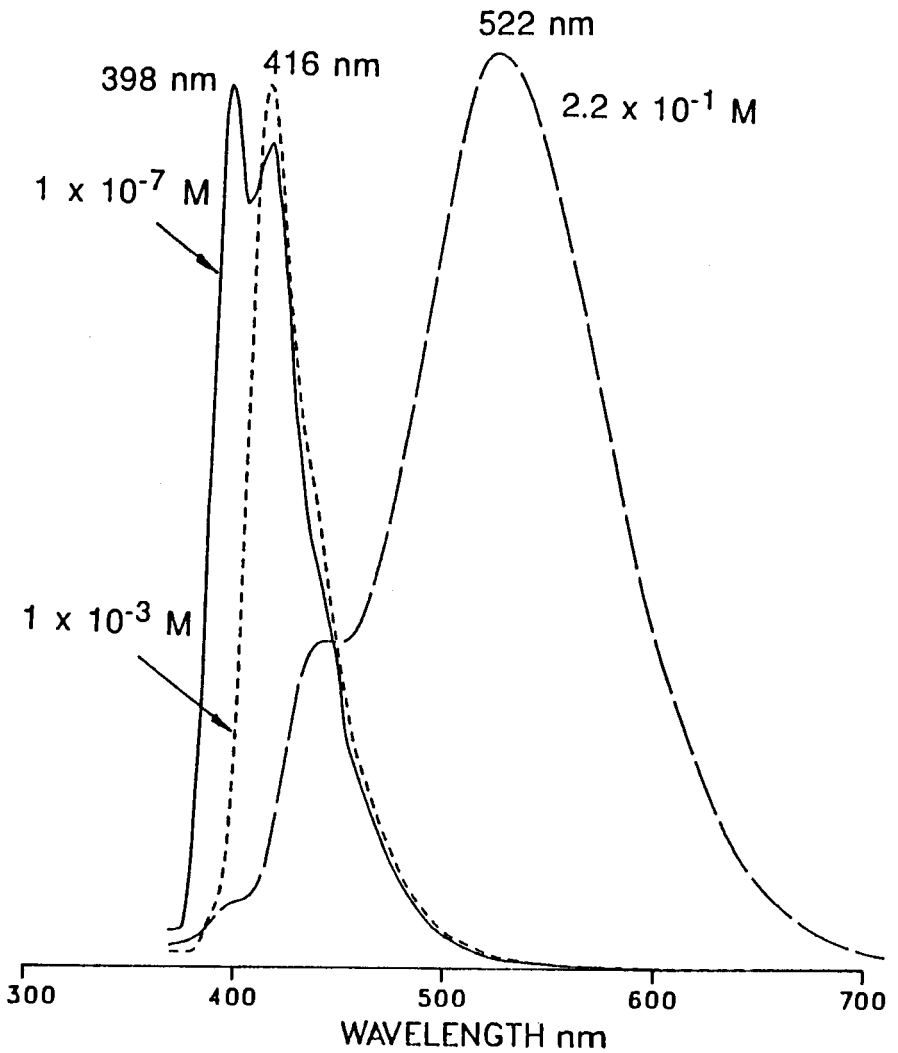

Figure 2-3. Normalized fluorescence emission spectra of $DBMBF_2$ at various concentration in CH_3CN (λ_{ex} = 365 nm).

398 and 416 nm (Fig.2-2). The corresponding excitation spectrum almost matched the absorption spectrum in terms of both position and shape. The 0-0 band of $DBMBF_2$ was estimated to be 392 nm which corresponded to the excitation energy of the lowest singlet state, E_s = 73.0 Kcal/mol. The relative

emission intensities, I, of the two peaks were found to be concentration dependent: the ratio I_{398}/I_{416} decreased as the concentration of $DBMBF_2$ increased and the peak at 398 nm disappeared when the concentration reached higher than 1 X 10^{-3} M. Further increases in concentration, however, resulted in the decrease of the peak at 416 nm accompanied by the appearance of a new, broad emission band centered at 522 nm with a shoulder at ~440 nm (Fig.2-3). The fluorescence emission band from the powder of $DBMBF_2$ resembled that found in saturated CH_3CN solution (~2.2 X 10^{-1} M, Fig.2-3).

The fluorescence of $DBMBF_2$ in ether or hexane also showed two λ_f^{max} (see Table 2-2). The relative intensities of the two peaks (390 and 410 nm) of the fluorescence in ether showed a concentration dependence similar to that found in CH_3CN

Table 2-2. The Data of Absorption and Fluorescence Spectra of $DBMBF_2$ in Various Solvents[a].

solvent	polarity[b] $E_T(30)$ (Kcal/mol)	UV/VIS λ_{max}(nm)	ε ($M^{-1}cm^{-1}$)	fluorescence λ_f^{max} (nm)
CH_3CN	46.0	365	45000	397,416
ether	34.6	361	43700	390,410
benzene	34.5	365	36500	426
hexane	30.9	358	38400	389,406

a. Measured at room temperature with [$DBMBF_2$] = 1 x 10^{-5} M. The accuracy of wavelength measurement was ± 0.5 nm.
b. The empirical parameters of solvent polarity, $E_T(30)$, are cited from ref.84.

solutions and only the peak at 410 nm remained when the concentration was increased to 1 X 10^{-3} M. The emission maximum then shifted to 417 nm as the concentration was further increased to ~1 X 10^{-1} M (saturated solution). Excluding the benzene solution (*vide infra*), a bathochromic shift for both absorption and fluorescence bands can be clearly seen from the data in Table 2-2.

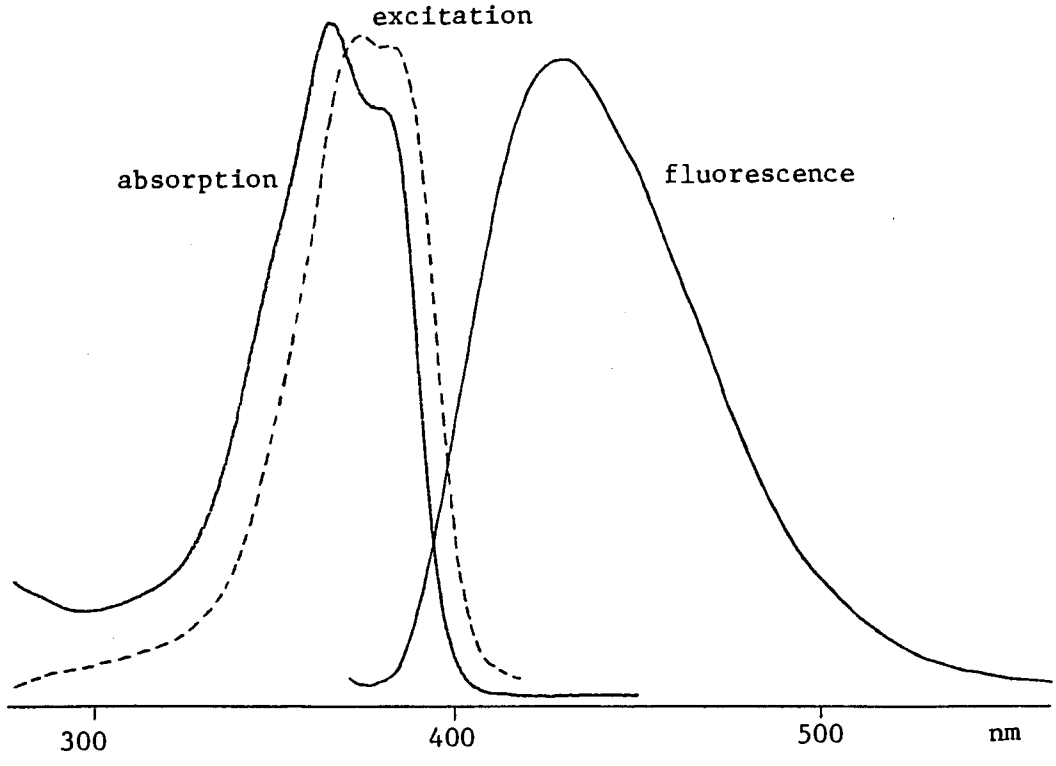

Figure 2-4. The fluorescence emission (λ_{ex} = 365 nm) and excitation (λ_{moni} = 425 nm) spectra of $DBMBF_2$ (1 X 10^{-6} M) in benzene. The absorption spectrum was recorded in benzene with [$DBMBF_2$] = 1 X 10^{-5} M (1 cm cell).

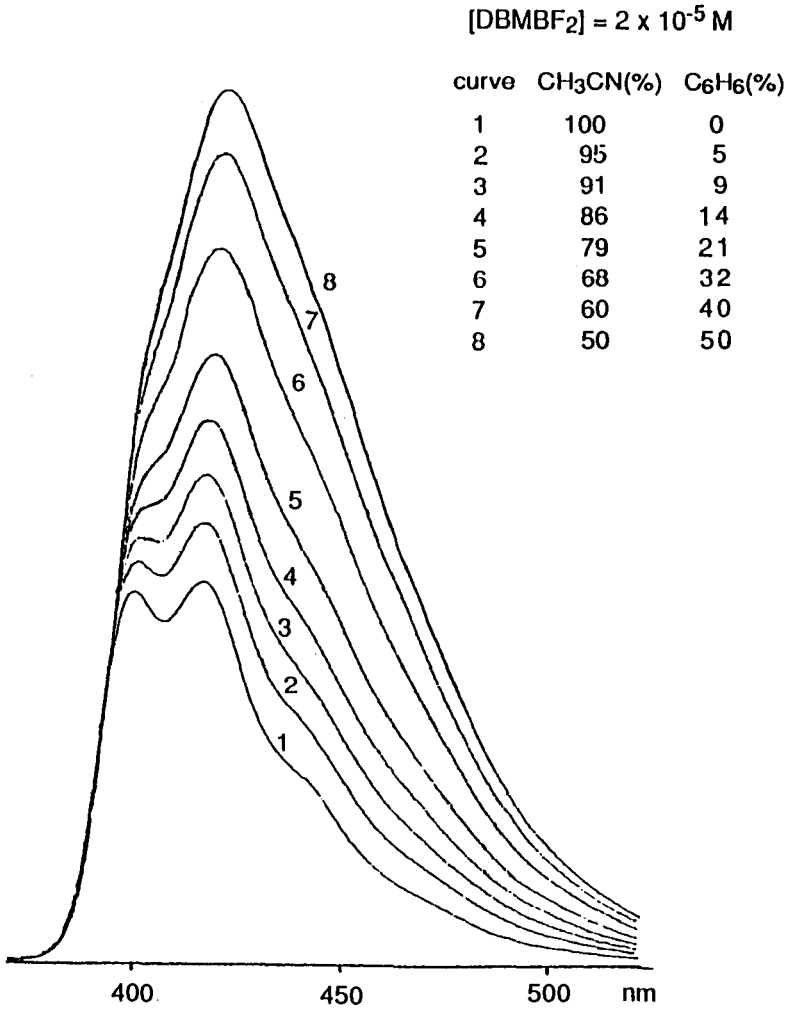

Figure 2-5. Fluorescence emission spectra of $DBMBF_2$ in CH_3CN-benzene binary solvents (λ_{ex} = 365 nm) with various composition (by volume).

However, the emission pattern of $DBMBF_2$ in benzene is totally different whereas the absorption spectrum did not show any notable changes with respect to that in CH_3CN (Fig.2-4). Only one broad emission peak (426 nm) appeared throughout the concentration range from 1 X 10^{-7} to ~5 X 10^{-2}

M (saturated solution in benzene). The λ_f^{max} remained at 426 nm in dilute solutions (< 1 X 10-3) but then shifted gradually to 436 nm in the saturated solution. The addition of benzene to a CH_3CN solution of $DBMBF_2$ resulted in an increase in emission intensity and a decrease in the intensity ratio I_{398}/I_{416} (Fig.2-5). It was also found that the bright yellow color of $DBMBF_2$ powder turned to pale white when it contacted benzene. Recrystallization of $DBMBF_2$ from benzene also gave pale white crystals which then gradually turned to bright yellow accompanying obvious deformations of crystal surfaces during the storage in desiccator. Nevertheless, a strong benzene odor could be detected from the crystals even after being dried for 12 h under reduced pressure in a desiccator.

The phosphorescence spectrum of $DBMBF_2$ in MCH-ether (1:1 by volume) at 77K showed two emission maxima at 486 and 512 nm. The excitation energy of the lowest triplet state $DBMBF_2$ (E_T) was estimated from the onset of the spectrum to be 62 Kcal/mol (461 nm). The corresponding excitation spectrum almost superimposed with the absorption spectrum of $DBMBF_2$ (Fig.2-6).

The concentration dependence found in the fluorescence emission of $DBMBF_2$ raised a question of whether the emission peak at 522 nm was from an excimer or from the excitation of a ground state complex. Considering that a molecular aggregation process was usually accompanied by changes in the spectroscopic properties,[85,86] we carried out the studies of

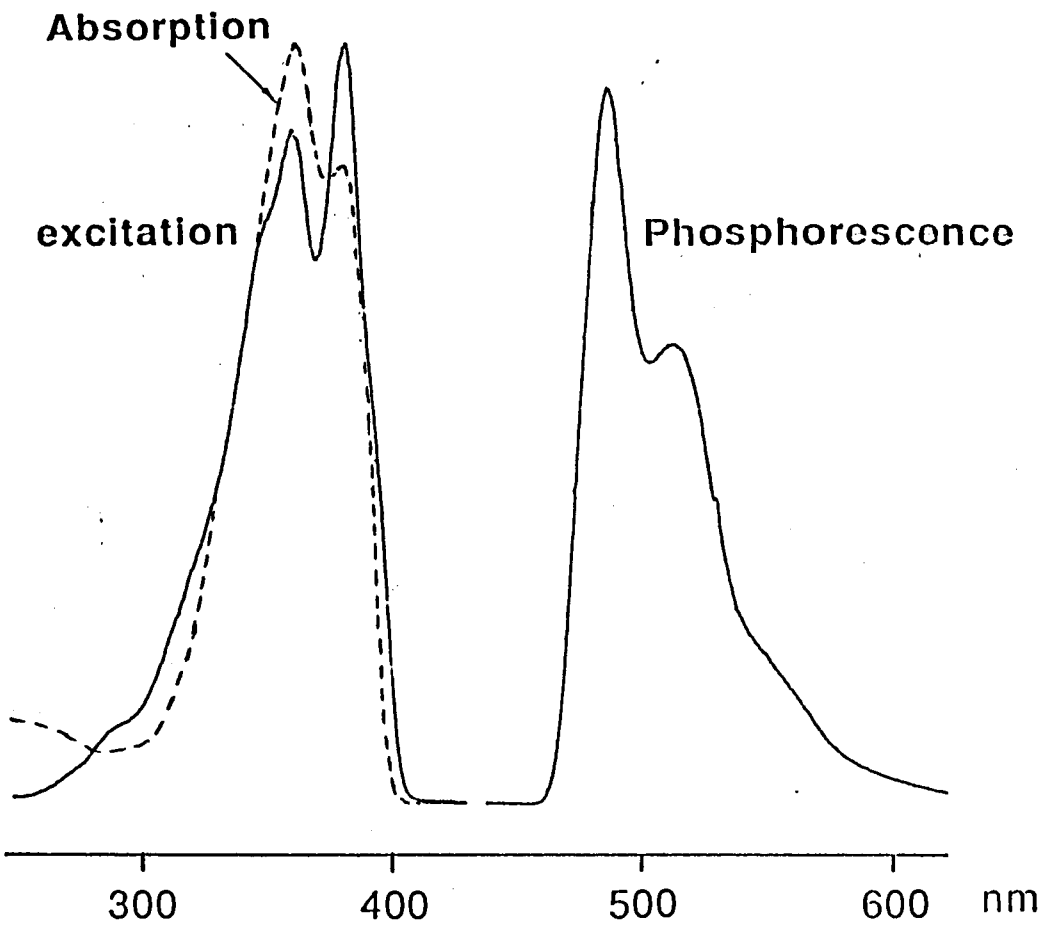

Figure 2-6. The phosphorescence emission (λ_{ex} = 365 nm) and excitation (λ_{moni} = 486 nm) spectra of $DBMBF_2$ (4.0 X 10^{-5} M) in ether/methylcyclohexane (1:1 v/v) at 77K. The absorption spectrum was taken in ether with [$DBMBF_2$] = 1 X10^{-5} M (1 cm cell).

the concentration effects on the absorption and NMR spectra. The absorption and fluorescence excitation spectra in CH_3CN

through a concentration range from 10^{-7} to 10^{-1} M were qualitatively given in Fig.2-7, showing no change in the band shape except in the excitation spectra taken at high concentration (0.01 - 0.1 M) due to the use of a right angle cell. The chemical shifts in ^{1}H, ^{11}B, and ^{19}F NMR spectra (Table 2-3) essentially did not vary with the concentration of $DBMBF_2$ going down from 10^{-1} to 10^{-3} M even to 10^{-5} M (only for ^{1}H).

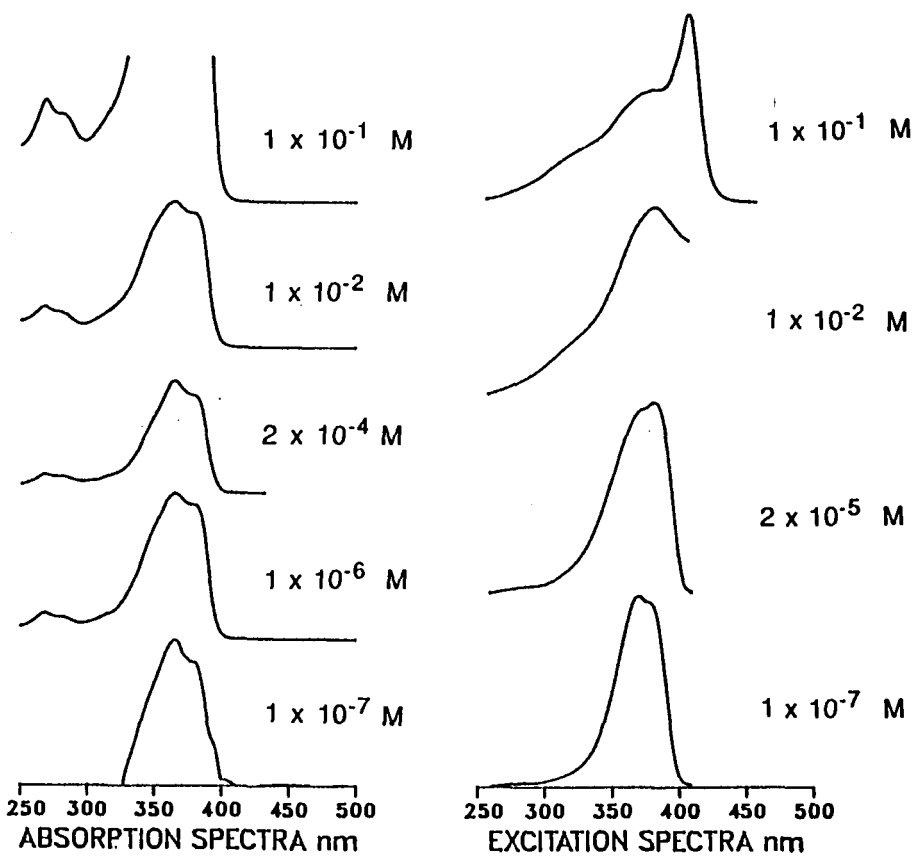

Figure 2-7. The absorption and fluorescence excitation spectra of $DBMBF_2$ at various concentrations in CH_3CN. The excitation spectra were recorded in a right angle cell at 416 nm for [$DBMBF_2$] = 1 x 10^{-7} M, 2 X10^{-5}, and 1 X 10^{-3} M; and 522 nm for 1 X 10^{-1} M.

Table 2-3. The Chemical Shifts (δ) of $DBMBF_2$ in $CDCl_3$ at Various Concentrations.

nuclei	δ (ppm)		
	$[DBMBF_2]$ = 1.0 X 10^{-1}	1.0 X 10^{-3}	1.0 X 10^{-5} M
^{1}H[a]	7.114	7.220	7.220
^{11}B[b]	-8.06	-8.13	/
^{19}F[c]	-61.76(^{11}B)	-61.96(^{11}B)	/
	-61.70(^{10}B)	-61.90(^{10}B)	/

a. The methine proton of $DBMBF_2$.

b. With $Na_2B_4O_7 \cdot 10H_2O$ in water as the external reference.

c. With CF_3COOH in $CDCl_3$ as the external reference.

2-1-2. The Absorption Spectra of $DBMBF_2$ in the Presence of Electron-Rich Olefins

The solution of $DBMBF_2$ in CH_3CN was originally pale white in color. However, a bright yellow color developed immediately upon mixing the solution with electron-rich olefins, i.e. quadricyclane (QC), norbornadiene (NBD), 2,4-dimethyl-1,3-pentadiene (**1**), 1,3-cylohexadiene (**2**), *trans*-anethole (**3**), 2,3-dihydropyran (**9**), ethyl vinyl ether (**11**), 1,3-cyclooctadiene (**13**), 1,3-pentadiene (**14**), or other good electron donors, i.e. triethylamine, *m*-dimethoxybenzene (**5**), N,N-dimethylaniline (**23**). Accordingly, the absorption spectra

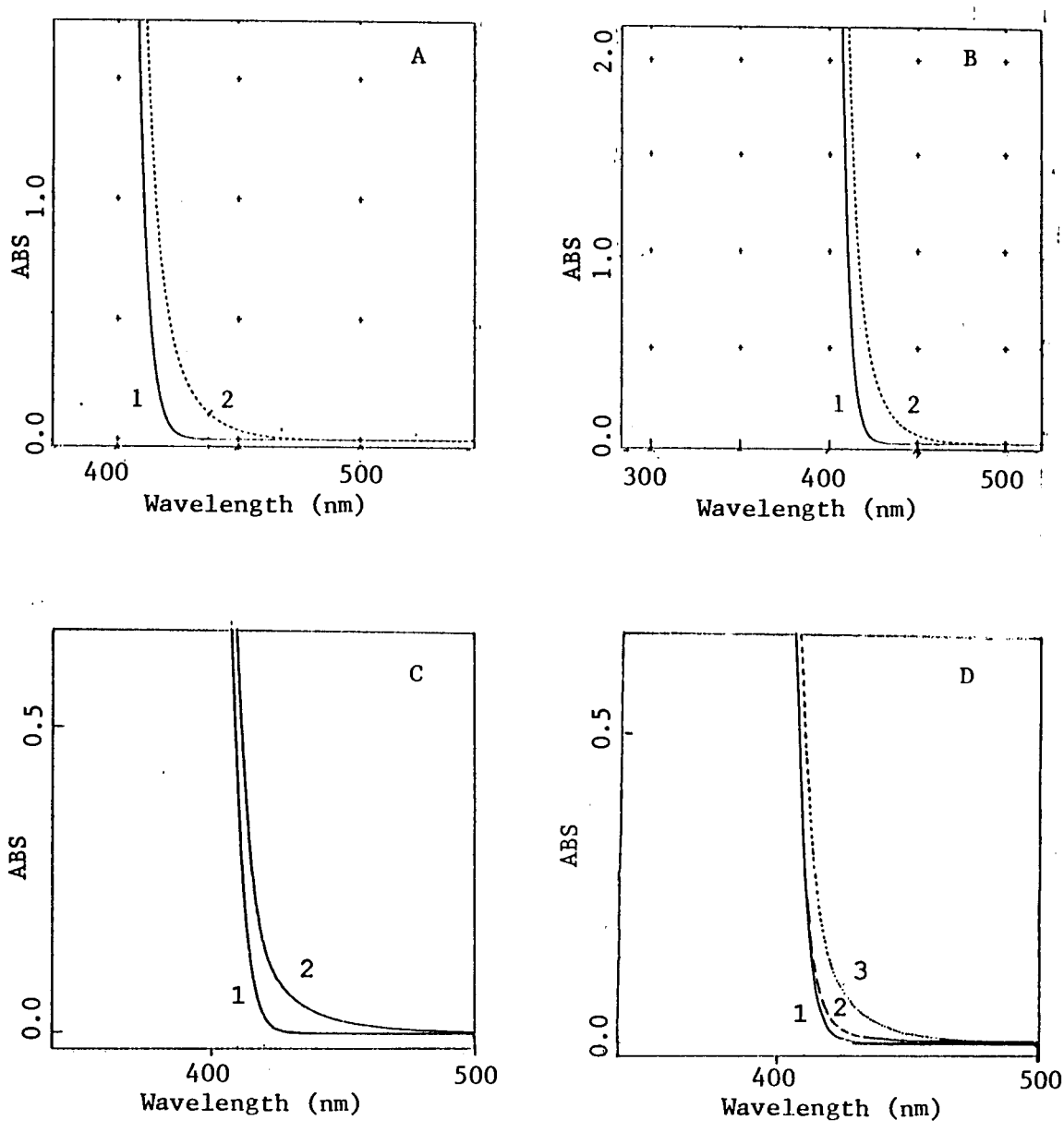

Figure 2-8. The absorption spectra of $DBMBF_2$ in CH_3CN in the presence of electron-rich olefins. A: $[DBMBF_2] = 2 \times 10^{-2}$ M; curve 1, [**1**] = 0; curve 2, [**1**] = 5×10^{-1} M; B: $[DBMBF_2] = 2 \times 10^{-2}$ M; curve 1, [**2**] = 0; curve 2, [**2**] = 5×10^{-1} M; C: $[DBMBF_2] = 1.0 \times 10^{-2}$ M; curve 1, [QC] = 0; curve 2, [QC] = 2.49×10^{-1} M; D: $[DBMBF_2] = 1.0 \times 10^{-2}$ M; curve 1, [**5**] = 0; curve 2, [**5**] = 1.7×10^{-2} M; curve 3, [**5**] = 1.02×10^{-1} M.

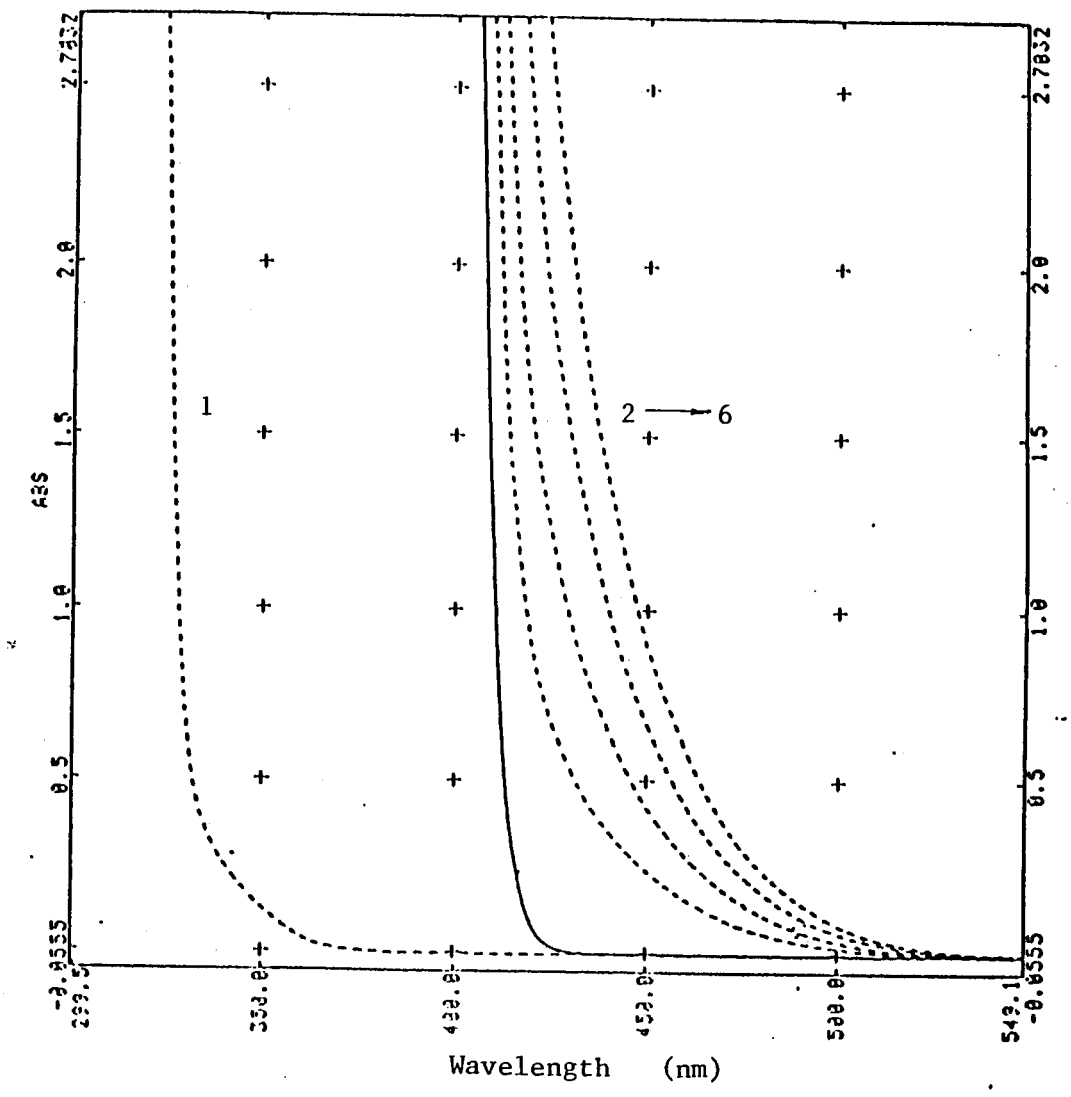

Figure 2-9. The absorption spectra of $DBMBF_2$ in CH_3CN with various concentration of **3**. Curve 1, $[DBMBF_2] = 0$, [**3**] = 5 X 10^{-1} M; curve 2-6, $[DBMBF_2] = 2.0 \times 10^{-2}$ M. curve 2, [**3**] = 0; curve 3, [**3**]= 0.985 X 10^{-1} M; curve 4, [**3**] = 1.941 X 10^{-1} M; curve 5, [**3**]= 3.174 X 10^{-1} M; curve 6, [**3**] = 4.650 X 10^{-1} M.

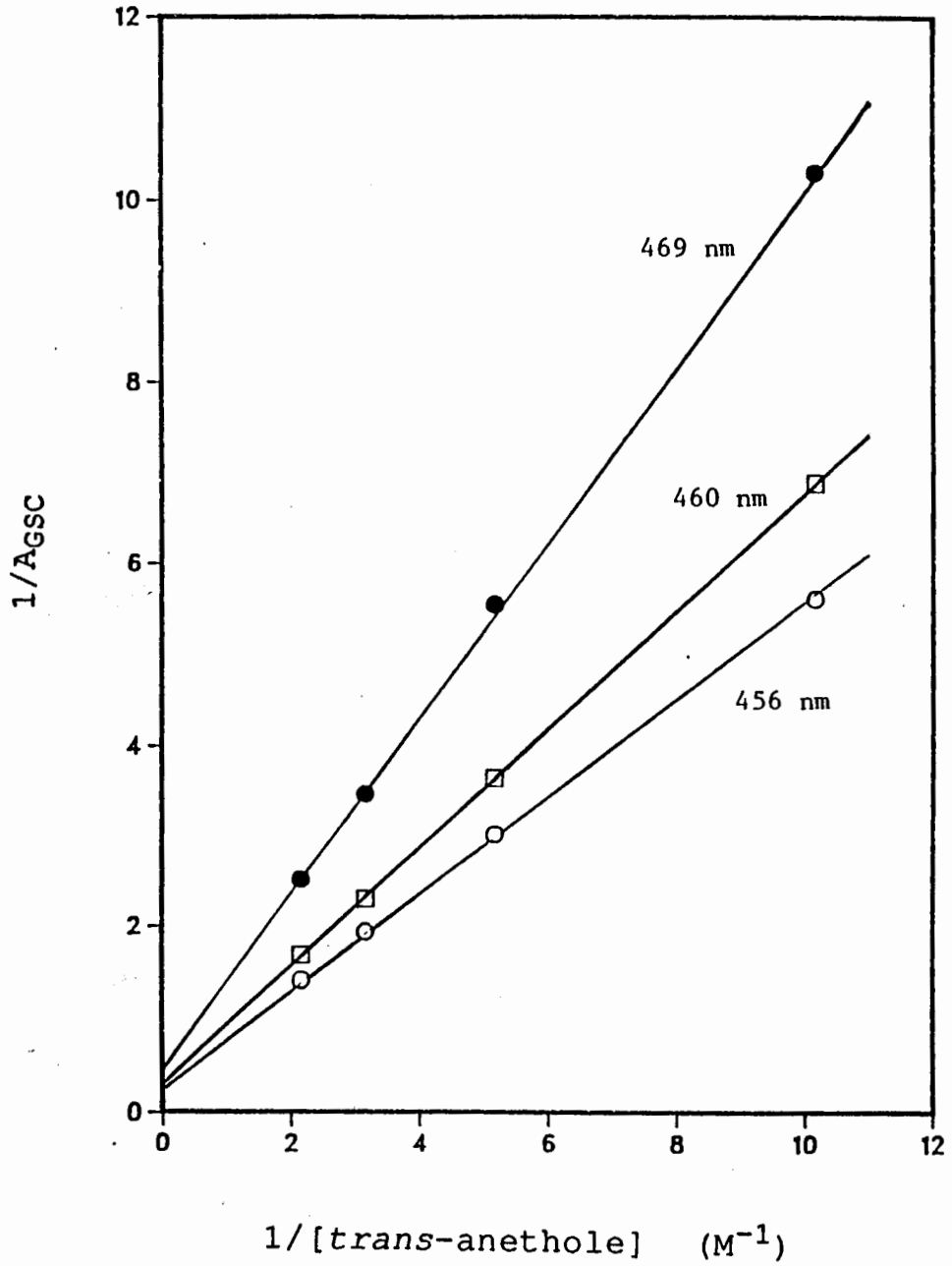

Figure 2-10. The Benesi-Hildebrand plots of $DBMBF_2$-**3** system. Data are adopted from Fig.2-9.

of $DBMBF_2$ changed upon addition of these electron donors,* the cut off of the absorption band shifted to longer wavelength and became more tailing as shown in Fig.2-8 and 2-9. These observations strongly suggested the formation of ground state complexes (GSC), more likely charge transfer complexes, between $DBMBF_2$ and the donors. Based on the data read from Fig.2-9, the formation constant (K) of $DBMBF_2$-**3** GSC was calculated by the Benesi-Hildebrand relationship,[87] where A_{GSC}

$$\frac{[DBMBF_2]}{A_{GSC}} = \frac{1}{\varepsilon_{GSC}} + \frac{1}{K\varepsilon_{GSC}[\mathbf{3}]}$$

and ε_{GSC} are the absorbance and extinction coefficient, respectively, at the given wavelength. Plots of $1/A_{GSC}$ *vs.* 1/[**3**] were taken at 469, 460 and 456 nm, giving K = 0.44, 0.45, and 0.43 M^{-1}, respectively. An average of K = 0.44 M^{-1} was adopted (Fig.2-10).

2-1-3. Quenching of $DBMBF_2$ Fluorescence Intensity

All the fluorescence intensity quenchings were carried out with undegassed solutions of $DBMBF_2$ (5×10^{-6} - 5×10^{-5} M) in CH_3CN since oxygen virtually did not quench the emission at 398 an 416 nm.

Biacetyl quenches the fluorescence intensity of $DBMBF_2$ in CH_3CN very efficiently. The decreases in intensity at 398 and 416 nm upon adding the quencher were different; ~15% faster

*Absorption spectra of $DBMBF_2$ in the presence of **1**, **2**, QC, **9**, and **3** were recorded respectively.

at 416 nm than at 398 nm (Fig.2-11). The $k_q\tau$ (60.0 M^{-1}) obtained by the quenching at 398 nm was referred to the "real" one (see 3-1-2). As the E_s of biacetyl (65.3 Kcal/mol)[88] is 7.7 Kcal/mol below that of $DBMBF_2$ (73.0 Kcal/mol), the quenching process can be regarded as diffusion controlled. By assuming k_q = 2.2 X 10^{10} M^{-1} sec^{-1}, the

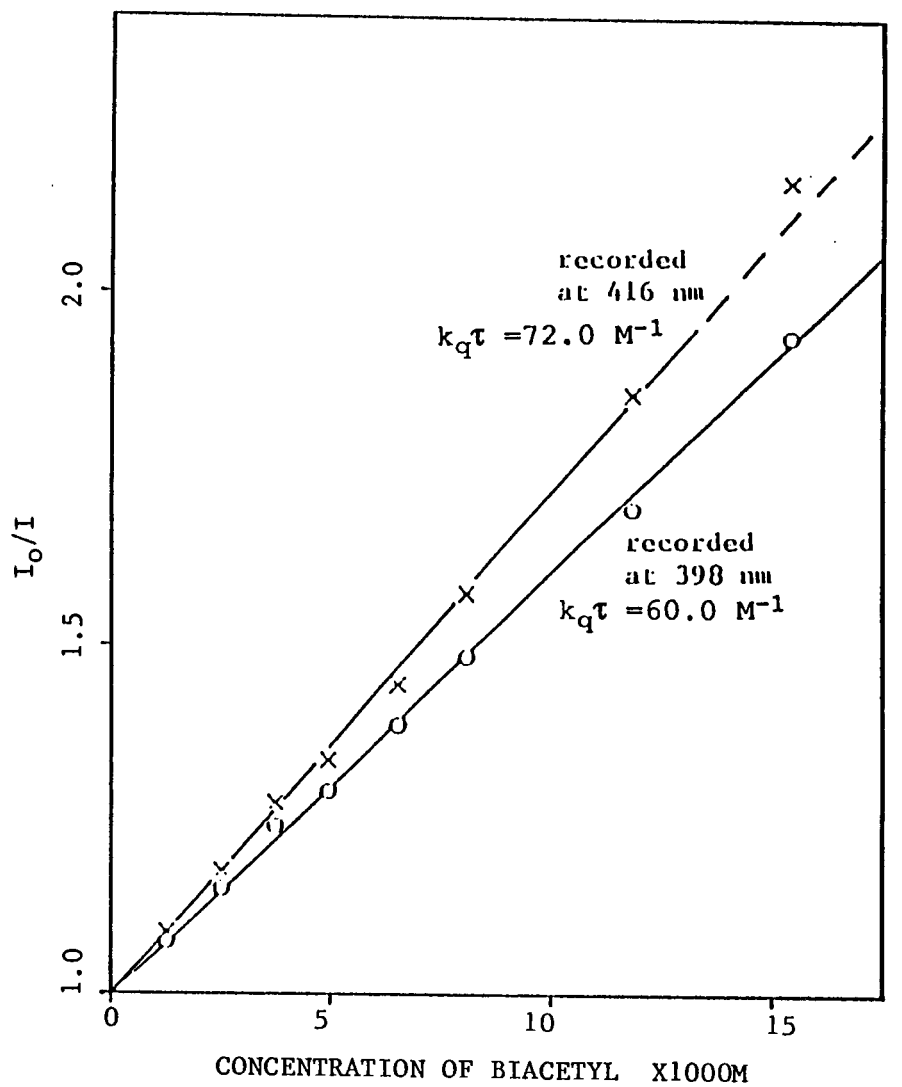

Figure 2-11. The Stern-Volmer plot of $DBMBF_2$-biacetyl system in CH_3CN ($[DBMBF_2]$ = 5 X 10^{-6} M).

fluorescence life time of $DBMBF_2$ in CH_3CN was estimated to be 2.73 ns.*

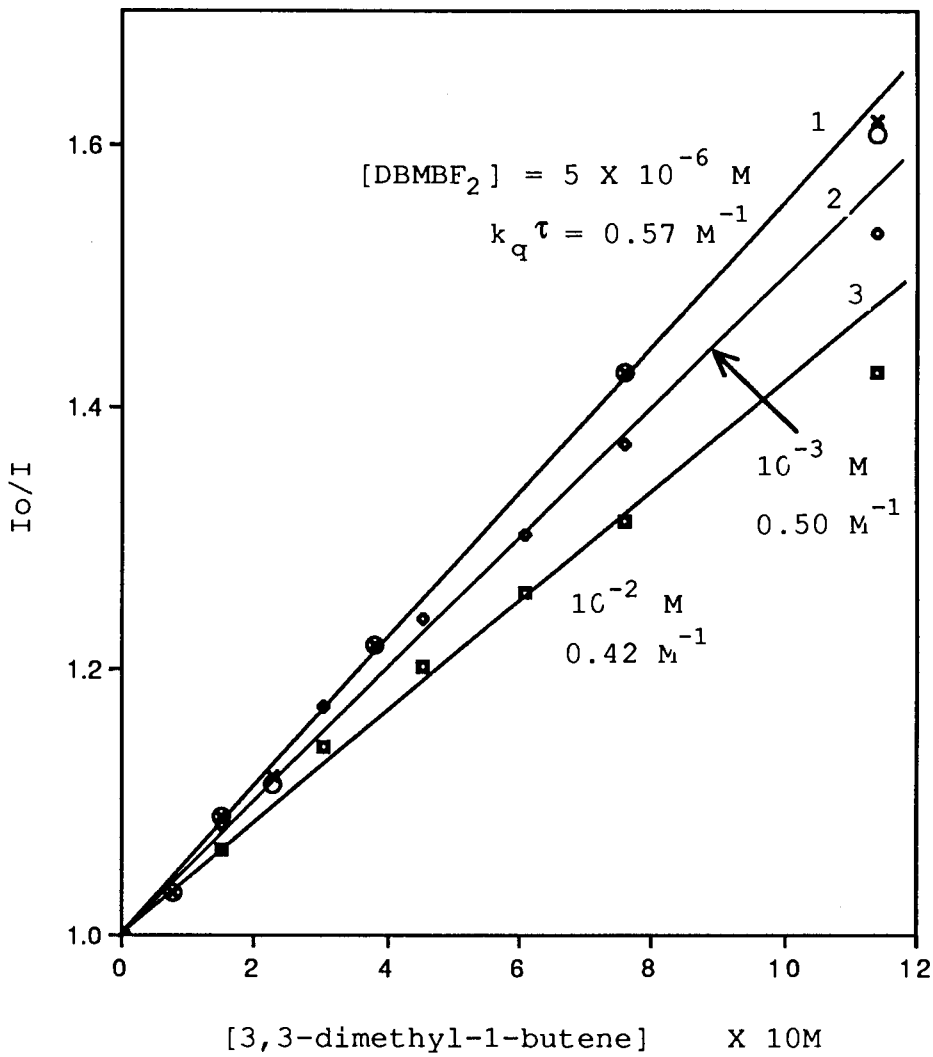

Figure 2-12. The Stern-Volmer plot of $DBMBF_2$-**7** system in CH_3CN. curve 1, measured at 398 (o) and 416 nm (x); curve 2 and 3, at 416 nm.

*The diffusion rate constant (2.2×10^{10} M^{-1} sec^{-1}) was cited from an experimental result (ref.31) obtained from a hexane solution which has a viscosity constant (η = 0.34 cp, at 22°) close to that of acetonitrile (0.36 cp, at 20°).

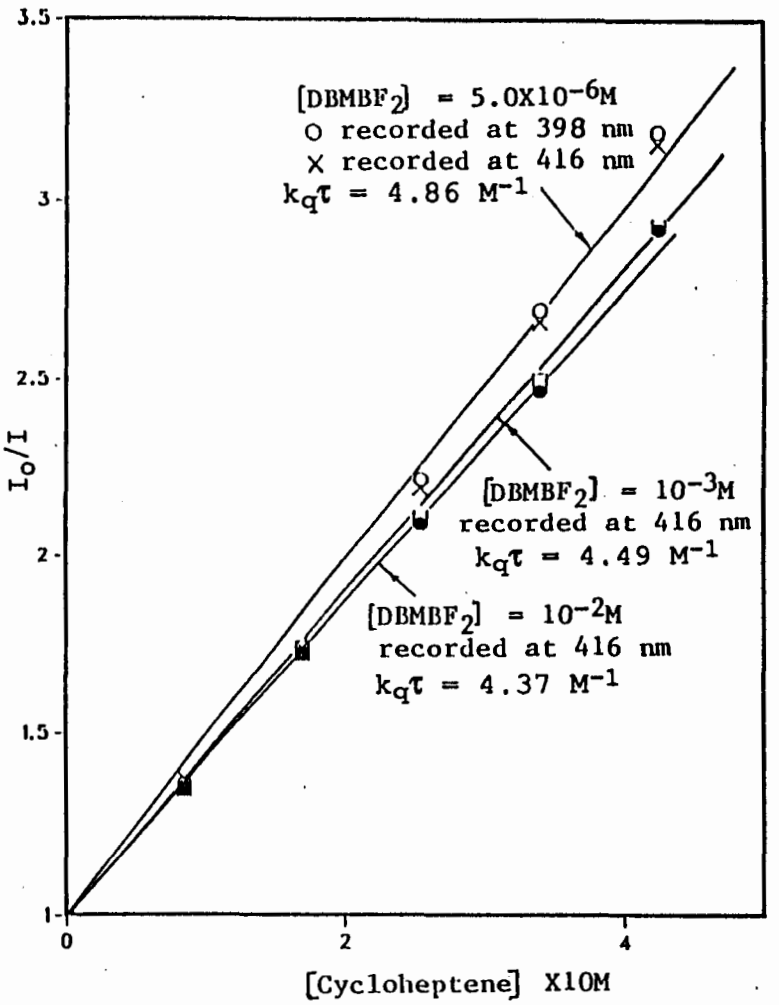

Figure 2-13. The Stern-Volmer plot of $DBMBF_2$-**8** system. Curve 1, measured at 398 (o) and 416 nm (x); curve 2 and 3,measured at 416 nm.

In contrast to the biacetyl quenching, the quenching efficiencies observed at 398 and 416 nm were identical in either $DBMBF_2$-**7** (Fig.2-12) or $DBMBF_2$-**8** (Fig.2-13) systems. However, the quenching efficiency slightly decreased as the

concentration of $DBMBF_2$ increased, which could be clearly seen from the slopes also given in the figures.

The fluorescence of $DBMBF_2$ was quenched by a large body of quenchers. The k_q values, obtained from linear Stern-Volmer relationships (Fig.4-3, 4-4), are listed in Table 2-4 along with the oxidation potentials ($E^{ox}_{1/2}$) and/or vertical ionization potentials (IP) of the quenchers.

The free enthalpy change (ΔG^o) of a photoinduced electron transfer process can be estimated by using the well-known equation derived by Rehm and Weller,[89,90] where $E^{red}_{1/2}$ is the

$$\Delta G^o = E^{ox}_{1/2} - E^{red}_{1/2} - E^* + \Delta E_{coul} \qquad (2\text{-}1)$$

reduction potential of $DBMBF_2$ (-1.30 v),[37] E^* is the energy of the singlet excited state of $DBMBF_2$ (3.17 eV), and ΔE_{coul} is the solvent stabilization energy for ion separation (-0.06 eV in CH_3CN at 20°).[91,92] A clear correlation of k_q values with ΔG^o (Fig.2-14) or IP (Fig.2-15) was found for all olefins except enones and their derivatives. Generally, the more electron-rich the quencher was, the faster the quenching occurred. However, some of enones quenched very efficiently though they were relatively electron-poor. And no correlation between the k_q values and IP's was found for these quenchers.

Table 2-4. Data of Fluorescence Intensity Quenching of $DBMBF_2$ in CH_3CN.[a]

quencher	$E^{ox}_{1/2}$ (V)[b]	IP (eV)[c]	ΔG^o (eV)[d]	$k_q\tau$ (M^{-1})	k_q (10^9 $M^{-1}s^{-1}$)	$\log k_q$
simple olefin						
4	0.91(93)	8.33(94)	-1.02	14.06	5.15	9.71
2	1.35(95)	8.30(96)	-0.58	10.51	3.85	9.59
9	1.46(31)	8.37(94)	-0.47	8.74	3.20	9.51
1	/	/	/	8.74	3.20	9.51
13	/	8.40(94)	/	7.45	2.73	9.44
11	1.74(31)	8.60(97)	-0.19	4.80	1.76	9.25
14	1.73(94)	8.61(96)[e]	-0.20	6.36	2.33	9.37
10	1.54(93)	8.70(94)	-0.39	6.83	2.50	9.40
8	/	8.87(97)	/	4.86	1.78	9.25
12	2.02(31)	8.94(98)	0.09	2.51	0.92	8.96
15	/	8.95(97)	/	4.12	1.51	9.18
7	/	9.45(99)	/	0.57	0.21	8.32
enone and derivative						
16	/	9.30(94)	/	18.26	6.69	9.83
19	/	9.33(94)	/	1.58	0.58	8.76
17	/	9.39(94)	/	9.86	3.61	9.58
18	/	9.65(94)	/	8.27	3.03	9.48
45	/	10.72(94)[f]	/	0.30	0.11	8.04
20	/	/	/	0.63	0.23	8.36
anethole and derivative						
3	1.11(100)	/	-0.82	13.13	4.81	9.68
21	/	/	/	30.85	11.30	10.05
22	/	/	/	20.39	7.47	9.87

To be continued at next page.

Table 2-4. (cont.)

other						
23	0.75(101)	7.36(101)	-1.18	21.70	7.95	9.90
100	/	8.85(38)	/	3.71	1.36	9.13

a. Measured at 20° with undegassed samples ([$DBMBF_2$]=$5X10^{-6}$ - $5X10^{-5}$ M).
b. Cited from references given in the parentheses and reported *vs.* SCE.
c. Vertical ionization potentials. Data measured by photoelectron spectroscopy are adopted preferentially. An average value is used for data cited from reference 94 where more than one source may appear.
d. Calculated from Eq.2-1.
e. The weighed average of IP's of the *trans* (70%) and *cis* (30%) isomers.
f. IP of the methyl analogue.

Notably, a very electron-poor olefin, acrylonitrile (IP = 10.92),[94] did not quench even at a very high concentration (1.38 M). The fluorescence emission at 522 nm in the concentrated $DBMBF_2$ solution (in CH_3CN, ~0.1 M) was not quenched by acrylonitrile either (Appendix 1).

Surprisingly, the fluorescence band at 522 nm in concentrated $DBMBF_2$ solutions was quenched by **8** and **7**. In a CH_3CN solution of $DBMBF_2$ (0.1 M), the peak at 522 nm was accompanied by another peak at 437 nm. Both peaks were quenched by addition of the olefins whereas the intensity of the peak at 522 nm decreased much faster (Fig.2-16, solid curves). As the quencher concentration was adjusted by

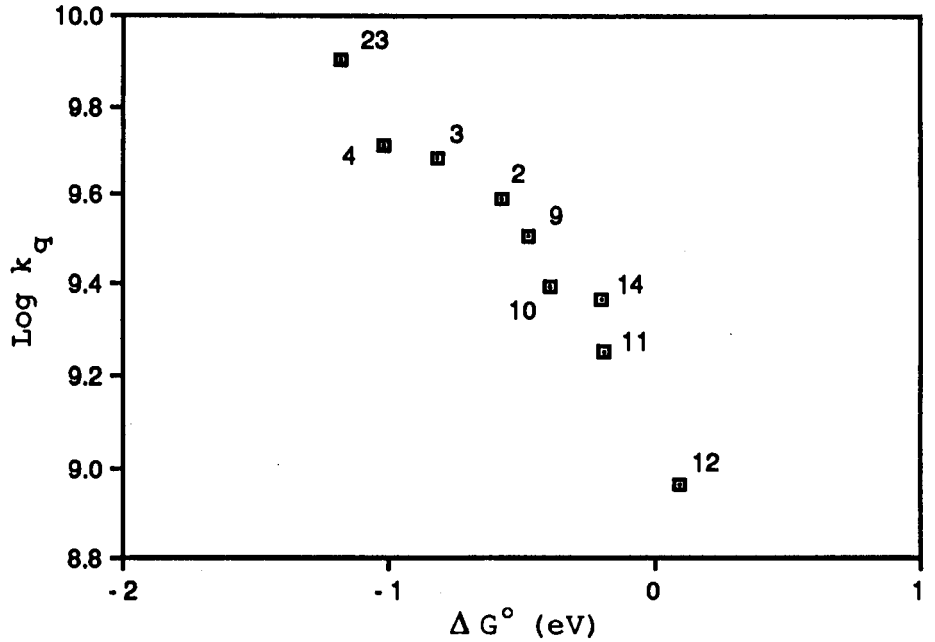

Figure 2-14. Semilogarithmic plot of the rate constant for fluorescence quenching of $DBMBF_2$ (5×10^{-6} - 5×10^{-5} M) in CH_3CN at 20°C as a function of the free enthalpy change for complete electron transfer.

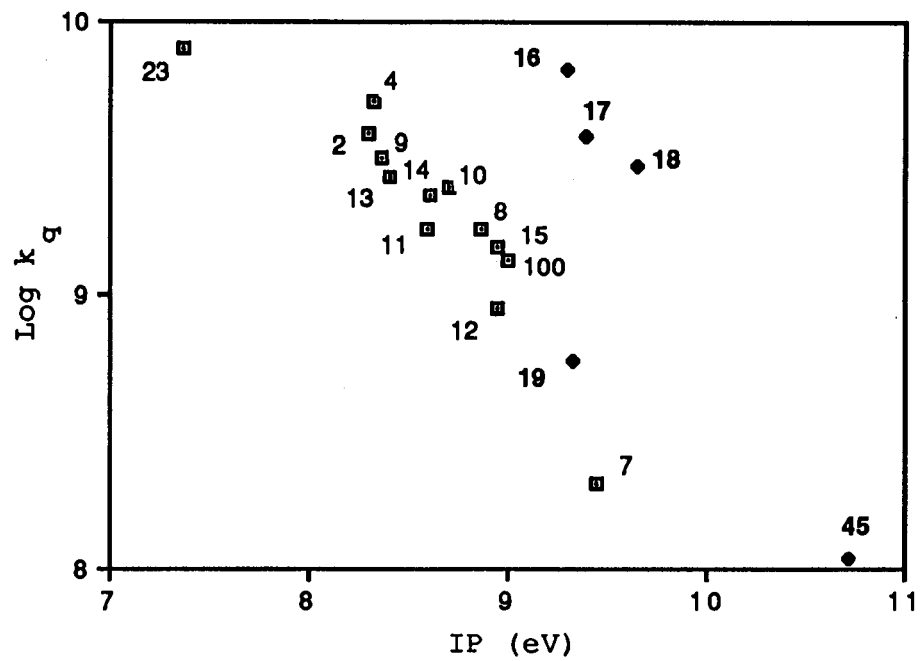

Figure 2-15. Semilogarithmic plot of the rate constant for fluorescence quenching of $DBMBF_2$ (5×10^{-6} - 5×10^{-5} M) in CH_3CN at 20°C as a function of the vertical ionization potential of quenchers.

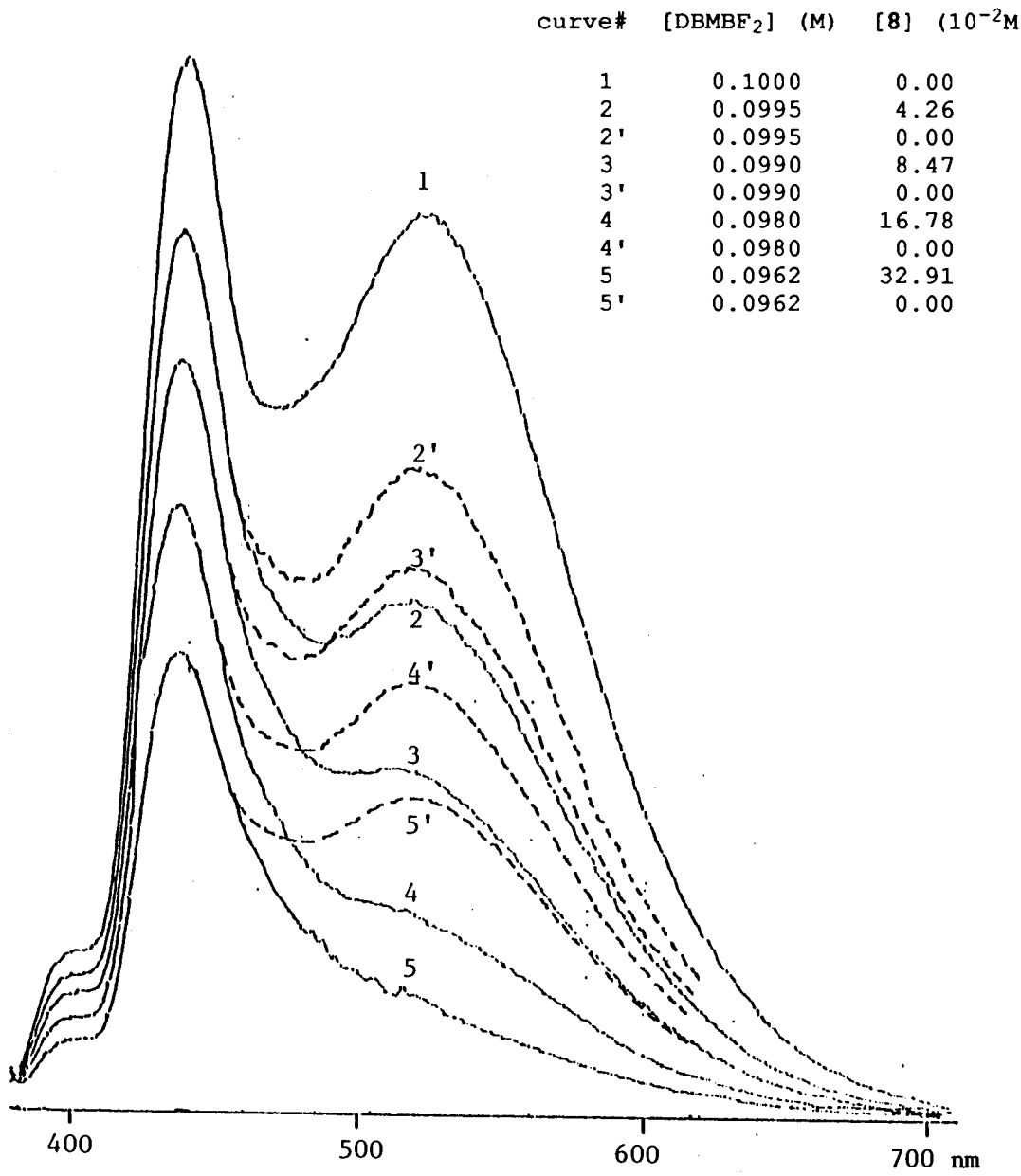

Figure 2-16. The quenching of $DBMBF_2$ excimer emission (λ_{ex} = 365 nm) by cycloheptene (**8**) in CH_3CN. The dashed curves are normalized with respect to the corresponding solid curves at 437 nm; see text for details.

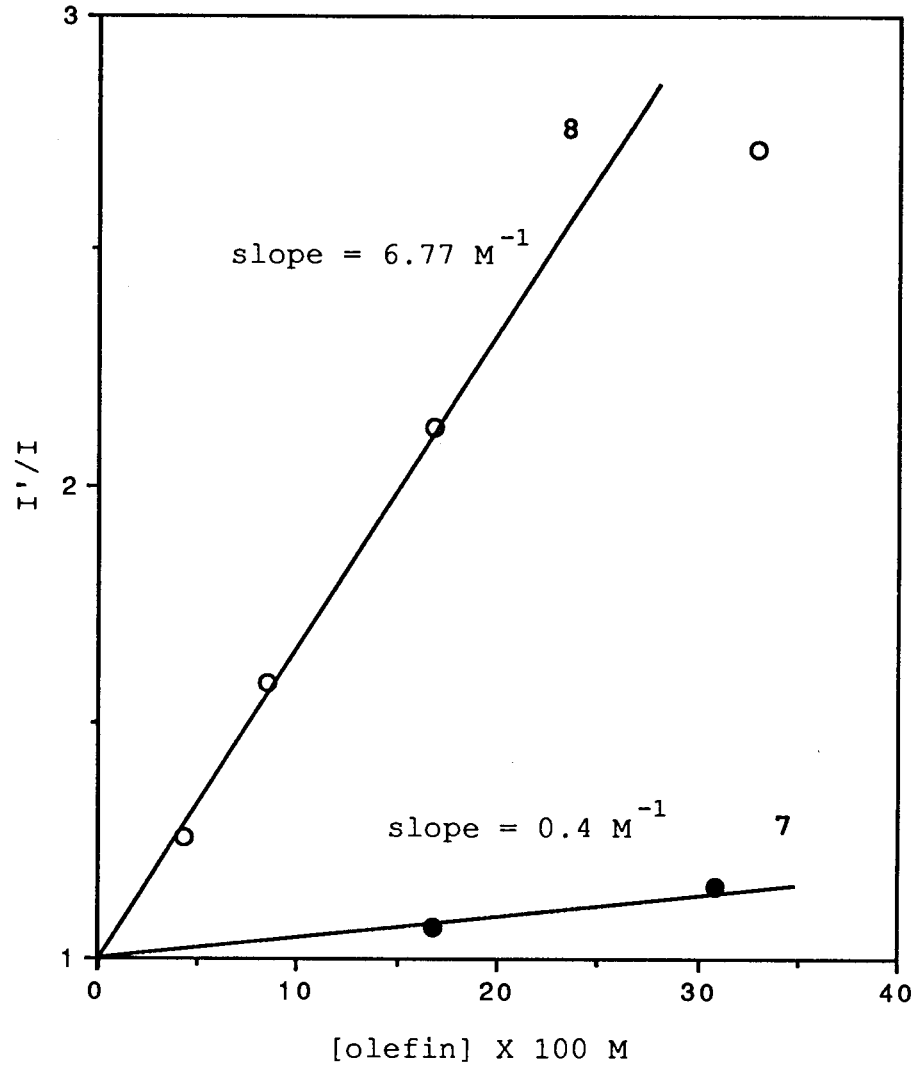

Figure 2-17. The Stern-Volmer plot of the quenching of $DBMBF_2$ excimer emission by **8**. Data are adopted from Fig.3-16, I' denotes the fluorescence intensity at 522 nm for the dashed curves, I for the corresponding solid curves.

injecting the neat quencher into the $DBMBF_2$ solution, the concentration of $DBMBF_2$ was slightly changed upon the addition of quencher. Therefore, the dilution effect on the intensity of the emission at 522 nm were examined by measuring the fluorescence spectra of $DBMBF_2$ solutions with concentration precisely the same as those resulting from addition of the quencher. The spectra thus obtained were then normalized with respect to the emission peak at 437 nm (Fig. 2-16, dashed curves). Comparing the intensities at 522 nm in related solid and dashed curves (I and I', respectively), one could get the real quenching efficiency of the excimer emission abstracted from both dynamic quenching and dilution effects. Indeed, the Stern-Volmer plot of I'/I *vs.* [**8**] gave a reasonable straight line (Fig.2-17) except the point for curve 5 at which the 522 nm peak almost disappeared (Fig.2-16). The $k_q\tau$ for the quenching by **8** was calculated from the plot to be 6.77 M^{-1}, far larger than that for the quenching by **7** (0.4 M^{-1}).

Pyridine behaved differently from other quenchers in the $DBMBF_2$ fluorescence intensity quenching. In CH_3CN, the decrease in fluorescence intensity at 398 and 416 nm upon addition of pyridine was accompanied by an increase in intensity at longer wavelength (> 450 nm) with an isoemissive point appears at ~445 nm (Fig.2-18, upper). However, no quenching but an enhancement in intensity was found in a nonpolar solvent, MCH (Fig.2-18, lower).

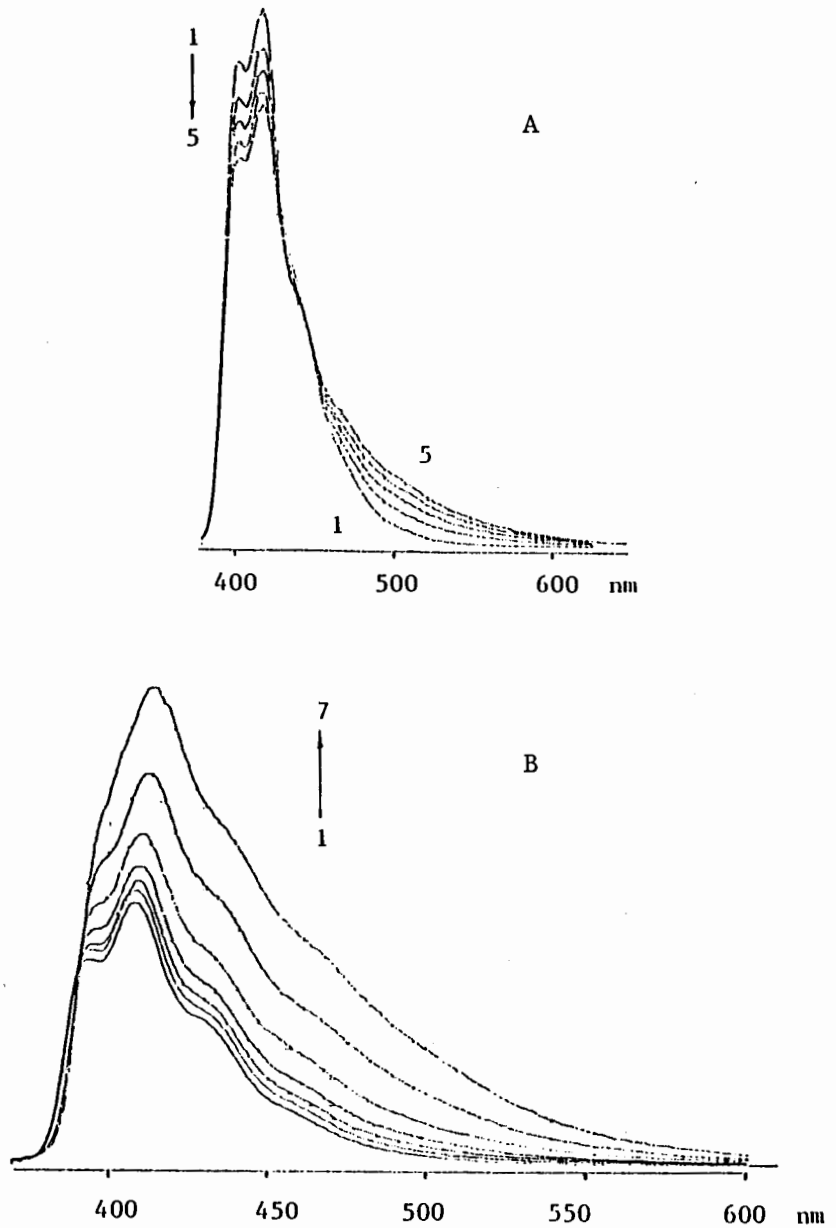

Figure 2-18. The quenching of $DBMBF_2$ fluorescence intensity by pyridine. [$DBMBF_2$] = 5.0 X 10^{-5} M; A, In CH_3CN [pyridine] (10^{-1} M): from curve 1 to 5, 0, 2.45, 4.80, 7.07, 9.25. B, In methylcyclohexane; [pyridine] (10^{-1} M): from curve 1 to 7, 0, 0.25, 0.62, 1.24, 2.45, 4.80, 9.25.

The fluorescence emission of $DBMBF_2$ in MCH had two peaks at 393 and 408 nm (curve 1 in Fig.2-18, lower). The addition of pyridine resulted in a clear increase at 408 nm and the emission maximum shifts to longer wavelength with increasing concentrations of pyridine. Meanwhile, the peak at 393 seemed to diminish as one could find from the figure. Noteworthy was the more significant increase in longer wavelengths of the emission band. For example, the intensity enhancement at 480 nm was about 6 folds (curve 7, Fig.2-18, lower), more then 3 times of that at 408 nm.

2-1-4. Fluorescence Emission in Neat Electron-Rich Olefins in the Presence of $DBMBF_2$

Extensive efforts were made to search for exciplex emission in the $DBMBF_2$-quencher systems. However, with few exceptions, the addition of quenchers (those mentioned in 2-1-3) only resulted in the decrease in fluorescence intensity but no appearance of new emission bands at longer wavelengths regardless whether the solvent used was a polar one (CH_3CN) or a nonpolar one (hexane). One of the exceptions was pyridine which has been described in 2-1-3. Others were two electron-rich olefins, **1** and **2**. In CH_3CN, the quenching pattern showed monotonic decreases, whereas a shoulder at ~550 nm on the fluorescence spectra was observed in the presence of either olefin in hexane solutions. In neat **1** and **2**, new fluorescence emissions centered at ~540 nm (for **1**) and ~570 nm (for **2**) appeared clearly (Fig.2-19). Both neat **1** and

2 had strong Raman peaks also shown in the spectra, the wavelength of which moved synchronously with the excitation wavelength. However, the emission bands at 540 nm (for **1**) and 570 nm (for **2**) did not change their positions as the excitation wavelength changed from 385 nm to 390 nm, and then to 398 nm. The blank samples (neat **1** and **2**) were also checked showing no emission but the Raman peaks. The corresponding excitation spectra recorded for both systems (Fig.2-19) exhibited the shape similar to the absorption spectrum of $DBMBF_2$ in a nonpolar solvent (e.g. hexane) except the tailing to ~440 nm, a much longer wavelength than the cut off of the absorption spectra (~400 nm). Comparing the excitation spectra with the absorption spectra of $DBMBF_2$ in the presence of **1** or **2** taken in CH_3CN (Fig.2-8,A,B), one can immediately find a notable similarity between the two in band shape at their tailing region.

The emission spectra of $DBMBF_2$ (2.0×10^{-5} M) in neat *trans*-anethole (**3**) was also examined showing no new emission at all though the olefin quenched the fluorescence very efficiently ($\log k_q = 9.68$) and formed a GSC readily with $DBMBF_2$ (Fig.2-9).

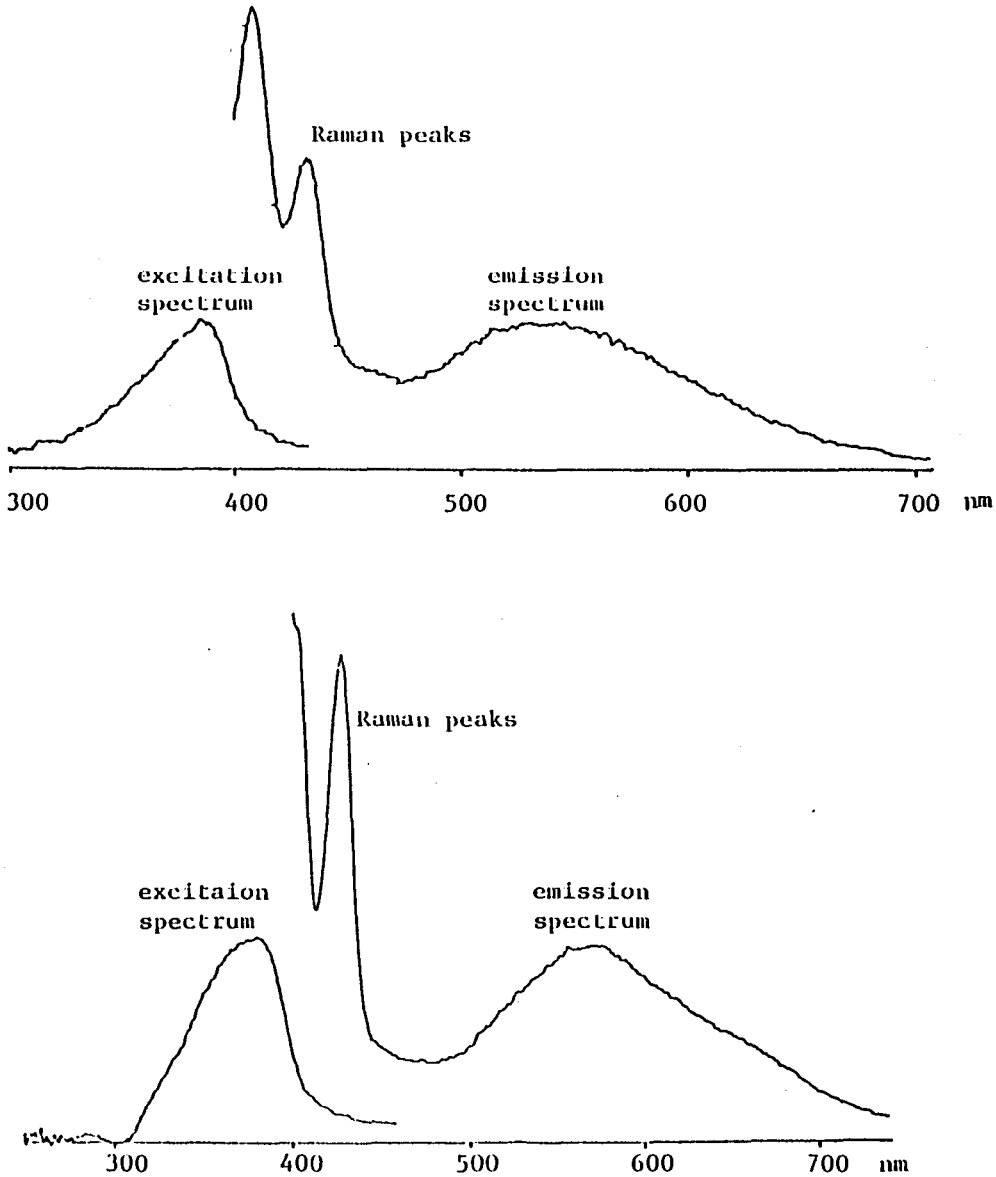

Figure 2-19. The emission and excitation of $DBMBF_2$ (2.0 X 10^{-5} M) in **1** (upper) and **2** (lower). For the upper spectra, λ_{ex} = 385 nm and the excitation spectrum was recorded at 540 nm. For the lower spectra, λ_{ex} = 380 nm, the excitation spectrum was recorded at 570 nm.

2-2. Photocycloaddition of β-Diketonatoboron Difluorides to Olefins

2-2-1. The Profile of Photocycloaddition

Irradiation of undegassed CH_3CN solutions of $DBMBF_2$ in the presence of various olefins gave rise to the adducts of DBM and the olefin in good yields. The general conditions and results of the photolyses of $DBMBF_2$-olefin systems are listed in Table 2-5. In most cases, the reaction was completed in a few hours as judged by the consumption of more than 90% $DBMBF_2$. The adduct(s) always appeared as the main fraction(s) on the GC trace of the photolysate and was(were) easily isolated by column chromatography mostly as pale yellow oil.

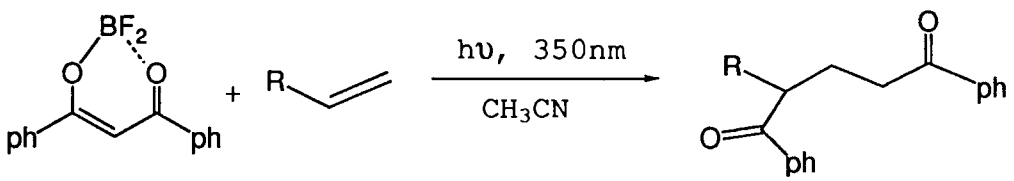

The GC-MS spectra of all products gave parent peaks which agreed with the molecular formula of adducts of DBM with corresponding olefins. The fragments resulted from McLafferty rearrangements, a typical fragmentation reaction for aromatic ketones, were found with fairly strong relative abundance for all adducts. Moreover, the fact that all products contained two carbonyl groups was clearly shown by IR and ^{13}C NMR data. Consistently, the adducts have two resolved strong carbonyl stretch bands* within a range of 24 cm^{-1} centered at υ = 1684

* Those for adduct **28** appear as a broad band at 1689 cm^{-1}.

Table 2-5. The General Profile of Photocycloaddition of $DBMBF_2$ to Olefins in CH_3CN.[a]

$DBMBF_2$ (0.05 M) + olefin (0.5 M) $\xrightarrow[CH_3CN,\ t\,(h)]{h\upsilon,\ 350\ nm}$ cycloadduct(s)

Olefin	t (h)[b]	consumption of $DBMBF_2$ (%)[c]	product[d]	yield(%)[e]
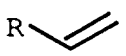			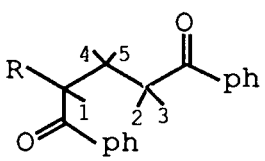	
R =				
$CH_3(CH_2)_3$ (**25**)	2.2	>80	**26**	78
$CH_2{:}CH(CH_2)_2$ (**27**)	3.5	>90	**28**	92
$(CH_3)_3C$ (**7**)	3.5	>90	**29**	69
			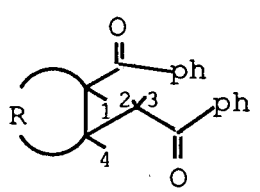	
R =				
$(CH_2)_3$ (**30**)	7.5	85	**31a** (*cis*)	58
			31b (*trans*)	10
$(CH_2)_4$ (**12**)	8.0	95	**32**	69
$(CH_2)_5$ (**8**)	6.0	>95	**33**	65
$(CH_2)_6$ (**34**)	2.2	>95	**35**	68
$(CH_2)_2CH{:}CH(CH_2)_2$ (**37**)	3.0	>95	**38**	50
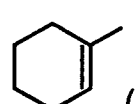 (**69**)	6	~0	no reaction[f]	

to be continued at next page.

Table 2-5. (cont.)

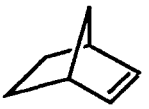			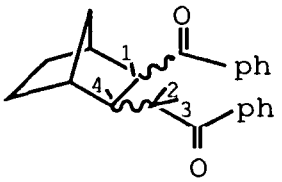	
(15)		3.5	>95	**36a** (*cis,endo*) 45 **36b** (*cis,exo*) 10
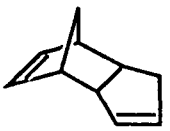	**(39)**	36	~50	**40a**[g] 27 **40b**[g] 38
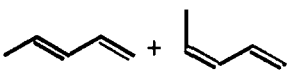			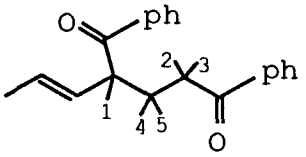	
70% **(14a)**	30% **(14b)**	6	>95	**41a** 32
			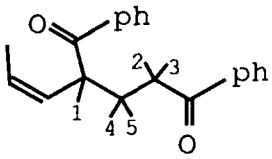	
				41b 11 **41c**[h] <3 **41d**[h] <3
	**(13)**	6	~0	no reaction[f]

a. CH_3CN solutions (30 ml) containing an olefin (0.5 M) and $DBMBF_2$ (0.05 M) were distributed in 6 Pyrex test tubes and irradiated with a 350 nm light source in a Rayonet photoreactor. Compound **31b** was not isolated; **36a** and **36b** could not be separated by either chromatography or recrystallization; **41a** and **41b** were obtained as a mixture; the yields were calculated from the GC peak ratios.

b. The irradiation time.

(to be continued)

Table 2-5. (cont.)

c. Estimated from GC analysis.

d. Unless otherwise specified, structures of the products have been assigned according to spectroscopic data. The numbers in the structure given are assigned for the protons, which are used in the text for descriptions of chemical shifts and coupling constants.

e. Calculated based on the products obtained from column chromatography and the consumption of $DBMBF_2$.

f.The starting materials were recovered.

g. An adduct of DBM and the olefin as suggested by the GC-MS data, whereas the detailed structures are still unknown.

h. An adduct of DBM as suggested by the GC-MS data.

cm^{-1}, a position common for carbonyls of acetophenone type.[104] Accordingly, the ^{13}C NMR spectra gave two singlet carbon signals, one at 199.61 ± 0.34 ppm and another at 203.96 ± 1.86 ppm. The fact that the two carbonyl groups were mutually δ-positioned for all the adducts was demonstrated by the coupling patterns of the protons between them (Table 4-6).

The photocycloaddition reactions of $DBMBF_2$ to olefins proceeded regioselectively or stereospecifically depending on the structure of the starting olefin. This was shown by the observations depicted as follows.

For monosubstituted olefin **25**, **27**, and **7**, all the products have the benzoyl group regiospecifically attached to the more substituted carbon of the double bond. The corresponding regioisomers, if any, must be formed in less than 1% relative yield because the main adducts appeared on the GC trace of the crude photolysates so cleanly that accompanied tiny peaks

were too small even for GC-MS analysis. The same regiospecificity also held for the reaction with 1,3-pentadiene. Moreover, the addition reaction predominantly, if not exclusively, occurred to the terminal double bond of the diene. The main adducts **41a** and **41b** showed allylic methyl signals at 1.65 and 1.69 ppm, respectively, both of which were coupled with adjacent olefinic protons. Since adduct **41b** had larger ^4J (coupling through 4 bonds, 1.8 Hz) for the methyl group than **41a** did (1.0 Hz), we assigned **41a** as the *trans* and **41b** as the *cis* isomer.[103] The relative yield of **41a** (75%) and **41b** (25%) was close to the *cis-trans* ratio (7:3) in the starting diene. Two minor products, **41c** and **41d**, were likely isomers of the main adducts since they had an identical GC-MS (CI mode) base peak at 293 (M^++1) identical to those of the main adducts, though we could not judge which double bond had reacted.

For the cycloadducts (**31a**, **31b**, **32**, **33**, **35**, and **38**) obtained from the photocycloaddition with cyclic olefins, spin-spin coupling constants between H_1 and H_4 of the adducts were compared with calculated values (Table 2-6) showing that they most likely have *cis* configuration. The calculations of vicinal coupling constants were carried out by using MM-2 program[211] (computer operating system: VAX/VMS version V4.5) in which not only the dihedral angles of the vicinal protons but also the polar interactions of the substituents were considered.[212] The envelope (for 5 membered ring), chair (6 membered ring), twisted chair (7 membered ring), and crown (8

membered ring) conformations were adopted in the calculations and the *trans* compounds were assumed equatorial-equatorial disubstituted which were expected thermally more stable than an axial-axial disubstituted one.

In the photocycloaddition of $DBMBF_2$ with norbornene (**15**), the major product **36a** has a *cis-endo* configuration as

Table 2-6. The Experimental and Calculated Vicinal Coupling Constants of H_1 and H_4 in the Cycloadducts.[a]

cycloadduct	n[b]	J(Hz)		
		trans(calc.)	*cis*(calc.)	found
31a	5	12	7	6.8
32	6	12	4	6.8
33	7	11	6	3.8
35	8	12	6	4.2
38	8	12	3	4.0

a. For the proton numbering, see structures in Table 2-5.
b. The ring size of starting olefins.

concluded by the NOE among H_1, H_4, and the *syn* bridge proton: irradiation of H_1 resulted in an enhancement (~20%) for both latter two (Fig.2-20). This was also supported by the zero coupling of H_1 and H_4 with the *anti* bridge proton ($J_{1,8} = J_{4,8} = 0$). Though the minor product **36b** has not been separated in pure form, its GC-MS spectra showed a base peak at m/e = 319

(CI mode, M^++1) and a parent peak at m/e = 318 (EI mode), implying that **36b** was one of the stereoisomers of **36a**. Interestingly, the fragmentations pattern (EI mode) of **36b** was notably different from that of **36a**. As one can find from Table 4-5, both **36a** and **36b** have fragments of m/e = 251 and 213 but with distinct relative abundances: more fragment of 213 (relative abundance 32%) and less fragment of 251 (5%) for **36a** whereas less 213 (6%) and more 251 (54%) for **36b**. The two fragments could be reasonably attributed to two

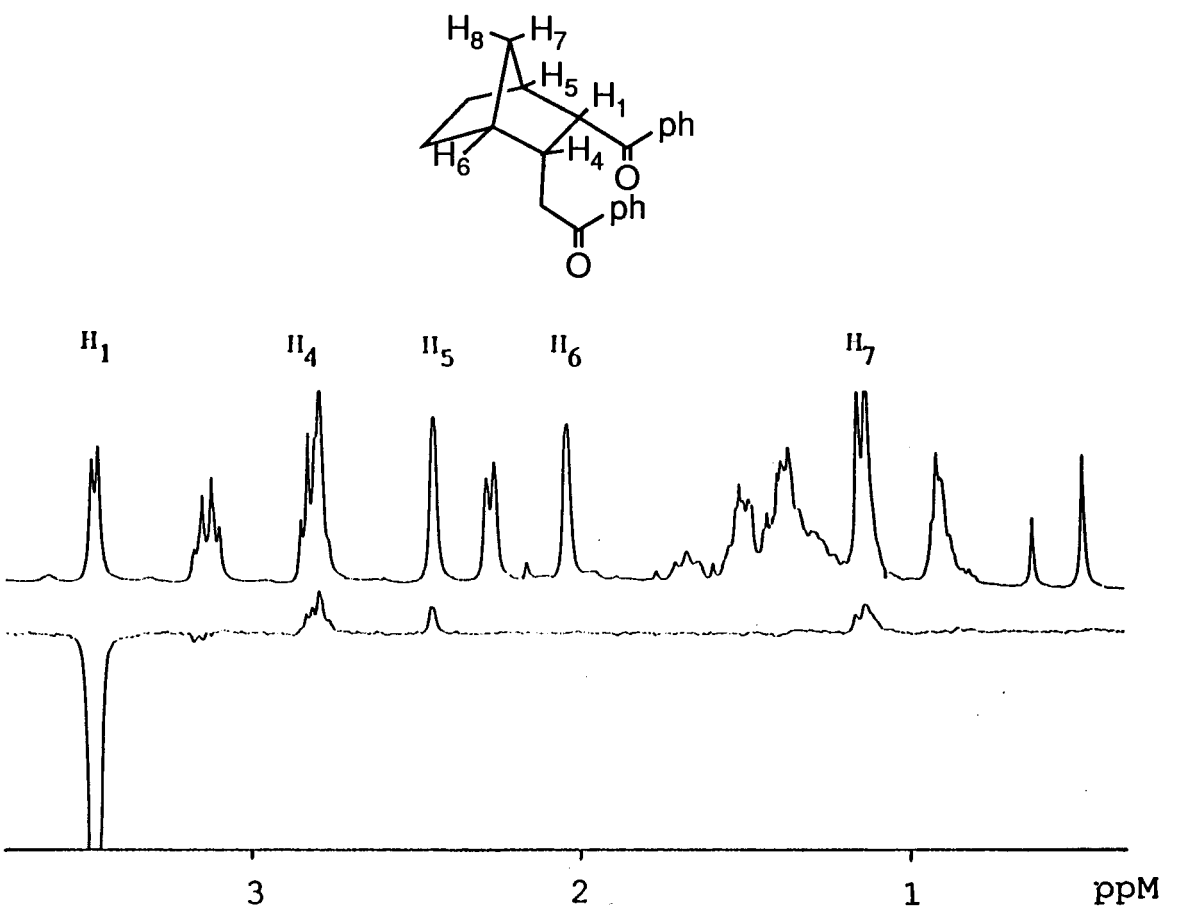

Figure 2-20. The ^1H NOE difference spectra of **36a** in C_6D_6.

Scheme 2-1:

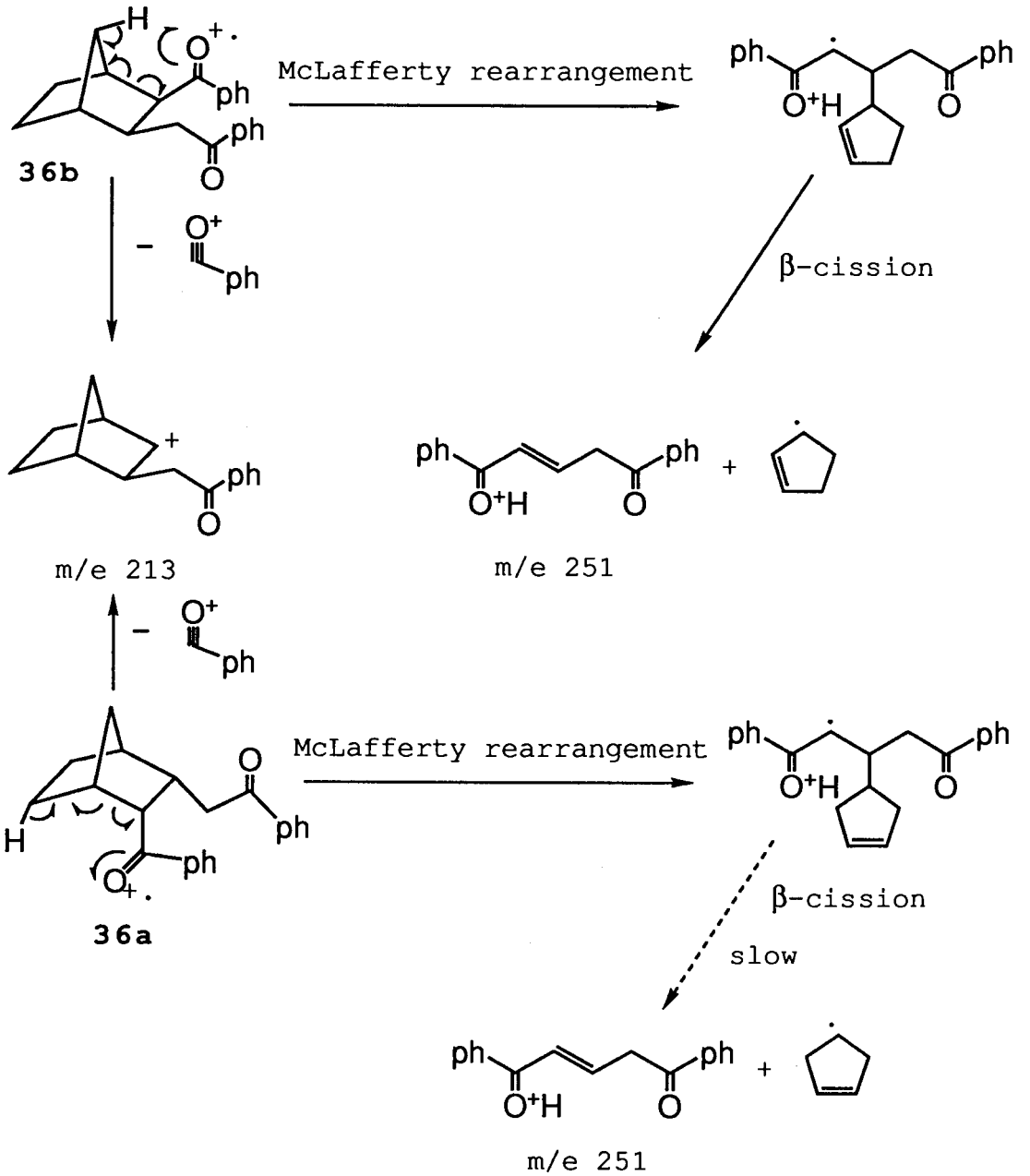

competitive fragmentation pathways starting from the parent cation radicals as shown in Scheme 2-1. Owing to facility of the McLafferty rearrangement[105] in an *exo*-carbonyl group followed by an equally facile β-scission (see Scheme 2-1),

36b probably had an *exo*-benzoyl. However, the *endo* benzoyl compound did not have a facile β-scission reaction so that the α-cleavage predominates, resulting in the fragment m/e = 213. At this junction, we still could not tell whether **36b** was a *cis, exo* isomer or a *trans* isomer with an *exo* benzoyl group, the latter could be formed *via* enolization of **36a**. However, the pure **36a** (20 mg) in an acidic acetone solution (2 ml with 0.05 ml HCl added) did not transfer to **36b** upon 6 h storage or 1 h at 60°, as shown by the GC and NMR spectra, leading to a conclusion that **31b** most likely was a *cis, exo* adduct.

Unexpectedly, $DBMBF_2$ failed to photocycloadd to 1-methyl cyclohexene (**69**) and 1,3-cyclooctadiene (**13**). Careful examinations by ^1H NMR and GC showed there was no hint of either isomerization, rearrangement, or other reactions of the two olefins upon irradiation in the presence of $DBMBF_2$ but only the reactants recovered.

2-2-2. Mechanistic Studies on the Photocycloaddition

The quantum yield of the photocycloaddition of $DBMBF_2$ to 3 cyclic (**8**, **34**, and **12**) and 3 acyclic olefins (**27**, **25**, and **7**) were measured under identical experimental conditions. The quantum yields obtained for these olefins are listed in Table 2-7. Apparently, the quantum yields correlate with the ionization potentials within a group of analogues. The trend was the same for both acyclic and cyclic olefins: the lower the IP was, the faster the reaction went.

The quantum yield of the photocycloaddition reactions of $DBMBF_2$ to 3,3-dimethyl-1-butene (**7**) and cycloheptene (**8**) were determined throughout an olefin concentration range (0.05 - 1.00 M) while the concentration of $DBMBF_2$ (1.0×10^{-2} M)

Table 2-7. Quantum Yields of the Photocycloaddition of $DBMBF_2$ to Selected Olefins.[a]

olefin	IP[b]	Φ
3,3-dimethyl-1-butene (**7**)	9.45	0.18
1-hexene (**25**)	9.34	0.28
1,5-hexadiene (**27**)	9.29	0.38
cyclohexene (**12**)	8.94	0.03
cycloheptene (**8**)	8.87	0.12
cyclooctene (**34**)	8.82	0.40

a. CH_3CN solutions (5 ml each) containing $DBMBF_2$ (0.01 M) and a freshly distilled olefin (1.0 M) were irradiated with a 350 nm light source according to **Method 3** described in 4-1-3.
b. Vertical ionization potential cited from Table 2-4.

maintained constant. The $k_q\tau$ values for the two olefins were calculated from the Stern-Volmer plots (Fig.2-21) and given in Table 2-8. The $k_q\tau$ values obtained from fluorescence intensity quenching are also listed for comparison. A good agreement in the $k_q\tau$ values obtained from the two methods was found for both olefins.

As the concentration of $DBMBF_2$ increased, the quantum yields of cycloadducts of $DBMBF_2$ with cyclic olefins (**12**, **8**, and **34**) increased, whereas, the quantum yield for an acyclic olefin, **7**, the quantum yield decreased instead. This is shown in Fig.2-22.

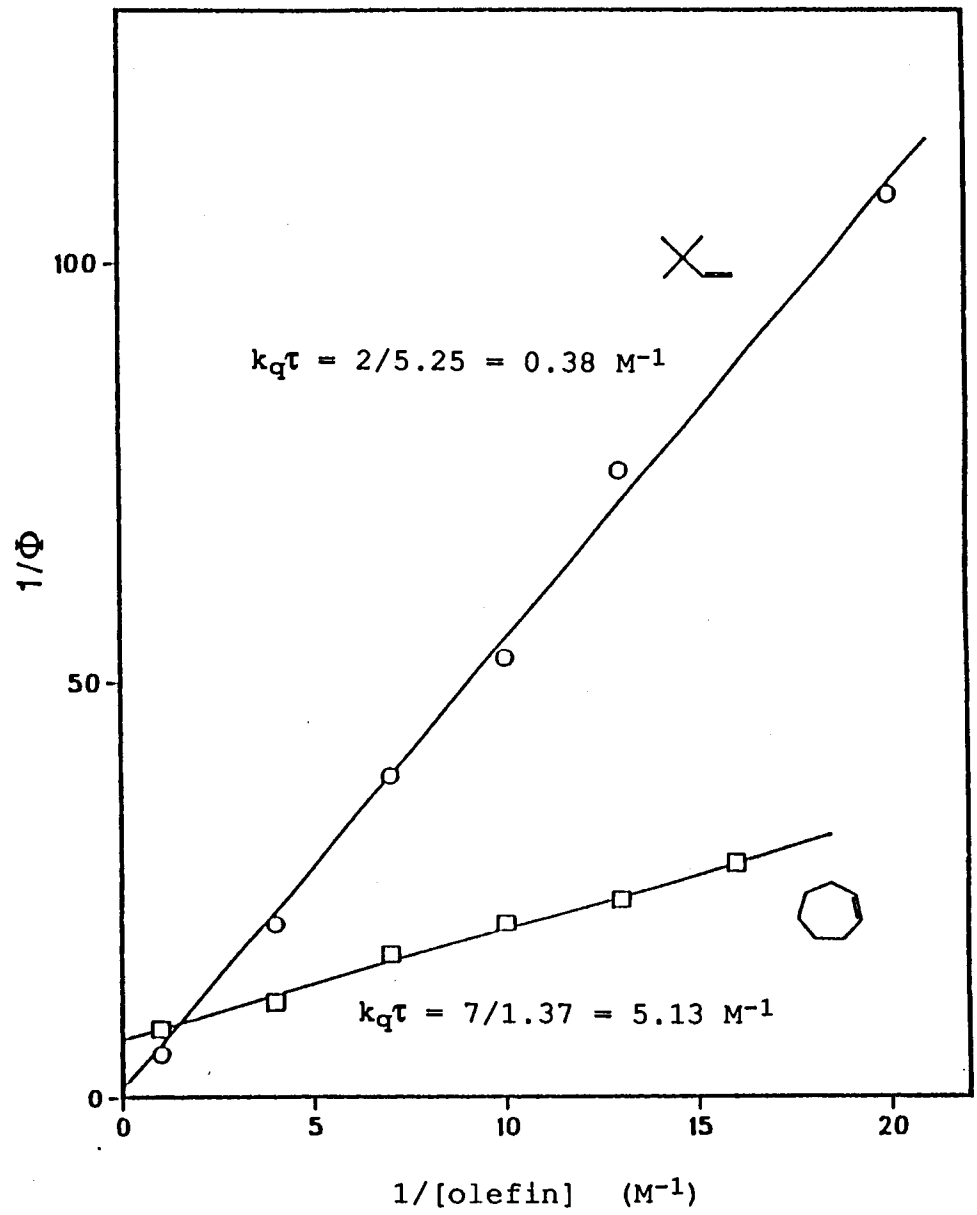

Figure 2-21. The Stern-Volmer plots of $1/\Phi$ vs. 1/[olefin]. $[DBMBF_2]$ = 1.0 X 10^{-2} M in CH_3CN.

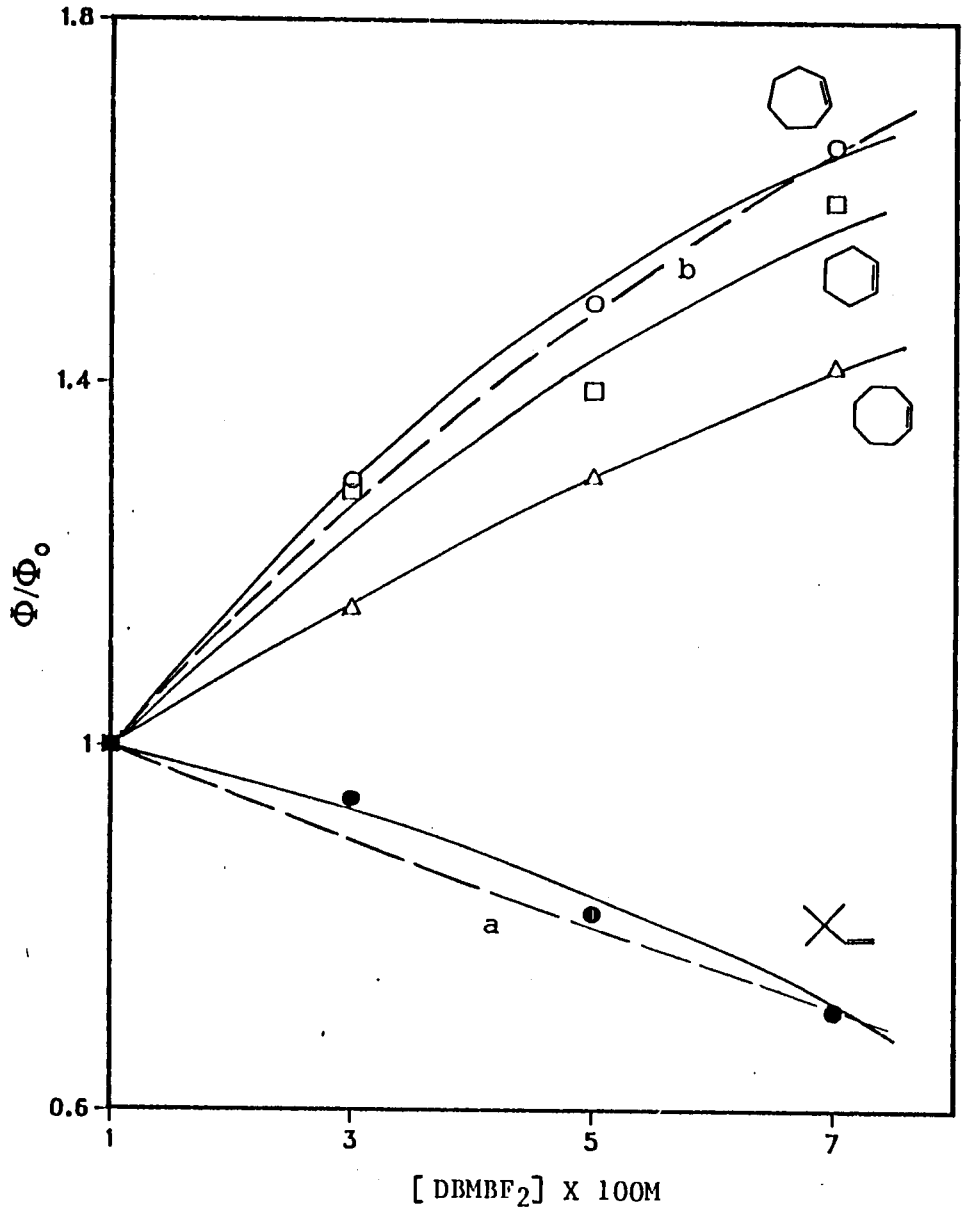

Figure 2-22. The dependence of quantum yields of the cycloadducts on the concentration of $DBMBF_2$ in CH_3CN. The quantum yield obtained at $[DBMBF_2] = 1.0 \times 10^{-2}$ M was denoted as Φ_o. The initial concentration of olefin was 1.0 M. The dashed curves were calculated from Eq.3-3 (see text in section 3-2-2); curve a is for **7** and b for **8**.

Table 2-8. Comparison of $k_q\tau$ values Obtained from Fluorescence Quenching and Cycloadduct Formation.

olefin	$k_q\tau$ (M^{-1})	
	by Φ_{add}[a]	by fluorescence quenching[b]
cycloheptene(**8**)	5.13	4.86
3,3-dimethyl-1-butene(**7**)	0.38	0.57

a. From quantum yield determination of the adducts, calculated from Fig.2-21.

b. Data are cited from Table 2-4.

Table 2-9. Quenching of Photocycloaddition Reactions of $DBMBF_2$ to **7** and **8** in CH_3CN.

olefin	sample[a]	yield of the adduct[b](%)
7	undegassed	46.5
	N_2 saturated	42.0
	O_2 saturated	37.4
	1M QC added	2.0
	1M NBD added	9.7
8	undegassed	76.0
	N_2 saturated	76.1
	O_2 saturated	69.7
	1M QC added	5.4
	1M NBD added	25.4

a. CH_3CN solutions (1 ml each) of $DBMBF_2$ (1.0×10^{-2} M), an olefin (1.0 M), and octadecane (2.0×10^{-3} M).

b. After 13.5 min irradiation (**Method a** described in 4-1-3); calculated based on the initial concentration of $DBMBF_2$.

The photocycloaddition were found quite inert towards oxygen, but strongly quenched by two good electron donors, QC and NBD. As one can find from the data in Table 2-9, QC acts as a better quencher than NBD, in accordance with the fact that QC is a better electron donor than NBD.

2-2-3. Photocycloaddition of $AABF_2$ and $BABF_2$ to Olefins

(a). $AABF_2$

The photolysis of a CH_3CN or THF solution of $AABF_2$ (0.05 M) and cyclohexene (**12**, 1.0 M) resulted in the formation of the adduct **42**, the same product obtained from the de Mayo

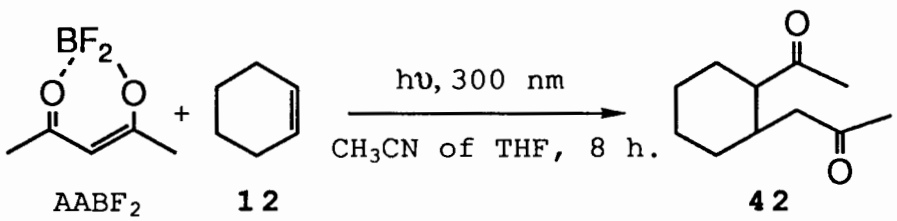

$AABF_2$ **12** **42**

0.05 M 1.0 M chemical yield: 5.1% in THF
(based on $DBMBF_2$) 7.0% in CH_3CN

reaction of acetylacetone with the olefin.[40] Though the reaction was fairly slow in terms of absolute yield, it proceeded 6.5 (in CH_3CN) or 14 (in THF) times faster than the de Mayo reaction carried on in the same solvent, as presented by the data in Table 4-8. The reaction of $AABF_2$ and **12** in a nonpolar solvent such as hexane could not be examined due to the instability of $AABF_2$.

(b). $BABF_2$

$BABF_2$ photoadded to norbornene (**15**) or cyclooctene (**34**) smoothly in a slower rate compared to the $DBMBF_2$ photoaddition. However, it failed to add to 3,3-dimethyl-1-butene (**7**) as no product peak was detected on GC trace but the starting materials recovered after 4 h of irradiation. The general conditions and outcomes of the reactions are given in Table 2-10.

The major one (**43a**) out of 3 products obtained from the reaction with norbornene had a *cis-endo* configuration with the benzoyl group attached to the norbornene frame. Since the structures **43a** and its regioisomer **43d** could not be

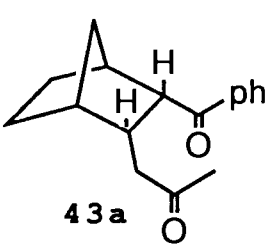

43a

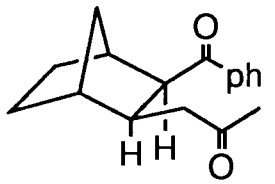

43b

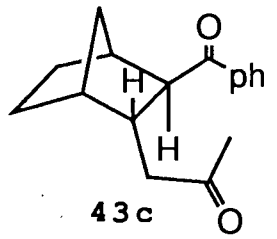

43c

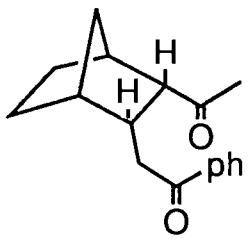

43d

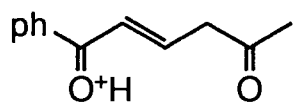

43e m/e 189

distinguished by the coupling pattern and chemical shifts in the ^1H NMR spectra, NOE difference spectra were utilized to solve the problem. The tertiary α proton, H_1, could be located easily in the ^1H NMR spectra based on its chemical shift (3.35 ppm) and the splitting pattern (a broad doublet

Table 2-10. The General Profile of the Photocycloaddition of $BABF_2$ to Olefins in CH_3CN.[a]

olefin	t (h)[b]	consumption of $DBMBF_2$ (%)[c]	product[d]	yield (%)[e]
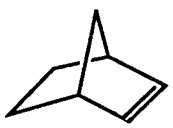 **(15)**	18	>90	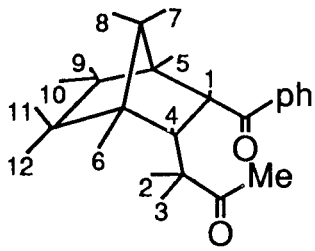 **43a** (*cis,endo*)	68.4
			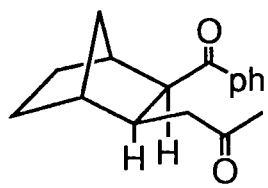 **43b** (*cis,exo*)	7.6
			43c (*trans*)[f]	
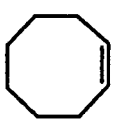 **(34)**	15.5	50	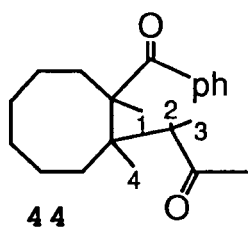 **44**	58.5
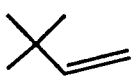 **(7)**	4.0	0	no reaction	

a. CH_3CN solutions (30 ml each) of $BABF_2$ (0.05 M) and an olefin (0.5 M) distributed in 6 Pyrex test tubes were irradiated with a 350 nm light source according to **Method 3** described in 4-1-3. Compounds **43b** and **43c** were not isolated, the yield were calculated from the GC peak ratio and the total amounts of the mixture obtained from chromatography.

b. The irradiation time.

(to be continued at next page)

Table 2-10. (cont.)

c. Shown by the GC analysis.

d. Unless otherwise specified, structures of the products have been assigned according to spectroscopic data. The numbers in the structure given are assigned for the protons, which are used in the text for descriptions of chemical shifts and coupling constants.

e. Calculated based on the products obtained from column chromatography and the consumption of $DBMBF_2$.

f. 2-exo-3-endo (*trans*) configuration.

H_8 and H_4.* The strong NOE effects observed on H_7 and H_4 when H_1 was irradiated confirms the *cis, endo* configuration. However, worthwhile to mention was no NOE effect was seen between H_4 and H_7. This observation suggests that the C_2-C_3 bond in the norbornene frame is somewhat twisted making H_4 pointing away from the vicinity of H_7 due probably to steric repulsion of two substituent groups. The minor product **43b** had a greater relative abundance (41%) of the McLafferty fragment (**43e**, m/e = 189) than the *cis, endo* adduct **43a** does (28%). Adduct **43a** was able to be converted readily to **43c** in acidic CH_3CN but not **43b**, supporting the structural assignment for **43b** and **43c** (Table 2-10).

The sole product (**44**) obtained from cyclooctene also has the benzoyl group attached to the ring frame. This is supported by the appearance of the fragment (m/e 215, M^+-CH_3COCH_2). Adduct **44** might also have a *cis* configuration for the same reason mentioned for compound **35**.

---

* For the proton numbering, see the structure in Table 2-10.

2-3. Photocycloaddition of $DBMBF_2$ to Enones

2-3-1. Acyclic Enones

The photolyses of undegassed CH_3CN solutions of $DBMBF_2$ (5.0×10^{-2} M) and an enone (5.0×10^{-1} M) under a 350 nm light source resulted in the consumption of the difluoride accompanied by the formation of two types of cycloadduct (Table 2-11). However, the reaction with an α,β-unsaturated ester **45**, only gave the "type b" product.

The structural assignment of "type a" for **47a** was straightforward because of two equivalent phenacyl groups attached to the same carbon. It showed only 4 types of phenyl ^{13}C signals and two pairs of chemically as well as magnetically equivalent methylene protons (H_2 and H_3, R_2 and R_3). The chemical shift of H_1 was at 5.57 ppm for **47a** and at 4.42 ppm for **47b**. For product **48a**, the chemical shift of H_1 was 5.74 ppm, about 1 ppm lower field than **48b** at 4.66 ppm. These data support the structural assignments. For adduct **49b** the chemical shift of H_1 was found to be 5.74 ppm (**49a** was not separated). However, its H_2 and H_3 appeared as a AB quartet (J = 17.8 Hz), indicating that **49b** had to have "type b" structure. Nevertheless, GC-MS data showed that for all "type a" products, a fragment of m/e = 224 was recorded, whereas for all "type b" products including product **48c*** no

---

* A fragment of m/e = 193 was obtained for **50b** instead.

Table 2-11. The General Profile of Photocycloaddition of $DBMBF_2$ to Acyclic Enones **18**, **17**, **46** and an α,β-Unsaturated Ester **45** in CH_3CN.[a]

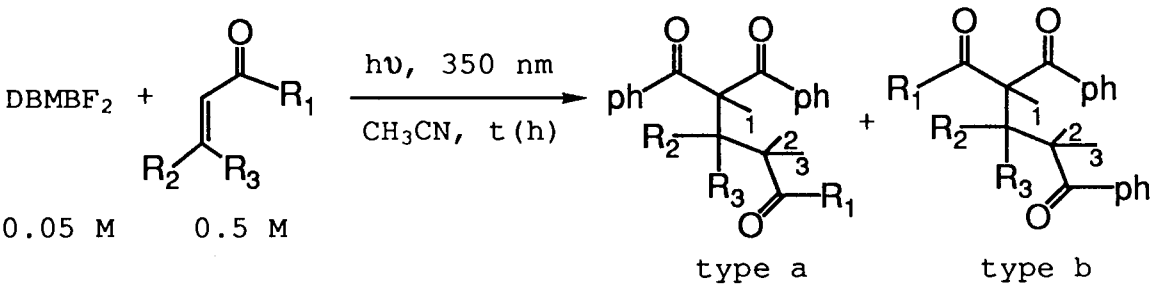

compd	R_1	R_2	R_3	t(h)[b]	consumption of $DBMBF_2$ (%)[c]	product[d]	yield(%)[e]
18	CH_3	H	H	7	95	**47a**	37.6
						47b	42.6
17	CH_3	CH_3	H	5	100	**48a**	36.3
						48b	34.3
						48c[f]	7.8
46	CH_3	CH_3	CH_3	5	100	**49a**[g]	27.8
						49b	50.6
45	C_2H_5O	H	H	14	100	**50a**	0.0
						50b	64.0

a. CH_3CN solutions (30 ml) containing an enone (0.5 M) and $DBMBF_2$ (0.05 M) were distributed in 6 Pyrex test tubes and irradiated with a 350 nm light source in a Rayonet photoreactor.

b. The irradiation time.

c. Estimated from GC analysis.

d. Unless otherwise specified, structures of the products have been assigned according to spectroscopic data. The

(to be continued at next page)

Table 2-11. (cont.)

numbers in the structure given are assigned for the protons, which are used in the text for descriptions of chemical shifts and coupling constants.

e. Calculated based on the products obtained from column chromatography and the consumption of $DBMBF_2$.

f. A diasteriomer of **48b** but not isolated, see the text.

g. The structure is assigned based on the GC-MS data, see the text. Compound **49a** was not isolated.

Scheme 2-2:

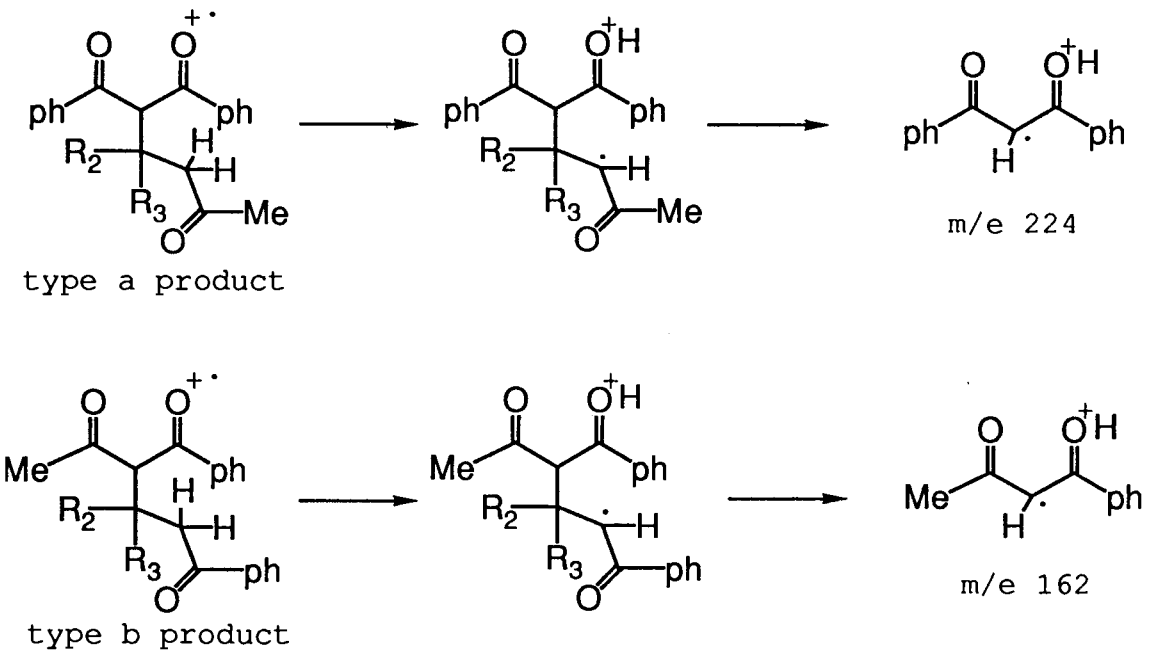

such fragment but the fragment of m/e = 162 (or 161) was recorded (Table 4-14). These two fragments obviously originated from the McLafferty rearrangements shown in Scheme

2-2. Based on this argument, the structures of **49a** and **49b** were assigned; **48c** was suggested as the diasteriomer of **48b** because they had an identical MS fragmentation pattern. The photocycloadduct to ethyl acrylate (**50b**), showing the H_1 signal at 4.69 ppm as a dd (J = 7.1, 7.1 Hz) coupled with two

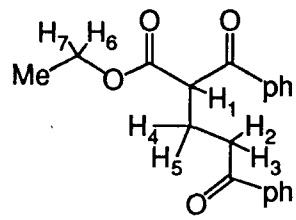

50b

nonequivalent methylene protons (H_4 and H_5), must have "type b" but not "type a" structure. The fact that the two methylene protons (H_6 and H_7) in the ester group appeared as two distinct doublets of quartet (Table 4-15) was also in agreement with the "type b" assignment.

2-3-2. Cyclic Enones

The photolyses of CH_3CN solutions containing $DBMBF_2$ (0.05 M) and 2-cyclohexenone (**16**, 0.5 M) or 2-cyclopentenone (**19**, 0.5 M) resulted in the formation of some adducts as suggested by the GC-MS data. However, the attempt to separate the products were not successful. In the case of **16**, all $DBMBF_2$ was consumed after 18 h of irradiation. The photolysate contained two groups of products as shown in its GC spectra. The first group (GC yield 31.3%) consisted of two peaks (at

RT = 2.20 and 2.26 min, respectively; OV-1, 25 M, 250°) that were the two dimers of the enone, **51** and **52** respectively, as

Table 2-12. The Relative Yields of **51**, **52**, and **53**, **54**.[a]

condition	relative yield(%)			
	53	**54**	**51**	**52**
$DBMBF_2$ sensitized[b]	54.2	45.8	33.7	66.3
direct irradiation[c]	59.2	40.8	37.1	62.9
direct irradiation[d]	56	44	33.3	66.6

a. Calculated from the ratio of the GC peaks. b. [$DBMBF_2$] = 5.0 X 10^{-2} M, [enone] = 5.0 X 10^{-1} M; irradiated with 350 nm light source for 1 h. c. Five ml of deaerated CH_3CN solution of the enone (5.0 X 10^{-1} M) was irradiated with a 200 W Hanovia lamp through a Pyrex filter for 55 min.
d. Data were cited from ref. 106, 107.

confirmed by coinjections with the authentic samples and the parent peak (m/e = 193) in their GC-MS (CI mode) spectra. The relative yields of **51** (33.7) and **52** (66.3) were similar to those obtained from the direct photolysis of the enone (Table 2-12). The second group included 5 peaks appeared closely at RT = 7.16-8.37 min with an identical MS (CI mode) parent peak at m/e = 321. The photolysis of 2-cyclopentenenone (**19**), proceeded slowly to consume only ~40% of $DBMBF_2$ after 20 h of irradiation. The GC pattern of the photolysate was similar to above, showing two groups of product peaks. The first group

(two peaks at RT = 1.79 and 1.82 min, respectively) was confirmed to belong to the dimers of **19** (**53** and **54**) by the coinjections with the authentic samples and the parent MS (CI mode) peak at m/e = 165. Also, the dimer **53** and **54** appeared in a ratio of 54.2/45.8, close to that resulted from the direct photolysis of the enone (Table 2-12). The second group consisted of two components at much longer RT (5.61 and 5.85 min, respectively). Since both components gave an identical parent MS (CI mode) peaks at m/e = 307, we assumed that they were adducts of DBM with **19**. In summary, the reaction pattern of $DBMBF_2$ with the cyclic enones can be described by Scheme 2-3.

Scheme 2-3:

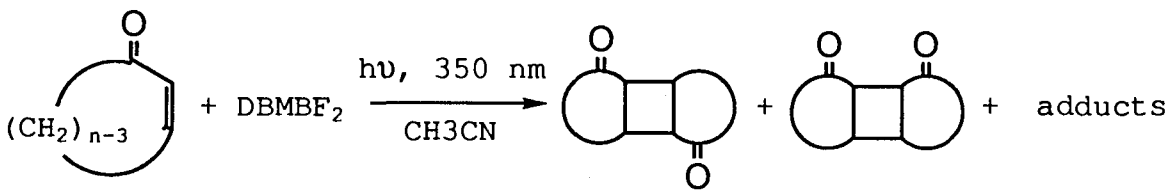

n = 6 (**16**) **51** **52**

5 (**19**) **53** **54**

2-4. Cation Radical Reactions Sensitized by β-Diketonatoboron Difluorides

2-4-1. Valence Isomerization of QC and NBD

The valence isomerization reactions of QC and NBD were examined in CH_3CN and CD_2Cl_2 solutions with acetylacetone, $AABF_2$, or $DBMBF_2$ being the sensitizers. The photolyses were carried out with a 300 nm light source for acetylacetone and $AABF_2$ and a 350 nm light source for $DBMBF_2$ sensitizations, i.e. under these conditions the sensitizers absorbed all incident light. The isomerizations, however, proceeded in strikingly different patterns depending on the nature of sensitizer.

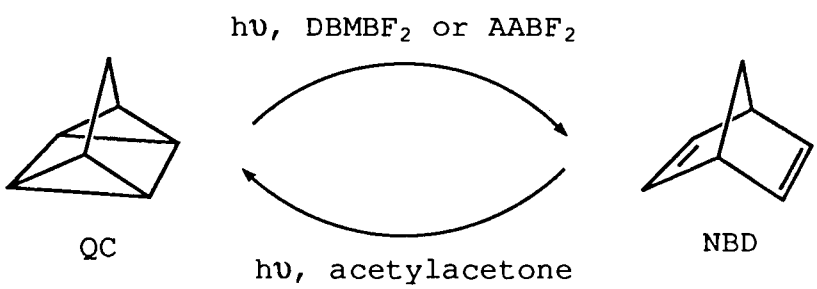

When acetylacetone was used as the sensitizer, NBD converted almost quantitatively to QC but QC remained unchanged upon irradiation. In both cases, acetylacetone was not consumed during the course of irradiation as shown in Fig.2-23. On the other hand, $AABF_2$ and $DBMBF_2$ acted as sensitizers to promoted only the isomerization from QC to NBD

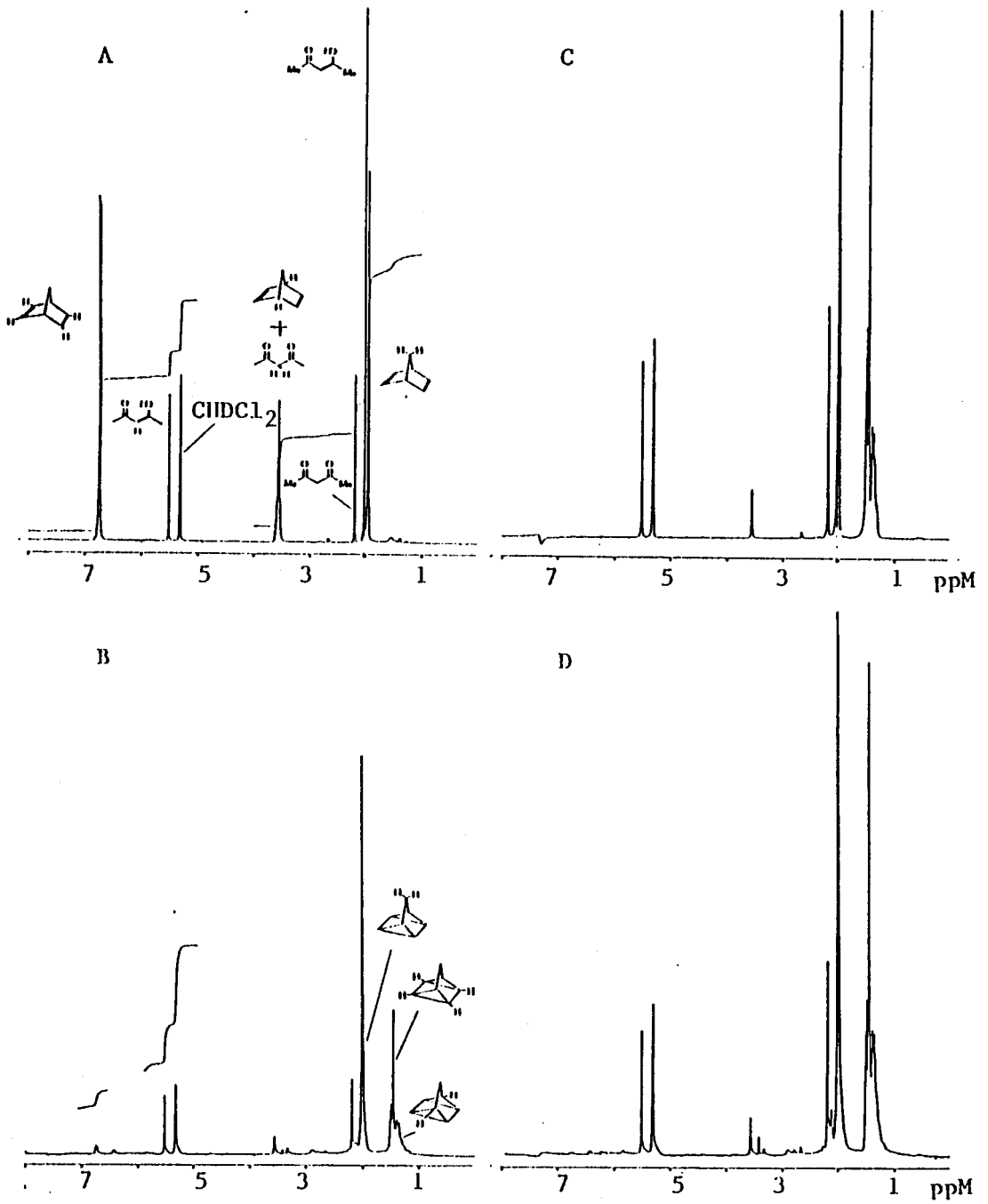

Figure 2-23. Acetylacetone-sensitized isomerization of QC and NBD in CD_2Cl_2. A. [NBD] = 6 X 10^{-2} M. [acetylacetone] = 5 X 10^{-2} M, before irradiation; B. The same solution as in A, after 12 h of irradiation; C. [QC] = 6 X 10^{-2} M, [acetylacetone] = 5 X 10^{-2} M, before irradiation; D. The same solution as in C, after 12 h of irradiation.

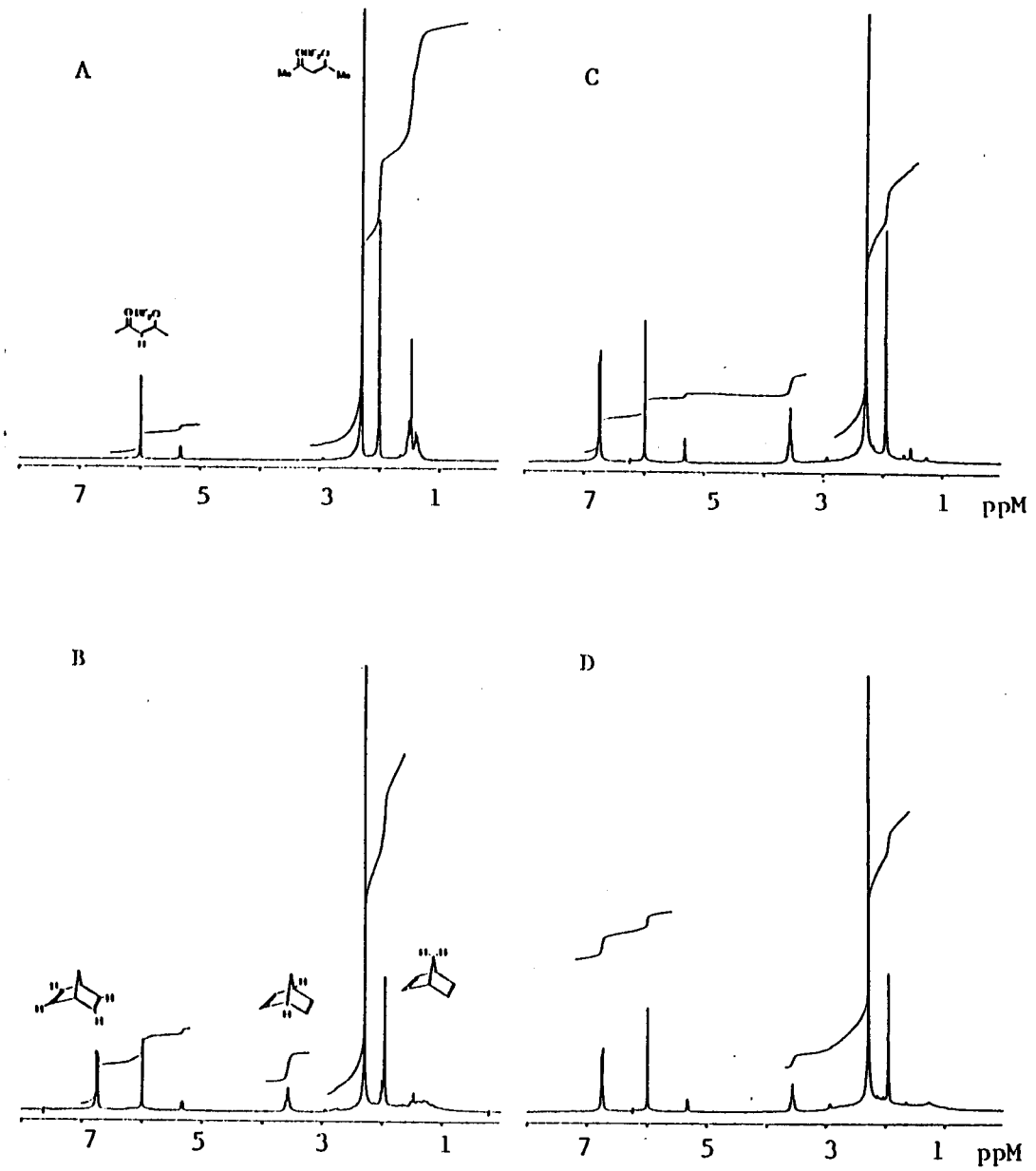

Figure 2-24. $AABF_2$-sensitized isomerization of QC and NBD in CD_2Cl_2. A. [QC] = 6 X 10^{-2} M, [$AABF_2$] = 4 X 10^{-2} M, before irradiation. B. The same solution as in A, after 12 h of irradiation. C. [NBD] = 2.5 X 10^{-2} M, [$AABF_2$] = 4 X 10^{-2} M, before irradiation. D. The same solution as in C, after 12 h of irradiation.

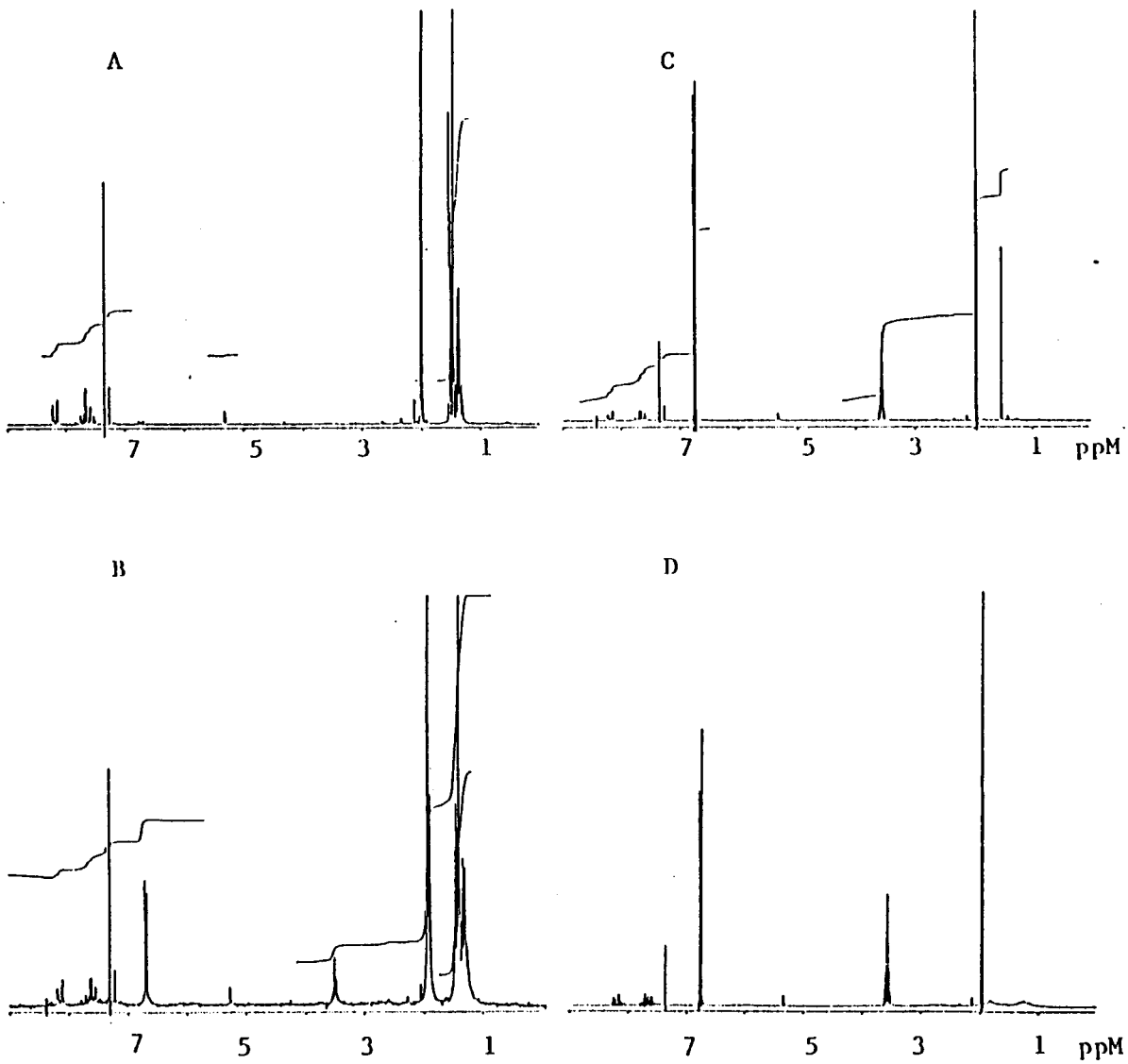

Figure 2-25. $DBMBF_2$-sensitized isomerization of QC and NBD in CD_2Cl_2. A. [QC] = 0.15 M, [$DBMBF_2$] = 5 X 10^{-3} M, before irradiation; B. The same solution as in A, after 2 h of irradiation; C. [NBD] = 0.15 M, [$DBMBF_2$] = 5 X 10^{-3} M, before irradiation; D. The same solution as in C, after 2 h of irradiation.

Table 2-13 Thermodynamic Parameters and Quantum Efficiencies (Φ) of the PET Mediated Valence Isomerization of QC and NBD.

sensitizer	solvent	$E_S(E_T)$ Kcal/mol	starting isomer	$E_S(E_T)$[a] Kcal/mol	ΔG^{Ob} Kcal/mol	Φ	ref.
$AABF_2$	CD_2Cl_2		QC			0.06	this work
	CD_3CN	<86[c]	QC	>95(~80)	-24.0	0.02	this work
	CD_2Cl_2		NBD			0.000	this work
	CD3CN	<86[c]	NBD	>95(~70)	-9.5	0.000	this work
$DBMBF_2$	CD_2Cl_2		QC			0.07	this work
	CD3CN	73(62)	QC	>95(~80)	-22.2	0.02	this work
	CD_2Cl_2		NBD			0.000	this work
	CD3CN	73(62)	NBD	>95(~70)	-7.6	0.000	this work
1-CN-Np	CD3CN	86.5	QC	>95(~80)	-22.8	~0.1	23
	CD3CN		NBD	>95(~70)	-8.3	~0.01	108
TCB	CD3CN	(62.3)[d]	QC	>95(~80)	-41.7	~0.6	108
	CD3CN	(62.3)[d]	NBD	>95(~70)	-27.2	0.000	109

a. The singlet excitation energies E_S > 95 are estimated from the fact that both QC and NBD have no absorption at l > 300 nm. The triplet excitation energies E_T are cited from ref. 24.

b. The change in free enthalpy for a complete PET process calculated according to Eq.2-1.

c. Estimated from the absorption spectra.

d. Cited from ref. 24.

but not in the reverse direction (NBD to QC). Again, the sensitizers remained unchanged during the irradiation. The quantum yields of the isomerization are estimated from NMR

spectra such as Fig.2-23 to 2-25 and listed in Table 2-13. Though the solvent effects on the isomerization have not been systematically studied, the $AABF_2$ or $DBMBF_2$ sensitizations appear to be more efficient in CD_2Cl_2 than in a more polar solvent, CD_3CN.

2-4-2. "Diels-Alder" Dimerization of 1,3-Cyclohexadiene (2) and 2,4-Dimethyl-1,3-Pentadiene (1)

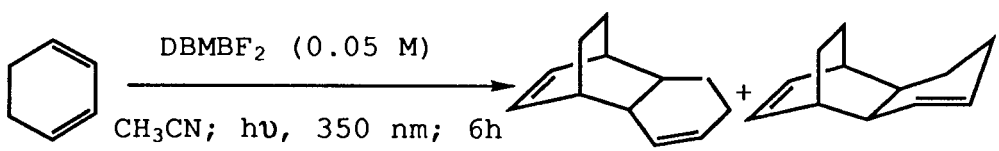

2 1.2 g, 0.5 M

55 (*endo*) yield 48%

56 (*exo*) 5%

The photolysis of a CH_3CN solution containing $DBMBF_2$ and **2** with a 350 nm light source afforded the 2+4 dimers **55** and **56** in a ratio of 9/1. A total yield of 53% was obtained after 6 h of irradiation at which the sensitizer was essentially not consumed. The 2+2 dimers **57** and **58** were not found at all in the reaction.

The dimerization of **2** is a known reaction which can be achieved by either thermolysis,[110,111] aminium salt catalysis,[112] or sensitized photolysis[9,113,114] but not by acid catalysis.[10] We decided, therefore, to compare the relative yields of the 4 possible dimers with respect to the nature of

Table 2-14. The Relative Yields of Dimers of **2**.[a]

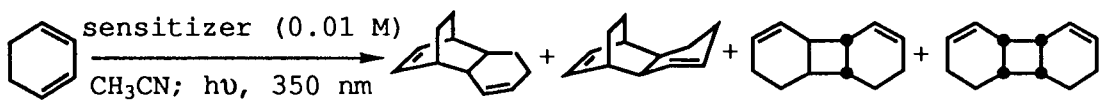

2 1.0 M **55** **56** **57** **58**

sensitizer	time(min)	relative yield				reference
		55	**56**	**57**	**58**	
$DBMBF_2$	25	93.5	6.5	0.0	0.0	this work
$BABF_2$	25	89.2	10.8	0.0	0.0	this work
9-CN-Ph	8	81.8	12.1	4.4	1.7	this work
	25	76.5	10.2	9.6	3.7	this work
1-CN-Np	8	74.4	15.0	7.9	2.8	this work
	25	71.6	11.5	12.1	4.9	this work
DCN-Np[b]		79	21	tr.	0.0	113
DCN-Np[b]		69	11		20[c]	114
DCN-An[d]		77	23	0.0	0.0	9
TCB	25	92.6	7.1	0.0	0.3	this work
DDB	10	83.5	13.2	1.7	1.6	this work
	25	71.4	10.1	13.3	5.1	this work
BAHA[e]	15	83	17	0.0	0.0	112
Δ, 200°	30	80	20	0.0	0.0	this work
Δ, 200°	120	80	20	0.0	0.0	110
1-MeO-Np	25	7.8	19.5	56.3	16.5	this work
benzophenone[f]	80	0.4	22.3	55.9	21.4	this work
benzophenone[f]		tr.	16	62	22	113
hυ (>330 nm)		0.0	40	44	23	115

Table 2-14 (cont.)

a. In CH_3CN unless otherwise specified.

b. 1,4-dicyanonaphthanlene.

c. The sum of **57** and **58**.

d. 9,10-dicyanoanthracene in CH_2Cl_2.

e. *Tris*-(4-bromophenyl)aminium hexachloroantimonate catalyzed reaction at -78°C.

f. In neat **2**.

sensitizer. The photolyses were conducted under parallel conditions and the results are listed in Table 2-14 along with those of thermolysis and previously published. The observations are listed below.

1. Both $DBMBF_2$ and $BABF_2$ lead to the exclusive formation of 2+4 dimers with the predominant yield of the *endo* dimer **55**, similar to those obtained from thermolysis, DCN-An sensitization, and BAHA catalysis.

2. The 2+4 dimers were obtained predominantly regardless of the multiplicity of sensitizers as long as they were good electron acceptors. This could be seen from the product distributions in TCB and DDB sensitizations.

3. For cyanoaromatics (except DCN-An) the 2+2 dimers are obtained as the minor products but in appreciable amount.

4. The 2+2 dimers became the major products in 1-MeO-Np and benzophenone sensitizations.

Table 2-15. The Dimerization of **1** Sensitized by Various Sensitizers in CH_3CN.[a]

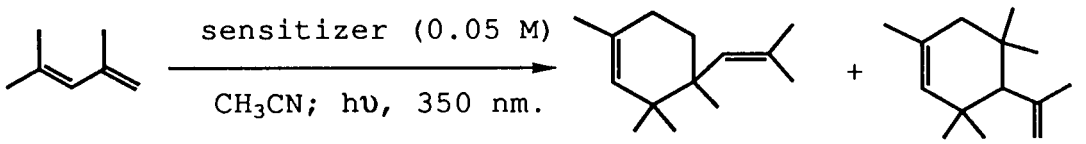

1 (0.2 M) **65** **66**

sensitizer	$E^{red.}_{1/2}$ (V)[b]	relative yield (%)		relative efficiency[c]
		65	**66**	
$DBMBF_2$	-1.30	99.2	0.8	1.00
$BABF_2$	-1.71	70.4	29.6	0.31
$AABF_2$[d]	-1.78	67.1	32.9	/
$TMHBF_2$[d]	/	98.0	2.0	/
9-CN-An	-1.70[e]	97.9	2.1	0.36
1-CN-Np	-2.00[e]	97.9	2.1	0.68
TCB	+0.02[e]	98.9	1.1	5.64
DDB	-0.51[f]	97.8	2.2	2.83
BAHA[g]	/	100.0	0.0	/

a. Irradiated with a 350 nm light source for 2 h unless otherwise specified.
b. Reported *vs* SCE.
c. The yield of **65** in the $DBMBF_2$ sensitization is taken as the unit.
d. Photolyzed according to **Method 2** in 4-1-3 with a 200 W Hanovia lamp through a Pyrex filter.
e. Sited from reference 23.
f. Cited from reference 116.
g. In the presence of pyridine, cited from ref. 10.

The photolysis of a CH_3CN solution of **1** (0.35 M) and $DBMBF_2$ (0.05 M) gave rise to two 2+4 dimers (**65** and **66**, total yield 63%) in a ratio of 82.5/17.5 after 12 h irradiation. About 95% of the sensitizer was recovered during the work up.

It was found that the "Diels-Alder" type photodimerization of **1** could be sensitized by a line of electron-deficient sensitizers as shown is Table 2-15. A character common to these sensitized dimerization reactions was that dimer **65** was obtained overwhelmingly except in the cases of $BABF_2$ and $AABF_2$ sensitizations. The relative efficiencies of the sensitizer with respect to $DBMBF_2$, where the experimental conditions were the same, are also given in Table 2-15, showing a correlation with the reduction potentials. TCB and DDB, having higher reduction potentials than $DBMBF_2$, appeared to be more efficient than $DBMBF_2$; whereas the two cyanoaromatics, bearing lower reduction potentials, were less efficient.

2-4-3. Dimerization of *Trans*-Anethole (3)

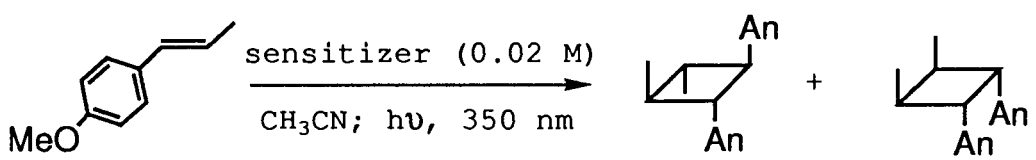

3 (0.5 M) **21** **22**

Irradiation of undegassed CH_3CN solutions of **3** (0.5 M) and a sensitizer (0.02 M) resulted in the formation of a mixture of the *anti* head-to-head dimer **21** and the *syn* head-to-head dimer **22**. While the appearance of the dimers was followed from time to time up to 4 h, the isomerization of **3** to *cis*-anethole was not examined.* The plots of composition *vs.* irradiation time shown in Fig.2-26 - 2-29 reveal several interesting features of the reaction.

For all the sensitized reactions, the formation of dimer **22** is slightly slower than that of **21** at the beginning (the first 30 min), then gradually levels off to a steady concentration (~0.005 M, corresponding to 1% yield with respect to the initial concentration of **3**). Meanwhile, the formation of **21** keeps increasing almost lineally along the time axis (Fig.2-26, 27, 28) except in the TCB sensitization where the curve has reached a plateau after about 1 h of irradiation (Fig.2-29). Before the irradiation, the solution containing **3** and $DBMBF_2$ was yellow in color; the solutions containing **3** and either $AABF_2$ or 9-CN-An were colorless. They all turned to brownish after 4 h of irradiation. The solution containing TCB was initially dark purple in color due to the formation of a charge transfer complex of TCB with **3** (see Appendix 2). The dark purple color faded upon the irradiation becoming light brownish.

---

*The *cis-trans* isomerization of **3** under PET conditions is known (ref. 8,117).

Photolysis of a CH_3CN solution (1 ml) of a dimer of **3** (**21** or **22**) in the presence of $DBMBF_2$ (0.02 M) resulted in the formation of **3** as the sole detectable product by GC analysis. As shown in the plots of composition *vs.* irradiation time (Fig.2-30 and 2-31), the rate of the disappearance of **22** was

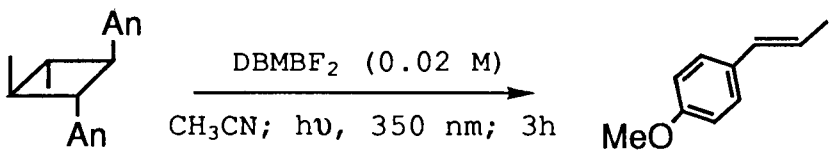

21 0.010 M **3** 18%

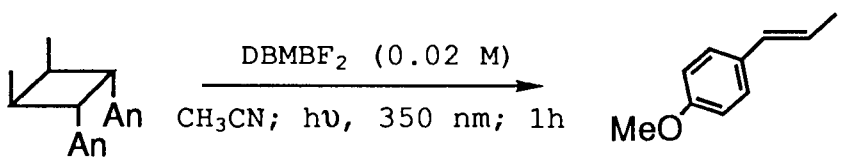

22 0.019 M **3** 71%

4 times faster than that of **21**. The yield of **3** from **21** was quite poor (18%) and that from **22** was moderate (71%). In the photocycloreversion of **22**, the concentration of **3** reaches the maximum when the dimer has been consumed more than 95%, then started to decrease accompanying by the formation of **21** (Fig.2-31). Apparently, the newly formed **21** was due to the sensitized dimerization of **3**. However, comparing the loss of **3** at 90 min (4.8×10^{-3} M) with the sum of the concentrations of **21** (0.88 X 10-3 M) and remained **22** (0.12×10^{-3} M), one can estimate the absolute yield of $DBMBF_2$ sensitized

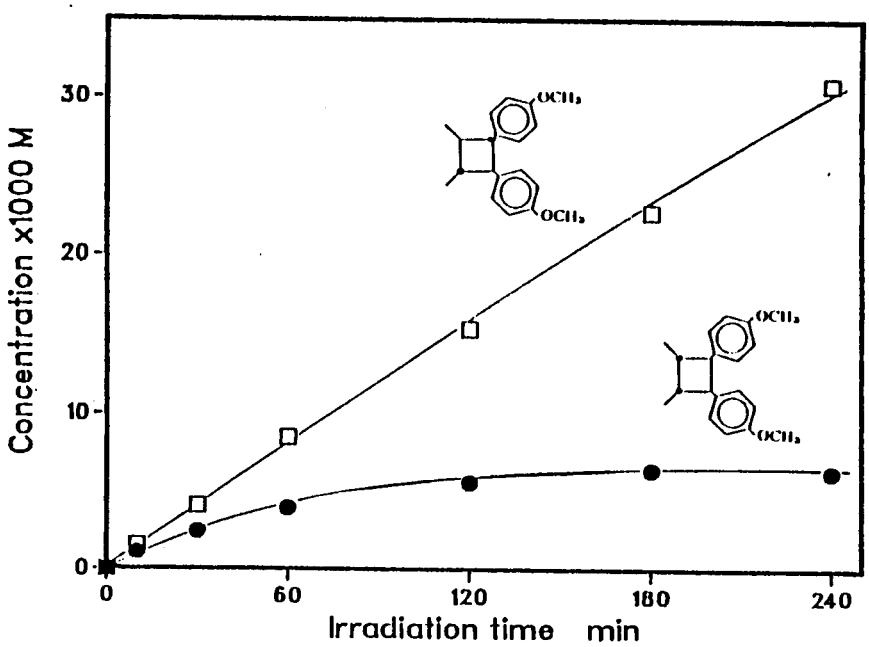

Figure 2-26. $DBMBF_2$ sensitized dimerizations of **3** in CH_3CN. The initial conc.: [**3**] = 5.0 X 10^{-1} M, [$DBMBF_2$] = 2.0 X 10^{-2} M.

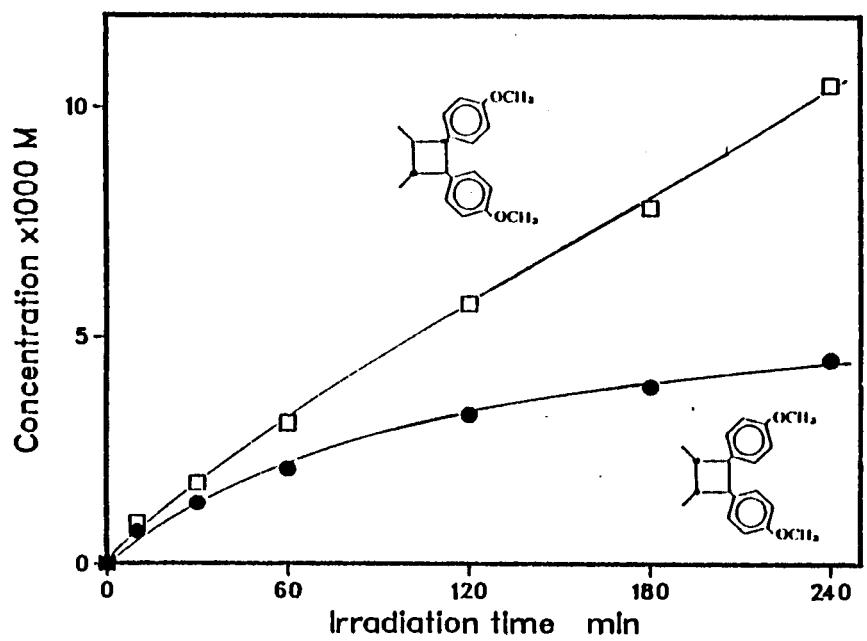

Figure 2-27. $BABF_2$ sensitized dimerizations of **3** in CH_3CN. The initial conc.: [**3**] = 5.0 X 10^{-1} M, [$BABF_2$] = 2.0 X 10^{-2} M.

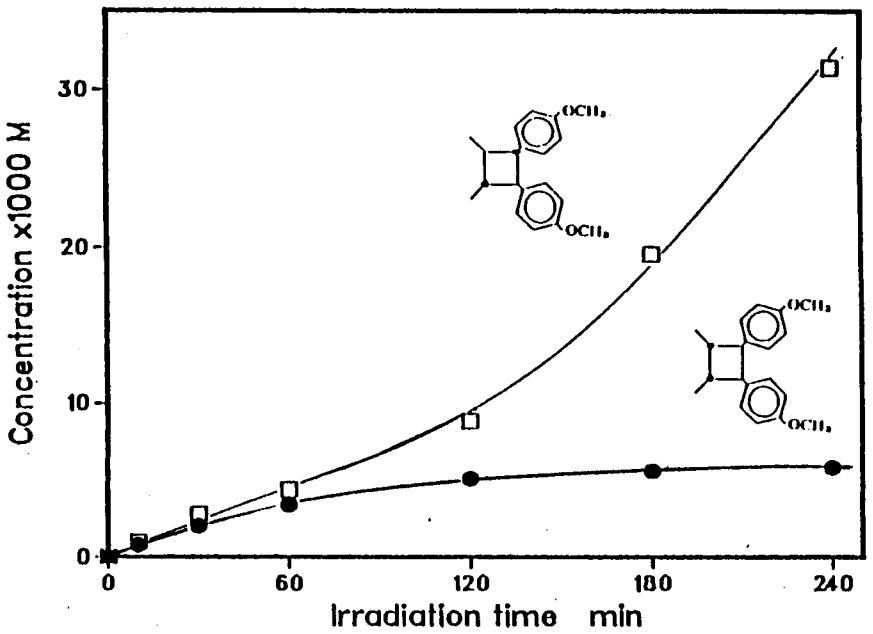

Figure 2-28. 9-cyanoanthracene (**67**) sensitized dimerizations of **3** in CH_3CN. The initial conc.: [**3**] = 5.0 X 10^{-1} M, [**67**] = 2.0 X 10^{-2} M.

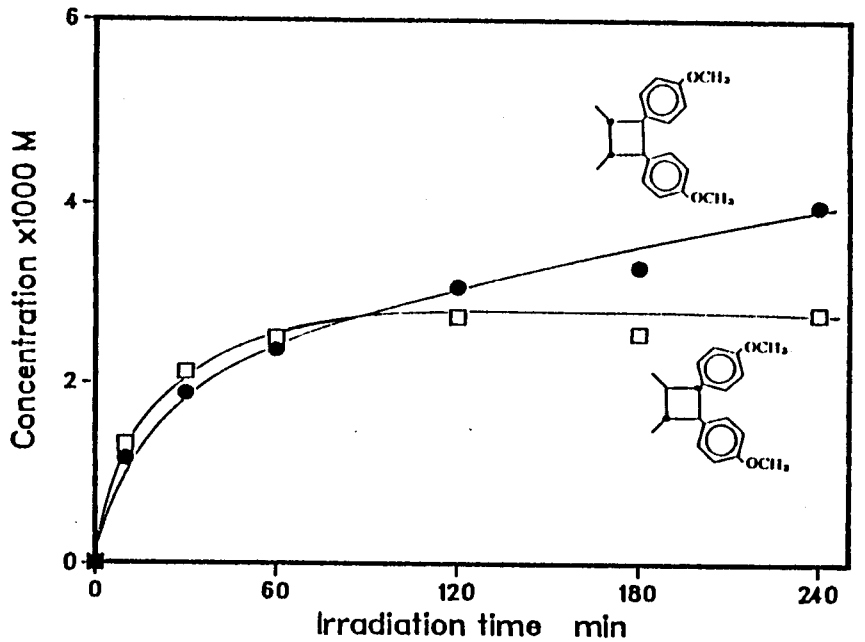

Figure 2-29. TCB sensitized dimerizations of **3** in CH_3CN. The initial conc.: [**3**] = 5.0 X 10^{-1} M, [TCB] = 2.0 X 10^{-2} M.

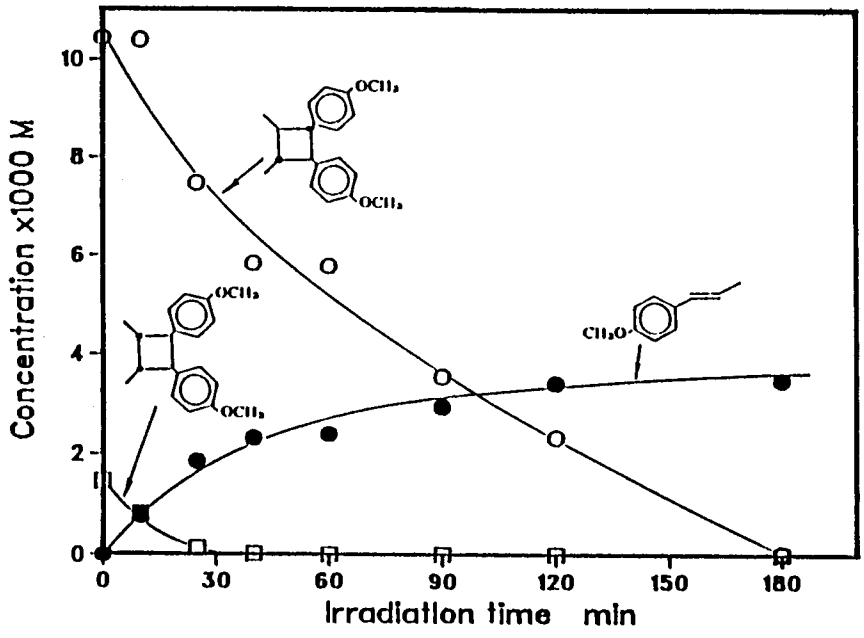

Figure 2-30. $DBMBF_2$ sensitized cycloreversion of **21** in CH_3CN. The dimer **21** was contaminated by about 12% of **22**. The initial conc.: [**21**] = 1.03 X 10^{-2} M, [$DBMBF_2$] = 2.0 X 10^{-2} M.

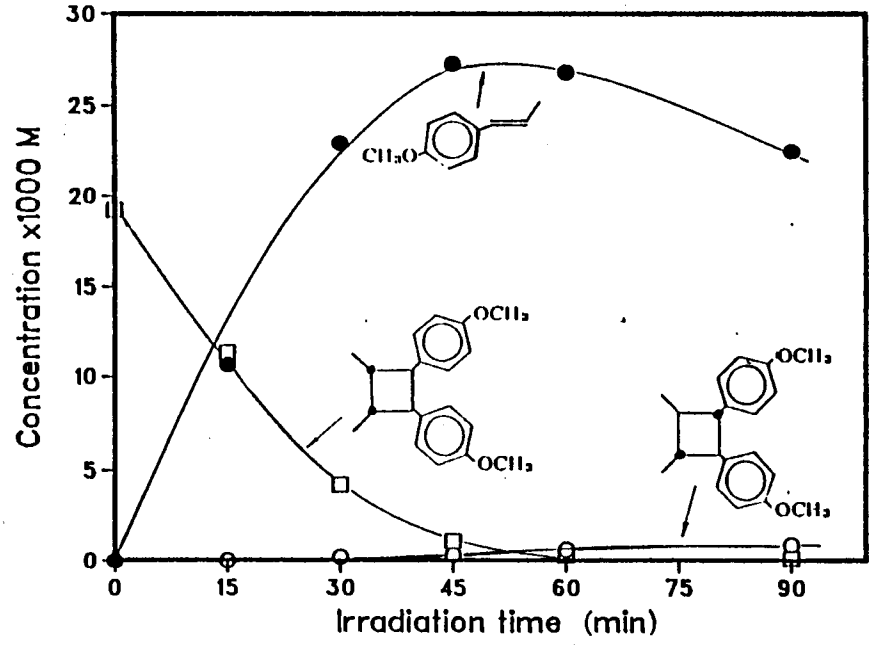

Figure 2-31. $DBMBF_2$ sensitized cycloreversion of **22** in CH_3CN. The initial conc. [**22**]=1.92 X 10^{-2} M, [$DBMBF_2$]=2.0 X 10^{-2}M.

dimerization of **3** is 20.8%. This poor yield is consistent with a reported value from DCN-An sensitized dimerization (~15%).[8] The poor yield of PET induced dimerization of **3** was due presumably to the cycloreversion of the formed dimers **21** and **22** as well as to the polymerization of **3** itself.[183] Worthwhile to mention was that none of dimers of **3** other than **21** and **22** was found during the sensitized cycloreversions.

The direct photolysis of **22** in CH_3CN with 300 nm light source was also examined, giving **3** as the sole detectable product (Fig.4-7).

2-4-4. Monochromatic Studies of $DBMBF_2$ Sensitized Dimerizations of 1, 2, and 3

Since $DBMBF_2$ has been found to be able to sensitize the dimerization of **1**, **2**, and **3**, the role played by their GSC in the sensitization become a critical question. The GSC formation constant of $DBMBF_2$-**3** system in CH_3CN is 0.44, and those for other two electron-rich olefins **2** and **3** can be assumed to be somewhat less than this value according to the less significant red shifts observed in the absorption spectra (Fig.2-8 and 2-9). To answer the question, monochromatic studies were carried out.

As shown by the absorption spectra (Fig.2-8 and 2-9), $DBMBF_2$ (0.02 M, in CH_3CN) does not absorb at wavelengths longer than 425 nm, while the absorption bands of the GSC's extend up to 460 nm. A 437 nm light beam is therefore used

for the selective irradiation of GSC's and a 312.8 nm light beam for the irradiation of the uncomplexed $DBMBF_2$. The experimental conditions and results are summarized in Table

Table 2-16. Monochromatic Photolyses of **2**, **1** and **3** in the Presence of $DBMBF_2$ in CH_3CN.[a]

diene	dimer	λ(nm)[b]	light absorbed[c] (%)	yield[d] (10^{-3} M)	relative quantum yield[e]
2	**55**	312.8	>80 ($DBMBF_2$)[f]	0.465	$\Phi(\mathbf{55})_{312.8}$
2	**55**	437.0	26 (GSC)[g]	<0.01[h]	$0-0.14\Phi(\mathbf{55})_{312.8}$
1	**65**	312.8	>80 ($DBMBF_2$)[f]	1.88	$\Phi(\mathbf{65})_{312.8}$
1	**65**	437.0	24 (GSC)[i]	<0.01[h]	$0-0.04\Phi(\mathbf{65})_{312.8}$
3	**21**[j]	312.8	8.4 ($DBMBF_2$)[k]	0.34	$\Phi(\mathbf{21})_{312.8}$
3	**21**[j]	437.0	98 (GSC)[l]	0.025[l]	$0.01\Phi(\mathbf{21})_{312.8}$

a. Undegassed solutions containing $DBMBF_2$ (0.02 M) and an olefin (0.5 M), irradiated for 120 min.
b. With a band width of 3.3 nm for **2** and **1**, 5.0 nm for **3**.
c. With the light-absorbing species in the parenthesis.
d. The concentration of the dimer resulted from irradiation.
e. The absolute quantum yields were unable to be measured due to too low light intensity.
f. By assuming that less than 20% of the light was absorbed by the GSC of $DBMBF_2$ with **3** at 312.8 nm.
g. The absorbance of the GSC at 437.0 nm is 0.13. $DBMBF_2$ did not absorb at 437 nm.
(to be continued at next page)

Table 2-16. (cont.)

h. The data were calculated by taking the sensitivity limit of the GC as the at-most possible yield. Actually no dimer peak was observed on the GC spectra.

i. The absorbance of the GSC at 437.0 nm is 0.12.

j. Another dimer **22** is also formed. We take the yield of **21** as the measure of the cation radical mediated dimerization, because **22** could be obtained by a direct irradiation of **3** (see footnote j).

k. 91.6% of the incident light is absorbed by **3** at 312.8 nm.

l. The absorbance of the GSC at 437.0 nm is 1.634.

m. For better accuracy, the yield is calculated from the yield measured in 480 min of irradiation (0.10×10^{-3} M) by assuming the formation of **21** proportional to the irradiation time.

2-16. In the cases of **2** and **1**, no dimer peak was detected by GC analysis when only the GSC were irradiated by 437 nm light beam (Fig.4-6). While the true yields could be zero, we rather assumed that the dimer (**55** or **65**) did have formed but in an amount too tiny to be detected by GC. Therefore, we take the sensitivity limit of the GC as the maximum possible yield of the dimers. On this basis, the upper limits of the relative yields at 437 nm with respect to those obtained at 312.8 nm are calculated.* As shown by the data in Table 2-16, the selective irradiation of the GSC in $DBMBF_2$-**3** system did give rise to the dimer **21** but with a quantum yield only 1% of that found in the selective irradiation of $DBMBF_2$ at 312.8 nm.

---

*For the details of calculation, see 4-5-4 and 4-5-5.

2-4-5. Dimerization of 2-Cyclopentenone Ethylene Ketal (20) - A False Photoreaction

Irradiation of a CH_3CN solution containing **20** (5×10^{-1} M) and $DBMBF_2$ (5×10^{-2} M) as the "sensitizer" with a 350 nm light source resulted in the formation of two head-to-tail (HT) dimers of the ketal, **95a** and **95b**, accompanied by a trace of a 2+2 dimer, **97**. These two diketal dimers spontaneously deketalized to give the corresponding monoketal dimers, **96a** and **96b**, respectively. The chemical yield of **96a** and **96b** was 26.5% after 2.5 h of irradiation. The hydrolysis of them in acidic water-CH_3CN binary solution afforded the two ketone dimers, **98a** and **98b**, respectively, as shown in Scheme 2-4. No product was detected from the dark control experiment.

The IR and MS data showed that **96a** and **96b** were compounds each containing a ketone and a ketal groups and having an identical molecular weight of 208. It was thought that they might have cyclobutane structures like **a** and **b** in Scheme 2-4, respectively, conversion of which to corresponding diketones **c** and **d** would loss the asymmetry raising the degree of difficulties in the structure determination. Therefore, the NMR studies were first focused on the dimer **96b**. The ^1H spectrum of **96b** was complicated in appearance due to signal overlapping and multiple long range couplings. More NMR methods such as COSY (Fig.2-32), NOESY (Fig.2-33), coupled ^{13}C spectra (Fig.2-34), selectively decoupled ^{13}C spectra (Fig.2-35), and ^{13}C-^1H correlation spectra (Fig.2-36) were invoked to

Scheme 2-4:

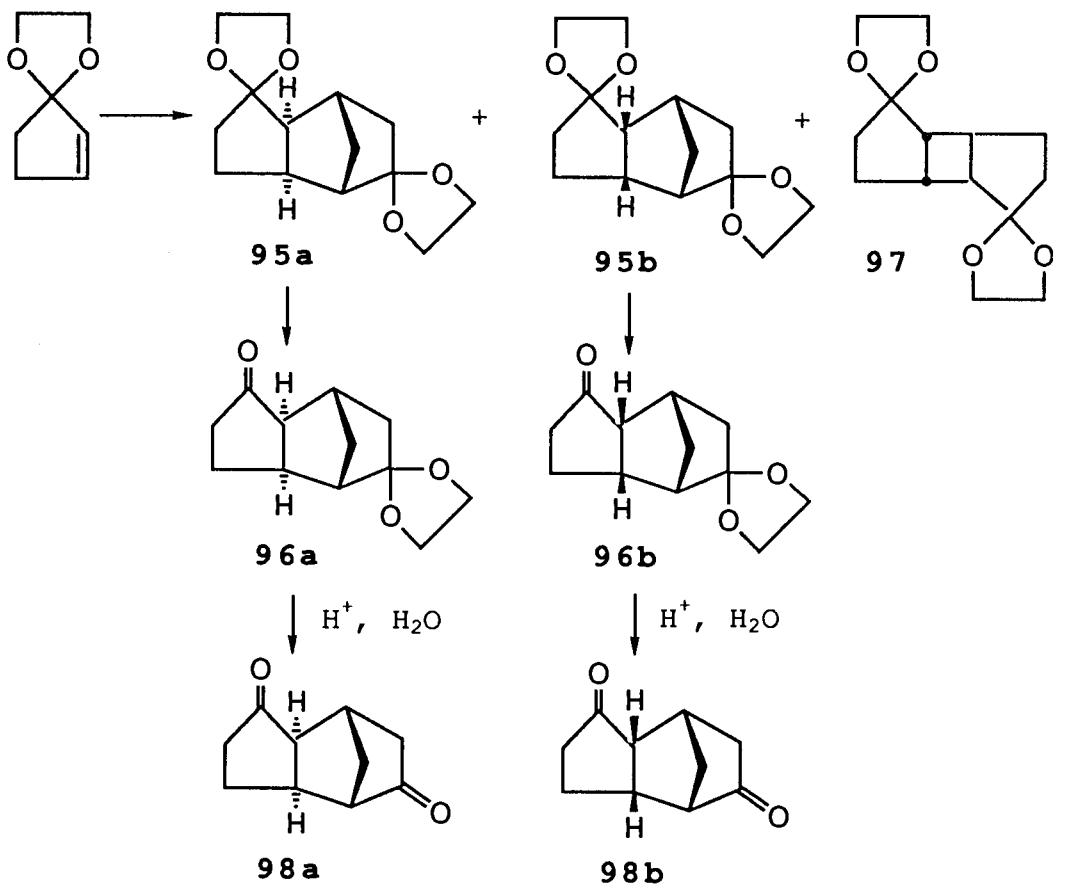

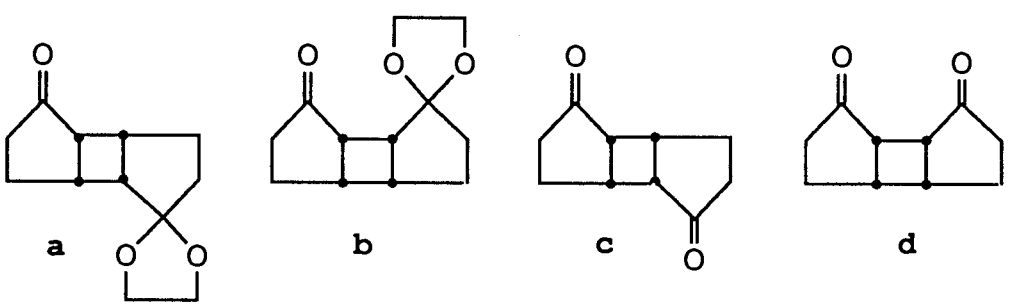

provide the structural informations. The finally assigned structure of **96b** was presented along with some of these spectra.

The ^{13}C NMR spectra showed 12 signals with two quaternary carbons at 220.64 and 115.85 ppm which apparently originated from the carbonyl carbon, C_1, and the ketal carbon, C_5, respectively. The other 10 signals consisted of 6 secondary and 4 tertiary carbons as clearly shown in Fig.2-34 and Fig.2-36. Once the position of C_2 was confirmed next to the carbonyl by the selectively decoupled ^{13}C spectra (Fig.2-35), all the ^{13}C and ^{1}H signals were located unambiguously by following the ^{13}C-^{1}H correlation (Fig.2-36) and the NOESY spectra (Fig.2-33). The cyclobutane structures (**a** or **b** in Scheme 2-4) were ruled out because the secondary carbon C_8 had to be a bridge carbon sited between two tertiary carbons, C_4 and C_7, as clearly shown by the ^{1}H coupling patterns ($J_{8\alpha,8\beta}$ = 9.9, $J_{8\alpha,4}$ = 1.6, $J_{8\beta,4}$ = 1.5, $J_{8\alpha,7}$ = 1.8, $J_{8\beta,7}$ = 1.5 Hz) and the NOE pattern among the protons (Fig.2-33). Therefore, we concluded that **96b** had a norbornane frame fused with a cyclopentanone and with the ketal group attached to C_5. The fact that the cyclopentanone moiety was *endo* fused to the norbornane frame was clearly shown by following observations. The NOE observed between H_7 and H_{7a} (slices I and J in Fig.2-33) as well as between H_4 and H_{3a} (slices E and F in Fig.2-33) strongly implicated that H_{7a} and H_{3a} were *exo* protons. The NOE between $H_{3\alpha}$ and H_{3a} was found stronger than

that between $H_{3\beta}$ and H_{3a} (slice E in Fig.2-33), also suggesting an *endo* configuration. Moreover, a weak but observable NOE between $H_{2\beta}$ and $H_{10\beta}$ (slice B in Fig.2-33) confirmed the *endo* assignment.

Noteworthy to mention was that the norbornane frame in **96b** was highly distorted as evidenced by following observations. The bridgehead proton H_7 was coupled with the *endo* proton $H_{6\beta}$ (J = 4.6 Hz) more strongly than with the *exo* proton $H6_{\alpha}$ (J = 1.0 Hz), in contrast to those found in a norbornane structure.[118,119] In addition, the bridge proton $H_{8\alpha}$ had a very strong diagonal NOE with $H_{6\alpha}$ (slice K in Fig.2-33) in sharp contrast to $H_{8\beta}$ which did not show any NOE with either H_{3a} or H_{7a} (slice L in Fig.2-33). The NOE between $H_{8\alpha}$ and $H_{6\alpha}$ was so strong that it became comparable with the NOE between the geminal protons $H_{8\alpha}$ and $H_{8\beta}$. This suggested that the bridge methylene group (C_8) was severely bent towards C_6 side. Even more surprisingly, there was a big long range coupling between $H_{8\alpha}$ and $H_{6\alpha}$ (3.1 Hz), which remained unexplainable (coupling though space?). However, once the monoketal dimer **96b** was converted to the corresponding diketone dimer **98b**, all these NMR phenomena mentioned above disappeared. In the ^1H spectrum of **98b** the coupling pattern in the norbornane frame was found to be typical for such structure (Table 4-19). The large coupling constant between H_7 and H_{7a} (J = 4.0 Hz) in **98b** reconfirmed the *endo* configuration.

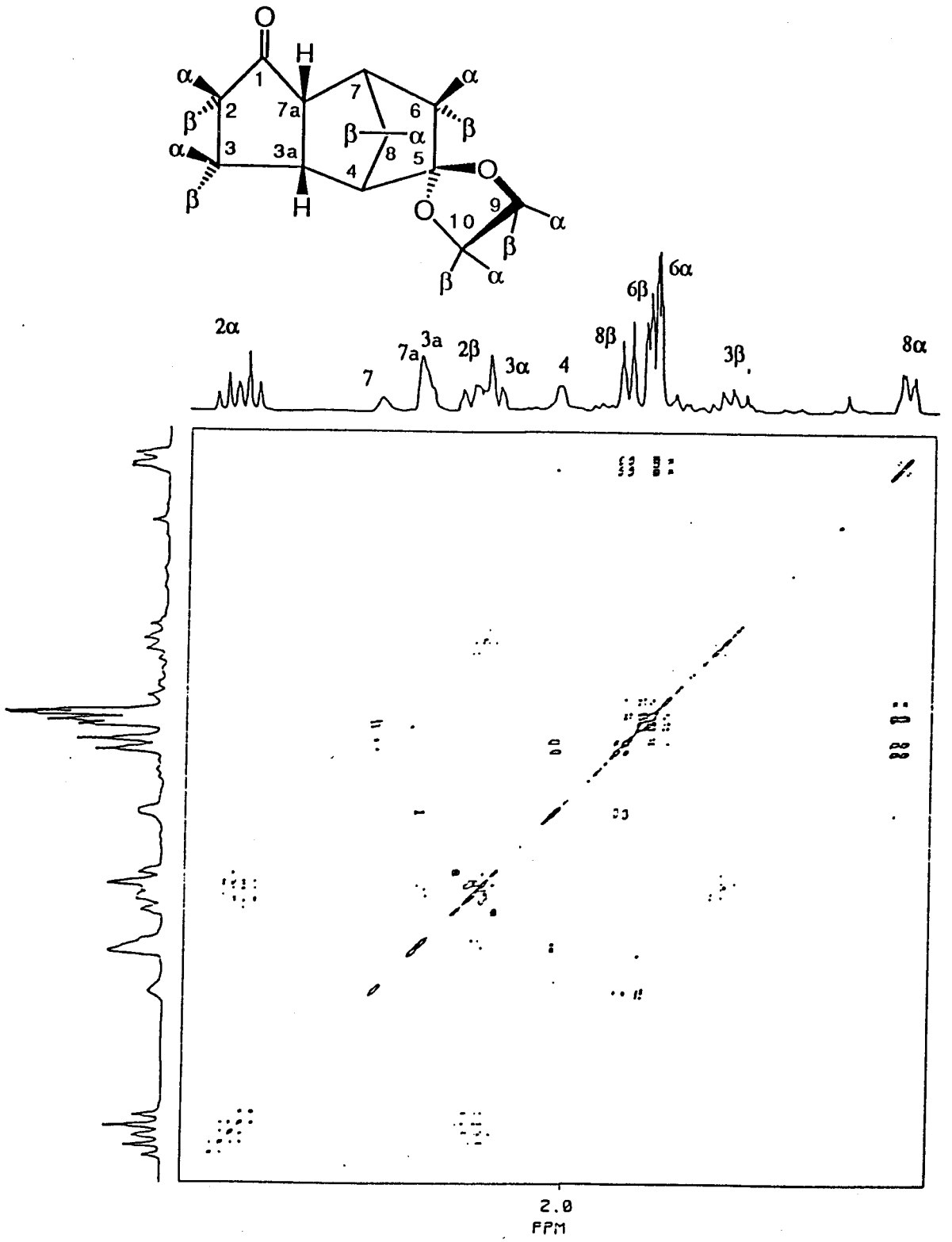

Figure 2-32. Contour plot of the ^{1}H COSY spectra of **96b** in C_6D_6. The ^{1}H spectrum of **96b** is given in both sides (the ketal protons are excluded).

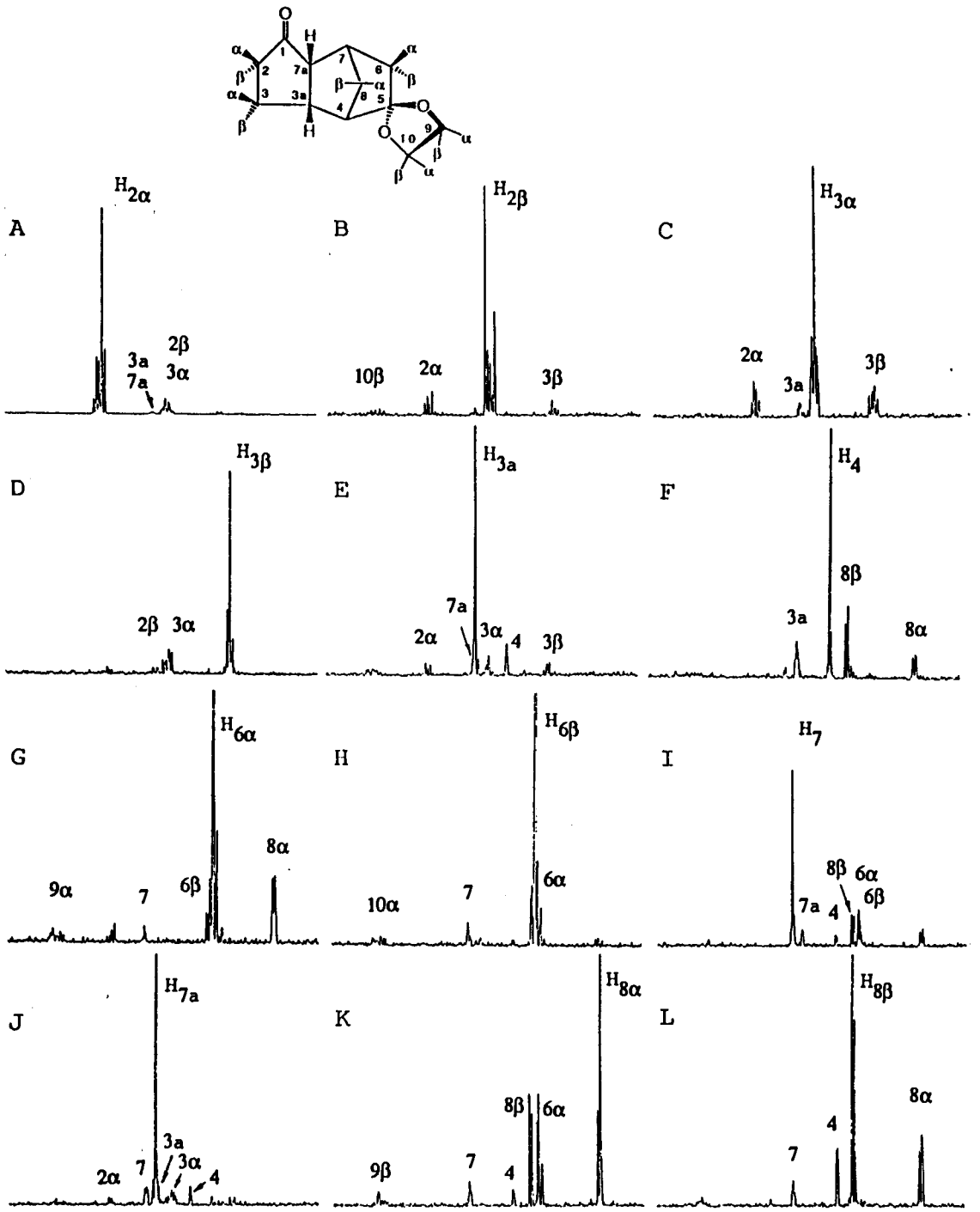

Figure 2-33. Cross-sectional plots of the ^{1}H NOESY spectra of **96b** in C_6D_6. The spectrum in slide A, for example, indicates that $H_{2\alpha}$ has NOE with H_{3a}, $H_{3\alpha}$, $H_{2\beta}$, and H_{7a}.

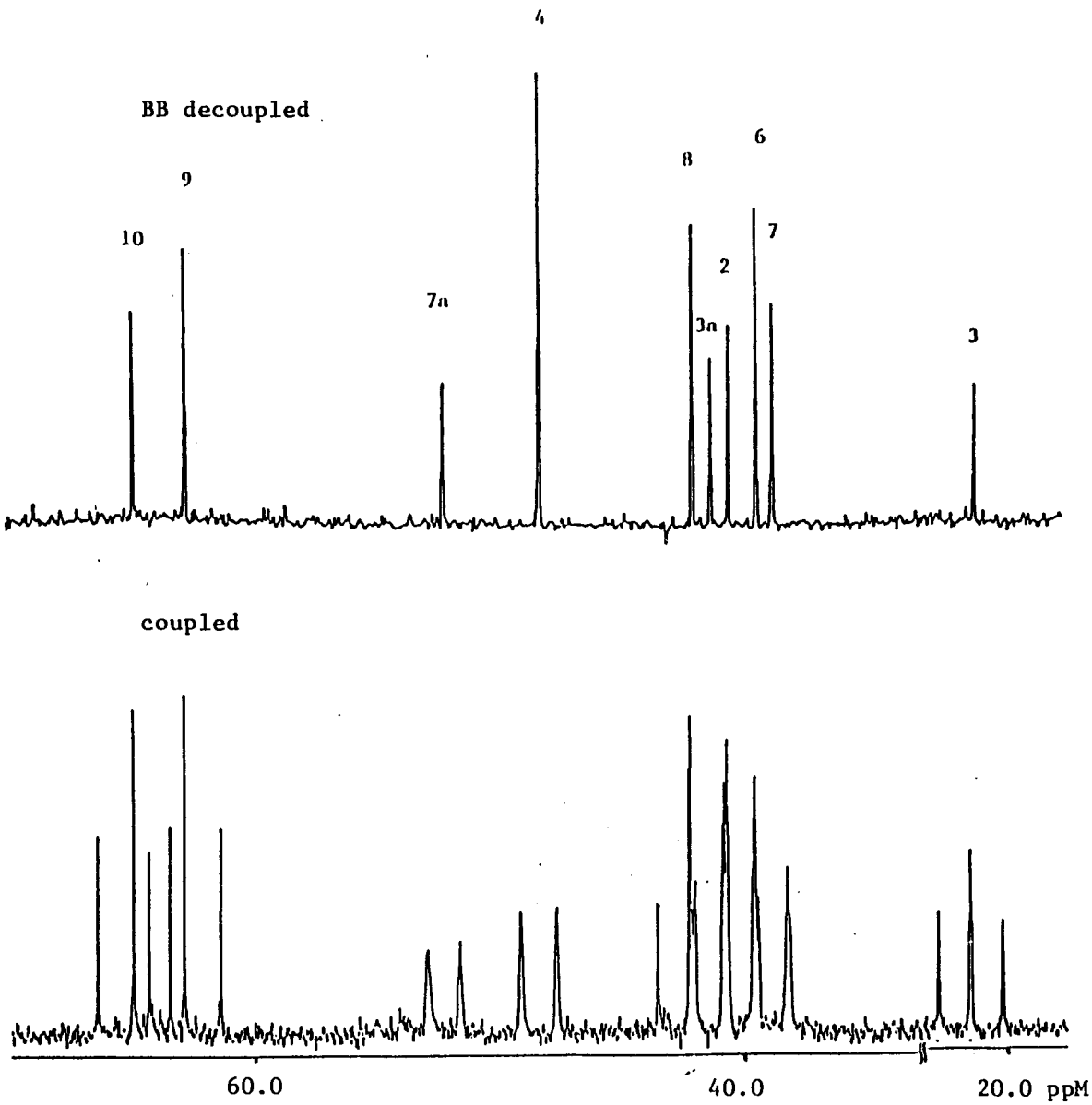

Figure 2-34. Coupled (lower) and decoupled (upper) ^{13}C NMR spectra of **96b** in C_6D_6.The quaternary carbons were excluded.

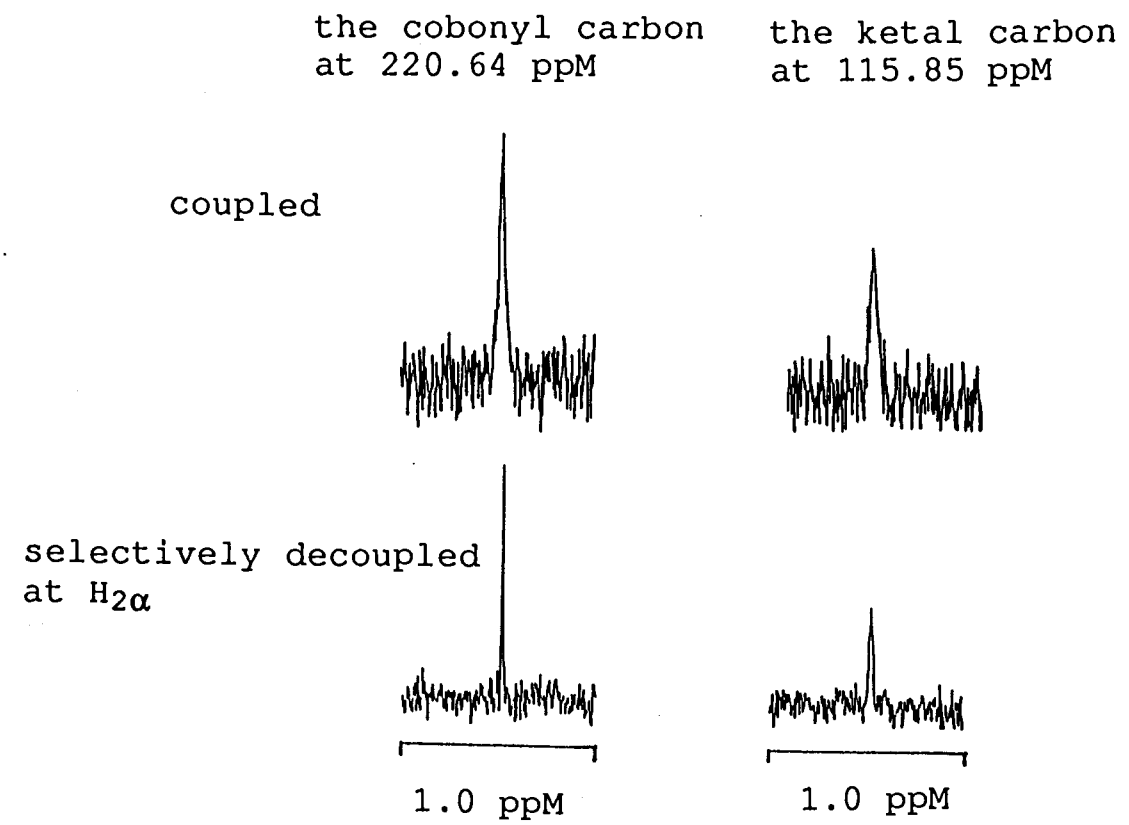

Figure 2-35. Selectively decoupled ^{13}C NMR spectra of **96b** in C_6D_6. Upper spectrum, coupled signals of C_1 (left) and C_5 (right); Lower, Selectively decoupled (at $H_{2\alpha}$) signals of C_1 (left) and C_5 (right).

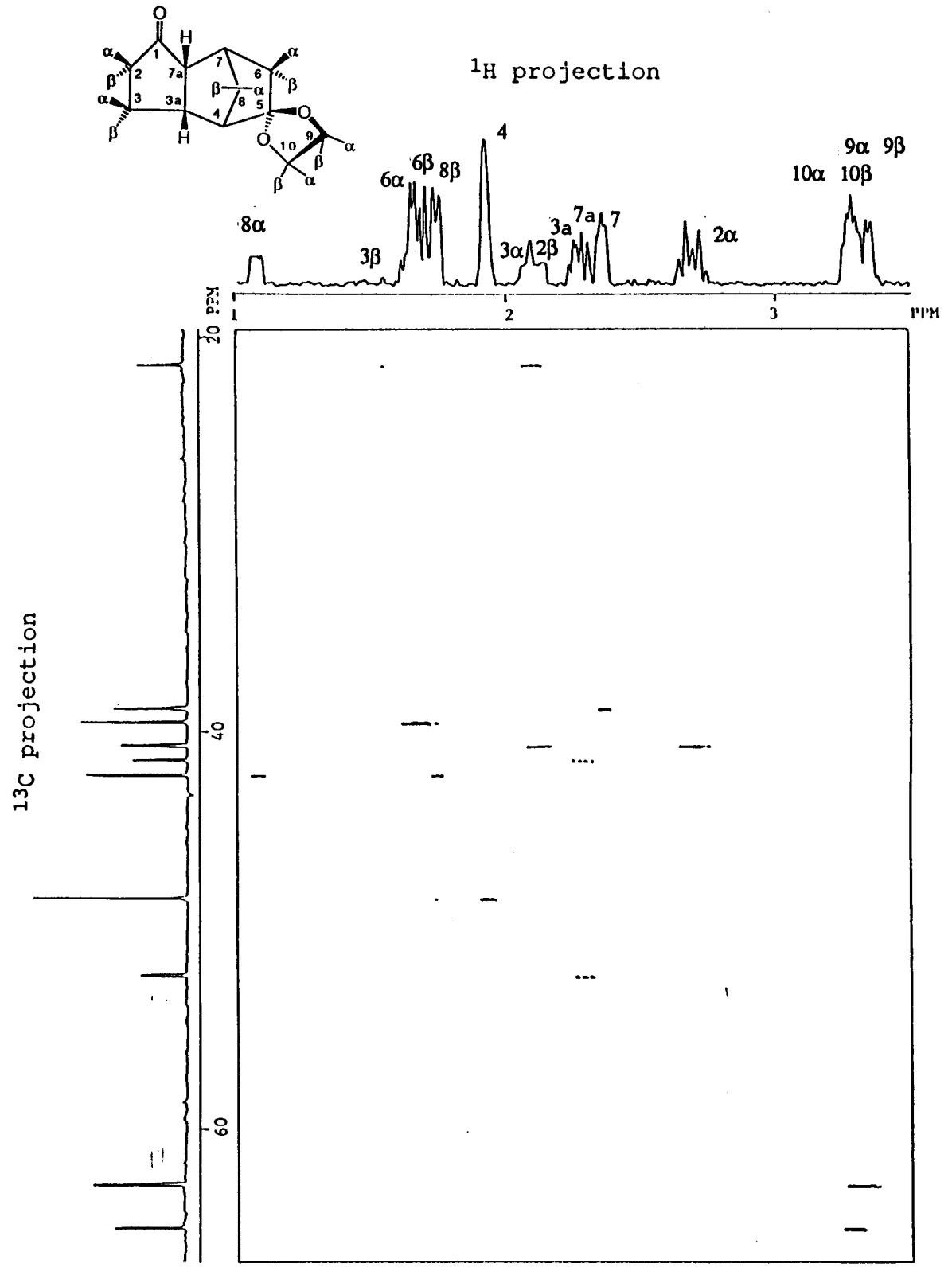

Figure 2-36. Contour plot of the ^{1}H-^{13}C correlation spectra of **96b** in C_6D_6.

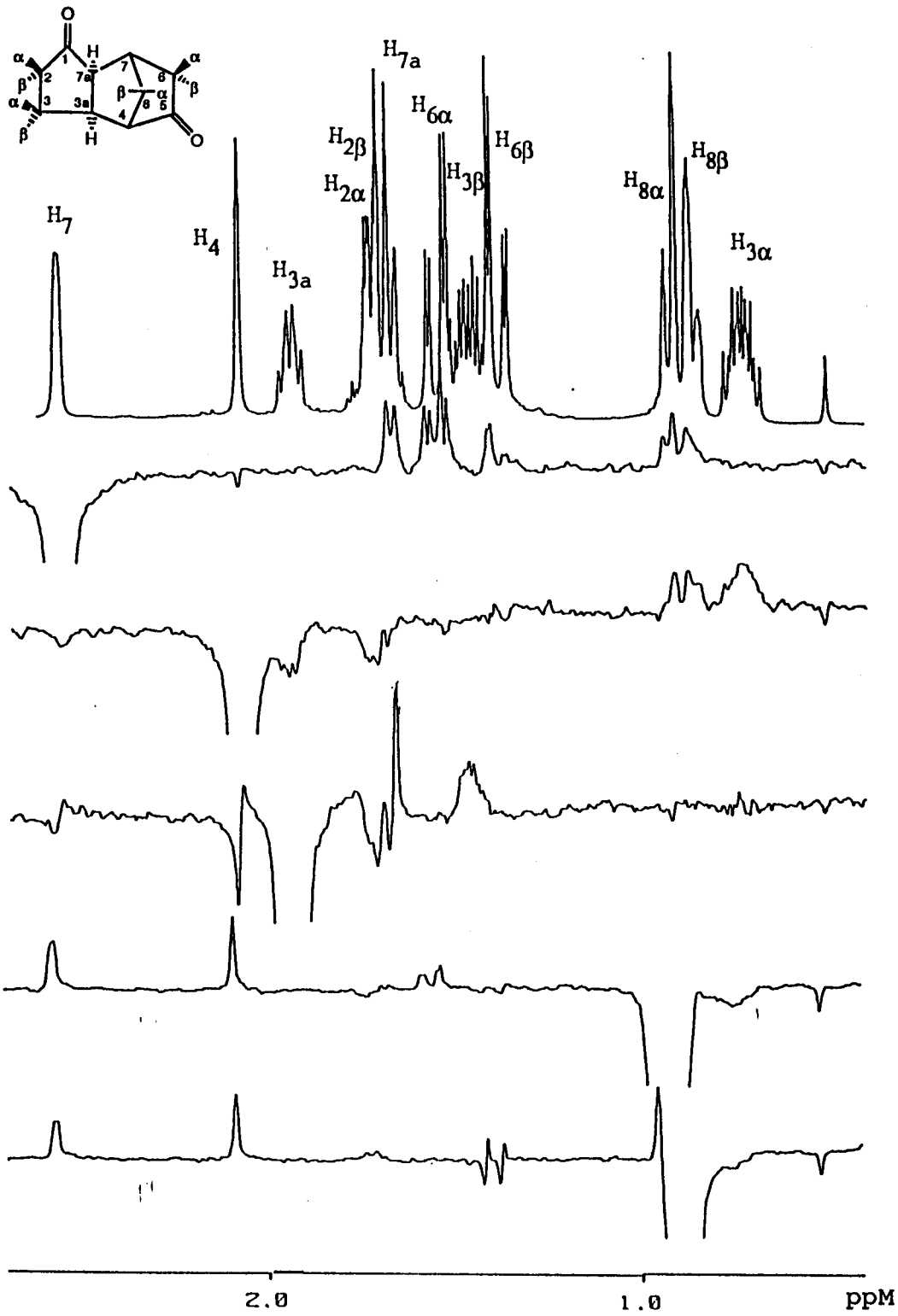

Figure 2-37. The ^1H NOE difference spectra of **98a** in C_6D_6.

The structure determination for the other diketone dimer **98a** was much easier because almost the ^1H NMR signals were first order and hence all the coupling constants were read out from decoupled spectra (Table 4-19). The ^1H coupling pattern was typical of norbornane derivative, showing smaller geminal coupling of bridge protons ($J_{8\alpha,8\beta}$ = 11.1 Hz), long range couplings between a bridge proton and *anti-endo* protons ($J_{8\beta,6\beta}$ = 4.0, $J_{8\alpha,7a}$ = $J_{8\alpha,3a}$ = 1.3 Hz), coupling of bridgehead protons with adjacent *exo* protons but not with *endo* protons ($J_{7,6\alpha}$ = 4.3, $J_{7,6\beta}$ = $J_{7,7\alpha}$ = $J_{4,3a}$ = 0 Hz). These data also indicated that the cyclopentanone was *exo* fused to the norbornane frame. However, we could not justify whether **98a** was a head-to-head or a head-to-tail diketone simply from the coupling pattern because the trace along the coupling relations was interrupted by the zero coupling between H_{3a} and H_4. Nevertheless, the tertiary proton H_{7a} was assigned α to the cyclopentanone carbonyl from the coupling relations in the cyclopentanone moiety (Table 4-19). The NOE spectra (Fig.2-37) showed that H_{7a} was adjacent to the bridge head proton H_7 which was also connected to two methylene groups (C_6 and C_8) as indicated by the coupling relations along the norbornane frame. Therefore, the other ketone group could only be at C_5, leading to the conclusion that **98a** was a head-to-tail diketone.

A similar result was obtained from a reaction of **20** in dry CH_2Cl_2 "catalyzed" by *tris*-(*p*-bromophenyl)aminium hexachloroantimonate (BAHA). After 30 min of reaction at 0°C,

the dimers were obtained in 56% yield and identified by coinjections with the samples obtained from the $DBMBF_2$ "sensitized" reaction. In both reactions mentioned above, significant amount of 2-cyclopentenone was found in the crude products.

Electron deficient sensitizers such as 9-CN-An and TCB failed to sensitize **20** to give the dimers, though a trace amount was detected in TCB "sensitization". Subsequently it was established that a CH_3CN solution of **20** (0.5 M) containing BF_3-etherate (0.1 M) was stirred for 15 min at room temperature to afford significant amounts of dimer **95a** and **95b** (~30%, by GC analysis). Sulfuric acid was also found to catalyse the dimerization in which **96a** and **96b** were obtained as the major products.

The $DBMBF_2$ "sensitized" photoreaction was then carried out in the presence of pyridine (0.1 M) as an acid trap, from which dimers were not obtained. The pH value of the photolysate thus obtained was 6.5 whereas that of the photolysate without pyridine was 4.0.* The addition of 2,6-lutidine (0.05 M) in the BAHA "catalyzed" thermal reaction also totally suppressed the dimerization.

It was therefore concluded that the dimerization of **20** was not a photoreaction but an acid catalyzed thermal reaction for which a possible mechanism was proposed as shown in Scheme 2-5.

---

* The pH values were measured by pH test paper using a mixture of equal volumes of the photolysate and water.

Scheme 2-5:

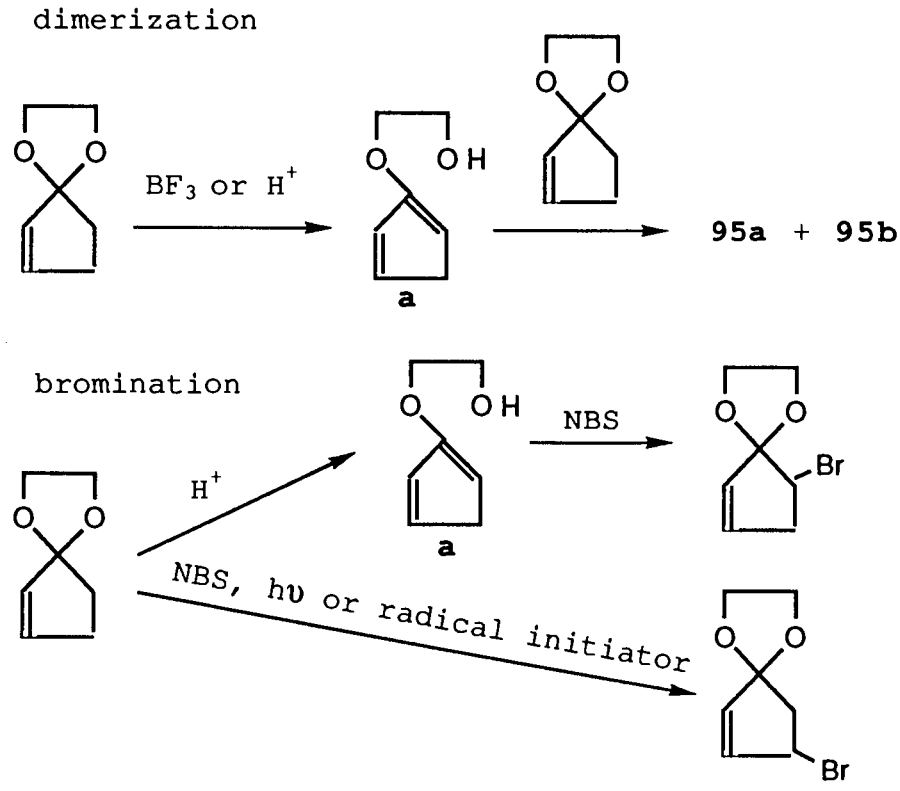

In the presence of an acid, the enone ketal is converted to an unstable diene intermediate (**a**) which undergoes the Diels-Alder reaction with another enone ketal molecule followed by reketalization to give the dimers **95a** and **95b**. The trace of HF is likely the catalytic species in the $DBMBF_2$[1] "sensitized" reaction. The diene intermediate **a** was originally suggested to be responsible for the bromination at C_5 position of 2-cyclopentenone ethylene ketal in acidic media.[120] It was claimed that the bromination by N-bromosuccinimide (NBS) in free radical condition gave only 4-bromocyclopetenone ketal, but in acidic solution without free radical initiators or light gave only 5-bromocyclopetenone ketal (Scheme 2-5).

2-5. Some Aspects of Photoreactions of Acetylacetone

2-5-1. The Photodimerization of Acetylacetone

Photolysis of acetylacetone in hexane with a 300 nm light source proceeded slowly to afford a 41% yield of dimer **70** which could readily be converted to the methyl ether **71** by treatment with acidic methanol. While the photodimerization also occurred in benzene, it did not in CH_3CN, CH_3OH, or CH_2Cl_2. 2,4-Hexanedione (**72**) and 6-methyl-2,4-heptanedione (**74**) were also irradiated under similar conditions in hexane giving trace amounts of dimers in 72 h as shown by GC-MS analysis. 2,2,6,6-tetramethyl-3,5-heptanedione (**73**) gave no dimer under similar reaction conditions. Because of the inefficiencies of dimerization these β-diketones were not investigated further.

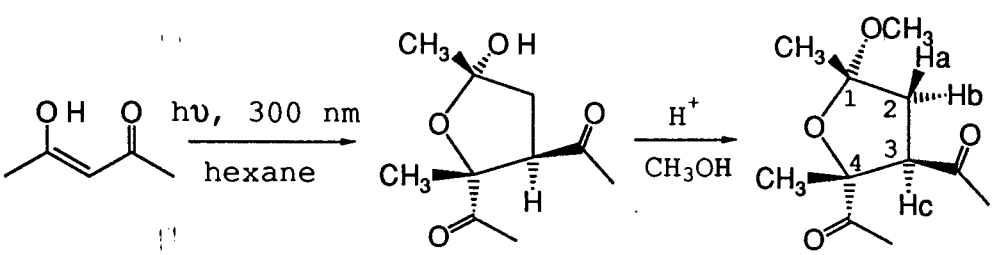

70 **71**

The dimer **70** was isolated from the crude material by flash chromatography and recrystallized slowly as parallelepiped crystals (mp, 73-4° C). The ^1H NMR studies (C_6D_6) showed that the dimer existed as an equilibrium mixture of three isomers in the solution. GC-MS showed a parent peak at m/e = 182 (M^+-18) by either EI or CI mode while X-ray crystallography reveal a dimeric structure shown above. The other two isomers detected by NMR spectroscopy were therefore assigned as the epimer and the ring opened isomer of **70**. Because of instability, the structure was determined primarily from the oily methyl ether **71** before the structure of **70** was solved by X-ray analysis.

The stable methyl ether also showed the highest molecular ion at m/e = 183 (M^+-OMe) in GC-MS by either EI or CI mode. The assignment of structure **71** is amply supported by ^1H and ^{13}C NMR data and by multiplicity sorting as well as selectively decoupled ^{13}C spectra that identified the ^{13}C signals. ^1H NOE spectra showed that the C_1-CH_3 and Ha were located on the one side of the furanoid plane and that the OCH_3, Hb, and Hc on the opposite side. The NOE experiments also showed that the two acetyl groups were *trans*-oriented. The ^1H coupling constants of the ABX system ($J_{Ha,Hb}$ = 12.9, $J_{Ha,Hc}$ = 11.4, and $J_{Hb,Hc}$ = 7.7 Hz) were reasonable for the ring system.

2-5-2. Photocycloaddition of Acetylacetone to Norbornene

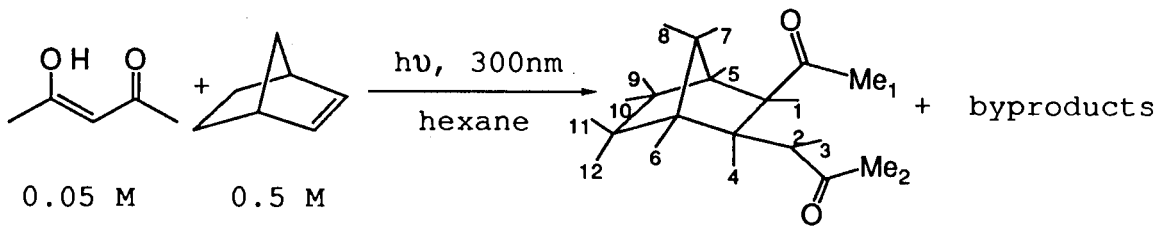

75 49.5%

Photolysis of acetylacetone in the presence of norbornene in hexane with a 300 nm light source lead to the isolation of a δ-diketone, **75**, as a colorless oil in 49.5% yield. The *cis-exo* configuration is strongly implied by the splitting pattern of the protons in the norbornane skeleton. The observations were that both H_1 and H_4 were coupled with the *anti* bridge proton ($J_{1,8}$ =1.1, $J_{4,8}$ = 1.8 Hz) but not with the adjacent bridgehead protons ($J_{1,5}$ = $J_{4,6}$ = 0 Hz).

While no other stereoisomer of **75** was found in the photolysate, significant amounts of byproducts were obtained (Table 4-21). These byproducts could be divided to 3 groups shown in Scheme 2-6. The first group consisted of the secondary photoreaction products of **75**, group 2 was the dimers of norbornene, and group 3, the adducts of norbornene with hexane. The structures of **76**, **77**, **80**, and **81** were assigned by comparison of their ^{1}H NMR spectra with authentic samples. For others, the structures were suggested by their GC-MS spectra (Table 4-22).

Scheme 2-6: by-products

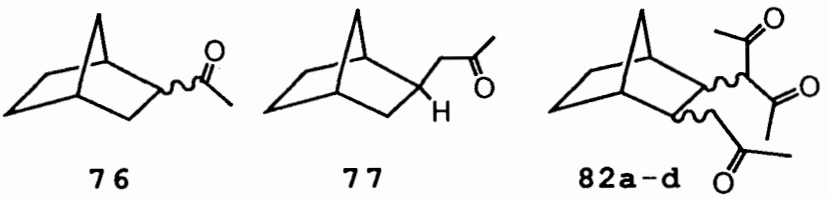

76 **77** **82a-d** group 1

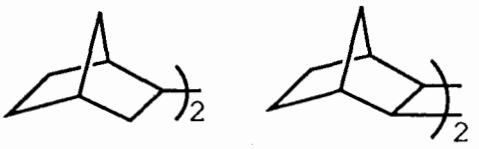

80 **81** group 2

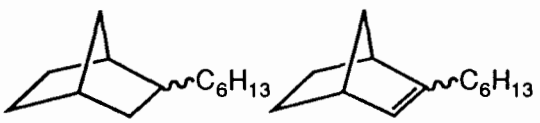

78 **79** group 3

The *cis-exo* δ-diketone **75** did not undergo Aldol condensation in acidic media but isomerized to the thermally more stable *trans* isomer **83**, which then readily condensed to give two products **84a** and **84b** (Scheme 2-7). As shown by the decoupled ^1H NMR spectra, the *trans* isomer **83** had an *exo* H_1 which was coupled with the adjacent bridgehead proton H_5 ($J_{1,5}$ = 3.3 Hz) but not with the *anti* bridge proton H_8 ($J_{1,8}$ = 0) while H_4 remains *endo* ($J_{4,6}$ = 0, $J_{4,8}$ = 1.5 Hz).

The *cis-trans* isomerization of **75** to **83** proceeded in acidic CH_3CN rapidly at room temperature to reach the equilibrium in 15 min with 93% of the *trans* isomer **83**. After 3.75 h reaction at room temperature in acidic CH_3OH, the

Scheme 2-7:

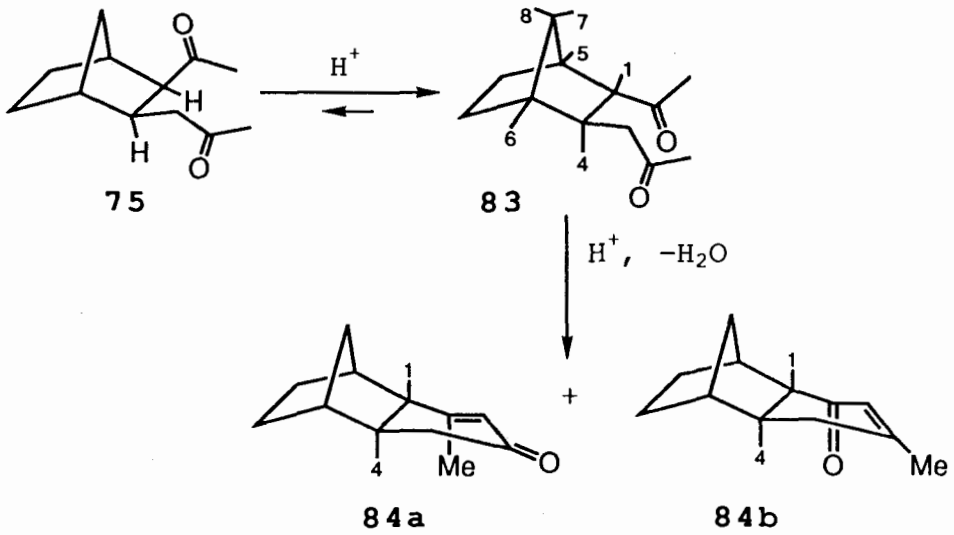

75 **83** **84a** **84b**

trans isomer **83** was also isolated as the major product along with the two condensed products in 20.6% yield. However, a solution of **83** in acidic CH_3OH gave **84a** and **84b** in 86.5% yield with no trace of **75** upon 11.6 h of reflux. Both **84a** and **84b** showed an identical parent peak of m/e = 176 in GC-MS spectra and carbonyl stretch at 1673, 1695 cm^{-1}, respectively, implying that they were condensed products of **83**. Only **84a** was isolated and analyzed by ^1H NMR spectroscopy. A small long range coupling (J = 1.2 Hz) between H_1 and the Me group was found in the ^1H NMR spectrum of **84a**. Based on this, the structure of **84a** was assigned and that of **84b** was suggested.

In the photolysis of acetylacetone-norbornene system, almost all the incident light was absorbed by acetylacetone. However, the photolysis also resulted in formation of the dimers of norbornene (**80** and **81**) as the byproducts which

obviously originated from the excited state or reactive state of norbornene. This observation raised a question: whether the excited state acetylacetone or the excited state norbornene was responsible for the formation of the cycloadduct **75**. Therefore, the quenching efficiency of 1,3-pentadiene on the formation of the dimers of norbornene (**80** and **81**) and that of the cycloadduct (**75**) were measured for comparison. As shown in Fig.2-38, the formation of **80** and **81** was indeed quenched by the addition of 1,3-pentadiene ($k_q\tau$ = 150 M^{-1}, curve 2) more than 20 times efficiently than **75** ($k_q\tau$ = 7.1 M^{-1}, curve 1). For comparison, the Stern-Volmer plot of the photocycloaddition of acetylacetone to cyclohexene in hexane was also measured and given as curve 3 in Fig.2-38.

For the same reason mentioned above, the concentration dependences of the composition of the photolysate were examined. We define the ratio of the amount of **75** formed to the internal standard as R and the ratio of the amount of **75** to the two dimers of norbornene **80** and **81** as r. At a fixed concentration of norbornene (0.5 M), the r value proportionally increased but R was kept essentially constant as the concentration of acetylacetone increased from 0.05 to 0.30 M (Fig.2-39). However, when the concentration of acetylacetone (0.052 M) was fixed, the r value decreased but R value proportionally increased as the concentration of norbornene increased from 0.05 to 0.6 M (Fig.2-40).

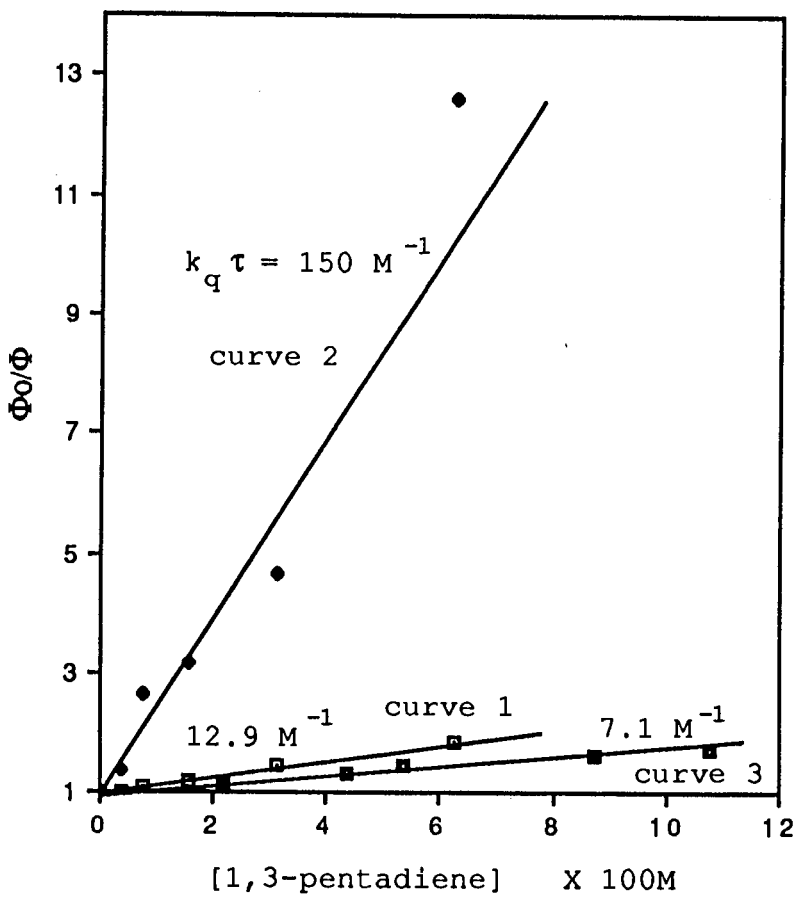

Figure 2-38. The Dependence of quantum yields of **75**, **80** and **81** on the concentration of 1,3-pentadiene. [acetylacetone] = 0.055 M, [norbornene] = 0.5 M. Φo denotes the quantum yields in the absence of the quencher. Curve 1, **75**, 14.5 h of irradiation; curve 2, the sum of **80** and **81**, 14.5 h of irradiation; Curve 3, the quantum yield of 42 obtained from the irradiation of acetylacetone (0.053 M) and cyclohexene (0.62 M) in hexane for 3 h.

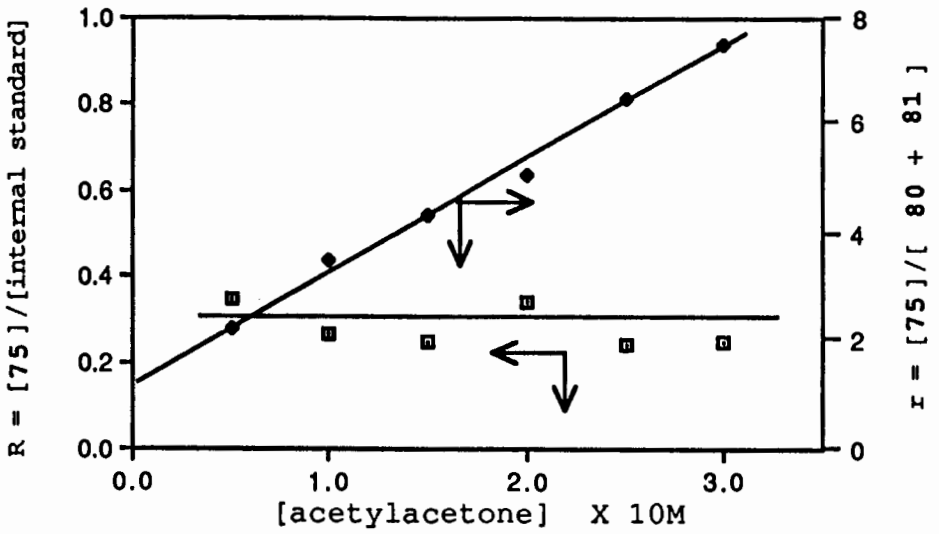

Figure 2-39. The dependence of the relative yields of **75**, **80** and **81** on the concentration of acetylacetone at [norbornene] = 0.5 M.

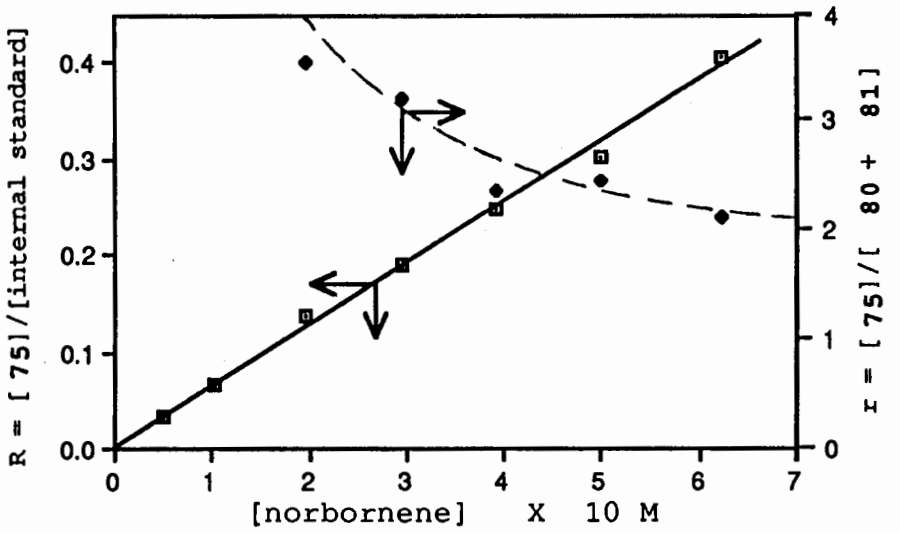

Figure 2-40. The dependence of the relative yields of **75**, **80** and **81** on the concentration of norbornene at [acetylacetone] = 0.052 M. The dashed curve is calculated according to Eq.3-10, see text in section 3-4-2.

2-5-3. Sensitized Solvent Addition Reactions of Norbornene

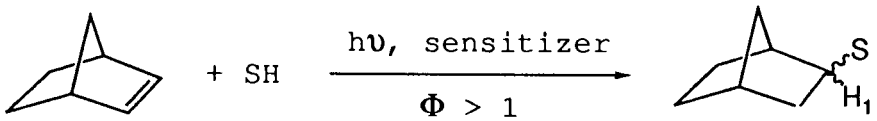

In an attempt to examine solvent effects of the cycloaddition reaction of acetylacetone to norbornene (2-5-2), it was found that in CH_2Cl_2, THF, CH_3CN the adduct **75** diminished to trivial or nil amounts while addition products of solvent to norbornene resulted. It was also found that the same solvent adducts were obtainable when acetylacetone was replaced by acetone. All the preparative photolyses were, therefore, conducted with acetone as the sensitizer.

The general profiles of the acetone sensitized photoreactions of norbornene in various solvents are given in Table 2-17. In acetone, CH_3CN, isopropanol, CH_2Cl_2, and $CHCl_2CH_3$, only one adduct was detected by GC analysis in each case and isolated by flash chromatography. Except the adduct of isopropanol, **89**, the configuration of which remains still unknown, all the adducts **77**, **85**, **90**, **92**, and **88a** had an *exo* configuration. The *exo* configuration of **77** and **85** were determined previously.[121,122] The *exo* configuration of **90**, **92**, and **88a** was decided from the splitting patterns of their ^1H NMR spectra, i.e. H_1 was not coupled with the adjacent bridgehead proton but weakly coupled with the *anti* bridge proton (1.4 Hz for **90**, ~0.9 Hz for **92**, and 1.8 Hz for **88a**).

Table 2-17. Experimental Conditions and Yields of the Adducts in Acetone-Sensitized Solvent Addition Reactions of Norbornene.

solvent	acetone % (by volume)	experimental conditions[a]	irradiation time (h)	product	yield[b] (%)
	100	C	10	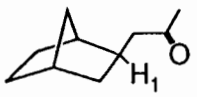 **77**	87.9
CH_3CN	12.5	A	12	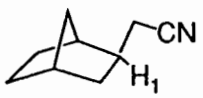 **85**	71.9
	12.5	A	12	 **86a + 86b**	61.2
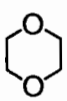	5	C	4	 **87a + 87b**	75.0
	10	B	2.5	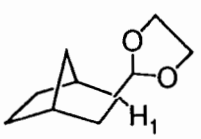 **88a**	62.5
				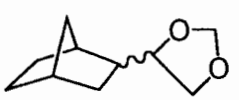 **88b + 88c**	14.7
	5	B	4	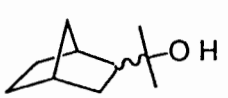 **89**	56.5
				77	~30

(to be continued at next page)

Table 2-17. (cont.)

solvent	acetone % (by volume)	experimental conditions[a]	irradiation time (h)	product	yield[b] (%)
CH_2Cl_2	12.5	A	12	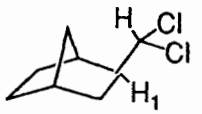 **90**	43.1
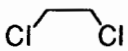	5	C	4	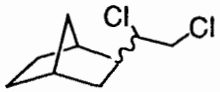 **91a** + **91b**	61.6
				77	~30
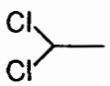	10	B	3	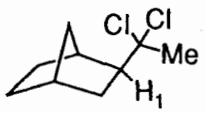 **92**	53.9
				77	~35

a. Condition A, a solution (280 ml) containing norbornene (5 g, 0.19 M) was irradiated with a 200 W Hanovia Medium pressure mercury lamp through a Pyrex filter according to **Method 1** described in 4-1-3; condition B, a solution (10 ml) in two Pyrex test tubes (100X13 mm) containing norbornene (95 mg, 0.1 M) was irradiated with a 300 nm light source according to **Method 3** described in 4-1-3; condition C, a solution (10 ml) containing norbornene (95 mg, 0.1 M) was irradiated according to **Method 2** described in 4-1-3. The light source was the same of Condition A.
b. Based on the amount of norbornene added.

The *exo* configuration of **88a** was also indicated by the NOE difference spectrum which showed no enhancement of the *syn* bridge proton signal when H_1 was irradiated. On the other

hand, the adducts resulted from THF, 1,4-dioxane, or 1,2-dichloroethane and the 4-substituted adducts of 1,3-dioxolane (**88b** and **88c**) were mixtures of two epimers as shown by the ^1H NMR spectra. As we failed to separate the epimers by either flash chromatography or preparative GC, we could not distinguish them unambiguously.

There were several common minor products found in the photolysates for all solvents. Among them, **77** obviously mainly originated from the addition of acetone and appeared in significant amounts when isopropanol, 1,2-dichloroethane, or 1,1-dichloroethane was used as the solvent (Table 2-16). Other two byproducts generally obtained in less than 15% GC yield were identified to be the two dimers of norbornene **80** an **81** by coinjection with the authentic samples. Another minor byproduct (<5%) found in the photolysate from 1,4-dioxane was likely a coupling product of the solvent as suggested by a parent peak at m/e = 174 and a base peak at m/e = 87 in the GC-MS (EI mode) spectrum.

The solvent addition reactions to norbornene sensitized by acetylacetone were examined in small scale experiments. Photolyses of solutions (5 ml each) containing norbornene (0.5 M) and acetylacetone (0.05 M) in a solvent (CH_3CN, THF, 1,4-dioxane, isopropanol, CH_2Cl_2, or 1,2-dichloroethane) gave the same adducts obtained from the corresponding acetone sensitized reactions, while acetylacetone remained essentially not consumed. In the acetylacetone sensitized solvent addition reactions the adduct(s) was(were) also

accompanied by several byproducts generally in less than 15% yield as judged by GC analysis. The byproducts were identified to be **77**, **80**, **81**, and the cycloadduct of acetylacetone with norbornene, **75**. However, **77** appeared always in tiny amount (<3%) for all runs.

The quantum yield measurements were performed for the reactions in CH_3CN, CH_2Cl_2 and THF. The photolyses of solutions (5 ml each) containing norbornene (~0.1 M) and acetylacetone (~0.05 M) lasted for 35 min by when the loss of norbornene was less then 5% as shown by quantitative GC analysis. The amounts of the adducts were determined by comparing their GC peak areas with the internal standard for

Table 2-18. The Quantum Yields of Acetylacetone-Sensitized Solvent Addition Reactions of Norbornene.[a]

solvent	[norbornene] (M)	[acetylacetone] (M)	product	Φ
CH_3CN	0.100	0.055	**85**	8.48
CH_2Cl_2	0.094	0.054	**90**	12.77
THF	0.102	0.054	**86a,86b**	2.83

a. Irradiated for 35 min with a 300 nm light source according to **Method 3** described in 4-1-3.

which calibration curves had been made earlier with authentic samples. The light intensity was recorded by using a benzophenone-benzhydrol actinometer under the same

irradiation conditions. As shown by the data in Table 2-18, quantum yields far greater than unity were found for all the three reactions.

2-5-4. The Photolysis of Norbornene-TCB System

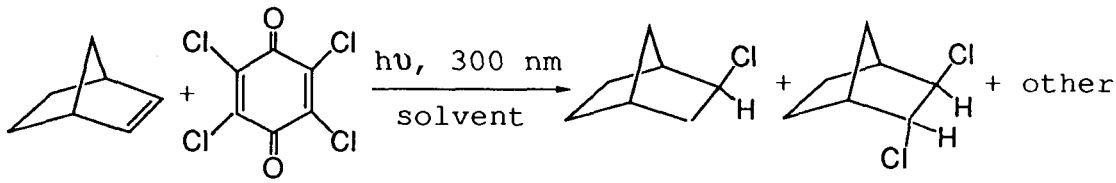

0.1 M 0.02 M **93** 75% **94** 15% 10%

relative yield

The photolyses of solutions containing norbornene (0.1 M) and TCB (0.02 M)* in various solvents (hexane, benzene, CH_2Cl_2, and CH_3CN) resulted in the formation of a major product and three minor products regardless which solvent was used. The major product and one of the minors were isolated from preparative GC and identified to be *exo*-2-chloronorbornane (**93**) and *trans*-2,3-dichloronorbornane (**94**), respectively. The GC-MS (CI) spectra clearly indicated that **93** was a monochloro compound and **94** was a dichloro compound. Their ^1H NMR spectra were essentially first order and all coupling constants were well established, in consistence with the assigned structures. No trace of solvent adducts to norbornene was found in any solvent.

* [TCB] = ~0.002 M when hexane was the solvent.

The ^1H NMR signals of norbornene in CD_2Cl_2 in the presence of TCB were found severely broadened upon irradiation (Fig.4-9). This finding led us to search for a paramagnetic species possibly generated in the system. Indeed, a strong ESR signal was observed in a benzene solution ([TCB] = 0.02 M, [norbornene] = 0.1 M) under irradiation (Fig.2-41,B). The signal built up in ~3 min after the light turned on and then gradually decreased due to the consumption of TCB. The signal was at least 10 times stronger than the neutral semiquinone radical (Fig.2-41,A)* and had a smaller g-value (2.0050) than the later did (2.0061). The difference in g-values (0.0011) was quite close to that between the anion radical of TCB and the neutral semiquinone radical in isopropanol (0.0008).[123] The signal was strongly quenched by addition of CF_3COOH as shown in Fig.2-41,C. All these observations allowed us to assign the signal to the anion radical of TCB. Both the neutral semiquinone radical and the TCB anion radical were trapped by *tert*-nitrosobutane showing different hyperfine splitting patterns (Fig.2-42) which remained still unexplainable.

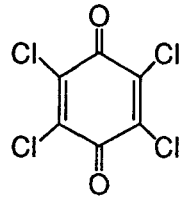

TCB

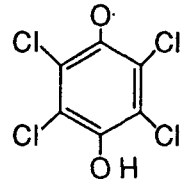

the semiquinone radical

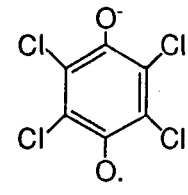

the anion radical

* The ESR signal of the neutral semiquinone radical was previously observed and assigned in isopropanol, see ref.123.

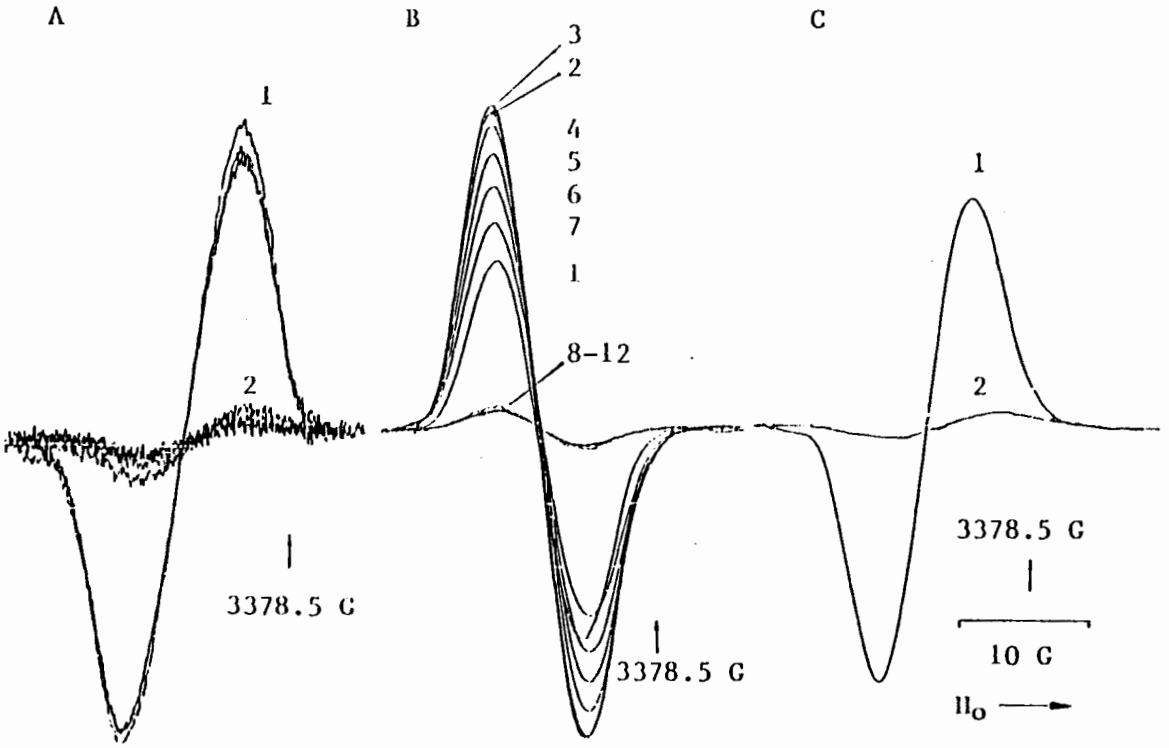

Figure 2-41. A. ESR signals from a benzene solution of TCB (2.0×10^{-2} M). Curve 1, taken after the light was turned on, consecutive scans with 1 min time intervals; curve 2, after the light was shut off. B. ESR signals from a benzene solution of norbornene (1.0×10^{-1} M) and TCB (2.0×10^{-2} M). curve 1 - 7, consecutively recorded after the light was turned on with 1 min time intervals; curve 8 - 12, recorded immediately after the light was turned off at the end of scan 7. C. ESR signals from a same sample of that in (B), both spectra were recorded immediately after the light was turned on; curve 1, without CF_3COOH; curve 2, with CF_3COOH (~1×10^{-2} M) added.

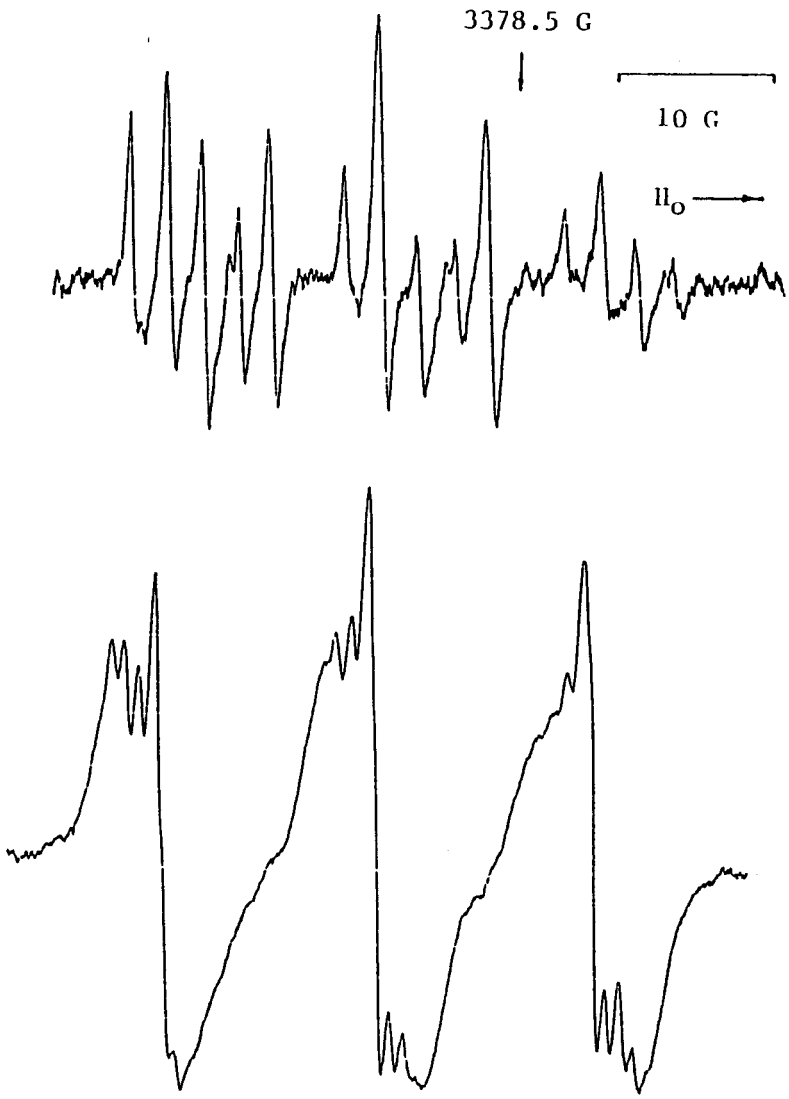

Figure 2-42. ESR signals trapped by *tert*-nitrosobutane (~1 X 10^{-6} M) in benzene. Upper spectrum, [TCB] = 2.0 X 10^{-2} M, the sample was irradiated for 1 min and then the spectrum was taken in the dark. Lower spectrum, [TCB] = 2.0 X 10^{-2} M, [norbornene] = 1.0 X 10^{-1} M, also taken in the dark after 1 min of irradiation.

CHAPTER 3 DISCUSSION

3-1. Photophysics of β-Diketonatoboron Difluorides

3-1-1. Ground State Complex (GSC) Formation of $DBMBF_2$ with Electron-Rich Compounds

GSC, especially charge-transfer (CT) complexes, combine electron donors and acceptors of sufficient strength such that they have a stable ground state equilibrium geometry. The related photophysical and photochemical phenomena have been known for a long time and well reviewed.[24,124,126] In analogy to the well known spectroscopic properties of GSC,[85] the commonly observed color change and red shifts in absorption spectra of $DBMBF_2$ solutions upon addition of various electron-rich compounds (2-1-2) are considered to be related to the formation of GSC between $DBMBF_2$ and the electron-rich compounds. The perfect linear Benesi-Hildebrand relation (Fig.2-10) obtained in $DBMBF_2$-anethole(**3**) system confirms that the red shifts in the absorption spectra is due to GSC formation. The absence of such color change or red shift in $DBMBF_2$ solutions on the addition of a less electron-rich olefin (e.g. **7**) or an electron-poor olefin (e.g. acrylonitrile) strongly indicates the charge-transfer character for the GSC observed.

The association constant, K = 0.44 M^{-1}, of $DBMBF_2$-**3** GSC formation implicates a moderate association: 29.5% of $DBMBF_2$ molecules are in the GSC in a solution containing 0.02 M of $DBMBF_2$ and 0.1 M of **3**. The GSC's formed with other electron donors, e.g. quadricyclane (QC), seem to have even smaller association constants as they show less significant red shifts in the absorption spectra (Fig.2-8), notwithstanding QC is at least as good as **3** in terms of being an electron donor as shown by their oxidation potentials (Table 2-4). The difference in K values between **3** and QC indicates the importance of "no-bond" interaction in GSC formation; **3** associates better because the benzene ring of **3** is expected to interact better with the chelate ring of $DBMBF_2$ causing stabilization. This is also in accordance with the theory and general observations for large body of GSC's. According to the Mulliken theory,[85] the ground state of CT complexes is described by a wave function which may be dissected into contributions from "no-bond" configuration, $\varphi(A,D)$, and a dative configuration in which an electron has been transferred, $\varphi(A^{-}\cdot,D^{+}\cdot)$. In Eq.3-1, the weighing coefficients

$$\varphi_{GSC} = a\varphi(A,D) + b\varphi(A^{-}\cdot,D^{+}\cdot) \qquad (3\text{-}1)$$

are generally considered to favor the "no-bond" configuration ($a >> b$). For example, less than 10% CT character for hexamethylbenzene complexes with various acceptors has been experimentally estimated.[127]

The substantial "no-bond" interaction between $DBMBF_2$ and aromatic compounds perhaps is the factor responsible for the unusual emissive behaviors of $DBMBF_2$ in benzene (Fig.2-4 and 2-5). The enhancements in intensity and red shift of the emission maxima indicate there are "new" emission peaks originated from GSC formed between $DBMBF_2$ and benzene. The observations during the recrystallization of $DBMBF_2$ in benzene (2-1-2) strongly suggest the formation of a rather stable GSC in the solid state. Considering a common assumption that the solution structures closely related to those determined for the solid state,[124] the observation of GSC in solid state, therefore, also support the conclusion that the GSC accounts for the enhanced fluorescence emission. On the other hand, the fluorescence spectra of $DBMBF_2$ in CH_3CN upon addition of pyridine (Fig.2-18,A) seem to imply an exciplex emission at about 500 nm. However, the emissive pattern in nonpolar MCH (Fig.2-18,B) clearly shows there is no new emission at ~500 nm but only broadening of the fluorescence band upon addition of pyridine. Therefore, we can not verify whether an exciplex formation or a GSC formation is responsible for the spectra shown in Fig.2-18,A.

While the GSC formation are demonstrated by the change in the absorption spectra, new fluorescence emissions at longer wavelengths are observed for two electron-rich olefins **1** and **2** (Fig.2-19). We assign them as the emissions from the GSC's rather than from exciplexes on the basis of similarity of the excitation spectra (Fig.2-19) with the corresponding

absorption spectra in the tailing region (400 - 440 nm, Fig.2-8), which has been referred to the GSC absorptions. In addition, we have demonstrate later on (see 3-2-3 and 3-3-3) that the quenching of singlet excited state $DBMBF_2$ by **1** or **2** is mainly due to the direct formation of solvent separated ion radical pairs rather than the exciplex formation. This is also in favor of the assignment to GSC for the origin of the new emissions. It has been claimed that CT complexes generally tend to have very low quantum yields of emission due to the prevalence of non-radiative decay,[124] therefore only few examples of fluorescence emission from the excitation of CT complexes have been reported.[128-130] This also explains why neat donors are needed to show the fluorescence of GSC's of $DBMBF_2$ with **1** or **2**. The failure of observing the emissions in CH_3CN (ε = 37.5)[84] is also in agreement with the general finding that the emission yield of CT systems drops sharply with increasing solvent polarity and virtually no fluorescence was found in solvents with $\varepsilon > 10$ due to a large reduction in radiative decay rate in polar media.[131,132] Worthwhile to mention is that in spite of clear evidence of the GSC formation between $DBMBF_2$ and **3**, no new emission was observed in neat **3**. Since **3** is a stronger electron donor than **1** and **2**, the lack of emission from $DBMBF_2$-**3** GSC is presumably due to a very fast electron transfer process within the excited GSC, which must result in the formation of the contact ion radical pair; this process supersedes emission.

3-1-2. Excimer Formation of $DBMBF_2$

The remarkable concentration dependence of $DBMBF_2$ fluorescence emission (Fig.2-3) resembles that found in a pyrene solution in heptane,[133-135] a classic example of excimer formation. The appearance of the structureless fluorescence band at 522 nm at the concentration of $DBMBF_2$ > 0.05 M in CH_3CN implicates the formation of the $DBMBF_2$ excimer. Despite the report that $DBMBF_2$ and $AABF_2$ exist only as monomer in benzene,[37] however, we still have to carefully rule out the possibility that the concentration dependence is due to a ground state molecular aggregation. Therefore, we have examined ^1H, ^{11}B, ^{19}F NMR (in $CDCl_3$) and electronic absorption (in CH_3CN) spectra of $DBMBF_2$ over a wide concentration range seeking signs of ground state molecular aggregations that should cause some changes to these spectra.[85,86] As shown by the results presented in Table 2-3 and Fig.2-7, the chemical shifts of the three nuclei and the band shape of electronic absorption spectra all demonstrate an independence to concentration changes. Moreover, the excitation spectra (Fig.2-7) taken at various concentrations do not show any notable changes in terms of band position and shape in comparison with the corresponding absorption spectra. All these observations agree with the conclusion that the emission at 522 nm originates from the excimer of $DBMBF_2$ and that the excimer is derived from dynamic process but not from a ground state complex. As an additional proof, we should cite that the fluorescence of crystalline $DBMBF_2$

superimposes with that observed in saturated CH_3CN solution ([$DBMBF_2$] = 0.22 M, Fig.2-3); a similar case has been found for pyrene.[135] Since the crystallographic studies of pyrene reveal that the molecules are arranged in parallel pairs with an interplanar distance of 3.53 Å,[136] a "face to face" structure is suggested for the pyrene excimer in solution.[122] Though the crystallographic data of $DBMBF_2$ has not been available till now, we suggest that the excimer of $DBMBF_2$ probably also has a "face to face" structure. In such a "face to face" structure the maximal overlap of π orbitals is expected, which in turn facilitates the charge resonance as well as exciton resonance between the partners of an aromatic excimer.[137]

Without more informations on the kinetic and thermodynamic parameters of the excimer formation, it is impossible to figure out the details of either the geometric structure or the dynamic course at this stage; the concentration dependence of $DBMBF_2$ fluorescence emissions at 398 and 416 nm complicates the problem. The coexistence of the two emissions of $DBMBF_2$ at 398 and 416 nm and their concentration dependence (Fig. 2-3) indicates that the peak at 416 nm might be a species derived from the monomer which is responsible for the emission at 398 nm. This is also supported by the observation in the fluorescence intensity quenching experiments. In the biacetyl quenching (2-1-6,a), which occurs by energy transfer owing to the singlet excited state energy (65.3 Kcal/mol)[88] of the quencher being 7.7 Kcal/mol

lower than that (73.0 Kcal/mol) of $DBMBF_2$, the peak at 416 nm ($k_q\tau$ = 71.7 M^{-1}) is quenched more efficiently than the peak at 398 nm ($k_q\tau$ = 60.0 M^{-1}). In contrast, in the case of 3,3-dimethyl-1-butene (**7**) or cycloheptene (**8**) being the quencher (2-1-6,b), which quenches *via* electron transfer mechanism (*vide infra*), the quenching efficiencies for both wavelengths are exactly the same. This observation can be rationalized by assuming that the species (tentatively denoted as species X) responsible for the emission at 416 nm is derived from the monomer of $DBMBF_2$ which emits at 398 nm, and the quenching by biacetyl *via* energy transfer affects both species whereas the quenching by the two olefins *via* electron transfer only affects the species that emits at 398 nm.

However, species X is distinctly different from the "conventional" excimer. The pyrene excimer has a difference between the fluorescence maxima of the monomer and the excimer as large as 6000 cm^{-1}, which corresponds to an energy difference of 17 Kcal/mol.[135] The corresponding difference for species X and the monomer of $DBMBF_2$ is only 1100 cm^{-1} (3.1 Kcal/mol). Moreover, both species coexist at $DBMBF_2$ concentration as low as 10^{-7} M. This means that if species X is some sort of excimer, the corresponding formation constant must be incredibly large (>10^5 M^{-1}). All these observations suggest that the concentration dependence of the ratio I_{398}/I_{416} is due to an unknown mechanism but not to an excimer formation. A rationalization is that the emissions at 398 and 416 nm are from two rotamers of $DBMBF_2$, respectively.

By analogy, we attribute the emission (~ 395 nm, Table 2-1) found in concentrated solution of $AABF_2$ (> 10^{-2} M) to the $AABF_2$ excimer.

3-1-3. $DBMBF_2$ Fluorescence Intensity Quenching at 398 nm

The dependence of quenching rate constant (k_q) for the fluorescence emission at 398 nm on either oxidation potentials (Fig.2-14) or IP (Fig.2-15) of the quenchers strongly indicate an electron transfer character of the quenching processes.[138,139] The k_q values in the exergonic ΔG^o region (Fig.2-14) are generally smaller by one order of magnitude than those predicated from Rehm-Weller relation[89,90] for a complete electron transfer mechanism, implying that a complete electron transfer from the quencher to $DBMBF_2$ can not be the rate limiting step.[31,140] We therefore suggest that the exciplexes of singlet excited state $DBMBF_2$ with the quenchers are involved in the quenching processes. However, later studies on the related photoreactions (3-3-3) reveal that the quenching of singlet excited state $DBMBF_2$ by some electron-rich olefins actually involves the direct formation of solvent separated ion radical pair (SSIP) in the competition with the exciplex formation. The competition of two quenching processes is also suggested by the correlation between k_q and IP of the quenchers as depicted below. A linear correlation (Eq.3-2) was reported[31,141] to hold for a fluorescence quenching process which is governed by exciplex

mechanism. In the equation, k_{diff} stands for the diffusion rate constant; A and C are constants. The plot of $\log[k_q/(k_{diff} - k_q)]$ *vs.* IP's of the quenchers (except enones) listed in Table 2-4 does

$$\log [k_q/(k_{diff} - k_q)] = A(IP) + C \qquad (3\text{-}2)$$

show a straight line in the IP > 8.4 eV region but a bent line in the IP < 8.4 eV region (Fig.3-1). This can be rationalized by assuming that the quenching process is operated predominantly by exciplex formation when IP > 8.4 eV

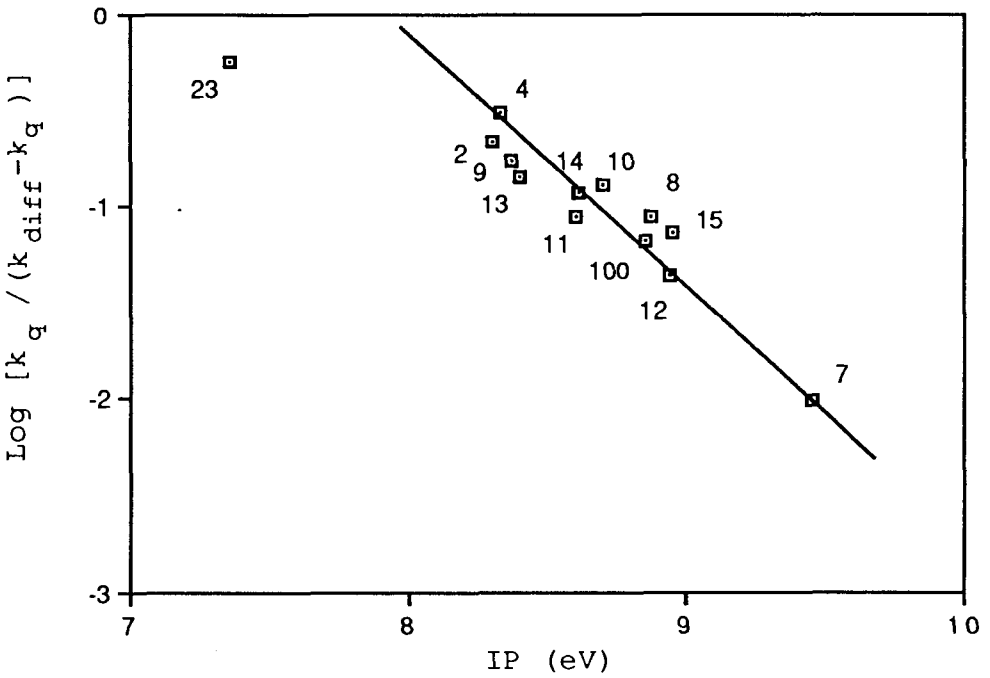

Figure.3-1. Dependence of rates of $DBMBF_2$ fluorescence quenching of various quenchers on their ionization potentials. k_{diff} = 2.2 X 10^{10} $M^{-1}s^{-1}$ is adopted for CH_3CN at 20° C.

whereas the direct formation of SSIP becomes competitive as IP goes down below 8.4 eV.

As mentioned in Chapter 1, acetylacetone may be regarded as an electron-rich species based on its redox parameters. Indeed, acetylacetone does quench the fluorescence of $DBMBF_2$ with a quenching rate constant fits excellently in the correlation curve shown in Fig.2-14 and Fig.3-1 (compound **100**). Enones also quench $DBMBF_2$ fluorescence. As one can find from Fig.2-15, there is no correlation of k_q with IP's. Though the lack of a correlation of k_q with IP does not necessarily indicate that the quenching is by energy transfer,[24,140] there seems to be a clue for an energy transfer mechanism for the quenching by enones. The quenching of singlet excited state $DBMBF_2$ by enones leads to the formation of the adducts of DBM and the enones (2-3). In the case of a cyclic enone (2-cyclopentenone **19** or 2-cyclohexenone **16**) being the quencher, two 2+2 dimers of the enone are also obtained accompanying the cycloaddition reactions (2-3-2) . Notably, the ratios of the head-to-head and head-to-tail dimers so obtained (34/66 for **16** and 54/46 for **19**) are very close to those resulted from the direct photolysis of the enone (37/63 for **16** and 59/41 for **19**). As the experiments are always carried out under conditions where virtually all the incident light is absorbed by $DBMBF_2$, this observation suggests that an energy transfer from singlet excited state $DBMBF_2$ to the enone must have occurred. And the

energy manifold of the reactive state of the enones has to be close to or below the E_s of $DBMBF_2$ (73.0 Kcal/mol). Because of the lack of fluorescence for these enones,[142] the E_s data have not been available except an E_s = 75.5 Kcal/mol was reported for **16**.[144] Nevertheless, the calculations by a modified INDO procedure (INDOUV) predict very low E_s (n,π^* transition) values for methyl vinyl ketone (**18**, 60.2 Kcal/mol) and 3-penten-2-one (**17**, 61.3 Kcal/mol).[143] However, the reactive state of enones in the quenching process does not have to be the spectroscopic singlet state. Further studies are, therefore, obviously needed to elucidate the mechanism.

3-2. Photocycloaddition

3-2-1. An overview

All products obtained from the photolyses of $DBMBF_2$-olefin systems are δ-diketones. According to a mechanism illustrated in Scheme 3-1 singlet excited state $DBMBF_2$ forms the exciplex with ground state olefin, within which a 2+2 cycloaddition reaction occurs to give a cyclobutane intermediate. The spontaneous ring opening of the cyclobutane gives rise to the final δ-diketone product. The chelate ring resonance no longer exists in such a intermediate and the BF_2 complex is hydrolyzed readily by trace of water in the solvent or the moisture encountered during work up.

The chemical outcome of the photolysis of $DBMBF_2$-olefin system is similar to that of the de Mayo reaction. DBM was reported to photoadd to styrenes,[145] probably *via* a triplet

Scheme 3-1.

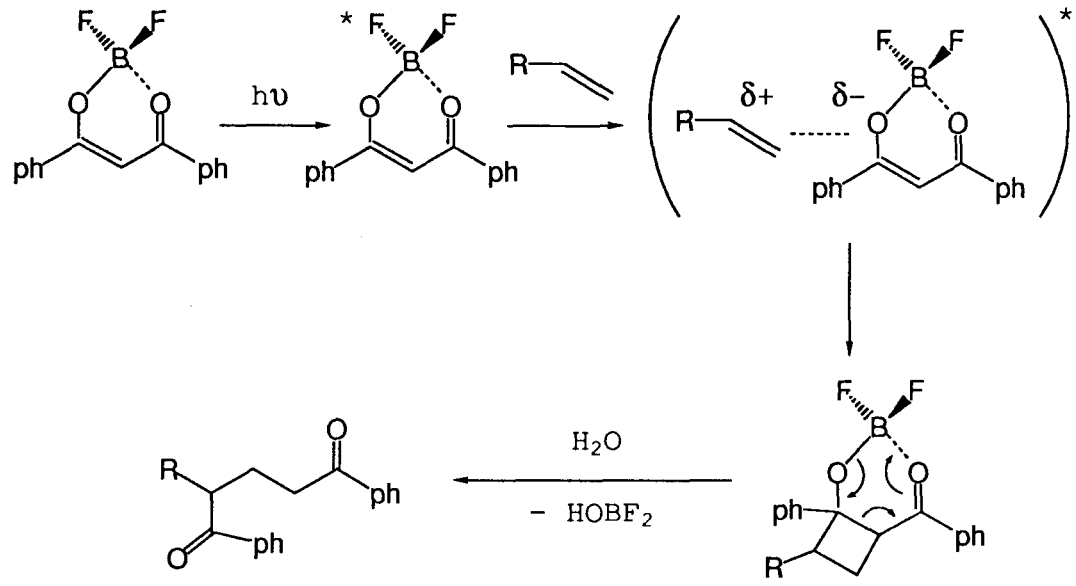

energy transfer from the β-diketone to styrenes followed by the cycloaddition of triplet styrenes to the ground state β-diketone. However, DBM does not photoadd to simple olefins (e.g.cyclohexene) as demonstrated by us and in the literature.[43] From mechanistic point of view, the photocycloaddition of $DBMBF_2$ to simple olefins (the cycloaddition) is entirely different from the de Mayo reactions. The cycloaddition is directly related to the quenching process of singlet excited state $DBMBF_2$ by the olefins. The coincidence of the $k_q\tau$ values obtained from fluorescence quenching with those obtained from the adduct quantum yield measurements (Table 2-8) concludes that the singlet excited state $DBMBF_2$ is involved in the reaction. The fact that the reaction is virtually not quenched by oxygen

but by electron donors such as QC and NBD (Table 2-9) is also in agreement with the conclusion. As the fluorescence quenching by simple olefins has been demonstrated to be electron transfer in nature and proceeds probably *via* exciplex formation, the cycloaddition must bear the same

Scheme 3-2.

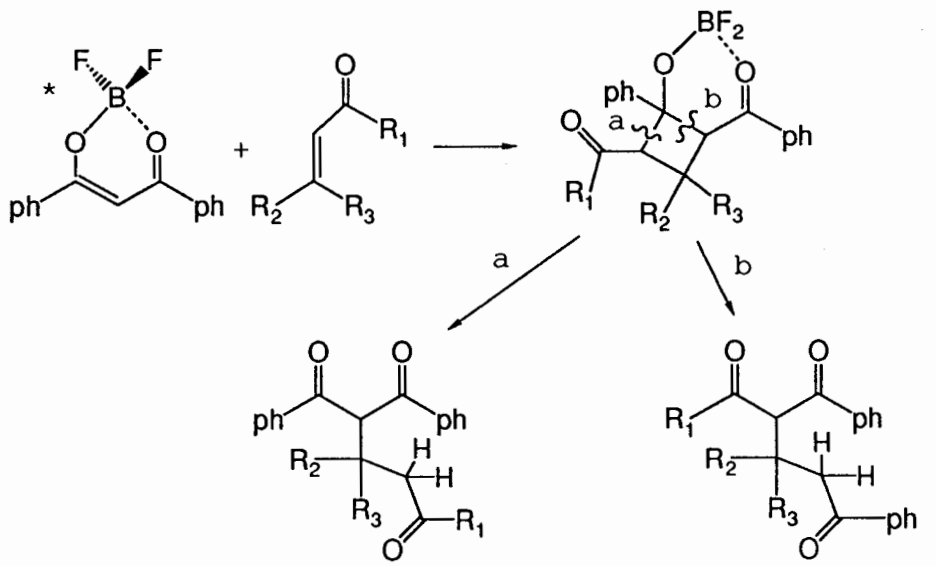

characteristics. For the cycloaddition with enones, A rationalization can be made by assuming that the reaction also proceeds *via* exciplex formation to regiospecifically give the cyclobutane intermediate (Scheme 3-2) which then undergoes ring opening in two directions affording "type a" and "type b" final products, respectively.

$DBMBF_2$ photocycloadds regiospecifically to acyclic olefins (**7**, **25**, **27**, and **14**) and enones (**17**, **18**, **45**, and **46**) with

the benzoyl attached to the more substituted carbon of the terminal double bond. Both $DBMBF_2$ and $BABF_2$ photoreact stereoselectively with norbornene to give predominantly the *endo* adducts. This contrasts strikingly to the general trend of *exo* attacks in ordinary additions by various reagents including nucleophiles, electrophiles, and radicals.[146] The stereochemistry of the $DBMBF_2$ cycloaddition reactions most likely is determined by the intermediacy of exciplex (bimolecular and/or termolecular, *vide infra*). A specific geometric orientation of the partners is required in the exciplex intermediates and therefore account for the selectivities in the structure of reaction products.

3-2-2. The Intermediacy of Triplexes

Photocycloaddition reaction occurring within exciplexes is most commonly seen and most extensively studied in donor-acceptor addition reactions, for which several reviews have been written.[20,147-150] The photocycloaddition reactions of $DBMBF_2$ with simple olefins seem also to involve an exciplex mechanism as described in 3-2-1. However, the experimental observations can not be explained by a simple exciplex mechanism.

The decreasing quantum yields of the photocycloaddition of $DBMBF_2$ with 3,3-dimethyl-1-butene (**7**) on increasing [$DBMBF_2$] (Fig.2-22) is a parallel phenomenon with the decreased fluorescence quenching rate ($k_q\tau$ for the monomer fluorescence at 398 and 416 nm) by **7** at high [$DBMBF_2$] (Fig.2-12). This is

attributed to the competition between exciplex formation and excimer formation (Scheme 3-3). In contrast, the quantum yields of photocycloaddition reaction with cyclic olefins (cyclohexene, cycloheptene, and cyclooctene) increase as [$DBMBF_2$] increases (Fig.2-22). Noticing that the $DBMBF_2$ monomer fluorescence quenching by cycloheptene also shows an decrease in the quenching rate as [$DBMBF_2$] increases (Fig.2-13), the dependence of the photocycloaddition reaction with cyclic olefins on [$DBMBF_2$] must be explained. We propose that the cycloaddition occurs from both a bimolecular exciplex and a termolecular exciplex intermediates, the latter of which consists of two acceptor ($DBMBF_2$) moieties and an olefin (Scheme 3-3). Termolecular exciplex has been known as triple exciplex,[151] or triplex,[152,153] or exterplex.[154] The existence of triplex has been claimed mainly based on fluorescence spectroscopic studies of donor-acceptor systems, e.g. arene/1,2,4,5-tetracyanobenzene,[155] 1,3-dinaphthylpropane/1,4-dicyanobenzene,[151] naphthalene/1,4-dicyanobenzene,[152,154] and 2,5-dimethyl-2,4-hexadiene/9,10-dichloranthracene.[153] A photoinduced Diels-Alder reaction of indene and cyclic dienes in the presence of cyanoaromatics is also claimed to proceed through the formation of a triplex intermediate that consisted of one cyanoaromatc, one indene, and one diene molecule.[156] In all systems mentioned above, the triplex have a D-D-A composition. However, in $DBMBF_2$-cyclic olefin systems, the triplex must have a D-A-A composition which is implied not only by the dependence of the quantum yield on

Scheme 3-3:

A = $DBMBF_2$ O = olefin $(A,A)^*$ = excimer

$(A,O)^*$ = exciplex $(A,A,O)^*$ = triplex

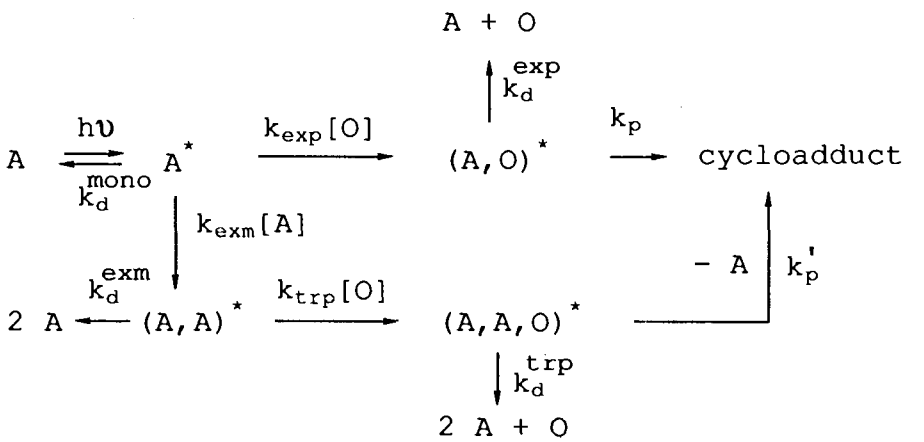

$DBMBF_2$ concentration, but also by the quenching of $DBMBF_2$ excimer emission by cycloheptene (Fig.2-16). This quenching process probably constituts a channel to the cycloaddition reactions of $DBMBF_2$ to cyclic olefins via triplex formation, it must be responsible for the observed monotonic increases of the reaction quantum yield with $DBMBF_2$ concentrations. As proposed in Scheme 3-3, the quantum yield of the cycloadduct formation (Φ_p) can be written as the sum of the quantum yields of cycloadduct from the exciplex (Φ_p^{exp}) and the triplex (Φ_p^{trp}), as shown by Eq.3-3*

* For derivation, see Appendix 3.

$$\Phi_p = \Phi_p^{exp} + \Phi_p^{trp}$$

$$= (Mk_{exp}[O]+Nk_{exm}[A])/(k_d^{mono}+k_{exp}[O]+k_{exm}[A]) \qquad (3\text{-}3)$$

where [O] and [A] stand for the concentration of the olefin and $DBMBF_2$, respectively; M and N are constants defined as follows.

$$M = k_p/(k_d^{exp}+k_p) \qquad (3\text{-}4)$$

$$N = \{k_p'/(k_d^{trp}+k_p')\}\cdot\{k_{trp}[O]/(k_d^{exm}+k_{trp}[O])\} \qquad (3\text{-}5)$$

Eq.3-3 shows that Φ_p is a function of [A] at constant concentration of olefin, the slope of which will be positive when $N > [k_{exp}[O]/(k_d^{mono}+k_{exp}[O])]M$ and negative when $N < [k_{exp}[O]/(k_d^{mono}+k_{exp}[O])]M$. The decay rate constant ($k_d^{mono} = 3.7 \times 10^8\ s^{-1}$) of the $DBMBF_2$ monomer has been obtained from biacetyl quenching of $DBMBF_2$ fluorescence and the concentration of olefins ([O] = 1 M) is fixed in the experiments for Fig.2-22. By adopting the $DBMBF_2$ monomer fluorescence quenching rate constants (k_q in Table 2-4) as the k_{exp} and assuming $k_{exm} = 6 \times 10^9\ s^{-1}M^{-1}$, (calculated from Foster's method[135] upon an assumption that the have-value concentration c_h for the excimer formation is 0.06 M, k_{exm} =

$1/c_h\tau = 1/2.73 \times 10^9 \times 0.06 = 6 \times 10^9\ s^{-1}M^{-1}$) Eq.3-3 can be simplified as Eq.3-6 for **7** and Eq.3-7 for **8**, respectively.

$$\Phi_p = (0.21M+6N[A])/(0.58+6[A]) \qquad (3\text{-}6)$$

$$\Phi_p = (1.78M+6N[A])/(2.15+6[A]) \qquad (3\text{-}7)$$

Based on the quantum yields measured at [A] = 0.01 and 0.07 M for both olefins,* the corresponding M and N values can be calculated; M = 0.53, N = 0.04 for **7**, and M =0.13, N = 0.69 for **8**. The Φ_p as function of [A] thus calculated are shown in Fig.2-22 as dashed curve a for **7** and dashed curve b for **8**, which match the experimental curves reasonably well. As an additional proof for the reliability of the calculations stated above, the M values obtained from calculation match the values experimentally obtained as depicted below. At a low concentration of $DBMBF_2$, e.g., 0.01 M, the cycloadditions proceed mainly through the bimolecular exciplex pathway (see Table 3-1). In this case the M value (Eq. 3-4) is the limiting quantum yield of the cycloadduct formation. Actually, we have experimentally obtained the limiting quantum yields for both $DBMBF_2$-**7** and $DBMBF_2$-**8** systems (Fig.2-21). The experimental data (M = 0.50 for **7** and 0.14 for **8**)

---

*The experimentally obtained quantum yields for the cycloaddition reactions at [$DBMBF_2$]=0.01 M are 0.18 for **7** and 0.12 for **8** (Table 2-7); those at [$DBMBF_2$]=0.07 M are 0.115 for **7** and 0.20 for **8** (Fig.2-22).

Table 3-1. Calculated Contributions of Exciplex (Φ_p^{exp}) and Triplex (Φ_p^{trp}) Pathways To the Total Quantum Yields of the Cycloaddition of $DBMBF_2$ with **7** and **8** As the Functions of $[DBMBF_2]$.[a]

olefin		$[DBMBF_2]$ (M)					
		0.001	0.005	0.010	0.050	0.100	0.220
7	Φ_p^{exp}(%)	99.8	98.9	97.9	90.3	82.3	67.8
7	Φ_p^{trp}(%)	0.2	1.1	2.1	9.7	17.7	32.2
8	Φ_p^{exp}(%)	98.2	91.8	84.8	52.8	35.9	20.3
8	Φ_p^{trp}(%)	1.8	8.2	15.2	47.2	64.1	79.7

a. The concentration of olefin is fixed at 1 M.

coincide the calculated ones (M = 0.53 for **7** and 0,13 for **8**) perfectly.

The relative contributions of Φ_p^{exp} and Φ_p^{trp} to the total quantum yield Φ_p can also be estimated from Eq.3-6 and Eq.3-7 as listed in Table 3-1. As shown by the data in Table 3-1, the bimolecular exciplex formation remains always the major pathway of the photocycloaddition for $DBMBF_2$-**7** system, whereas for $DBMBF_2$-**8** system this gradually gives way to the triplex mechanism as [A] increases to above 0.06 M. In the extreme, for example, in saturated CH_3CN solutions ($[DBMBF_2]$ ≈

0.22 M) the contributions of Φ_p^{trp} are expected to be 32% and 80% for **7** and **8**, respectively. Furthermore, this analysis reveals the differences between $DBMBF_2$-**8** and $DBMBF_2$-**7** systems, i.e. in the former system, the excimer must be quenched by the olefin very efficiently ($ktrp[O] >> k_d^{exm}$) and the rate of cycloaddition from the triplex also must be fast ($k_p' >> k_d^{trp}$), whereas the rate of cycloaddition from the exciplex must be slow ($k_p << k_d^{exp}$). Indeed, **8** has been shown to be a strong quencher of the excimer emission ($k_q\tau$ = 6.77 M^{-1}). Substituting the $k_q\tau$ and N values into Eq.3-5,* and M value into Eq.3-4, we can get $k_p' = 3.8\ k_d^{trp}$ and $kp = 0.15k_d^{exp}$ (at [O] = 1 M), respectively. However, these relations mentioned above must be reversed for $DBMBF_2$-**7** system. Olefin **7** is a much weaker quencher for the excimer emission ($k_q\tau$ = 0.47 M^{-1}). By the same procedure of calculation, we now get $k_p' = 0.14k_d^{trp}$ and $kp = 1.13k_d^{exp}$ for **7**. Of interest is the fact that in the exciplex pathway, the rate of cycloaddition (k_p) is large for the less electron-rich olefin **7** ($kp = 1.13k_d^{exp}$) but small for the more electron-rich olefin **8** ($kp = 0.15k_d^{exp}$) with respect to the corresponding exciplex decay rates (k_d^{exp}). This can be rationalized by quoting a commonly observed

---

* The term $k_{trp}[O]/(k_d^{exm} + k_{trp}[O])$ in Eq.3-5 can be rewritten as $k_q\tau/(1 + k_q\tau)$ since $k_{trp} = k_q$, [O] = 1 M, and $k_d^{exm} = 1/\tau$.

phenomenon in donor-acceptor addition reactions which proceed by a bimolecular exciplex mechanism, i.e. increasing the extent of charge transfer within an exciplex generally impedes the cycloaddition process.[1] For example, decreases in quantum yield as the donor and acceptor become energetically more favorable electron transfer partners have been recorded from cycloaddition reactions of *trans*-stilbenes with α,β-unsaturated esters,[157,158] cyanobenzene with olefins,[159] and N-methylphthalimide with olefins.[160] A hypothesis was therefore proposed[1] that cycloaddition from exciplex intermediates is inherently a non-ionic process, which is also supported by the solvent dependence of several donor-acceptor photocycloaddition reactions.[161,162] Namely, nonpolar solvents are found to be more favorable to these reactions than polar ones. Therefore, a lower k_p could be expected for **8** (IP =8.87 eV) and a higher k_p for **7** (IP = 9.45 eV) due to the non-ionic character of donor-acceptor cycloaddition from bimolecular exciplex intermediates.

3-2-3 Energetics in $DBMBF_2$-donor Interactions

Viewing the interactions of singlet excited state $DBMBF_2$ with various donors, one can find a relation between the reaction patterns and the energetics of the donor-acceptor pairs. When a complete electron transfer process is fairly endergonic (ΔG^o > +0.1 eV, e.g. **7**, **25**, **27**) cycloaddition reactions resulted mainly from the bimolecular exciplex. In the region of -0.4 eV < ΔG^o < +0.1 eV (e.g. **8**, **12**, **30**) the

triplex formation becomes the major pathway at high concentration of $DBMBF_2$ (> 0.06 M). Nevertheless, once the electron donating ability of donor olefins further increases to very exergonic region (ΔG^o < -0.4 eV, e.g. **1**, **2**, **3**) the donor-acceptor cycloaddition reactions vanish and cation radical mediated self-dimerizations take place instead, which has been proposed to be initiated by the direct formation of SSIP *via* an electron transfer process within encounter complexes (section 3-3). A general illustration shown in Scheme 3-4 summarizes the possible pathways* of $DBMBF_2$-donor interactions and their chemical consequences. Obviously, the fate of the reaction is decided by the relative significance

Scheme 3-4:

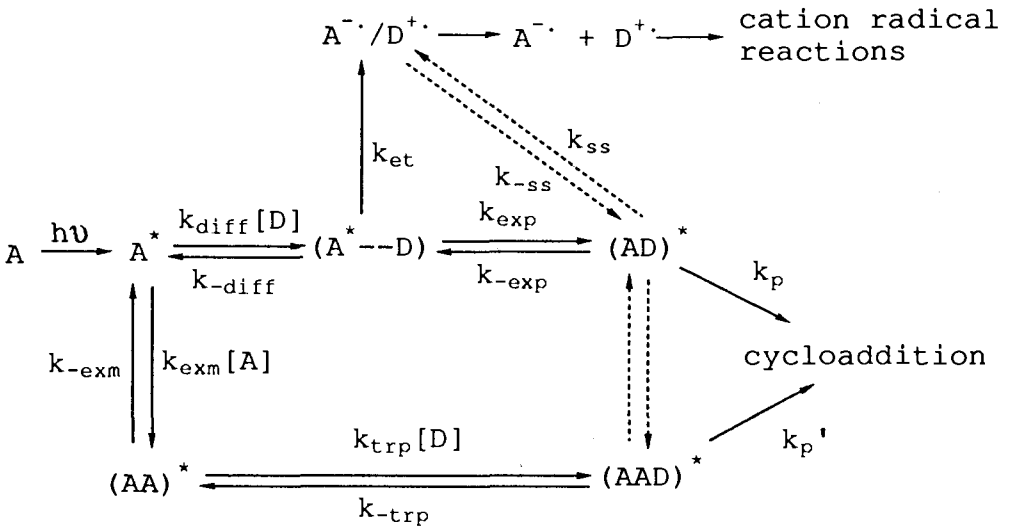

A = $DBMBF_2$; A^* = singlet excited state $DBMBF_2$;
D = donor olefin; $(A^*\text{--}D)$ = encounter complex;
$(AD)^*$ = exciplex; $(AA)^*$ = excimer;
$(AAD)^*$ = triplex; k = rate constant; $A^{-\cdot}/D^{+\cdot}$ = SSIP.

* The radiative and radiationless decay process of the excited species in Scheme 3-5 are omitted for simplicity.

of the rate constants of various processes given in Scheme 3-4, and therefore governed by the energetic feature of the donor-acceptor pair. For acyclic olefins, $k_{exp} >> k_{et}$ and $k_p >> k_p'$, the major pathway is the formation of exciplex from which donor-acceptor cycloadditions occur. In the case of cyclic olefins, $k_{et} << k_{exm}[A]$, and k_p' becomes competitive with k_p, i.e. the triplex channel is opened. However, when strong electron donors are involved, $k_{et} >> k_{exp}$; $k_{et} >> k_{exm}[A]$, a complete electron transfer predominates resulting in cation radical reactions of the donor olefins. In Scheme 3-4 we draw dashed arrows between (AD)* and (AAD)* because it is an assumed process with no experimental evidence. On the other hand, the direct traffic between (AD)* and $A^{-}\cdot/D^{+}\cdot$ is also designated by dashed arrows due to $k_{ss} << k_{et}$ for strong donors. As will be discussed in Section 3-3, the monochromatic photolyses of $DBMBF_2$ in the presence of very electron-rich olefins, i.e., **1**, **2**, and **3**, lead to a conclusion, exactly the same as the one suggested by Farid,[188] that the electron transfer quenching of the free acceptors does not proceed *via* the intermediacy of a contact ion pair but resulted in the formation of the solvent separated ion pair directly.

As stated above, the ΔG^{o} value for a D-A pair is crucial in determining the reaction pathway. A complete electron transfer approaches diffusion controlled constant and may become the major pathway when ΔG^{o} goes down below -0.4 eV, which is predicted by the well known Rehm-Weller relation

[89,90] and also demonstrated to be the case in $DBMBF_2$-diene (**1**, **2**) systems. As a comparison, these dienes do undergo 2+2 cycloaddition reaction in CH_3CN *via* an exciplex mechanism with 1- or 2-cyanonaphthalene ($E^{red}_{1/2}$ = 1.98, V),[163] and 9,10-dichloranthracene ($E^{red}_{1/2}$ = 1.51 V),[164] which are electron acceptors weaker than DBMBF2 ($E^{red}_{1/2}$ = 1.30 V).

On the other hand, while $DBMBF_2$-olefin cycloaddition reactions proceed well in the endergonic region (ΔG^o > +0.1 V), we still don't know the upper limit of ΔG^o for the cycloaddition reactions. Presumably, the rate of the cycloaddition reactions is determined by the rate of exciplex formation (k_{exp} in Scheme 3-4) if ΔG^o is positive. Further increases in ΔG^o are expected to lower the rate of exciplex formation as indicated by the very low $DBMBF_2$ fluorescence intensity quenching rate constants and consequently lower the yield of the cycloaddition reaction. Once the ΔG^o value becomes so positive that the exciplex formation can no longer competes with other decay processes of singlet excited state $DBMBF_2$, the cycloaddition reaction vanishes. Perhaps the failure of cycloaddition between $BABF_2$ and 3,3-dimethy-1-butene (**7**) can give a rough idea about how positive the ΔG^o value should be to stop the donor-acceptor cycloaddition by assuming that singlet excited state of $DBMBF_2$ and $BABF_2$ have similar lifetimes. The oxidation potential of **7** is estimated to be 2.49 V from its vertical ionization potential (IP = 9.45) by the correlation[101] of $E^{red}_{1/2}$ with IP. The singlet

excited state energy (E_s) of $BABF_2$ is c.a. 79 Kcal/mol (3.43 eV) estimated from its absorption spectrum. Therefore, the ΔG^o value of a PET process for $BABF_2$-**7** system is ~0.8 V as calculated from Eq.2-1.

3-3 $DBMBF_2$ Sensitized Cation Radical Reactions

3-3-1 The Valence Isomerization of QC and NBD

The isomerization of QC and NBD *via* intramolecular valence rearrangement has been extensively studied due to its unique reaction pattern and significant mechanistic interests. At the early stage of studies, it was found that if the sensitized isomerization of QC and NBD is energy transfer in nature, triplet sensitizers only promote the isomerization of NBD to QC[165,166] whereas singlet sensitizers favor the isomerization in the reverse direction of QC to NBD.[167] The striking influence of multiplicity of the sensitizer involved has been rationalized in terms of the distinction in the structure of intermediates resulted from singlet and triplet sensitizations.[168] In early 80's, the involvement of PET in the isomerization of QC and NBD in the presence of an electron acceptor-sensitizer, e.g. cycanoaromatics and TCB, was proved by a series of work.[5,23,108,169-178] Generally, the isomerization under PET conditions proceeds predominantly (in the cases of cyanoaromatics sensitization)[23,108] or only (in the case of TCB sensitization)[109] from QC to NBD.

Our observation in the isomerizations of QC and NBD sensitized by acetylacetone and β-diketonatoboron difluoride ($AABF_2$ and $DBMBF_2$) is fully consistent with the reaction patterns mentioned above. From energetic point of view (Table 2-13), the energy transfer from acetylacetone (E_T = 69 - 74 Kcal/mol)[41] to NBD (E_T = ~70 Kcal/mol) is feasible and hence promotes the isomerization from NBD to QC in analogy to acetone or acetophenone sensitization.[166] On the other hand, an energy transfer from singlet $AABF_2$ (E_S < 86 Kcal/mol)* or $DBMBF_2$ (E_S = 73 Kcal/mol) to QC (E_S > 95 Kcal/mol)* seems impossible. As we have proven the PET characters of $DBMBF_2$ fluorescence quenching by QC and NBD, the isomerization from QC to NBD must be promoted by the PET from QC and NBD to $AABF_2$ or $DBMBF_2$ and mediated by the cation radicals of the donors.

As shown by the data in Table 2-13, the negative free enthalpy changes (ΔG^o) in $AABF_2$ and $DBMBF_2$ sensitizations indicate exergonic PET reaction for both systems. The efficiency (Φ) of the isomerization on sensitization by $AABF_2$ or $DBMBF_2$ is reduced with the change of solvent from CD_2Cl_2 (Φ = 0.06 - 0.07) to more polar CD_3CN (Φ = 0.02), in agreement with the solvent effects found in 1-CN-Np sensitizations.[172] The lack of isomerization from NBD to QC in $AABF_2$ and $DBMBF_2$ sensitizations can be explained by quoting the difference in potential energy of the cation radical

---

* Estimated from the corresponding absorption spectra in CH_3CN.

species.[109] The potential energies of ion radical pairs (E_{IRP}) produced in an electron transfer reaction can be calculated by Eq.3-8, where E_D^{ox} and E_A^{red} are the oxidation potential of

$$E_{IRP} = E_D^{ox} - E_A^{red} + \Delta E_{coul} \qquad (3\text{-}8)$$

the donor and the reduction potential of the acceptor, respectively; and ΔE_{coul} is the solvent stabilization energy for ion separation (-0.06 eV in CH_3CN).[91,92] The potential energies of species involved in the $DBMBF_2$ sensitized QC-NBD

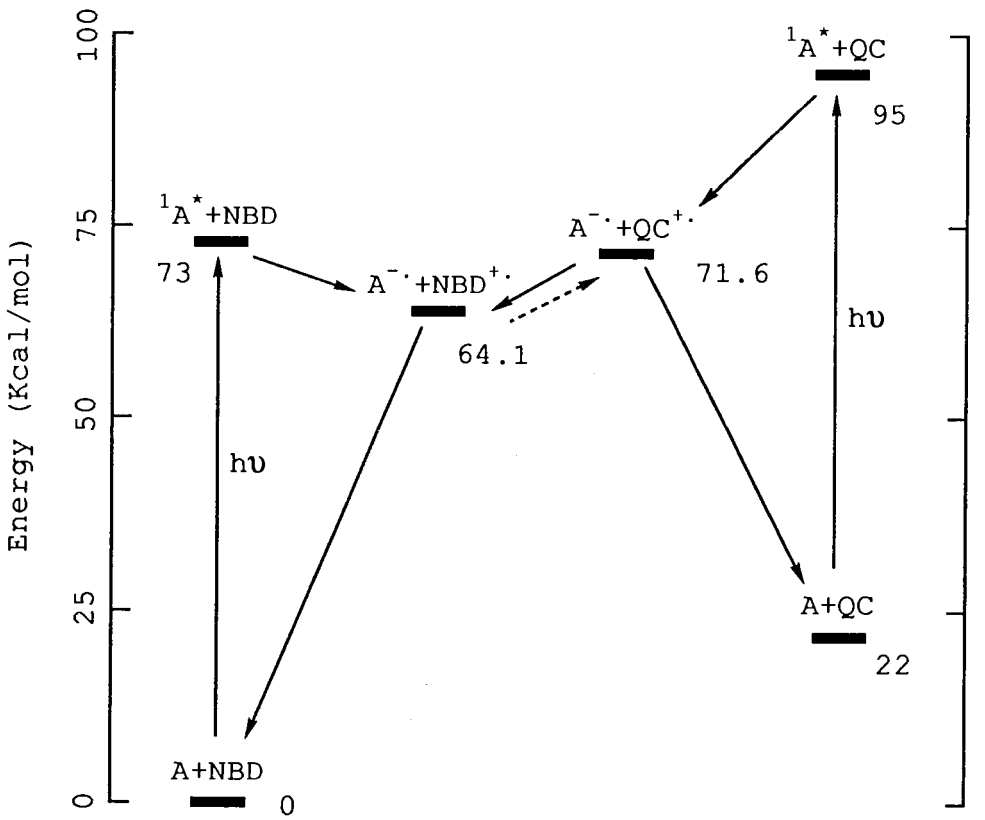

Figure 3-2, Energy levels of relevant species in the $DBMBF_2$ sensitized isomerization of QC and NBD.

isomerization are given in Fig.3-2, in which an energy gap of 22 Kcal/mol for ground state QC and NBD is adopted.[109] The energy of $QC^{+\cdot}$ lies at least 7.5 Kcal/mol above that of $NBD^{+\cdot}$. This energy difference is sufficient to account for the substantially different interconversion rates of the two cation radical species.

However, a notable difference of 1-CN-Np sensitization from $AABF_2$ or $DBMBF_2$ sensitization is that the isomerization from NBD to QC also occurs in the former though with a much lower efficiency (Φ = 0.01) than the isomerization from QC to NBD (Φ = 0.1).[108] The course of isomerization in 1-CN-Np sensitization has been rationalized by a mechanism involving an intersystem conversion to triplet ion radical pair[109] which

Scheme 3-5:

$$^1A + NBD \longrightarrow {}^1\overline{A^{-\cdot} + NBD^{+\cdot}} \quad (1)$$

$${}^1\overline{A^{-\cdot} + NBD^{+\cdot}} \rightleftharpoons {}^3\overline{A^{-\cdot} + NBD^{+\cdot}} \quad (2)$$

$${}^1\overline{A^{-\cdot} + NBD^{+\cdot}} \longrightarrow A + NBD \quad (3)$$

$${}^3\overline{A^{-\cdot} + NBD^{+\cdot}} \longrightarrow A + {}^3NBD \quad (4)$$

$$^3NBD \longrightarrow QC \quad (5)$$

is shown in Scheme 3-5 where A denotes the electron acceptor-sensitizer. The energy of the ion radical pair (79.8 Kcal/mol) generated by PET from NBD ($E^{ox}_{1/2}$ = 1.54 V) to 1-CN-Np ($E^{red}_{1/2}$ = -1.98 V) lies well above the triplet states of both

the donor (E_T = 70 Kcal/mol) and the acceptor (E_T = 57 Kcal/mol)[174,175] so that the triplet recombination (step 4 in Scheme 3-5) is energetically feasible. In contrast, the energy (64.1 Kcal/mol) of the ion radical pair generated by PET from NBD and DBMBF2 ($E^{red}_{1/2}$ = -1.30 V) is lower than the triplet state energy of NBD (70 Kcal/mol). The triplet recombination in $DBMBF_2$-NBD system, and consequently the formation of QC (step 5 in Scheme 3-5) are prohibited. Nevertheless, this argument is not applicable to $AABF_2$-NBD system where the energy of resulted ion radical pair is high (75.2 Kcal/mol). The lack of the isomerization from NBD to QC could presumably be due to an inefficient intersystem crossing (step 2 in Scheme 3-5).

3-3-2 "Diels-Alder" Reactions of Conjugated Diene 1 and 2 Sensitized by $DBMBF_2$

Cation radical mediated "Diels-Alder" reaction of two electron-rich dienes, **1** and **2**, have received much attention during the last decades,[1,10,176] and could become a potent synthetic method.[177,178] These reactions, distinct from the corresponding acid catalyzed Diels-Alder in terms of product structures, can be initiated either thermally by *tris*-(4-bromophenyl)aminium hexachloroantimonate (BAHA) [10,112,176,180] or photochemically by PET[9,10,11,114,181] (Scheme 3-6, and 3-7).

Data in Table 2-15 show that the "Diels-Alder" dimerization of **1** can be achieved by the sensitization of β-

diketonatoboron difluorides and other electron acceptor-sensitizers which have not been examined in previous work. While BAHA catalyzed and DCN-An sensitized dimerization give no dimer **66** but only **65**,[10] trace or appreciable amounts of **66** were detected in our experiments. Since dimer **66** is the product of protic acid catalyzed reaction which is claimed at least 100 times faster than the corresponding electron transfer pathway leading to the formation of **65**,[10] the appearance of **66** in PET conditions could be the result of the thermal reaction catalyzed by trace of photogenerated acids in the systems. The data also shows a correlation between the electron acceptabilities of sensitizers and the efficiency of the dimerization. Namely, the efficiency increases as the sensitizer becomes stronger electron acceptor regardless the multiplicity of excited state. As this type of cation radical mediated dimerization catalyzed by BAHA has been proved to be

Scheme 3-6:

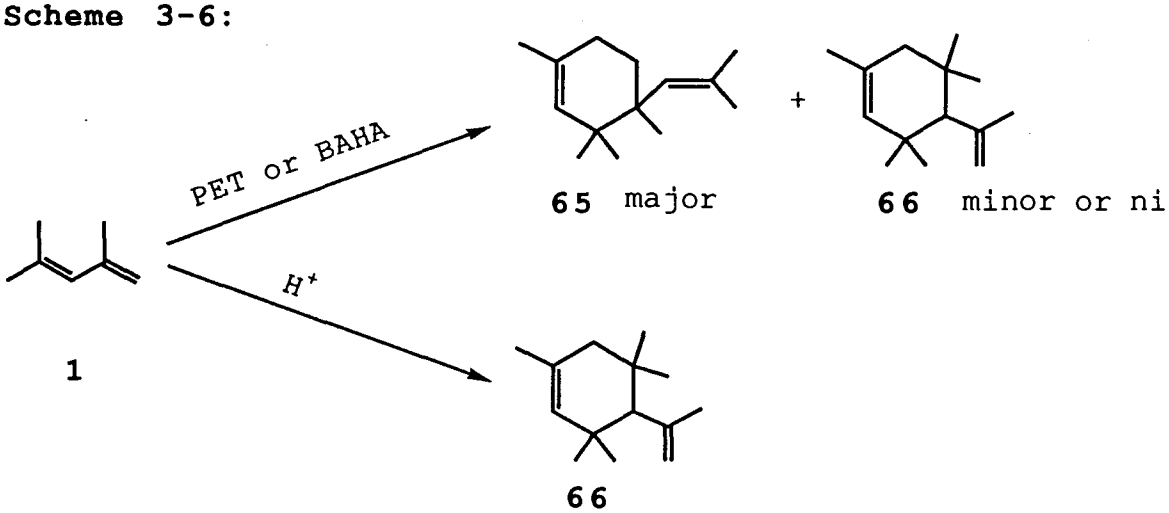

Scheme 3-7:

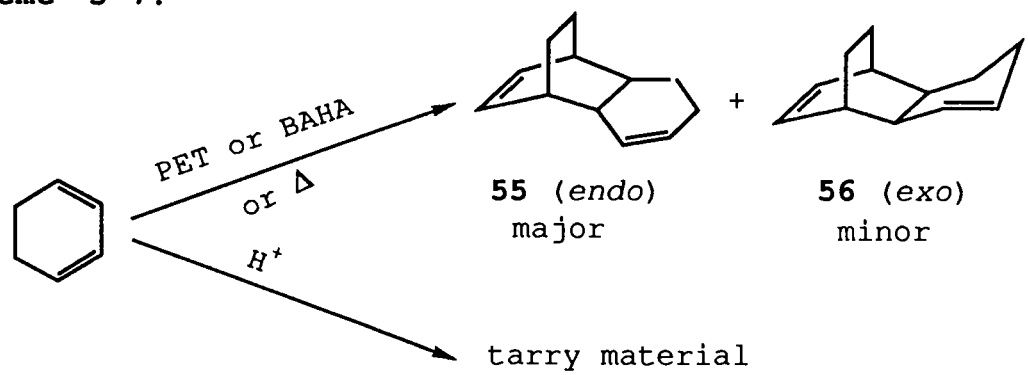

Scheme 3-8:

D = **1**, **3**; D_2 = dimer; A = sensitizer

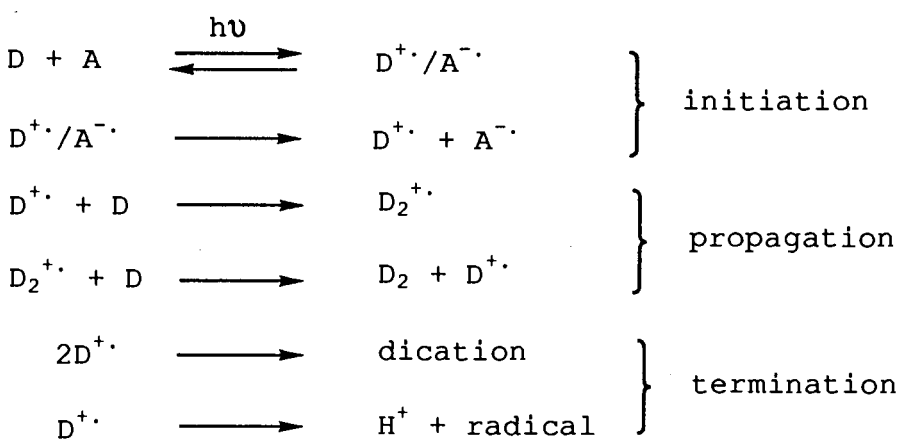

a chain reaction,[100] we assume that the formation of **65** in PET conditions also arises from a similar chain mechanism shown in Scheme 3-8.

Though the role of the anion radical of sensitizers ($A^{-}\cdot$) in the chain mechanism remains still unknown, the correlation with the reduction potentials of sensitizers seems to imply

that efficiency of the dimerization is mainly decided by the chain initiation step. This chain initiation step involves a predominate formation of solvent separated radical ion pairs rather than the formation of contact radical ion pairs, on which a detailed discussion will be given later on (section 3-3-3).

In the PET induced "Diels-Alder" reactions of **2**, the formation of dimer **55** (major product) and **56** is almost exclusive in the cases of $DBMBF_2$, $BABF_2$, TCB, DCN-Np, or DCN-An sensitizations, whereas the products are accompanied by the formation of appreciable amounts of the 2+2 dimers **57** and **58** when 1-CN-Np, 1-CN-Ph, or DDB is used (Table 2-14). Apparently, the 2+2 dimers are mainly derived from the

Scheme 3-9:

D = **2**; D_2 = 2+4 dimers; A = sensitizer

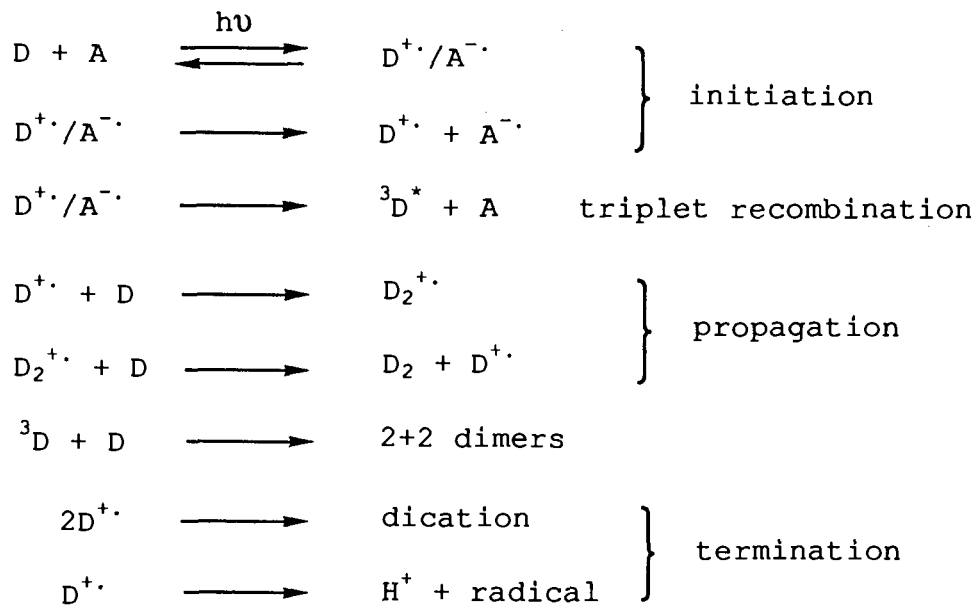

triplet diene reactions which can be generated by a triplet sensitization (e.g. in benzophenone sensitization). However, an additional route leading to triplet **2** can be envisaged by triplet recombination (or back electron transfer) as we have seen in the valence isomerization of QC and NBD (Scheme 3-5). Indeed, triplet recombination has been demonstrated to be responsible for the formation of **57** and **58** in the dimerization of **2** sensitized by 1,4-dicyanobenzene.[115] Therefore, the formation of the 2+2 dimers in 1-CN-Np, and 1-CN-An sensitizations might be attributed to the triplet recombination (Scheme 3-9) of the donor-acceptor ion radical pair though we can not completely rule out the competition of direct triplet energy transfer from triplet excited state sensitizers to the diene.

In an ideal circumstance, the formation of triplet **2** *via* a triplet recombination is determined by the rate of the back electron transfer within the sensitizer$^{-\cdot}$ - **2**$^{+\cdot}$ pair and therefore correlates to the free enthalpy change of triplet recombination, ΔG^{o}_{-et}. Consequently, some sort of correlation between ΔG^{o}_{-et} and the product ratio, **(57+58)/(55+56)** should hopefully presents itself. The ΔG^{o}_{-et} can be estimated by Eq.3-9[13,182] where $(E_T)_D$ and E_D^{OX} stand

$$\Delta G^{o}_{-et} = (E_T)_D - E_D^{OX} - E_A^{red} \qquad (3\text{-}9)$$

for the triplet energy (2.27 eV)[88] and oxidation potential (1.35 eV)[95] of **2**, respectively; and E_A^{red} for the reduction potential of sensitizers. Indeed, a rough correlation for the singlet sensitizers can be seen from the data listed in Table 3-2. The triplet recombination becomes competitive with

Table 3-2. Product Distribution and Free Enthalpy Change in PET Induced Dimerization Reactions of 1,3-Cyclohexadiene in Acetonitrile.

sensitizer	E_A^{red} (V)	ΔG^o_{-et} (eV)	**(57+58)/(55+56)** %
1-CN-Np	-1.98	-1.06	20.5
1-CN-Ph	-1.88	-0.96	15.3
$BABF_2$	-1.71	-0.79	0.0
$DBMBF_2$	-1.30	-0.38	0.0
DCN-Np	-1.28	-0.36	0.0
DCN-An	-0.89	0.02	0.0
DDB	-0.45	0.41	22.5
TCB	+0.02	0.94	0.3

respect to the separation of free radical ions (Scheme 3-9) when ΔG^o_{-et} decreases to below -0.9 eV (1-CN-Np and 1-CN-Ph sensitizations). On the other hand, in the cases of two triplet sensitizers TCB (E_T = 2.70 eV)[23] and DDB, the triplet recombination is energetically prohibited. Therefore, the 2+2 dimers **57** and **58** must arise from an efficient energy transfer

which is in competition with the primary electron transfer process (the first initiation step in Scheme 3-9).

3-3-3 PET Induced Dimerization of 3 and Corresponding Cycloreversions

In comparison with **1** and **2**, the PET induced dimerization of *trans*-anethole (**3**) had not been reported until two papers[7,8] emerged in December 1988, shortly after we finished the investigation. While our observations in the reaction pattern agree with those reported, our discussion will focus on some mechanistic features viewed from different directions.

Our first conclusion that the PET induced dimerization of **3** is a concerted process is based on the simple principle of microscopic reversibility. The $DBMBF_2$ sensitized cycloreversions of either **21** or **22** under PET conditions ($DBMBF_2$ sensitization) resulted in the formation of **3** with

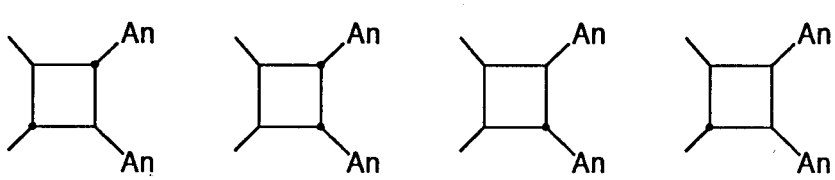

21 **22** **a** **b**

absolutely no formation of either *cis*-anethole or the 2+2 dimers **a** and **b** that are expected to be thermally more stable than **22**; these two cyclobutanes would have been formed by a rapid single bond rotation if the cycloreversion and cycloaddition had underwent by a stepwise mechanism.

Therefore the cation radical mediated dimerization most likely follow a concerted mechanism leading to the formation of **21** and **22**. A similar conclusion has been made for the dimerization of **3** *via* thermally induced electron transfer on the basis of theoretical calculations,[183] and also in the 9-CN-An sensitized PET dimerization of **3** on the basis of by-product analysis.[8]

As shown by Scheme 3-10, the formation of free ion radical species (FIS) is the consequence of ion separation from solvent separated ion radical pair (SSIP). However, SSIP can be formed *via* two pathways,[24,184] either directly from the encounter complex or from contact ion radical pair (CIP) derived from exciplex. An alternative way to CIP is the excitation of the charge transfer (CT) complex of ground state D and A, which has been first theoretically predicted[85] and then experimentally verified.[185-187] Therefore, the relative importance of each pathway with respect to FIS formation can be estimated by comparison of quantum yield of FIS obtained from selective irradiation of monomeric acceptor and the CT complex, respectively.[188] In $DBMBF_2$-**3** system the quantum yield of **21** resulted from the irradiation of $DBMBF_2$ is found about 100 times larger than that obtained from irradiation of the CT complex of $DBMBF_2$ and **3** (Table 2-16). This observation strongly suggests that neither the exciplex nor the excitation of CT complex but the direct formation of SSIP from the encounter complex of excited state $DBMBF_2$ with **3** is responsible for the PET induced dimerization of **3**.

Scheme 3-10.

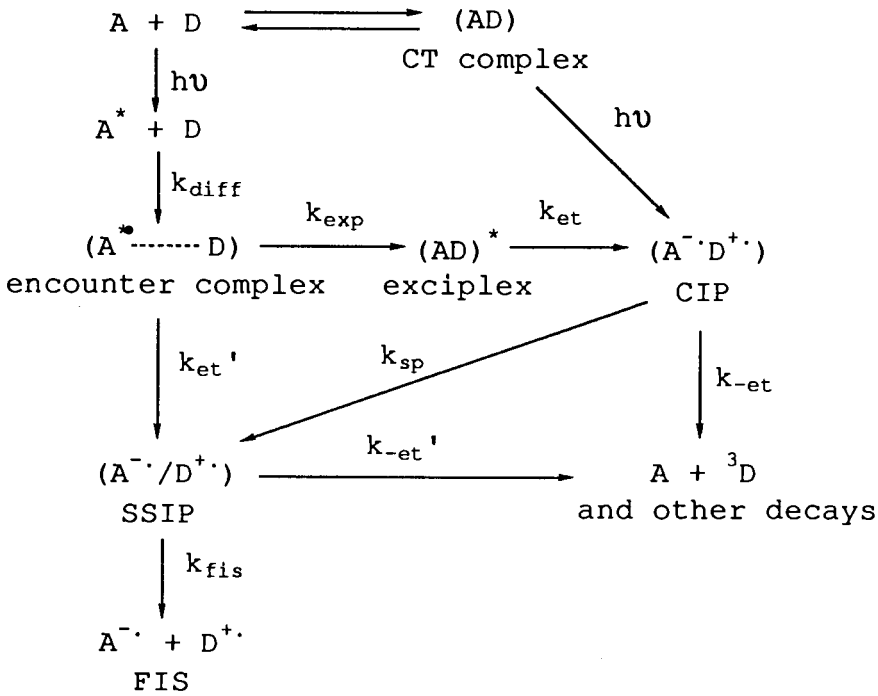

Since the encounter complex is known to be *en route* to exciplex, the observation mentioned above implicates that the primary electron transfer from D to A* within the encounter complex (k_{et}') is fast enough to compete with the exciplex formation (k_{exp}). Such an electron transfer must occur over a distance of ~7 Å, the center-to-center distance suggested for encounter complex in polar solvents.[184] However, few reports for the direct formation of SSIP as the major reaction pathway in intermolecular systems have been seen.[188,193] In our work we find that this is the case not only for $DBMBF_2$-**3** system but also for other two $DBMBF_2$ systems where **1** and **2** are the donors (Table 2-16). Both **1** and **2** can form CT complexes (referred as GSC) with $DBMBF_2$ in CH_3CN as evidenced by the absorption spectra (3-1-2). Irradiation of these CT

complexes do not give any detectable amount of dimers (**55**, **56**, and **65**, **66**) but irradiations of $DBMBF_2$ do. The nil importance of CIP found for the three PET induced cation radical reactions perhaps implies the commonality of the direct formation of SSIP as the major reaction pathway for favorable electron donor-acceptor pairs. This results also support the assumed SSIP mechanism for $DBMBF_2$ fluorescence quenching by **1**, **2**, **3**, and other electron donors with IP < 8.4 eV (see Section 3-1-3, Fig.3-1).

This fact also furnishes a better understanding of the correlation of the yield of triplet recombination products with corresponding ΔG°_{-et} values in the PET induced dimerization of **2** (Table 3-2). The increase in ΔG°_{-et} has been concluded to be responsible for the diminishing of triplet recombination products **57** and **58** but hard to explain why the drop in the yield is so sharp within a rather narrow ΔG°_{-et} range (-0.96 to -0.79 eV). Considering the triplet recombination has more chance $[k_{-et}/(k_{-et} + k_{sp}) + k_{-et}'/(k_{-et}' + k_{fis})]$ to occur in a reaction *via* exciplex formation than that $[k_{-et}'/(k_{-et}' + k_{fis})]$ in a reaction *via* the direct formation of SSIP, the sharp drop may be an indication of change in the reaction mechanism. Namely, the weaker acceptors 1-CN-Np and 9-CN-Ph might react with the donor olefin mainly *via* exciplex whereas better acceptors $BABF_2$, $DBMBF_2$, DCN-Np, and DCN-An *via* a direct formation of SSIP.

3-4 Related Photoreaction of Acetylacetone

3-4-1 Dimerization

The photodimerization of acetylacetone can be visualized as a special case of the de Mayo reactions: an excited acetylacetone molecule (most probably in the triplet manifold)[41,42,104,194,195] cycloadds to a ground state acetylacetone molecule giving the cyclobutane intermediate followed by a spontaneous ring opening process and then a furanoid ring closure as shown in Scheme 3-11. Of particular interest is that only **70** out of many possible stereoisomers is obtained. The 2+2 cycloaddition of excited and ground state acetylacetone molecules most likely proceeds through a polar interaction, a mechanism commonly assumed for de Mayo reactions.[142,196] By assuming the hydrogen bond of enolized acetylacetone is kept intact during the reaction, a head-to-head arrangement of two reaction partners is required by the opposite polarization (Scheme 3-11) of electron density along the double bonds in π-π^* excited and ground state molecules, which has been predicted by theoretical MO calculations.[197] The parallel and *anti*-parallel orientations are two possible approaches that should give rise to the cyclobutane intermediates **a** and **b**, respectively, both of which lead to a same acyclic intermediate **c**. The ring closure of **c** produces only dimer **70** but not its epimer **d** due presumably to the high conformational energy of the transition state leading to the latter. The epimerization from **70** to **d** should be slow in the

presence of H^+; this is the reason why methyl ether **71** with configuration retention is quantitatively obtained under acidic condition.

Scheme 3-11.

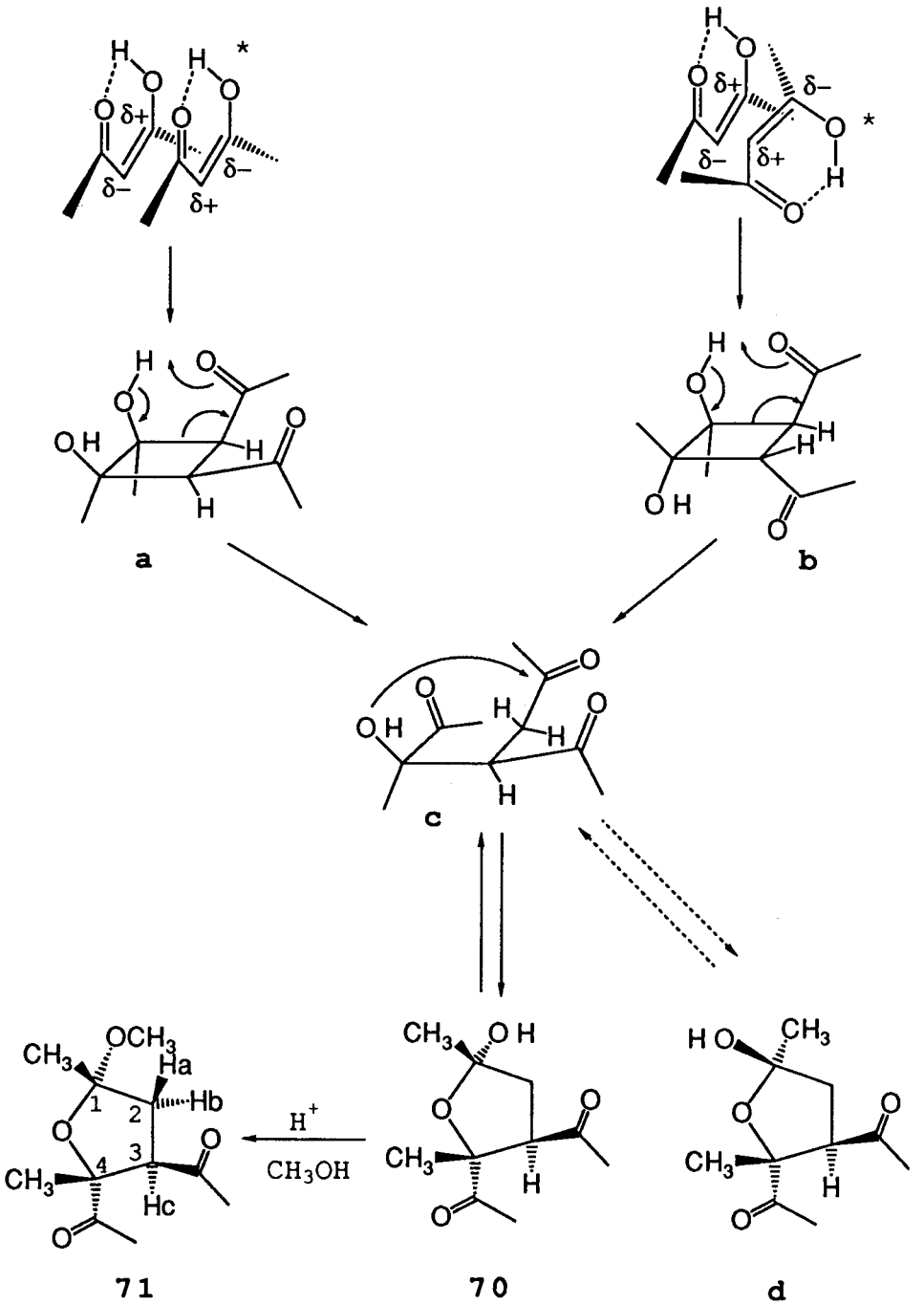

3-4-2 Cycloaddition with Norbornene

The triplet energies are 69 - 74 Kcal/mol for acetylacetone[41] and 72 Kcal/mol for norbornene.[198] A reversible energy transfer is therefore expected to coexist with the cycloaddition reaction in the photoreactions of acetylacetone-norbornene system. This has been confirmed by the appearance of norbornene dimers (**80, 81**) and solvent addition products (**78, 79**) as the byproducts of the cycloaddition reaction under conditions virtually all the incident light is absorbed by acetylacetone. A question therefore arises: which excited state species is responsible for the cycloaddition reaction? The 1,3-pentadiene quenching efficiency (Fig.2-38) for the cycloadduct (**75**) formation ($k_q\tau$ = 12.9 M^{-1}) is close to that for the acetylacetone-cyclohexene adduct (**42**) formation ($k_q\tau$ = 7.2 M^{-1}) but much different from that for norbornene dimer (**80** + **81**) formation ($k_q\tau$ = 150 M^{-1}). The notable discrepancy in $k_q\tau$ values for **75** formation and the norbornene dimer formation clearly indicates that they do not originate from a same excited state species. In another word, the triplet excited state norbornene is involved in the dimerization of itself[209,210] but not in the cycloaddition with acetylacetone. Worthwhile to mention is that the low $k_q\tau$ values for both **75** and **42** formations seems to disagree the involvement of triplet acetylacetone in the de Mayo reaction, a mechanism previously proposed.[41,42,104,194,195] Therefore, we rather assume that an unknown excited state acetylacetone is responsible for the

unknown excited state acetylacetone is responsible for the cycaddition reactions upon which a mechanism is proposed in Scheme 3-12 where A and N denote acetylacetone and norbornene, respectively. The mechanism has been simplified by assuming either A^* and N^3 have roughly the same lifetime or the unimolecular decays of A^* and N^3 are negligible due to very fast bimolecular interactions in the presence of large amounts of ground state reactants. Based on this, one can predict that the quantum yield of **75** (Φ_{add}) should be

Scheme 3-12:

$$A^* + N \xrightarrow{k_{add}} \mathbf{75}$$

$$A^* + N \underset{k_{-1}}{\overset{k_1}{\rightleftharpoons}} A + N^3$$

$$N^3 + N \xrightarrow{k_{dim}} \text{dimers}$$

proportional to the concentration of norbornene as has been observed (Fig.2-40). Furthermore, (Eq.3-9)* derived according to the mechanism (Scheme 3-12) reveals that the ratio of quantum yields for the **75** formation (Φ_{add}) and norbornene dimer formation (Φ_{dim}) is proportional to the concentration

$$r = \Phi_{add}/\Phi_{dim} = \frac{dP}{dt} \Big/ \frac{dD}{dt} = \frac{k_{add}}{k_1} + \frac{k_{add}k_{-1}[A]}{k_1 k_{dim}[N]} \qquad (3\text{-}9)$$

* For derivation, see Appendix 4.

of acetylacetone and to the reciprocal concentration of norbornene. This is also experimentally found to be true (Fig.2-39, 2-40). As indicated by the intercept (1.2) and slope (21 M^{-1}) obtained from the plot of r value (yield of **75**/yield of dimers) *vs.* acetylacetone concentration (Fig.2-39), the rate constant of cycloaddition (k_{add}) is close to the rate constant of energy transfer ($k_1 = 0.83\ k_{add}$) whereas the rate constant of norbornene dimerization (k_{dim}) is much slower than the rate constant of the reverse energy transfer from triplet norbornene to acetylacetone ($k_{-1} = 8.8\ k_{dim}$). Assuming the triplet energy gap between acetylacetone and norbornene is zero, the rate constant of energy transfer in hexane can be estimated by the theoretical calculation:[88,199] $k_1 = k_{-1} = 0.5\ k_{diff} = 1.1 \times 10^{10}\ s^{-1}M^{-1}$. On the basis of this assumption the rate constants for the cycloaddition (k_{add}) and the dimerization (k_{dim}) are calculated to be 1.3×10^{10} and $1.3 \times 10^{-9}\ s^{-1}M^{-1}$, respectively. According to the intercept and slope of Eq.3-9 obtained from Fig.2-39, r value should be a function of norbornene concentration presented by Eq.3-10, if the concentration of acetylacetone is fixed at 0.052 M. The

$$r = 1.2 + 0.55/[N] \qquad (3\text{-}10)$$

dashed curve in Fig.2-40 is calculated from Eq.3-10, showing a good agreement with the experimental data.

The cycloaddition reaction of acetylacetone with norbornene proceeds most likely by the mechanism for the de

Mayo reactions (Scheme 1-2). The *cis-exo* configuration of the sole adduct **75** is determined by the intermediacy of the cyclobutane and the steric effects.[146,200] Though the *trans* isomer **83** is obviously thermally more stable than **75**, it is not formed in the cycloaddition but readily formed from acid-catalyzed epimerization of **75**. The failure to obtain Aldol condensation products from **75** is due not only to the fast epimerization but also to the much higher activation energy required by the transition state leading to the *cis*-fused multicyclic compounds (Scheme 3-13). This is because that a twisting around C_2-C_3 bond of norbornene frame is required by the favorable chair conformation of the cyclohexanone moiety in the transition state **a**. Such a twisting will increase its potential energy in comparison with that in transition state **b** where no such twisting is needed.

Scheme 3-13:

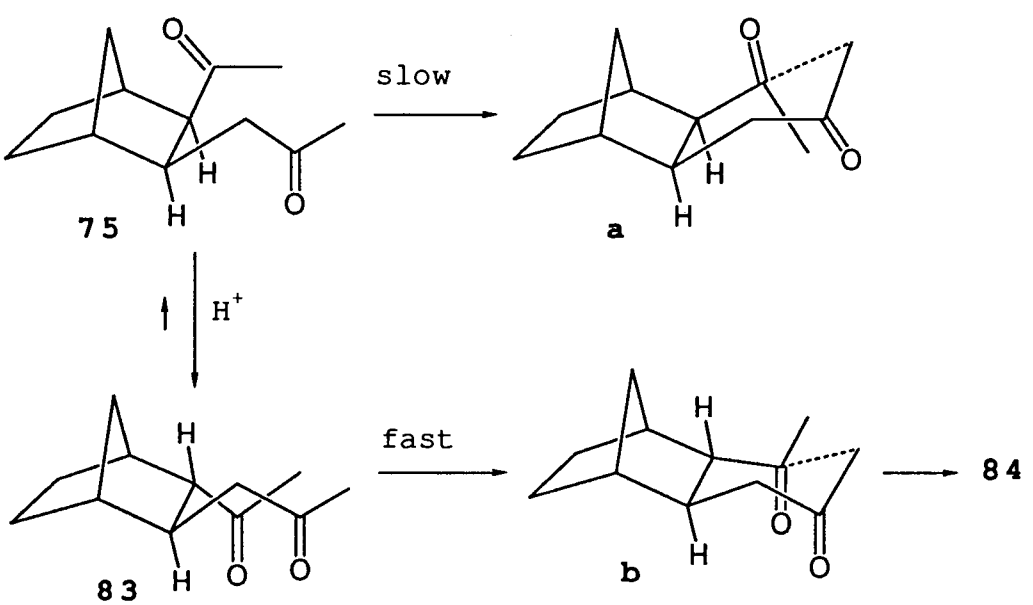

3-4-3 Solvent Addition

Acetylacetone can act as a triplet sensitizer as we have seen in the sensitized valence isomerization of NBD to QC (3-3-1) and in the energy transfer from excited state acetylacetone to norbornene to give byproducts such as **80**, **81**, and minor amounts of solvent (hexane-norbornene) addition products **78** and **79**. However, solvent addition products turn out to be the major products when other solvents are used (those listed in column 1 in Table 2-17). Several triplet excited state sensitized solvent addition reaction of norbornene have been found scattered in literature, i.e. xylene sensitized addition of methanol,[198] acetophenone or xylene sensitized addition of CH_3CN,[122,201] and the photoaddition of acetone.[121] We found that acetylacetone or acetone sensitized photoaddition reactions of a number of solvents to norbornene give the adducts in high chemical yields. This type of reaction perhaps can serve as a convenient synthetic method for norbornane derivatives some of which are commercially useful, e.g. the adducts of 1,3-dioxolane (**88a**) have been used in the fragrance industry.[202]

A chain radical mechanism has been proposed for the addition reaction of CH_3CN and acetone,[122,198,201] which is supported by the observation that the addition reaction of acetone to norbornene can be thermally induced by peroxides.[203,204] The quantum yields far greater than unity for the acetylacetone sensitized solvent addition reactions found in our work (Table 2-18) provide a compelling evidence

for the chain mechanism proposed in Scheme 3-14. Triplet norbornene is generated by energy transfer from excited state acetylacetone (A) or acetone and undergoes hydrogen

Scheme 3-14:

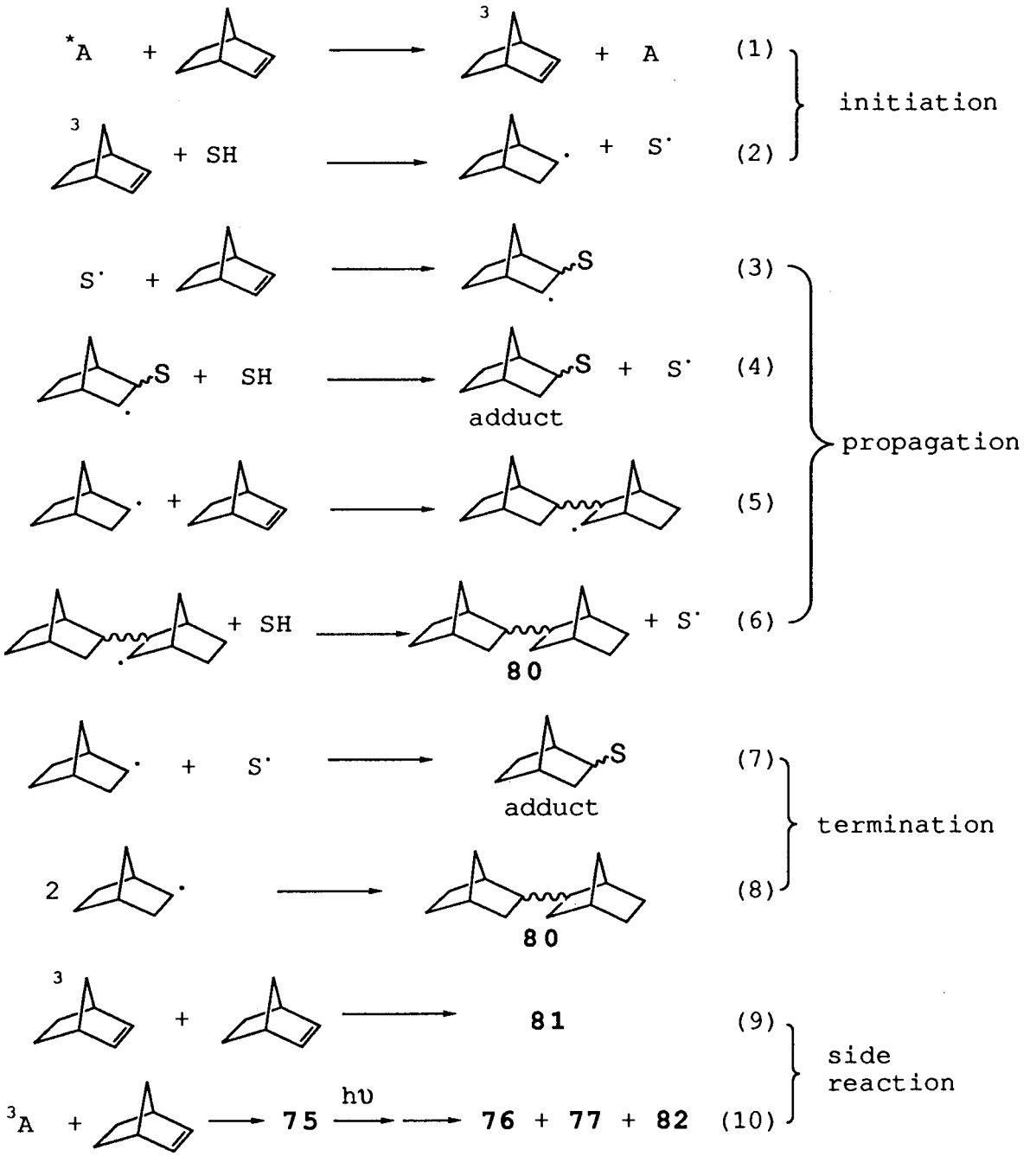

abstraction from the solvent (SH) in the chain initiation steps. The radical chain is operated with the solvent radical(S·) as the chain carrier (step 3 and 4). Step 5 and 6 probably constitute another chain propagation process leading to the formation of a byproduct **80**. There are several side reactions, i.e. steps 8, 9, 10, accounting for the formations of the byproducts. While none of the byproducts seems to have connection with the chain termination, we suggest that the combination of norbornene radical and S· (step 7) could be the major termination step, which most likely occurs within the solvent cage immediately after the hydrogen abstraction. This radical combination has been previously suggested to be one possible reaction pathway to the formation of CH_3CN addition product.[122,201] Moreover, the in-cage coupling (step 7) probably can be used to explain why only *exo* adducts are exclusively obtained from acetone, CH_3CN, CH_2Cl_2, and 1,1-dichloroethane but epimeric mixture are resulted for other solvents. For example, the two epimers from 1,2-dichloroethane are obtained with a yield ratio of 16/20. It is well known that ground state norbornene tends to be attacked preferentially from the *exo* side by various reagents including radicals.[146,205] However, this stereospecificity might be lost (or partially lost) in a coupling reaction of two radical species. Therefore, the formation of significant amount of *endo* adduct could be an indication of the importance of the in-cage coupling for certain solvents, e.g. 1,2-dichloroethane.

The addition of CH_3CN to norbornene was reported to be initiated by silver(I) salt[122] obviously by an electron transfer pathway. Is it possible to conduct the solvent addition reactions mentioned above under PET conditions? As described in 2-2, the interaction of singlet excited state $DBMBF_2$ with norbornene in CH_3CN only results in the donor-acceptor cycloaddition but not solvent addition reaction. This is reasonable because generation of norbornene cation radical in the system is energetically forbidden, i.e. the free enthalpy change for a complete electron transfer process in this system is positive ($\Delta G^\circ \sim 0.1$ eV).* Therefore, we use a stronger electron acceptor-sensitizer, TCB, to generate the norbornene cation radical by the PET, the process of which is highly exothermic ($\Delta G^\circ \sim -0.7$ eV). Indeed, free radical species are generated upon irradiation in the TCB-norbornene system as demonstrated by the NMR and ESR studies (2-5-3c). However, instead of the solvent addition products, chloronated norbornanes **93** and **94** are obtained from hexane, benzene, CH_2Cl_2 or CH_3CN. Presumably, the expected solvent addition reaction is buried by other concurrent complicated radical reactions, the study of which is beyond the scope of this work.

---

* See Table 2-4, and compare norbornene (**15**) with cyclohexane (**12**).

3-5 Concluding Remarks and Proposals for Further Studies

In summary, the studies we have been carried out on the photophysics and photochemistry of β-diketonatoboron difluorides and related photoreactions of acetylacetone lead to the following conclusions.

(1). The fluorescence of $DBMBF_2$ is quenched by various electron donors including simple olefins. The quenching rate constants correlate well with ionization potentials of the donors and free enthalpy changes (ΔG^o) in the corresponding PET processes.

(2). The quenching of singlet excited state $DBMBF_2$ by electron donors proceeds mainly by exciplex formation whereas a complete electron transfer mechanism incorporates in the quenching leading to the direct formation of solvent separation ion radical pair when the quenching becomes very exergonic ($IP < 8.4$ eV, $\Delta G^o < -0.4$ eV).

(3). $DBMBF_2$ excimer fluorescence emission (522 nm) is found in concentrated CH_3CN solutions (> 0.05M), which is quenched by cycloheptene.

(4). $DBMBF_2$ can form ground state complexes with a series of electron donors. The emissions of the ground state complex was observed from neat 1,3-cyclohexadiene and 2,4-dimethyl-1,3-pentadiene or their solutions in hexane.

(5). The β-diketonatoboron difluorides photocycloadd to donor olefins regiospecificly and/or stereoselectively in CH_3CN to give δ-diketones. The photocycloaddition of $DBMBF_2$ only occurs

to olefins with IP > 8.4 eV, and proceed predominantly *via* a bimolecular exciplex intermediate for the acyclic olefins (IP > 9 eV) but mainly *via* a triplex intermediate at [$DBMBF_2$] > 0.06 M for cyclic olefins (8.4 eV < IP < 9 eV).

(6). The singlet excited state β-diketonatoboron difluorides can induce cation radical reactions for several donor olefins (IP < 8.4 eV), i.e. the valence isomerization of QC to NBD, the "Diels-Alder" reaction of 1,3-cyclohexadiene and 2,4-dimethyl-1,3-pentadiene, and the 2+2 dimerization of *trans*-anethole. These reactions are suggested to be initiated mainly by the solvent separated ion radical pairs formed from an electron transfer from the donor to singlet $DBMBF_2$ over ~7Å distance in encounter complexes.

(7). Acetylacetone photodimerizes regio and stereoselectively in non-polar solvents *via* the photocycloaddition of an excited state molecule with a ground state molecule to give a furanoid compound as the final product. The stereochemistry is controlled by stereoelectronic effects in the transition state of the cycloaddition and the steric effects in the furanoid closure step.

(8). The photocycloaddition of acetylacetone with norbornene in hexane proceeds *via* the interaction of excited state acetylacetone with ground state norbornene. Meanwhile, an energy transfer from excited state acetylacetone to norbornene also occurs causing the dimerization of norbornene.

(9). Acetylacetone can sensitize a series of solvent addition reactions to norbornene. The involvement of radical chain mechanism is strongly supported by the quantum yield measurement ($\Phi >> 1$).

Based on this, we have good reason to regard β-diketonatoboron difluorides as a new type of electron acceptor-sensitizers. The complexation with BF_2 also drastically modify the reactivities of the parent diketone, therefore may provide a useful synthetic pathway. In comparison with cyanoaromatics, $DBMBF_2$ is better than monocyano compounds and comparable to dicyano compounds in terms of electron acceptability. Generally, the BF_2 complexes have fairly large extinction coefficients, a necessity for being a good sensitizer. The synthesis of BF_2 complexes is easy and can be made *in situ*, which is of great convenience, especially to synthetic applications. However, the poor solubility and photoinstability in non-polar solvents restrict their use. Precaution also has to be taken to avoid protic acid which will destroy BF_2 complexes.

The study of the photochemistry of β-diketonatoboron difluorides now deserves a variety of in-depth investigations. Some of them are tabulated below.

(1). There is an immediate need to conduct time-resolved emission spectroscopic studies to verify the excimer formation of β-diketonatoboron difluorides. As stated in section 3-1-2, we still can not ascertain the reason for the concentration dependence of the relative fluorescence

intensities of $DBMBF_2$ at 398 and 416 nm. Following the build-up and decay manners of the two peaks will hopefully supply more information about the origins of the emissions.

(2). To use ESR and transient absorption spectroscopy to investigate the structure and dynamic properties of the anion radicals of BF_2 complexes.

(3). Flash photolysis studies of $DBMBF_2$-donor systems may reveal more mechanistic details of the PET interactions. A group of analogues covering a wide IP range, e.g. conjugated dienes,[96] alkyl benzenes,[188] and 1,3-dioxoles,[31] are good candidates for the donor. In the case of alkyl benzene, the transient absorption of both donor and acceptor might be recorded simultaneously.

(4). We have proposed a mechanism for the photocycloaddition of $DBMBF_2$ with enones, in which both "type a" and "type b" adducts are attributed to the interaction of singlet state $DBMBF_2$ with ground state enones (section 3-2-1, Scheme 3-2). As a singlet energy transfer from $DBMBF_2$ to enones has been demonstrated to occur, we can not vigorously exclude the possibility that the excited state enones participate in the cycloaddition reactions. Therefore, this reaction obviously needs more mechanistic studies, e.g. oxygen quenching. Since oxygen virtually does not quench either the fluorescence or the cycloadditions of $DBMBF_2$, we may conduct oxygen quenching to the cycloaddtion with enones. If the addition of oxygen does influence the yields and the distributions of the two

type of cycloadducts, this will be a clue of the participation of excited state enones.

(5). While a large number of other β-diketonatoboron difluorides[62-69] can be photochemically studied, of particular interest is what will happen to dialkyl- or diarylboron β-diketonate[62] under PET conditions.

(6). Instead of BF_2 complexes, silicon and phosphorus complexes of β-diketones are also promising as being electron

Table 3-3: Some Silicon and Phosphorus Complexes of β-Diketones.[a]

compound	formula	reference
101	$(AA)_3SiCl\cdot HCl$	54
102a	$(AA)_2SiAc_2$	55,56
102b	$(AA)_2Si(C_6H_5)_2$	57
102c	$(AA)_2Si(CH_3CH_2CO_2)_2$	58
102d	$(AA)_2Si(CH_3CH_2CH_2CO_2)_2$	58
102e	$(AA)_2Si(C_6H_5CO_2)_2$	58
102f	$(AA)_2Si(CH_2ClCO_2)_2$	58
102g	$(DBM)_2Si(CH_2ClCO_2)_2$	58
103a	$(AA)PF_4$	52
103b	$(DBM)PF_4$	52
103c	$(BA)PF_4$	52
103d	$(AA)PF_3CF_3$	53
103e	$(AA)PF_2(CF_3)_2$	53
103f	$(AA)PF(CF_3)_3$	53
103g	$(AA)PCH_3(CF_3)_3$	53

a.AA stands for the acetylacetonato group; DBM, dibenzoylmethanato group; BA, benzoylacetonato group.

acceptor-sensitizer. The complexes listed in Table 3-3 are thermally stable but their photophysical and photochemical properties have not been examined at all. Unfortunately, the electrochemical data of these complexes are not available either. However, the structures of these compounds and NMR data of some of them have been published. For example, **101** and **103a** showed significant down field shifts of the methine proton signals by 0.86 and 0.74 ppm with respect to that of acetylacetone, respectively. Compounds **103d - 103g** also showed similar down field shifts. These large down field shifts are even larger than that found in $AABF_2$ (0.65 ppm), indicating deficiencies in electron densities at the diketone moiety of these complexes. Moreover, **103a** has been claimed to be electron-accepting and used as a sensitizer in electrophotography.[206] Of particular interest among these complexes listed in Table 3-3 is compound **102b**. Unlike other hexacoordinated silicon complexes which exist in an equilibrium of *cis* and *trans* isomers in solution, **102b** only takes the *trans* configuration with no isomerization at room temperature.[57] This could avoid any complexity arising from a possible photoinduced *cis-trans* isomerization in this type of complexes. In addition, attaching functional groups to the phenyl rings in **102b** would vary the electron acceptability and hence facilitate systematic studies.

CHAPTER 4 EXPERIMENTAL

4-1. General Conditions and Material

4-1-1. Chemicals

(a). Solvents

Reagent grade acetonitrile (Fisher or Caledon) was used as supplied in preparative photolysis and spectro grade acetonitrile (BDH) in spectroscopic measurements. Methylcyclohexane (BDH, reagent) for the phosphorescence measurements was fractionally distilled twice. Hexanes (Mallinkrodt, AR grade) and ethyl acetate (BDH, AR grade) were used as supplied in either photolysis or chromatography. Dichloromethane (Fisher, Reagent grade) was distilled over phosphorus pentoxide under nitrogen atmosphere. Benzene (Fisher, Reagent grade) was distilled before use.

All deuterated solvents for NMR studies, chloroform-d (MSD), methylene-d_2-chloride (MSD), benzene-d_6 (MDS), acetonitrile-d_3 (MSD), and acetone-d_6 (ICN) were used as supplied.

(b). Diketones

Acetylacetone (BDH, regent grade), dibenzoylmethane (Aldrich), and benzoylacetone (Aldrich) for the preparation of BF_2 complexes were used without purification. Acetylacetone, 2,4-hexanedione (Aldrich,98%), 6-methyl-2,4-heptanedione (Aldrich,99%), and 2,2,6,6-tetramethyl-3,5-

heptanedione (Aldrich,95%) were distilled prior to use in the photolysis.

(c). Olefins

All olefins except norbornene (Aldrich) employed in photolysis and/or fluorescence quenching were distilled right before use. They were 1-hexene (Aldrich), 1,5-hexadiene (Aldrich), 3,3-dimethyl-1-butene (Aldrich), cyclopentene (Aldrich), cyclohexene (BDH, AR grade), cycloheptene (Aldrich), cylooctene (Matheson, practical), 1,3-cyclooctadiene (Columbian Carbon), 1,5-cyclooctadiene (Aldrich), 1-methylcyclohexene (Aldrich, Technical), norbornadiene (Aldrich), quadricyclane (Aldrich)*, cyclopentadiene dimer (Aldrich), 1,3-pentadiene (Matheson, technical), 2,4-dimethyl-1,3-pentadiene (Aldrich), 1,3-cyclohexadiene (Aldrich), *trans*-anethole (Eastman), methyl vinyl ketone (Aldrich, Technical), 3-penten-2-one (Aldrich, technical), ethyl acrylate (Aldrich), 2-cyclopentenone (Aldrich), 2-cyclohexenone (Aldrich), and 2-cyclopentenone ethylene ketal (Aldrich).

(d). Sensitizers

Acetone (BDH, AR grade) and acetophenone (Matheson, practical) were distilled. Benzophenone (Fisher, certified), 2,3,5,6-tetrachloro-1,4-benzoquinone (Aldrich, 99%), and 2,3-

*Quadricyclane is mentioned here for convenience.

dichloro-5,6-dicyano-1,4-benzoquinone (Aldrich) were recrystallized from methanol, methanol/acetonitrile, and dichloromethane/ethyl acetate, respectively. 1-cyanonaphthanlene (Eastman,), 9-cyanoanthracene (Aldrich,), 9-cyanophenanthrene (Aldrich, 97%), and 1-methoxynaphthanlene (Aldrich) were sublimed.

(e). Others

Octadecane (Eastman), decane (Aldrich), dodecane (Eastman), and decalin (Fisher, purified grade) were used as supplied as the internal standards for GC analysis. *Tris*(*p*-bromophenyl)aminium hexachloroantimonate (Aldrich) and benzhydrol (Aldrich) were also used as supplied.

4-1-2. Analytical Equipment

Gas chromatography (GC) analyses were performed on a Hewlett-Packard 5790 chromatograph using a flame ionization detector. The chromatograph was equipped with an OV-1 (12 m X 0.20 mm) or HP-1 (25 m X 0.20 mm) capillary column and connected to a Hewlett-Packard 3390A chart integrator. Preparative GC was conducted on a Varian 1700 chromatograph equipped with an OV-1 packed column (4' X 0.25", 15%, chromsorb A, 60-80 mesh). Melting points were determined on a Fisher-Johns apparatus (uncorrected). Infrared (IR) spectra were recorded on the following spectrophotometers. Perkin-Elmer 1310 (neat film), Perkin-Elmer 559B (neat film or KBr), Bruker IFS 85 (GC-FTIR), and Bomen Michelson 120 (FT-IR). The

relative intensities of IR signals are reported as s (strong), m (medium), or w (weak). Letter "b" stands for a broad peak and "sh" for a shoulder peak. Mass spectra (MS) and gas chromatography - mass spectra (GC-MS) were taken with a Hewlett-Packard 5985 GC-MS system by electron impact ionization (EI) and/or chemical ionization (CI) mode. Routine nuclear magnetic resonance (NMR) spectra were obtained on either a Bruker 100SY spectrometer equipped with Aspect 2000 software or a Bruker WH400 spectrometer. Two dimension (2D) NMR spectra were recorded on the latter. Chemical shifts (δ) for ^{1}H and ^{13}C spectra are reported in ppm with tetramethylsilane as the reference, whereas those for ^{19}F and ^{11}B will be specified where the spectra appear. The splitting patterns of ^{1}H signal are presented as s (singlet), d (doublet), t (triplet), q (quartet), or m (multiplet). A broadened signal is denoted as bs, bd, and so on. The multiplicities of ^{13}C signal are specified as q (primary), t (secondary), d (tertiary), and s (quaternary). Coupling constants are reported in Hz. Attempted chemically induced dynamic nuclear polarization (CIDNP) studies were conducted on a Varian EM360 spectrometer equipped with a quartz light pipe. Electron spin resonance (ESR) spectra were obtained on a Varian E-4 spectrometer. Ultraviolet and visible (UV/VIS) spectra were recorded on a Varian Cary 210 or a Philips PV8720 spectrophotometer. Emission spectra were obtained on a Perkin-Elmer MPF44B spectrophotometer (uncorrected).

4-1-3. Photolysis Apparatus

Method 1. (Large scale preparations)

A cylindrical Hanovia type photocell of 280 or 175 ml capacity was fitted with a side arm at the top and a gas inlet extended to the bottom. A Pyrex water-cooled lamp housing was inserted into the cell which contained the reaction solution. During irradiation, the photolysate was magnetically stirred while a slow stream of purified nitrogen was allowed to purge through from the gas inlet and escape from the side arm. A condenser with a mercury seal was connected to the side arm in order to reduce the solvent loss and secure the oxygen-free condition. The light source was a 200 W (654A36) or 450 W (679A36) Hanovia medium pressure mercury lamp.

Method 2. (Qualitative experiments)

The light sources and the lamp housing were the same as described in **Method 1.** Pyrex test tubes (13 X 100 mm) containing reaction solutions were placed around the water-cooled lamp housing.

Method 3. (Quantum yield measurements and small scale preparations)

Pyrex test tubes containing samples were evenly mounted in a "merry-go-round" which was placed in the center of a Rayonet photoreactor equipped with either RPR-3000 Å (16 X 21

W) or RPR-3500 Å (16 X 24 W) lamps depending on the requirement of the experiment being carried out. The temperature of the reaction mixture was 30-35°, maintained by ventilation throughout the irradiation.

Method 4. (Quantum yield measurement)

The monochromator set consisted of a LPS251HR power supply, a LH150 lamp housing with a Oriel 200W Xenon-mercury lamp (cat No:6291) as the light source, and a Kratos GM252 grating monochromator. The set and the photocell mounted on a cell holder were aligned up on a photobench to ensure the focused incident light fallen into the photolysate solution in the photocell (Fig.4-1). The distance between the front face of the photocell and the exit-end of the grating monochromator was fixed at 15.0 mm for all experiments. The current, wavelength, and band width were kept identical for all experiments.

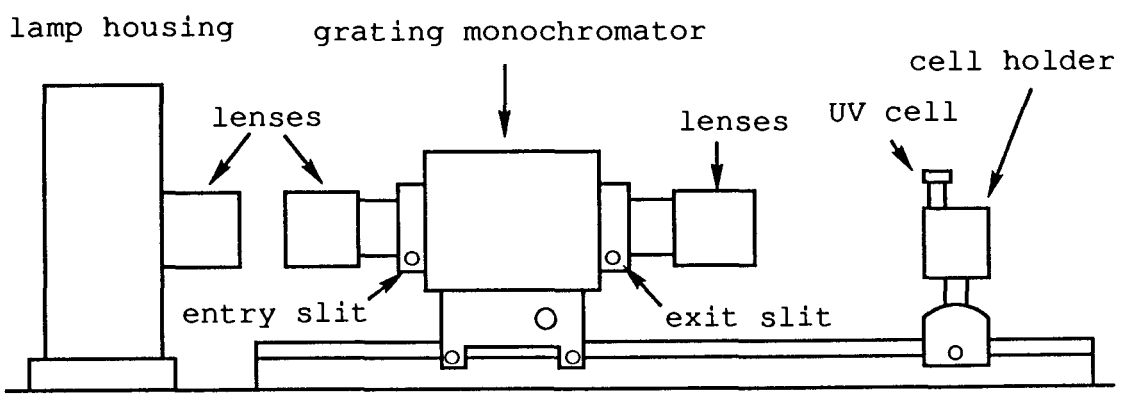

Figure 4-1. The set-up of monochromatic photolysis.

4-2. Spectroscopic Studies on β-Diketonatoboron Difluorides

4-2-1. Preparation of BF_2 Complexes

(a). Acetylacetonatoboron Difluoride ($AABF_2$)

To a 50 ml round-bottom flask equipped with nitrogen sweep was placed boron trifluoride-ether (5.06 g, 0.035 mol). Acetylacetone (3.5 g, 0.035 mole) was then added dropwise under magnetic stirring. While hydrogen fluoride was evolved during the reaction, the reaction mixture became warm and turned gradually to brown in color. After the hydrogen fluoride evolution ceased, the mixture was transferred to a distillation apparatus. Crude $AABF_2$ (4.8 g, 91%) as a pale liquid that solidified upon scratching was obtained from the distillation under reduced pressure. Recrystallization twice in anhydrous ether gave white crystals (3.1 g, 59%) with m.p.= 40.5 - 41.5° close to the reported melting points, 39-40° [37] and 43°.[61] MS (m/e, EI mode) 148 (M^+,40,^{11}B), 147 (M^+,10,^{10}B), 133(94), 132(22), 129 (56), 128(14); IR (film) 2970, 2930, 1560, 1385, 1365, 1170, 1080, 1021, 958, 817cm^{-1}; NMR, δ(ppm): ^1H (in C_6D_6) 1.25 (6H,S), 4.61 (1H,S); ^{13}C (in C_6D_6) 23.1, 101.1, 192.1; ^{11}B (in CD_3CN, $N_aB_4O_7 \cdot 10H_2O$ in H_2O as the reference) -9.06(S);

(b). Dibenzoylmethanatoboron Difluoride ($DBMBF_2$)

To a CH_3CN solution (10 ml) containing dibenzoylmethane (2 g, 8.9 mmol) was slowly added boron trifluoride-ether (1.42 g, 10 mmol). The reaction mixture was magnetically stirred overnight under dry nitrogen. After remained hydrogen fluoride and the solvent were removed by purging nitrogen through the reaction mixture followed by flash evaporation, the crude $DBMF_2$ was obtained as yellow powder. Recrystallization in benzene gave bright yellow crystals (2.1 g, 86.7%) with m.p.= 192-4° (lit.[37] 193-4°). All samples for spectroscopic measurements were recrystallized twice from CH_3CN which resulted in a lower yield (~70%, m.p. 193-4°). the absorption spectra of $AABF_2$ and $DBMBF_2$ are shown in Fig.4-2.

(c). 1-Benzoylacetonatoboron Difluoride ($BABF_2$)

1-Benzoylacetone (18.11 g, 50 mmol) was dissolved in 75 ml of dry acetonitrile, to which was added dropwise boron trifluoride-ether (10.6 g, 75 mmol). The resulting solution was magnetically stirred at ambient temperature for 3 h. The solvent and liberated hydrogen fluoride were then removed under reduced pressure. The residue was taken up in dichloromethane, washed with saturated sodium bicarbonate and water and then dried over magnesium sulfate. The yellow

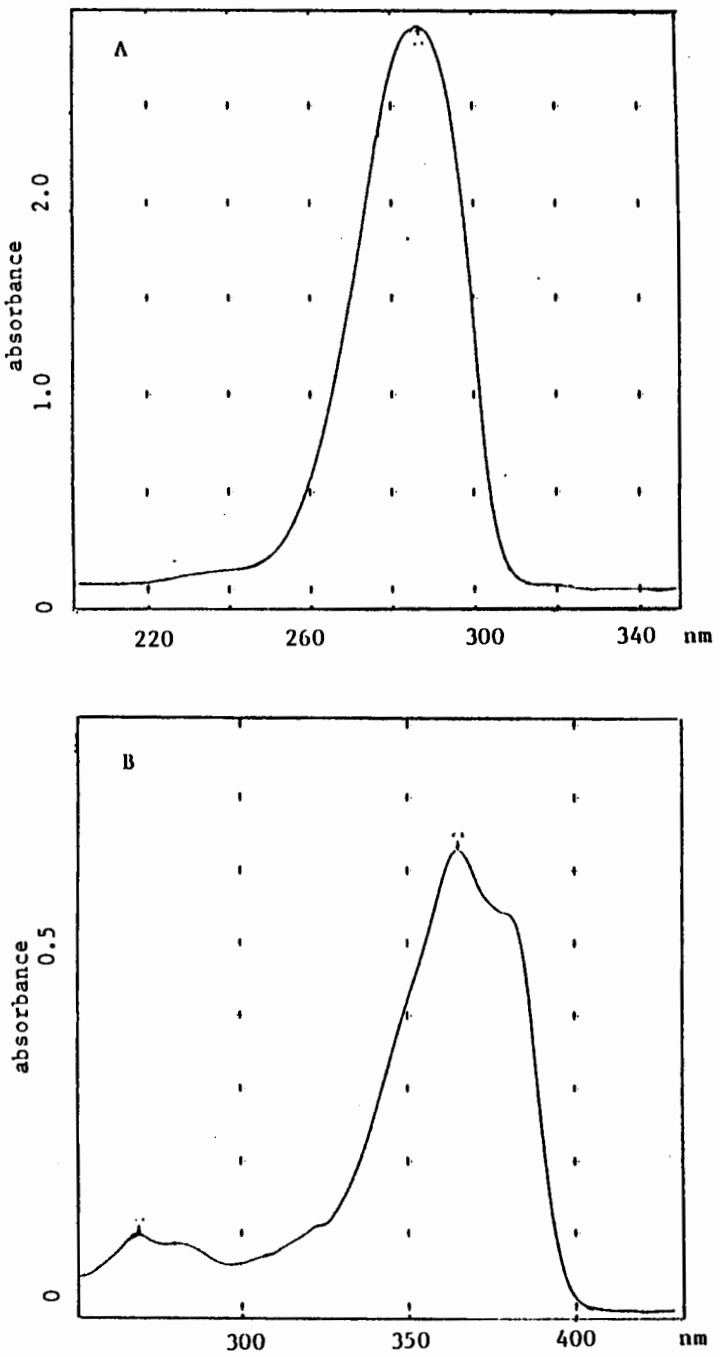

Figure 4-2. The absorption spectra of $AABF_2$ and $DBMBF_2$ in CH_3CN. A, $[AABF_2] = 2.00 \times 10^{-4}$ M, 1.000 cm cell; B, $[DBMBF_2] = 2.00 \times 10^{-4}$ M, 0.100 cm cell.

powder obtained after evaporation of the solvent was recrystallized twice from CH_2Cl_2-hexanes (8/2 v/v) giving bright yellow crystals (4.2 g, m.p.= 153-4° lit.[61] 157°). Evaporation of the solvent from the mother liquor followed by recrystallization from benzene gave additional 4.0 g of the product with brownish yellow color (m.p. 152-4°) raising the total yield to 78.1%.

(d). 2,6-Tetramethyl-3,5-Heptanedionatoboron Difluoride ($TMHBF_2$)

To an CH_3CN solution (15 ml) containing the diketone (2.5 g, 13.6 mmol) was added dropwise boron trifluoride-ether (2.15 g, 15.1 mmol) under stirring at ambient temperature. After 2 h of reaction, nitrogen was purged through the reaction mixture for 15 min. Evaporation of the solvent by flash distillation gave the crude $TMHBF_2$ as pale powder which was recrystallized from CH_2Cl_2-hexane (5/95 v/v), giving white crystals (2.75 g, 87%); m.p. 98-99°, (lit.[62] 83°), ^1H NMR (in C_6D_6), δ (ppm): 6.14 (1H,s), 1.29 (18H,s).

4-2-2. The Emission Spectra of $AABF_2$ and $DBMBF_2$

A stock solution of $AABF_2$ (1.00 X 10^{-1} M) or $DBMBF_2$ (1.00 X 10^{-1} M) in a spectroscopic grade solvent was prepared by weighing appropriate amount of the substrate into a 5 ml volumetric flask. The solvent was added to dissolve the sample to make the stock solution. The working solutions were

made by consecutive dilutions with the same solvent in volumetric flasks starting from the stock solution. The solutions of $DBMBF_2$ in hexane and methylcyclohexane were made by adding an appropriate amount of the stock solution in CH_3CN into 3 ml of the nonpolar solvents. Neither precipitation nor phase separation upon mixing was observed when the concentration of $DBMBF_2$ was below 5×10^{-5} M. Samples for fluorescence measurement were undegassed while those for phosphorescence measurement were purged with nitrogen for 5 min prior to use in a septum-sealed quartz phosphorescence cell.

4-2-3. The Concentration Dependence of Absorption and NMR Spectra of $DBMBF_2$

The $DBMBF_2$ solutions in CH_3CN for absorption spectrum measurement were made by following the procedure described in 4-2-2. The qualitative measurements of the absorption spectra of concentrated samples (1×10^{-2} M and 1×10^{-1} M) were conducted in a film cell made from two pieces of quartz plats tied up with rubber bands at both ends. The thickness of the solution film formed by injecting a solution into between the plats was estimated to be ca. 0.03 mm as OD = 1.5 was obtained from a CH_3CN solution of $DBMBF_2$ (1×10^{-2} M). However, the measurements had to be carried out quickly to avoid the interference of evaporation along the edges of the cell. More diluted samples were measured in standard UV cells with path lengths of 0.10 to 5.00 cm.

The stock solution for NMR studies was made by weighing 27.2 mg of $DBMBF_2$ into 1 ml of $CDCl_3$ ($[DBMBF_2] = 1 \times 10^{-1}$ M). Subsequent dilutions of the stock solution afforded the samples with adequate concentration. The measurements were carried out on a Bruker WH400 spectrometer.

4-2-4. Quenching of $DBMBF_2$ Fluorescence Intensity

(a). General Procedure

$DBMBF_2$ solutions (5×10^{-6} - 5×10^{-5} M) in CH_3CN (spectroscopic grade) used for the quenching experiments were freshly made from a stock solution of $DBMBF_2$ (1.00×10^{-1} M). The concentration of quenchers were adjusted by direct addition of a quencher into a fluorescence cell which contained $DBMBF_2$ solution (2 ml) or by dissolving an appropriate amount of a quencher with a stock solution of $DBMBF_2$ in volumetric flasks. A correction for the dilution effect was made when the direct addition method applied. A right angle cell was used when the concentration of $DBMBF_2$ was lower than 1×10^{-4} M. Otherwise a front face cell was used. In both case the excitation wavelength was fixed at 365 nm. The fluorescence intensity ratio, I_o/I, was determined at 398 nm unless otherwise specified. All I_o/I ratio and/or corresponding Stern-Volmer plots are given as follows.

(b). Biacetyl

Table 4-1. The Quenching of $DBMBF_2$ (1.0×10^{-5} M) Fluorescence Intensity by Biacetyl in CH_3CN.

[biacetyl] 10^{-3} M	I_o/I 398 nm	416 nm
0	1	1
0.42	1.036	1.041
1.26	1.080	1.094
2.51	1.157	1.182
3.73	1.246	1.279
4.94	1.296	1.340
6.52	1.388	1.444
8.08	1.484	1.573
11.83	1.692	1.857
15.42	1.900	2.161

(c). 3,3-Dimethyl-1-Butene (7)

Table 4-2. The Quenching of $DBMBF_2$ Fluorescence Intensity by **7** in CH_3CN. The Wavelength and Concentration Dependence.

		Io/I			
	$[DBMBF_2]$ (M) =	5×10^{-6}		1×10^{-3}	1×10^{-2}
[7] 10^{-1}M	λ_{moni} (nm) =	398	416	416	416
0.00		1	1	1	1
0.76		1.033	1.032	/	/
1.52		1.088	1.088	1.065	1.082

to be continued at next page.

Table 4-2. (cont.)

2.28	1.113	1.119	/	/
3.04	/	/	1.142	1.172
3.80	1.217	1.218	/	/
4.56	/	/	1.201	1.238
6.08	/	/	1.258	1.303
7.60	1.425	1.426	1.312	1.372
11.40	1.607	1.617	1.426	1.532

(d). Cycloheptene (8)

Table 4-3. The Quenching of $DBMBF_2$ Fluorescence Intensity by **8** in CH_3CN. The Wavelength and Concentration Dependence.

		Io/I			
	$[DBMBF_2]$ (M) =	5 X 10^{-6}		1 X 10^{-3}	1 X 10^{-2}
[7] 10^{-1}M	λ_{moni} (nm) =	398	416	416	416
0		1	1	1	1
0.85		1.362	1.376	1.346	1.346
1.69		1.746	1.744	1.694	1.726
2.54		2.219	2.196	2.541	2.113
3.39		2.691	2.660	3.388	2.499
4.26		3.189	3.156	4.235	2.928

(e). Olefins, Enones, and Other Quenchers

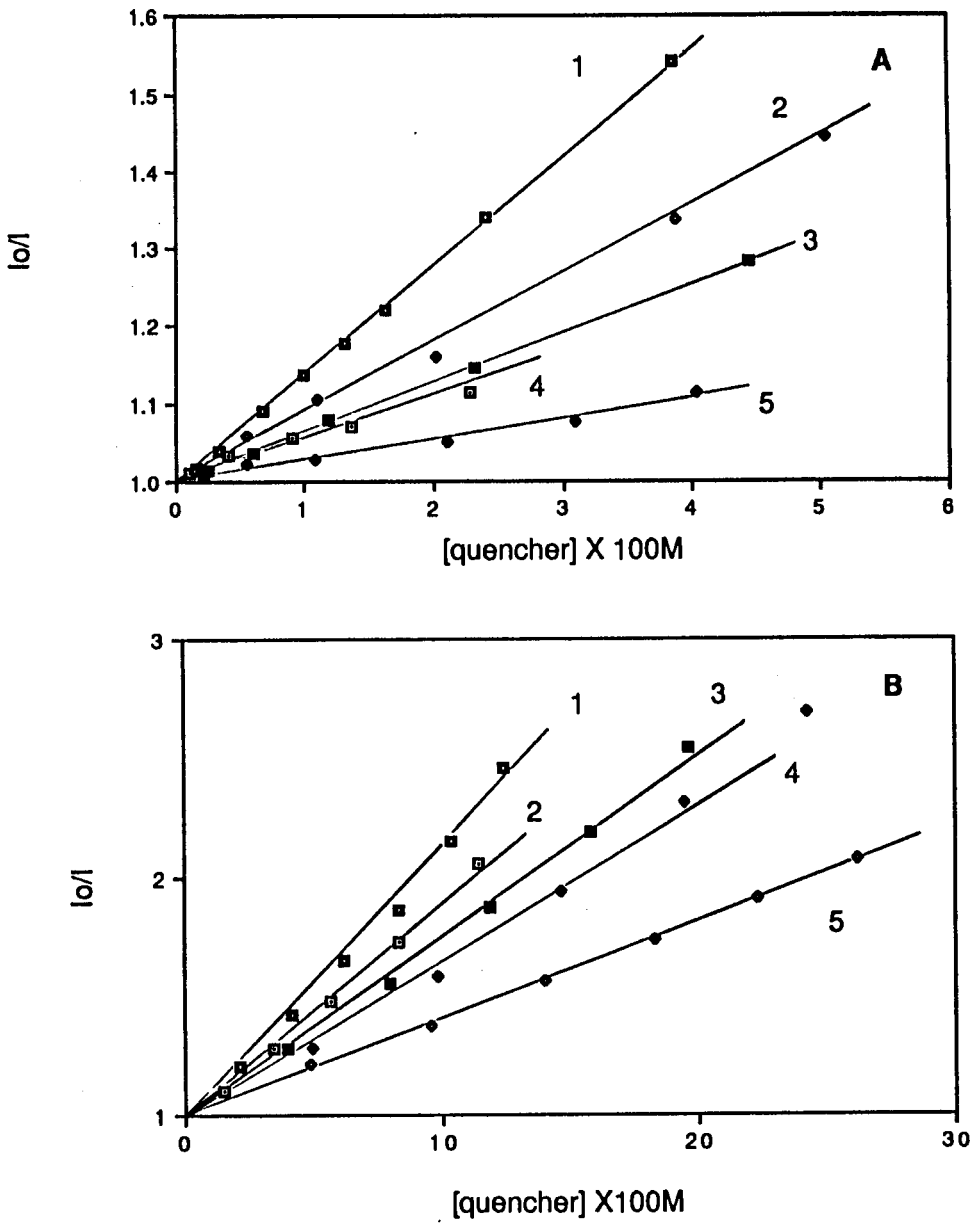

Figure 4-3. Stern-Volmer plots of $DBMBF_2$ fluorescence quenching in CH_3CN. A, $[DBMBF_2] = 2.0 \times 10^{-5}$ M; curve 1, quadricyclane (**4**); curve 2, 2,3-dihydropyran (**9**); curve 3, norbornadiene (**10**); curve 4, ethyl vinyl ether (**11**); curve 5, cyclohexene (**12**). B, $[DBMBF_2] = 5.0 \times 10^{-5}$ M; curve 1, 1.3-cyclohexadiene (**2**); curve 2, 2,4-dimethyl-1,3-pentadiene (**1**); curve 3, 1,3-cyclooctadiene (**13**); curve 4, 1,3-pentadiene (**14**); curve 5, norbornene (**15**).

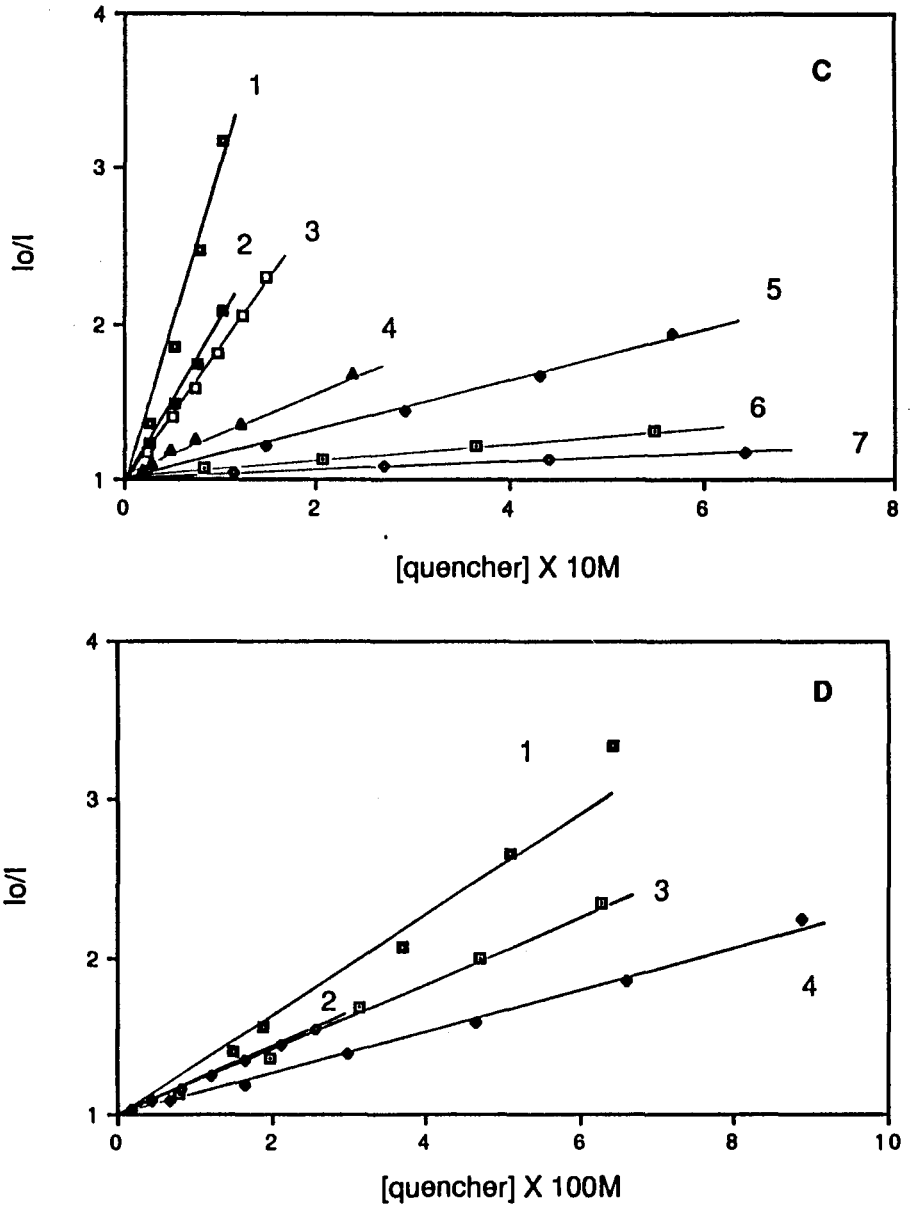

Figure 4-4. Stern-Volmer plots of $DBMBF_2$ fluorescence quenching in CH_3CN. C, $[DBMBF_2] = 5.0 \times 10^{-5}$ M; curve 1, 2-cyclohexenone (**16**); curve 2,3-penten-2-one (**17**); curve 3, methyl vinyl ketone (**18**); curve 4, acetylacetone; curve 5, 2-cyclopentenone (**19**); curve 6, 2-cyclopentenone ethylene ketal (**20**); curve 7, ethyl acrylate (**45**). D. $[DBMBF_2] = 5.0 \times 10^{-5}$ M; curve 1, *trans-anti-trans* dimer of anethole (**21**); curve 2, *trans-syn-trans* dimer of anethole (**22**); curve 3, N,N,-dimethylaniline (**23**); curve 4, *trans*-anethole(**3**).

4-3. Photocycloaddition of β-Diketonatoboron Difluorides with Simple Olefins

4-3-1. General Procedure of Preparative Photolysis

Unless otherwise specified, the general procedure described below was followed throughout the preparative photolysis of β-diketonatoboron difluoride-olefin systems. To a CH_3CN solution (30 ml) of a difluoride (1.5 mmol, 5.0×10^{-2} M) was added a freshly distilled olefin (15 mmol, 5.0×10^{-1} M). Six Pyrex test tubes (100 X 13 mm) loaded with the solutions were placed in a "merry-go-round" mounted in a Rayonet photoreactor. $DBMBF_2$ and $BABF_2$ systems were irradiated with a 350 nm light source, whereas $AABF_2$ systems with a 300 nm light source. The reaction time was controlled by monitoring the disappearance of the BF_2 complex on GC. The reaction was interrupted when the consumption of the BF_2 complex reached greater than 80% except for very slow reactions.

At the end of reaction, the photolysates usually showed yellow or brown in color. Most crude products obtained from flash evaporation of the solvent were directly taken for flash chromatography. In the case of low conversion of the difluoride, the crude products were treated with 30-50 ml of hexanes to precipitate out most of the unreacted difluoride before column separation. Hexanes containing 20-30% volume of ethyl acetate were used as the eluent.

The general reaction profiles are given in Section 2-2 and spectroscopic data of the products are given as follows.

4-3-2. $DBMBF_2$ to Olefins

Table 4-4. IR Data of the Cycloadducts of $DBMBF_2$ with Olefins.[a]

adduct	υ (cm^{-1})
with acyclic olefins	
26	3075(w), 2970(m), 2944(m), 2876(w), 1694(s,sh), 1687(s), 1605(m), 1589(m), 1456(s), 1375(m,b), 1232(s,b), 981(m), 762(w), 715(m), 701(m).
28	3080(w), 2944(m,b), 2872(w), 1689(s,b), 1649(w), 1605(m), 1589(m), 1457(s), 1421(w), 1375(m,b), 1234(s,b), 1190(w), 1011(m), 983(m), 926(m,b), 761(m), 719(m), 701(m).
29(KBr)	2972(m), 2960(m), 2918(w), 2882(w), 1693(s), 1672(s), 1604(m), 1586(w), 1455(m), 1415(w), 1373(w), 1360(w), 1268(m), 1230(s), 1209(w), 1196(w), 1010(w), 984(w), 961(w), 770(m), 760(s), 704(s).
with cyclic olefins	
31a	3072(w), 2962(s), 2886(w), 1695(s,sh), 1684(s), 1604(m), 1589(w), 1456(s), 1372(m,b), 1226(s,b), 1189(w), 1011(m), 763(m), 719(m), 701(m).

to be continued at next page.

Table 4-4. (cont.)

32	3075(w), 2942(s), 2872(m), 1696(s,sh), 1687(s), 1605(m), 1589(m), 1456(s), 1368(m), 1289(m), 1260(s), 1221(s), 1188(m), 1020(m), 1011(m), 991(m), 972(w), 956(w), 898(w), 866(w), 801(w), 762(s), 701(s).
33	3079(W), 2942(s), 2874(m), 1695(s,sh), 1686(s), 1606(m), 1589(m), 1457(s), 1280(m,b),,1224(s), 1190(m), 1012(m), 765(m), 704(s).
35	3076(w), 2938(s), 2872(w), 1696(s,sh), 1688(s), 1605(s), 1589(m), 1456(s), 1365(m,b), 1298(s), 1229(s,b), 1189(w), 1169(w), 1011(m), 977(m), 856(w), 762(m), 703(s).
36a(86%) +**36b**(14%) (KBr)	3082(w), 2993(w), 2963(s), 2901(w), 2891(m), 1692(s,sh), 1681(s), 1606(s), 1589(m), 1458(s), 1376(m), 1339(m), 1300(s), 1246(m), 1230(s), 1012(m), 777(s), 760(m), 751(w), 716(m), 700(s), 662(m), 620(m).
38	3075(w), 3030(w), 2945(s,b), 2880(w), 1692(s,sh), 1680(s,b), 1603(s), 1597(m), 1455(s), 1279(m,b), 1226(s,b), 1189(m), 1011(m), 760(s), 706(s).
with 1,3-pentadiene	
41a(76%) +**41b**(24%)	3078(W), 3020(w), 2980(m), 2951(m), 2874(w), 1694(s,sh), 1685(s), 1605(s), 1589(m), 1457(s), 1372(m,b), 1283(m), 1221(s), 1190(w), 1169(w), 1011(m), 982(s,b), 855(w), 764(m), 701(s).

a Measured by neat films unless otherwise specified.

Table 4-5. GC-MS Data of the Cycloadducts of $DBMBF_2$ with Olefins.

adduct	m/e (CI)	m/e (EI)
with acyclic olefins		
26	309(M^++1)	308(M^+,10), 252(50), 224(30), 189(65), 105(100), 77(25).
28	307(M^++1)	306(M^+,4), 265(58),252(50), 224(15), 105(100), 77(45).
29	309(M^++1)	308(M^+,8), 252(25),251(30), 224(38), 105(100), 77(46).
with cyclic olefins		
31a		292(M^+,6), 173(82), 105(100), 77(43).
31b		292(M^+,6), 173(92), 105(100), 77(40).
32		306(M^+,22), 187(45), 105(100), 77(30).
33		320(M^+,5), 201(20), 105(100), 77(50).
35		334(M^+,6), 224(20), 215(15), 105(100), 77(55).
36a		318(M^+,30), 251(5), 213(32), 199(52), 105(100), 77(42).
36b		318(M^+,26), 251(54), 213(6), 199(43), 105(100), 77(42).

to be continued at next page.

Table 4-5. (cont.)

38		332(M^+,12), 331(18), 214(22), 213(22), 105(100), 77(34).
40$_a$		356(M^+,28), 288(15), 251(30), 207(28), 185(22), 105(100), 77(34).
40$_b$		356(M^+,34), 288(10), 251(38), 207(24), 185(26), 105(100), 77(44).
with 1,3-pentadiene		
41a	293(M^++1)	292(M^+,2), 105(100), 77(60), 51(12).
41b	293(M^++1)	292(M^+,2), 105(100), 77(60), 51(12).
41c	293(M^++1)	105(100), 77(48), 51(8), 44(25).
41d	293(M^++1)	105(100), 77(65), 51(10), 44(18).

Table 4-6. ^1H Chemical Shifts (δ) and Coupling Constants (J) of the Cycloadducts of $DBMBF_2$ with Olefins.[a]

adduct	δ (ppm) and J (Hz)
with acyclic olefins	
26	δ: H_1,3.56(m);H_2,2.64(ddd);H_3,2.84(ddd); H_4,2.08(dddd); H_5,2.38(dddd); other H's:0.83(3H,t);1.22(4H,m);1.45(1H,m); 1.87(1H,m);7.0-8.1(10H,m,phenyl). J: $J_{1,4}$=7.8; $J_{1,5}$=7.8; $J_{2,3}$=17.6; $J_{2,4}$=7.7; $J_{2,5}$=7.8; $J_{3,4}$=8.1; $J_{3,5}$=6.1; $J_{4,5}$=14.1.

to be continued at next page.

Table 4-6. (cont.)

28	δ: H_1,3.58(m);H_2,2.61(ddd);H_3,2.79(ddd); H_4,2.00(m); H_5,2.32(dddd); other H's:1.53(1H,m);2.0(3H,m);4.96(2H,m); 5.69(1H,m);7.0-8.1(10H,m,phenyl). J: $J_{1,5}$=8.1; $J_{2,3}$=17.3; $J_{2,4}$=7.1; $J_{2,5}$=6.6; $J_{3,4}$=6.0; $J_{3,5}$=7.4; $J_{4,5}$=16.0.
29	δ: H_1,3.59(dd);H_2,2.53(ddd);H_3,2.68(ddd); H_4,2.21(dddd); H_5,2.43(dddd); other H's:1.01(9H,s.Me); 6.95-8.0(10H,m,phenyl). J: $J_{1,4}$=2.9; $J_{1,5}$=12.0; $J_{2,3}$=16.9; $J_{2,4}$=7.1; $J_{2,5}$=5.0; $J_{3,4}$=7.3; $J_{3,5}$=5.1; $J_{4,5}$=13.2.
with cyclic olefins	
31a	δ: H_1,3.86(ddd);H_2,2.87(dd);H_3,3.04(dd); H_4,2.96(m); other H's:1.52(1H,m); 1.78(2H,m); 1.93(1H,m); 2.11(1H,m); 6.95-8.00(10H,m,phenyl). J:$J_{1,4}$=6.8; $J_{2,3}$=16.5; $J_{2,4}$=6.9; $J_{3,4}$=6.3.
32	δ: H_1,3.57(m);H_2,2.97(dd);H_3,3.04(dd); H_4,2.80(m);other H's:1.60(6H,m); 1.90(1H,m); 2.18(1H,m); 7.0-8.1(10H,m,phenyl). J: $J_{1,4}$=6.8; $J_{2,3}$=16.2; $J_{2,4}$=7.4; $J_{3,4}$=6.0.
33	δ: H_1,3.65(ddd);H_2,2.85(dd);H_3,3.10(dd); H_4,2.85(m);other H's:1.15-2.15(10H,m); 7.00-7.95(10H,m,phenyl). J: $J_{1,4}$=3.8; $J_{2,3}$=20.6; $J_{3,4}$=8.7.

to be continued at next page.

Table 4-6. (cont.)

35	δ: H_1,3.82(ddd);H_2,2.76(dd);H_3,3.11(dd); H_4,3.00(m);other H's:1.37-2.02(12H,m); 7.0-8.0(10H,m,phenyl).
	J: $J_{1,4}$=4.2; $J_{2,3}$=16.3; $J_{2,4}$=8.7; $J_{3,4}$=4.1.
36a	δ: H_1,3.48(d);H_2,2.82(dd);H_3,3.13(dd); H_4,2.79(m);other H's:0.9-1.5(4H,m); 1.15(1H,m,syn bridge H); 2.04(1H,m, bridge head);2.27(1H,m,anti bridge H); 2.45(1H,m,bridgehead); 7.0-8.1(10H,m,phenyl).
	J: $J_{1,4}$=7.4; $J_{2,3}$=19.9; $J_{2,4}$=8.1; $J_{3,4}$=9.0.
38	δ: H_1,3.87(ddd);H_2,2.86(dd);H_3,2.50(dd); H_4,3.05(m);other H's:1.48-2.57(9H,m); 5.58(1H,m); 5.76(1H,m); 7.05-8.05(10H,m,phenyl).
	J: $J_{1,4}$=4.0; $J_{2,3}$=15.5; $J_{2,4}$=10.2; $J_{3,4}$=4.4.
with 1,3-pentadiene	
41a($CDCl_3$)	δ: H_1,4.17(ddd);H_2,2.98(m);H_3,3.08(m) H_4,1.99(m);H_5,2.33(m);other H's: 1.65(3H,dd.Me,J=6.6,1.0Hz);5.52(1H,m); 5.58(1H,m); 7.42-8.05(10H,m,phenyl).
	J: $J_{1,4}$=6.9; $J_{1,5}$=8.2.
41b($CDCl_3$)	δ: H_1,4.57(ddd);H_2,~3.0(m);H_3,~3.1(m) H_4,~2.0(m);H_5,~2.3(m);other H's: 1.69(3H,dd.Me,J=7.5,1.8Hz);5.45(1H,ddq); 5.66(1H,dq);7.42-8.05(10H,m,phenyl).
	J: $J_{1,4}$=7.3; $J_{1,5}$=7.7.

a. In C_6D_6 unless otherwise specified. H_1 denotes the tertiary α proton; H_2 and H_3, the secondary α protons; H_4 and H_5, the protons β to both carbonyls.

Table 4-7. ^{13}C Chemical Shifts of the Cycloadducts of $DBMBF_2$ with Olefins (in $CDCl_3$).

adduct	δ (ppm)
with acyclic olefins	
26	13.64, 22.61, 26.09, 29.34, 32.07, 35.76, 45.01, 127.82, 128.05, 128.34, 128.50, 132.75(2C), 136.78, 137.29, 199.56, 203.70.
28	26.02, 31.15, 31.20, 35.51, 44.09, 115.06, 127.70,128.01, 128.26, 128.43, 132.68, 132.76, 136.63, 137.10, 137.58, 199.27, 203.34.
29	23.29, 28.16(3C), 34.20, 36.70, 53.37, 127.75, 127.90, 128.30, 128.44, 132.59, 132.68, 136.69, 140.03, 199.58, 204.81.
with cyclic olefins	
31a	23.57, 28.94, 32.22, 39.08, 39.61, 48.32, 127.73, 128.11, 128.20, 128.40, 132.63(2C), 137.00, 137.63, 199.54, 202.98.
32	22.91, 23.51, 25.89, 29.21, 33.67, 38.94, 46.31, 127.91, 128.06, 128.34, 128.53, 132.61, 137.02, 137.22, 199.53, 203.32.
33	26.04, 26.40, 27.39, 28.64, 32.42, 36.10, 40.51, 48.76, 127.98, 128.13, 128.37, 128.61 132.71, 137.18, 138.20, 199.70, 204.22.

to be continued at next page.

Table 4-7. (cont.)

35	25.58(2C), 26.15, 26.74, 28.41, 31.27, 34.45, 41.35, 45.57, 127.84, 128.07, 128.25, 128.53, 132.60, 137.06, 137.17, 199.48, 204.18.
36a	29.42, 29.55, 34.92, 39.95, 41.24, 41.77, 43.09, 52.06, 127.84, 128.10, 128.35, 128.55, 132.70(2C), 137.32, 138.40, 199.65, 202.31.
38	24.76, 27.33, 31.34, 34.73, 39.07, 44.81, 55.65, 128.01, 128.12, 128.40, 128.58, 131.87, 132.70, 132.76, 136.72, 136,96, 199.75, 204.16.
with 1,3-pentadiene	
41a	18.00, 26.72, 35.70, 49.60, 127.51,128.06, 128.46, 128.60, 128.85, 129.25, 129.44, 132.99, 136.80, 137.12, 199.95, 201.10.

4-3-3. $AABF_2$ to Cyclohexene (12)

Five ml THF or CH_3CN solution containing 5 X 10^{-2} M $AABF_2$ and 1 M cyclohexene (**12**) was irradiated with a 300 nm light source for 8 h giving, in both cases, a sole product **42** as confirmed by coinjection in GC with the authentic sample. For a comparison, solutions of acetylacetone (5 X 10^{-2} M) and **12** (1M) in various solvents were also photolyzed under same conditions. Decalene (2 X 10^{-3} M) was added as the internal standard in all runs before irradiation in order to determine the yields of photoadducts. The results are given in Table 4-8.

Table 4-8. Photolysis of $AABF_2$-**12** and Acetylacetone-**12** System in Various Solutions.[a]

solvent	$[AABF_2]$ (M)	[acetylacetone] (M)	yield of **42** (%)[b]
THF	$5.03X10^{-2}$	0	5.05
THF	0	$5.15X10^{-2}$	0.36
CH_3CN	$5.06X10^{-2}$	0	6.98
CH_3CN	0	$5.25X10^{-2}$	1.08
hexane	0	5.97	41.2

a. [**12**] = 1 M. 8 h irradiation.
b. Calculated based on the amount of acetylacetone or $AABF_2$ in the beginning of the reaction.

4-3-4. $BABF_2$ to Olefins

Table 4-9. IR Data of the Cycloadducts of $BABF_2$ to Olefins.[a]

compound	υ (cm^{-1})
43a	3012, 2963, 2866, 1718, 1683, 1456, 1376, 1233, 1171.
44	2936, 2874, 1720, 1684, 1603, 1588, 1454, 1363, 1226, 1209, 1188, 1170.

a Neat film.

Table 4-10. GC-MS Data of the Cycloadducts of $BABF_2$ to Olefins.

compound	m/e (EI)
43a	256(M^+,35), 238(10), 213(55), 199(35), 189(28), 105(100), 77(80), 43(85).
43b	256(M^+,44), 238(20), 213(18), 199(40), 189(41), 105(88), 77(86), 43(100).
43c	256(M^+,100), 238(10), 213(40), 199(82), 189(38), 105(80), 77(76), 43(100).
44	272(M^+,22), 254(16), 215(20), 105(100), 77(58), 43(72).

Table 4-11. ^1H Chemical Shifts (δ, in C_6D_6) and Coupling Constants (J) of the Cycloadducts of $BABF_2$ to Olefins.

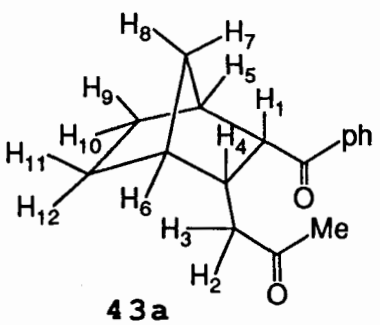

43a

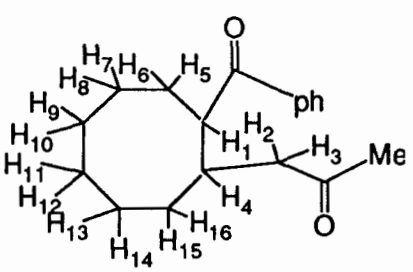

44

to be continued at next page.

Table 4-11. (cont.)

adduct	δ (ppm) and J(Hz)
43a	1.09(H_7, dm), 1.25-1.55(4H,H_{9-12},m), 1.47(3H,Me,s), 1.91(H_6,bd), 2.08(H_3, dd), 2.13(H_8,dm), 2.41(H_5,bd), 2.45(H_2,dd), 2.57(H_4, ddd), 3.35(H_1,d), 7.15(3H,phenyl,*meta* and *para*,m), 7.97(2H,phenyl,*ortho*,dd). $J_{1,4}$=9.1, $J_{2,3}$=17.6, $J_{2,4}$=6.5, $J_{3,4}$=8.3, $J_{7,8}$=10.1, $J_{6,11}$=3.7, $J_{5,9}$=1.9, $J_{7,5}$=$J_{7,6}$=$J_{7,10}$=$J_{7,12}$=1.4, $J_{8,5}$=$J_{8,6}$=1.8.
44	1.50-1.90(12H,H_{5-16},m), 1.57(3H,Me,s), 2.04(H_3,dd), 2.40(H_2,dd), 2.78(H_4,ddddd), 3.75(H_1,ddd), 7.1-8.0(5H,phenyl). $J_{1,4}$=4.0, $J_{1,5}$=9.2, $J_{1,6}$=4.0, $J_{2,4}$=4.9, $J_{2,3}$=17.6, $J_{3,4}$=8.3, $J_{4,5}$=4.0, $J_{4,16}$=8.3.

Table 4-12. ^{13}C Chemical Shift (in C_6D_6) of the Cycloadducts of $BABF_2$ to Olefins.

compound	δ (ppm)
43a	29.60, 29.70, 29.80, 35.04, 41.77, 42.16, 42.84, 45.15, 51.95, 128.48, 128.64, 132.47, 139.03, 201.62, 205.98.
44	26.18, 26.37, 27.29, 27.48, 28.38, 29.79, 31.69, 33.76, 45.75, 46.78, 128.39, 128.78, 132.60, 137.98, 203.49, 205.77.

4-3-5. Quantum Yield Measurement

Quantum yield measurements for the photocycloaddition reactions of $DBMBF_2$ with selected olefins (**7**, **25**, **27**, **12**, **8**, and **34**) were conducted in a air-cooled "merry-go-round" - Rayonet photoreactor set as described in 4-1-3 (**Method a**) or on a monochromator (**Method b**). In **Method a**, the actinometer and sample photocells (Pyrex test tube, 100 X 13 mm) were evenly placed on the "merry-go-round" which revolved slowly at the center of the Reyonet photoreactor. The volume of actinometry solution and those of sample solutions were kept identical. Whenever a tube was pulled out of the reactor for analysis, another tube loaded with $DBMBF_2$ solution (at same concentration of the sample solution) was immediately put in the place to maintain the consistency of irradiation.

Benzene solutions of benzophenone (5×10^{-2} M) and benzhydrol (1×10^{-1} M) were degassed and then irradiated for 5 min. The consumption of benzophenone was measured spectrophotometrically at 340 nm from which the absorbed light intensity (in Einstein/min) was determined.[88] A quantum yield of 0.74 was adopted for the actinometer.[207] Octadecane (2.0×10^{-3} M) was added into the sample solutions before irradiation acting as the internal standard for GC analysis. The conversion of $DBMBF_2$ was controlled less than 30% at the end of irradiations.

4-4. Photocycloaddition of $DBMBF_2$ to Enones

4-4-1. General Methods

A CH_3CN solution (30 ml) of $DBMBF_2$ (1.5 mmol, 5.0 X 10^{-2} M) and a freshly distilled enone (15 mmol, 5.0 X 10^{-1} M) were distributed into 6 Pyrex test tubes (100 X 13 mm) and then irradiated with a 350 nm light source according to **Method 3** described in 4-1-3. The disappearance of $DBMBF_2$ was monitored by GC analysis. The reaction solutions turned to brownish after a few hours of irradiation. The crude products obtained from flash evaporation of the solvent were directly taken for flash chromatography. In the case of low conversion of the difluoride, the crude products were treated before column separation with 30-50 ml of hexanes to precipitate out most of the unreacted $DBMBF_2$. Hexanes contained 25-30% volume of ethyl acetate were used as the eluent.

4-4-2. Photolysis of $DBMBF_2$ with 18, 17, and 45 in CH_3CN

The preparative photolyses were interrupted when the consumption of $DBMBF_2$ reached ~85%. All the cycloadducts obtained from chromatography were oils with pale yellow color. The general reaction conditions and profiles are given in Table 2-11 and spectroscopic data of the products are shown as follows.

Table 4-13. IR Data (neat film) of the Cycloadducts of $DBMBF_2$ with Enones.

compound	υ (cm^{-1})
47a	3089, 2960, 1710, 1700, 1674, 1603, 1590, 1550, 1457, 1374, 1300, 1255, 1220, 1189, 1171, 1054, 1011, 946, 768, 702, 654, 611.
47b	3074, 2946, 1738, 1695, 1680, 1603, 1588, 1484, 1361, 1225, 1189, 1166, 1010, 981, 766, 740, 702.
48a	3076, 2980, 2948, 2892, 1715, 1700, 1673, 1602, 1587, 1454, 1360, 1270, 1208, 1189, 1009, 950, 768, 717, 702.
48b	3080, 2992, 2950, 2898, 1720, 1685, 1606, 1589, 1457, 1368, 1278, 1223, 1190, 1011, 993, 950, 768, 704.
49b	3074, 2980, 2946, 1715, 1700, 1674, 1602, 1574, 1454, 1360, 1270, 1208, 1188, 1009, 950, 768, 717, 703, 672.
50b	3080, 2998, 2954, 2921, 1740, 1690, 1605, 1589, 1457, 1377, 1270, 1230, 1165, 1030, 1011, 986, 760, 703.

Table 4-14. GC-MS Data of of the Cycloadducts of $DBMBF_2$ with Enones.

adduct	m/e(CI)	m/e(EI)
47a	295	294(M^+,4), 276(22), 236(45), 224(46), 189(68), 172(18), 105(100), 77(74).
47b	295(100) 163(74)	294(M^+,4), 276(22), 251(66), 234(61), 189(77), 105(100), 77(60).
48a	309	290(M^+-H_2O,8), 250(10), 224(35), 203(18), 186(37), 171(35), 105(100), 77(50).
48b	309	290(M^+-H_2O,20), 265(32), 203(26), 189(44), 162(58), 105(100), 77(52).
48c	309	290(M^+-H_2O,20), 265(28), 203(25), 189(46), 162(51), 105(100), 77(55).
49a	323	322(M^+,2), 304(3), 265(10), 224(68), 185(22), 147(12), 105(100), 77(54).
49b	323	304(M^+-H_2O,4), 203(22), 161(25), 105(100), 77(62).
50b	325(100) 279(19) 193(20)	324(M^+,3), 306(3), 279(25), 250(21), 216(8), 105(100), 77(32).

Table 4-15. ^1H Chemical Shifts (δ) and Coupling Constants (J) of the Cycloadducts of $DBMBF_2$ with Enones (in C_6D_6).

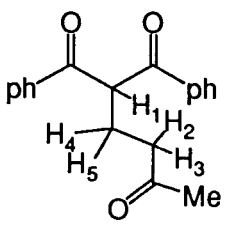

47a

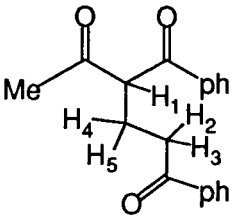

47b

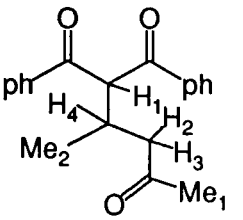

48a

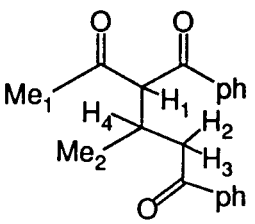

48b

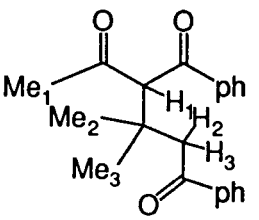

49b

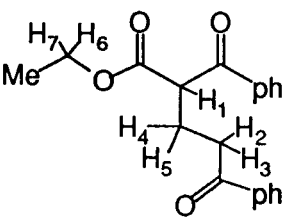

50b

compound	δ(ppm) and J(Hz)
47a	δ: 1.54(3H,s,Me), 2.31(2H,t,H_2H_3), 2.04(2H,td,H_4H_5), 5.57(1H,t,H_1), 7.0-8.2(10H,m,phenyl). J: $J_{1,4}=J_{1,5}=6.5$, $J_{2,4}=J_{2,5}=J_{3,4}=J_{3,5}=5.8$.
47b	δ: 1.81(3H,s,Me), 2.37(1H,dddd,H_4), 2.44(1H,dddd,H_5), 2.64(1H,ddd,H_2), 2.89(1H,ddd,H_3), 4.42(1H,dd,H_1), 7.0-8.2(10H,m,phenyl). J: $J_{1,4}=J_{1,5}=6.8$, $J_{2,3}=18.1$, $J_{2,4}=J_{2,5}=6.5$, $J_{3,4}=7.3$, $J_{3,5}=6.8$, $J_{4,5}=26.8$.

to be continued at next page.

Table 4-15. (cont.)

48a	δ: 1.20(3H,d,Me_2), 1.59(3H,s,Me_1), 2.26(1H,dd,H_2), 2.70(1H,dd,H_3), 3.26(1H,dddq,H_4), 5.74(1H,d,H_1), 6.94-8.20(10H,m,phenyl). J: $J_{1,4}$=6.7, $J_{2,3}$=18.0, $J_{2,4}$=6.3, $J_{3,4}$=6.0, $J_{4,Me2}$=6.9.
48b	δ: 1.07(3H,d,Me_2), 1.78(3H,s,Me_1), 2.57(1H,dd,H_2), 3.23(1H,dd,H_3), 3.25(1H,m,H_4), 4.66(1H,d,H_1), 6.95-8.25(10H,m,phenyl). J: $J_{1,4}$=7.3, $J_{2,3}$=13.9, $J_{2,4}$=6.6, $J_{3,4}$=5.0, $J_{4,Me2}$=6.9.
49b	δ: 1.25(3H,s,Me_2), 1.49(3H,s,Me_3), 1.84(3H,s,Me_1), 2.96(1H,d,H_2), 3.63(1H,d,H_3), 5.74(1H,s,H_1), 7.0-8.3(10H,m,phenyl). J: $J_{2,3}$=17.8.
50b	δ: 0.81(3H,t,Me), 2.59(2H,m,H_4H_5), 2.76(1H,ddd,H_2), 3.01(1H, ddd, H_3), 3.86(1H,dq,H_6), 3.96(1H,dq,H_7), 4.69(1H,dd,H_1), 7.00-8.25(10H,m,phenyl). J: $J_{1,4}$=$J_{1,5}$=7.1, $J_{2,4}$=$J_{3,4}$=6.1, $J_{2,5}$=$J_{3,5}$=6.8, $J_{2,3}$=18.0, $J_{6,7}$=10.5, $J_{6,Me}$=$J_{7,Me}$=6.6.

Table 4-16. ^{13}C Chemical Shifts (δ, in C_6D_6) of the Cycloadducts of $DBMBF_2$ with Enones.

adduct	δ(ppm)
47a	23.57, 29.27, 40.47, 55.48, 128.87, 128.99, 133.28, 136.77, 196.06, 207.11.
47b[a]	22.30, 28.10, 35.77, 61.60, 128.61, 128.95, 129.06, 132.84, 133.45, 137.02, 137.29, 196.61, 198.65, 202.74.
48a	17.78, 29.76, 30.55, 59.99, 128.70, 128.96(3C), 133.17, 133.35, 137.16, 137.64, 195.97(2C), 207.00.
49b	26.46, 27.45, 30.86, 37.19, 47.59, 64.82, 128.58, 128.82, 128.97(2C), 132.75, 133.24 138.52 139.05, 198.08, 199.90, 202.65.
50b	13.82, 23.65, 35.74, 53.15, 61.12, 128.22, 128.61, 128.85, 129.00, 132.87, 133.36, 136.75, 137.24, 169.90, 195.19, 198.61.

a. One signal was buried into the solvent peaks.

4-4-3. The Identification of Dimers of cyclopentenone (16) and cyclohexenone (19).

A solution of **19** (1 M) in CH_3CN (5 ml) was placed in a Pyrex test tube (100 X 13 mm) and irradiated for 55 min with a 200 W Hanovia medium pressure mercury lamp according to **Method 2** described in 4-1-3. The photolysate was analyzed by GC, showing two products with a area ratio of 40.8:59.2. Both fractions gave a same parent peak at m/e = 144 on the GC-MS spectra. The minor product (40.8%) was then assigned as the head-to-head, *cis-anti-cis* dimer, **54**, and the major one (59.2%) as the head-to-tail analogue, **53**, according to the literature.[106] The authentic samples of **51** and **52** were prepared from **16** and identified by the same procedure described above. The product distributions of the dimers are listed in Table.2-12.

4-5. Cation Radical Reactions Sensitized by Diketonatoboron Difluorides.

4-5-1. The Sensitized Valence Isomerization of Quadricyclane (QC) and Norbornadiene (NBD)

(a). General procedure

Acetylacetone, $AABF_2$, and $DBMBF_2$ were used as the sensitizers in the sensitized isomerization of QC and NBD. Solutions of a sensitizer and a substrate (QC or NBD) in a deuterated solvent (CD_2Cl_2 or CD_3CN, 0.5 ml each) placed in a Pyrex NMR tube (5 mm in diameter) was irradiated according to **Method 3** described in 4-1-3 and monitored by NMR spectroscopy. A benzophenone-benzhydrol actinometer was irradiated under the identical conditions to record the absorbed light intensity. A 300 nm light source was used for acetylacetone and $AABF_2$ sensitizations and a 350 nm light source for the $DBMBF_2$ sensitization.

The solvent peaks ($CHDCl_2$ in CD_2Cl_2, CHD_2CN in CD_3CN) were taken as internal standards for calculations of the isomerization yields. Based on the integral ratios of the NBD signals over the solvent peaks (R_{int}^{NBD} = [integral of the 4 olefinic protons of NBD]/[integral of the solvent]) and that of the QC signals over the solvent peaks (R_{int}^{QC} = [integral of the 6 tertiary protons of QC]/[integral of the solvent]) and the initial concentration (C, in M) of the substrate, the yields of the isomerization (Y) were calculated according to

Eq.4-1a or 4-1b with an accuracy of 10-20%. Eq.4-1a is for the isomerization from QC to NBD and Eq.2-1b for the isomerization from NBD to QC,

$$Y = 6R_{int}^{NBD}/4R_{int}^{QC}(0) \qquad (4\text{-}1a)$$

$$Y = 4R_{int}^{QC}/6R_{int}^{NBD}(0) \qquad (4\text{-}1b)$$

where $R_{int}^{QC}(0)$ and $R_{int}^{NBD}(0)$ denote the signal area ratio before irradiation. The quantum yields (Φ) were then estimated by Eq.4-2, where V was the volume of reaction solution

$$\Phi = (Y \cdot C \cdot V)/(t \cdot I) \qquad (4\text{-}2)$$

(in liter); t, the irradiation time (in min); and I, the absorbed light intensity (in Einsteins/min, 2.08 X 10^{-5} for the 300 nm light source and 1.61 X 10^{-5} for the 350 nm light source). The quantum yields obtained wherefrom are listed in Table 2-13.

(b). Attempted CIDNP Studies on the Isomerization of QC and NBD Sensitized by $AABF_2$ and $DBMBF_2$

Deaerated solutions of QC (5 X 10^{-2} M) or NBD (5 X 10^{-5} M) and a sensitizer ($AABF_2$ or $DBMBF_2$, 1 X 10^{-2} M) in CD_2Cl_2 or CD_3CN (0.5 ml each) were examined. To a Pyrex NMR tube (5 mm in diameter) containing a sample was inserted a quartz rod

(4.8 mm in diameter) the lower end of which was merged into the solution with no air bubble in between. The quartz rod was used as a light pipe to introduce the light into the sample. As shown in Fig.4-5, the NMR tube was placed in the cavity of a Varian EM360 spectrometer and adjusted to ensure that the lower end of the light pipe sat right above the probe coil. A 1000 W high pressure mercury lamp (Wild) was used as the light source. The light beam passed through a Pyrex filter (for $AABF_2$ sensitization) or GWV filter (for $DBMBF_2$ sensitization) was reflected by an UV mirror then focused onto the upper end of the light pipe. Five scans (2 min each) were recorded immediately after the light was turned on. No CIDNP signal was observed in either $AABF_2$ or $DBMBF_2$ sensitization.

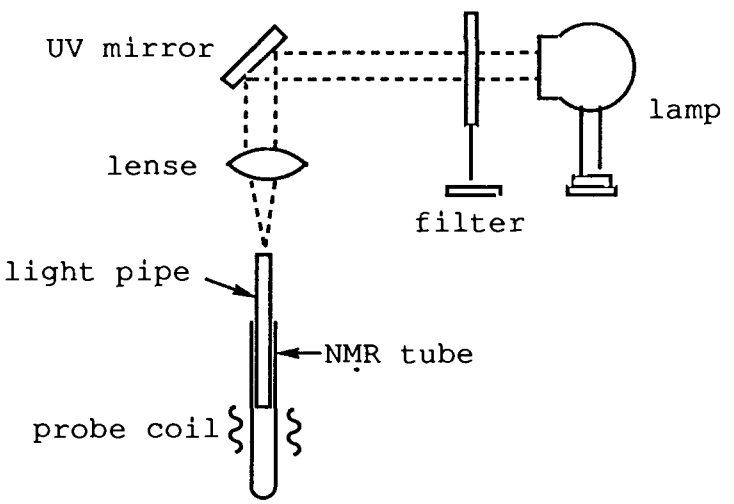

Figure 4-5. A schematic illustration of the set-up for CIDNP studies.

4-5-2. The "Diels-Alder" Reaction of 1,3-Cyclohexadiene (2)

(a). The Preparative Photolysis

A solution of **2** (1.2 g, 5 X 10^{-1} M) and $DBMBF_2$ (407 mg, 5 X 10^{-2} M) in CH_3CN (30 ml) was irradiated for 6 h with a 350 nm light source according to **method 3** described in 4-1-3. $DBMBF_2$ remained essentially unconsumed after irradiation as estimated from the GC analysis. The residue obtained after evaporation of the solvent was chromatographed (5% ethyl acetate in hexanes) affording the crude products (640 mg, 53%) which contained 2 dimers of **2** as suggested by two GC peaks which showing the same parent peak at m/e = 160. The crude products was chromatographed again on the same column (2% ethyl acetate in hexanes) to give a major product (380 mg); ^1H NMR (C_6D_6), δ(ppm) 1.0-1.6(6H,m), 1.8(1H,m), 1.9(1H,m), 2.15(1H,m), 2.30(1H,m), 5.65(1H,m), 5.90(1H,m), 6.25(2H,m). This compound was confirmed to be the *endo* 2+4 dimer (**55**) by coinjection with the authentic sample obtained from the thermal dimerization of **2** (*vide infra*). The pure minor product was not isolated but identified to be the *exo* 2+4 dimer (**56**) by coinjections with the authentic samples obtained from the thermal dimerization and the benzophenone-sensitized dimerization of **2** (*vide infra*). The 2+2 dimers **57** and **58** were not found in the photolysate according to the GC analysis.

(b). Comparison of Various Sensitizers

The photodimerizations of **2** sensitized by $DBMBF_2$, $BABF_2$, tetrachloro-1,4-benzoquinone (TCB), 2,3-dichloro-5,6-dicyano-1,4-benzoquinone (DDB), 9-cyanophenanthrene (9-CN-Ph), 1-cyanonaphthanlene (1-CN-Np), 1-methoxynaphthanlene (1-MeO-Np), and benzophenone were examined under identical conditions. Solutions containing **2** (1 M), a sensitizer (1 X 10^{-2} M), and the internal standard (decane, 5 X 10^{-3} M) in CH_3CN (1 ml each) were irradiated for 1 h with a 350 nm light source according to **Method 3** described in 4-1-3. The resulting photolysates were directly taken for GC analysis. The irradiation time and the relative yields of the 4 dimers of **2** in the presence of various sensitizer are listed in Table 2-14 along with the results of the thermal dimerization and previously published results.

(c). Preparation of the Authentic Samples

The authentic samples of **55** and **56** were made by the thermal dimerization of **2**. A sealed capillary tube containing 10 μl of **2** was heated at 200° for 30 min in a silicone oil bath. The reactant was then taken up in acetone (10 ml) for GC analysis. Two peaks with a area ratio of 4:1 were found as the sole products on the GC trace. The major product was assigned as the endo dimer, **55**, and the minor as the exo dimer, **56**, according to the previous report.[23]

The authentic samples of **57** and **58** were obtained by benzophenone (**63**) sensitized dimerization of **2**. A Pyrex NMR tube (5 mm in diameter) loaded with neat **2** (0.5 ml) containing the sensitizer (~5 X 10^{-2} M) was irradiated with a 350 nm light source for 1 h. The resulting reaction mixture was diluted with acetone (30 ml) for GC analysis. Three main peaks were detected, one of which was identified to be **56** by comparison with the thermolysis products of **2**. Other two peaks have a ratio of *ca.* 3:1; the major one was assigned to **57** and the minor to **58** according to the literature.[23]

4-5-3. The "Diels-Alder" Reaction 2,4-Dimethyl-1,3-pentadiene (1)

(a). The Preparative Photolysis

A solution of **1** (1 g, 3.5 X 10^{-1} M) and $DBMBF_2$ (0.41 g, 5 X 10^{-2} M) in CH_3CN (30 ml) was distributed in 6 Pyrex test tubes (100X13 mm) and irradiated for 12 h with a 350 nm light source according to **Method 3** described in 4-1-3. The crude products obtained from evaporation of the solvent was a mixture of oil and solid material, which was then treated with hexanes (30 ml) resulting in the separation of the crude dimers of **1** (630 mg, 63%) as a colorless liquid and recovered $DBMBF_2$ (390 mg) as a bright yellow powder which was identified by GC analysis. The crude product was analyzed by GC, showing two components with relative yields of 82.5% and 17.5%, respectively. The crude product was chromatographed

(3% ethyl acetate in hexanes) to give two pure compounds; the major one (~250 mg) and the minor one (~25 mg) were assigned as the dimers **65** and **66**, respectively, based on the MS and ^1H NMR data and coinjections with the authentic samples made by Gassman's method.[10] **65**, GC-MS (m/e, EI mode) 192(M^+,36), 177(7), 149(54), 135(10), 121(20), 96(100), and 81(44); ^1H NMR (C_6D_6) δ: 1.02(3H,s), 1.11(3H,s), 1.23(3H,s), 1.66(3H,s), 1.70(1H,m), 1.74(6H,m), 1.92(2H,m), 5.17(1H,m), and 5.51(1H,m). **66**, GC-MS (m/e, EI mode) 192(M^+,11), 177(20), 149(28), 135(34), 121(68), 96(100), and 81(44); ^1H NMR (C_6D_6) δ: 1.01(3H,s), 1.08(3H,s), 1.12(3H,s), 1.13(3H,s), 1.60(2H,m), 1.67(3H,s), 1.83(3H,s), 1.99(1H,bs), 4.84(1H,bs), 5.05(1H,bs), and 5.20(1H,bs).

(b). Comparison of Various Sensitizers

Solutions containing **1** (2.0 X 10^{-1} M), a sensitizers (5 X 10^{-2} M), and the internal standard (decane, 5,0 X10^{-3} M) in CH_3CN (1 ml each) were irradiated for 2 h and then analyzed by following the procedures described in 4-5-2(b). The GC traces showed that **65** and **66** were the major products with a total GC yield* greater than 85% for all samples. The distribution of the two dimers and the relative efficiencies of the dimerization with respect to the $DBMBF_2$ sensitization are given in Table 2-15.

---

*the ratio of GC peak area over the total peak area appeared on the GC trace except those of the solvent and reactants)

4-5-4. Monochromatic Photolysis of 2 and 1 in the Presence of $DBMBF_2$

CH_3CN solutions (2 ml each) of a diene (**2** or **1**, 5 X 10^{-1} M) and $DBMBF_2$ (2.0 X 10^{-2} M) in an 1 cm UV cell were photolyzed for 120 min on a monochromatic apparatus described in **Method 4** (section 4-1-3). Decane (5.0 X 10^{-3} M) was added in the solvent before the reaction as the internal standard for GC analysis. The current of power supply for the lamp was kept at 8.20 A throughout the experiments. The band width (3.3 nm) and the height of entry and exit slits (15 mm for both) were also fixed. The photolyses were conducted at 312.8 and 437 nm respectively. The 200 W xenon-mercury lamp (Oriel) had an output* of 43 $\mu W/cm^2$,nm at 312.8 nm where the majority of incident light was absorbed by $DBMBF_2$. The lamp had an output of 27 $\mu W/cm^2$,nm at 437 nm where $DBMBF_2$ did not absorb but its ground state complexes (GSC) with either **2** or **1** did.# While the irradiation at 437 nm ended up with nothing showed up on the GC traces, the irradiation at 312.8 nm did result in the formation of **55** and **65** respectively from **2** and **1** in a tiny but detectable amount as shown in Fig.4-6. The relative light intensities absorbed by the reaction solutions at each wavelength were calculated based on the output ratio of the lamp and the absorbances of solutions at the given wavelength. By assuming that the sensitivity limit of the GC

---

* The output data of the lamp were cited from the manual (cat. No 6219) supplied by the maker. Conditions of output measurement were identical for all wavelengths.

The absorption spectrum of $DBMBF_2$ and those of the ground state complexes of $DBMBF_2$ with **2** or **1** are given in Fig.4-2 and Fig.2-8, respectively.

was 10^{-5} M, the upper limit of the relative quantum yields at 312.8 nm (Φ_{437}) with respect to those at 312.8 nm ($\Phi_{312.8}$) were estimated by Eq.4-3. The quantum yields thus calculated are given in Table 2-16.

$$\Phi_{437} = \text{(output ratio of the lamp, 43/27)} \times \text{(1/light absorbed by the GSC at 437 nm)} \times \text{(yield at 437 nm/yield at 312,8 nm)} \times \Phi_{312.8} \quad (4\text{-}3)$$

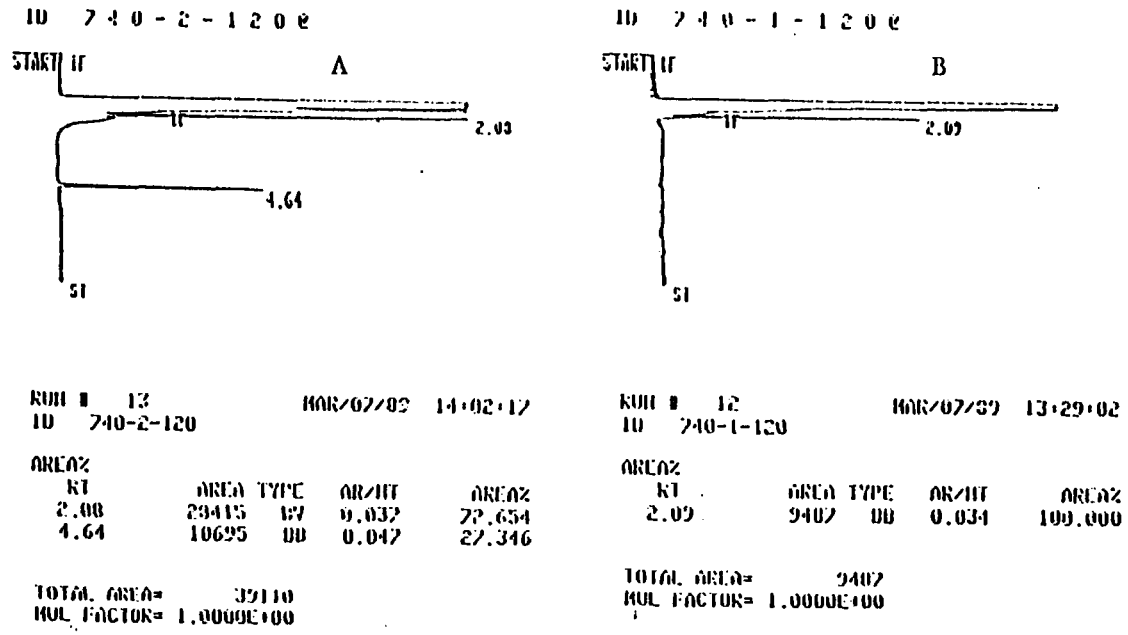

Figure 4-6. The GC spectra of the monochromatic photolysis of $DBMBF_2$-**1** system at 312.8 (spectrum A) and 437.0 nm (spectrum B). The peak at RT = 4.64 min is of the dimer **65**.

4-5-5. The Sensitized Dimerization of *trans*-Anethole (3)

(a). Preparation of Dimer 21

A nitrogen-purged solution of *trans*-anethole (**3**, 1.60 g, 3.6 X 10^{-1} M) and TCB (0.37 g, 5 X 10^{-2} M) in dry CH_2Cl_2 (30 ml) were irradiated for 140 min according to **Method 3** described in 4-1-3. The residue obtained from evaporation of the solvent was allowed to pass through a short column (silica gel, 60 mash, 3 cm in length and 2 cm in diameter) to remove the remained sensitizer and a minor amount of tars formed during the irradiation. The column was then washed by haxanes/ethyl acetate (90/10) binary solvent(100 ml). The eluents were combined and then evaporated under reduced pressure to give the crude dimers (300 mg). The GC trace showed that the crude products contained a major fraction (73%) and a minor fraction (27%). The crude product was chromatographed (3% ethyl acetate in hexanes) to afford 120 mg of the major product (120 mg, contaminated by 12% of the minor product); GC-MS m/e (CI mode) 297(M^++1); (EI mode) 296(M^+,2), 148(100); ^{1}H NMR ($CDCl_3$) δ: 1.21(6H,d,Me), 1.70-2.00(2H,m,methine), 2.83(2H,d,benzylic), 3.80(6H,s,OMe), 6.8-7.2(8H,m,phenyl); ^{13}C NMR ($CDCl_3$) δ: 18.80, 43.29, 52.64, 55.26, 113.87, 127.73, 136.04, 158.15. The ^{1}H NMR data matched those of **21** reported in the literature.[100] Therefore, the two products were assigned as the dimers **21** (major) and **22** (minor), respectively.

(b). Preparation of Dimer 22

Following the procedures reported,[41] a solution of **3** (15 g) in cyclohexane (175 ml) was irradiated under nitrogen for 20 h. The light source was a 200 W Hanovia medium pressure mercury lamp through a Pyrex filter. The removal of the solvent under reduced pressure gave rise to yellow oily crude products which contained only one major fraction with 93% purity. The crude products were chromatographed (2.5% ethyl acetate in hexanes) to afford a pure oily product (2.2 g); GC-MS m/e (CI mode) 297(M^++1); (EI mode) 296(M^+,2), 148(100); ^{1}H NMR ($CDCl_3$) δ: 1.24(6H,d,Me), 2.80(2H,m,methine), 3.46(2H,d,benzylic), 3.73(6H,s,OMe), 6.7-7.2(8H,m,phenyl). The ^{1}H NMR data matched those of **22** reported in the literature.[41]

(c). Dimerization of 3 Sensitized by $DBMBF_2$, $BABF_2$, 9-CN-An, and TCB

A CH_3CN solution (1 ml) containing **3** (5.0 X 10^{-1} M) and a sensitizer (2 X 10^{-2} M) was irradiated with a 350 nm light source according to **Method 3** described in 4-1-3.* The samples were taken for GC analysis in certain time intervals and then put back into the "merry-go-round" for further photolysis. Octadecane (2.0 X 10^{-3} M) was added to the solutions prior to irradiation as the internal standard for GC analysis. For the quantitative analysis of **21** and **22**, the

* When TCB (1 X 10^{-2} M) was used as the sensitizer, the sample was deaerated by purging nitrogen through for 3 min prior to irradiation.

calibrations with respect to the internal standard were carried out with the authentic samples of **21** and **22**. The yields of **21** and **22** along the irradiation time scale for each sample are shown in Fig.2-26 - 2-29. At the end of photolysis (4 h), $DBMBF_2$ and $BABF_2$ remained essentially not consumed as shown by the GC analysis and the photolysates showed a yellow-brown color. In the case of 9-CN-An being the sensitizer, two GC peaks other than the peaks of **21** and **22** appeared at RT = 4.8 - 5.0 min (250°, HP-1, 25 m) both having a parent peak at m/e = 351 on the GC-MS spectra. The GC trace showed that about 40% of 9-CN-An was consumed in 4 h of irradiation. In TCB-**3** system, the original dark purple color had faded after 4 h of irradiation. The change in the concentration of TCB upon the irradiation could not be monitored by the GC that was equipped only with an FID detector.

(d). $DBMBF_2$ Sensitized Cycloreversion of 21 and 22

CH_3CN solutions (5 ml each) of **21** (1.03×10^{-2} M) or **22** (1.92×10^{-2} M) with $DBMBF_2$ (2.0×10^{-2} M) added as the sensitizer and octadecane (2.0×10^{-3} M) added as the internal standard for GC analysis were placed in Pyrex test tubes and irradiated with a 350 nm light source according to **Method 3** described in 4-1-3. The disappearance of the dimers and the formation of **3** were followed by GC analysis and the results are shown in Fig.2-30 and 2-31. A yellow color was developed immediately upon adding $DBMBF_2$ into the solutions of **21** or **22**

and remained at the end of irradiation. In both cases $DBMBF_2$ did not show any observable decrease in concentration at the end of irradiation as shown by GC analysis.

(e). The Direct Photolysis of 22 in CH_3CN

A undegassed solution of **22** (2.0×10^{-2} M) in CH_3CN (5 ml) containing octadecane (2.0×10^{-3} M) as the internal standard for GC analysis was irradiated with a 300 nm light source for 4 h according to **Method 3** described in 4-1-3. The photolysate was directly analyzed by GC at certain time intervals. The results are shown in Fig.4-7.

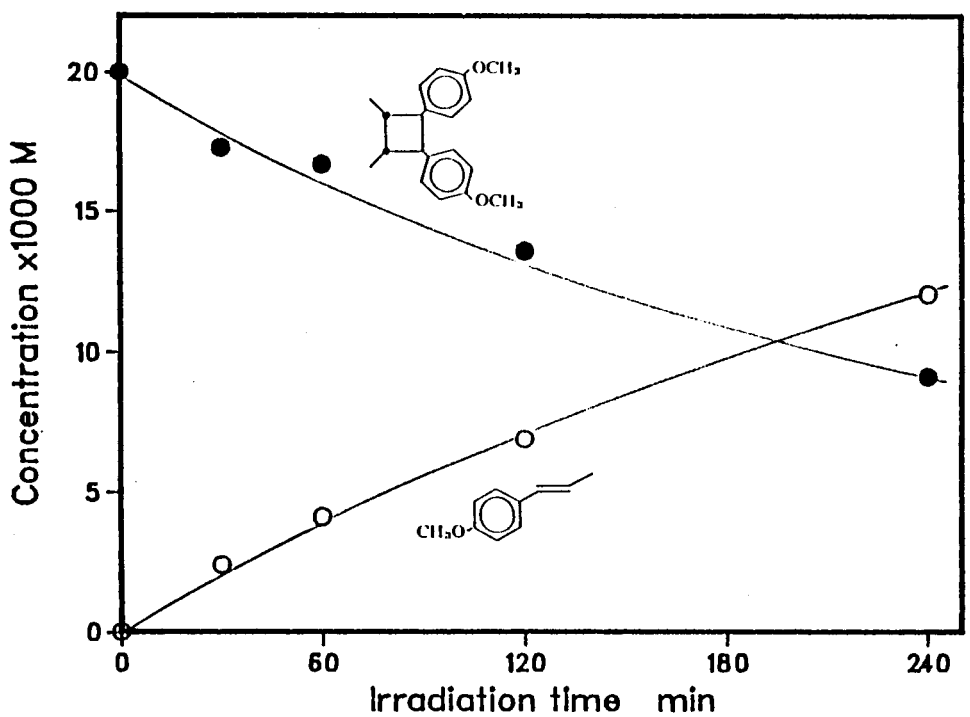

Figure 4-7. The direct photolysis of **22** in CH_3CN. The initial concentration of **22** was 2.0×10^{-2} M.

(f). The Monochromatic Photolysis

A CH_3CN solution of **3** (5.0×10^{-1} M) and $DBMBF_2$ (2.0×10^{-2} M) was irradiated monochromaticly at 312.8 nm and 437 nm, respectively, under the conditions same as those described in 4-5-4 except octadecane (2.0 X 10-3 M) was added as the internal standard prior to the photolysis and a wider band width (5 nm) was used instead. The photolysate was directly analyzed by GC, showing both **21** and **22** formed upon irradiation at either wavelength. The yields of the two dimers were calculated form the GC peak area ration with respect to that of the internal standard and listed in Table 2-16.

At 312.8 nm, the distinction coefficient of **3** (ε_3) was 1833 and that of $DBMBF_2$ (ε_{DBMBF_2}) was 4100. Therefore, only 8.2% of the incident light was absorbed by $DBMBF_2$. At 437 nm, $\varepsilon_3=0$, $\varepsilon_{DBMBF_2}=0$, whereas the absorbance of the ground state complex (GSC) of $DBMBF_2$ with **3** was 1.634 (read from Fig.2-9), corresponding to 98% of the incident light absorbed at the wavelength. The ratio of outputs of the lamp at 312.8 nm and 437 nm is 43/27. Taking the yield of **21** as the measure of the quantum yield of anethole cation radical and assuming the yield is proportional to the irradiation time in low conversion range, the relative quantum yield of the cation radical in the monochromatic photolysis at 437 nm with

respect to that at 312.8 nm was calculated by the equation shown below.

Φ_{437} = [(yield of **21** at 437nm)/(yield of **21** at 312.8nm)]
X(output ratio of the lamp)
X(fraction of light absorbed by $DBMBF_2$)
X[1/(fraction of light absorbed by the GSC at 437nm)]
$X\Phi_{312.7}$
= $(0.025/0.34)X(43/27)X0.082X(1/0.98)X\Phi_{312.7}$
= $0.01\Phi_{312.7}$.

4-6. Photolysis of $DBMBF_2$ in the Presence of 2-Cyclopentenone Ethylene Ketal (20) - A False Photoreaction

4-6-1. $DBMBF_2$ "Sensitized" Dimerization of 20

A CH_3CN solution (30 ml) containing freshly distilled **20** (1.89 g, 5 X 10^{-1} M) and $DBMBF_2$ (0.41 g, 5 X 10^{-2} M) was placed in 6 Pyrex test tubes (100 X 13 mm) and irradiated with a 350 nm light source according to **Method 3** described in 4-1-3. After 2.5 h irradiation, the pale yellow reaction mixture turned to brownish yellow. The solvent was removed by flash distillation to give a wet yellow residue which was treated with 30 ml of hexanes. A yellow precipitate (0.35g) was filtered out and identified to be a mixture of $DBMBF_2$ and

dibenzoylmethane by the GC analysis. The filtrate contained significant amount of 2-cyclopentenone as shown by GC analysis. The enone, unreacted ketal, and the solvent were removed from the filtrate by flash evaporation to give a crude product (0.5 g) which contained fraction A (19%),fraction B and C (81%), and trace of fraction D shown by the GC analysis. The crude product was then passed through a flash chromatography column (30% ethyl acetate in hexanes) affording pure fraction A (33 mg), fraction B (73 mg), and fraction C (100 mg). Fraction A (**95**) showed up on the GC spectra as a broadened single peak but proved to be a mixture of two compounds (**95a** and **95b**) by ^1H NMR spectroscopy. **95** was treated with hydrochloric acid in CH_3CN/H_2O (1:1 v/v) binary solvent to give two new compounds **98a** and **98b** with a ratio of 4/6 as shown by the GC analysis. Fraction B (**96a**, 50 mg) and C (**96b**, 50 mg) were also treated with hydrochloric acid in CH_3CN/H_2O (1:1 v/v) binary solvent for 1h at room temperature to give **98a** and **98b**, respectively, as confirmed by coinjections. The hydrolysates were neutralized with aqueous $NaHCO_3$ followed by abstraction with ether. The crude products obtained from evaporation of ether were chromatographed (10% ethyl acetate in hexanes) to give pure **98a** (35 mg, 89%) and **98b** (33 mg, 84%), respectively. The spectroscopic data of **95**, **96a**, **96b**, **98a**, and **98b** are given in Table 4-17 - 4-20.

The control experiment in the dark gave no product after 12 h storage as checked by GC analysis.

Table 4-17. IR Data of **95**, **96a**, **96b**, **98a**, and **98b**.

dimer	υ (cm^{-1})
95 (neat)	2975, 2896, 1470, 1347, 1321, 1217, 1171, 1108, 1031, 958, 896.
96a (neat)	2980, 2900, 1740, 1483, 1341, 1298, 1140, 1027, 956, 906, 863.
96b (neat)	2980, 2898, 1736, 1453, 1361, 1312, 1180, 980, 1028, 957, 899, 869.
98a (C_6D_6)	2963, 2915, 2890, 1755, 1736.
98b (C_6D_6)	2959, 2926, 1750, 1736.

Table 4-18. MS Data of **95**, **96a**, **96b**, **98a**, and **98b**.

dimer	MS (m/e)	
	CI (M^++1)	EI
95	253	252(M^+,8), 207(59), 125(36), 99(100), 86(32), 55(16).
96a	209	208(M^+,39), 152(21), 126(41), 99(100), 86(75), 55(10).

to be continued at next page.

Table 4-18. (cont.)

96b	209	208(M^+,21), 152(11), 126(55), 99(30), 86(100), 55(13).
98a		164(M^+,100), 146(3), 136(20), 121(22), 108(19), 93(24), 79(87), 66(53), 55(19).
98b		164(M^+,100), 146(1), 136(27), 121(22), 107(21), 93(24), 79(72), 66(45), 55(17).

Table 4-19. ^{1}H NMR Data of **96a**, **96b**, **98a**, and **98d**.

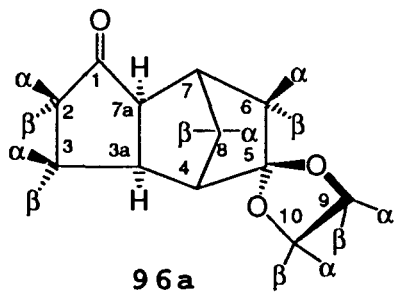

96a

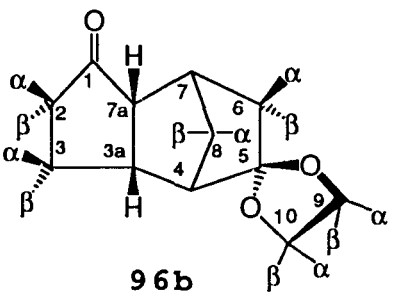

96b

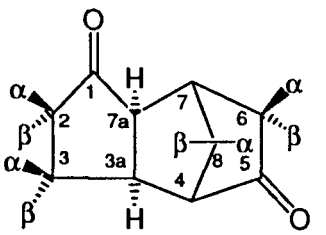

98a

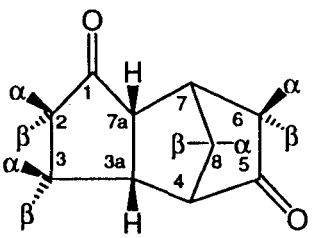

98b

Compound	δ(ppm) and J(Hz) in C_6D_6
96a	0.93(1H,m), 0.98(1H,dm), 1.40 (1H,dm), 1.55(1H,dm), 1.71(1H,m), 1.81-1.90(3H,m), 1.99(1H,bd), 2.34(1H,dm), 2.61(1H,dm), 2.71(1H,ddd), 2.32-2.53(4H,m).

to be continued at next page.

Table 4-19. (cont.)

96b	1.13($H_{8\alpha}$,dm), 1.57($H_{3\beta}$,m), 1.73($H_{6\alpha}$,dd), 1.80($H_{6\beta}$,ddm), 1.83($H_{8\beta}$,dm), 1.99(H_4,bs), 2.15($H_{3\alpha}$,dm), 2.19($H_{2\beta}$,m), 2.30(H_{3a},m), 2.33(H_{7a},bs), 2.44(H_7,bs), 2.79($H_{2\alpha}$,ddd), 3.25-3.34($H_{10\alpha}$,$H_{10\beta}$,m), 3.25-3.40($H_{9\alpha}$,$H_{9\beta}$,m); $J_{2\alpha,2\beta}$=20.9, $J_{2\alpha,3\alpha}$=$J_{2\alpha,3\beta}$=10.6, $J_{3\alpha,3\beta}$=14.0, $J_{3\alpha,2\beta}$=12.0, $J_{7,6\alpha}$=1.0, $J_{7,6\beta}$=4.6, $J_{8\alpha,8\beta}$=9.9, $J_{8\alpha,4}$=1.6, $J_{8\alpha,6\alpha}$=3.1, $J_{8\alpha,7}$=1.8, $J_{8\beta,4}$=$J_{8\beta,7}$=1.5, $J_{6\alpha,6\beta}$=14.1.
98a	0.73($H_{3\alpha}$,dddd), 0.86($H_{8\beta}$, dddd), 0.93($H_{8\alpha}$,ddddd), 1.39($H_{6\beta}$,dd), 1.56($H_{6\alpha}$,dd), 1.64-1.80($H_{2\alpha}$,$H_{2\beta}$,m), 1.68,(H_{7a},bd), 1.74($H_{3\beta}$,dddd), 1.95(H_{3a}, ddd), 2.09(H_4,bs), 2.54(H_7,bs); $J_{3\alpha,3\beta}$=14.0, $J_{3\beta,3a}$=9.8, $J_{2\beta,3\beta}$=5.6, $J_{3\beta,2\alpha}$=9.8, $J_{3\alpha,3a}$=6.1, $J_{2\beta,3\alpha}$=10.2, $J_{2\alpha,3\alpha}$=10.2, $J_{3a,7a}$=9.2, $J_{3a,4}$=0, $J_{3a,8\alpha}$=1.3, $J_{7,6\alpha}$=4.3, $J_{7,6\beta}$=0, $J_{7,8\alpha}$=1.3, $J_{7,8\beta}$=2.2, $J_{6\alpha,6\beta}$=17.3, $J_{6\beta,8\beta}$=4.0, $J_{7a,8\alpha}$=1.3, $J_{7,7a}$=0, $J_{4,8\alpha}$=1.3, $J_{4,8\beta}$=1.1, $J_{8\alpha,8\beta}$=11.1.
98b	1.01($H_{8\beta}$,ddddd), 1.14($H_{8\alpha}$,ddd), 1.38($H_{3\beta}$,m), 1.52($H_{3\alpha}$,dddd), 1.57($H_{6\alpha}$,dd), 1.76($H_{6\beta}$,dd), ~1.88($H_{2\beta}$,m), ~1.89($H_{2\alpha}$,m), 2.16(H_{3a},m), ~2.19(H_{7a},m), 2.23(H_4,bs), 2.38(H_7,bs) $J_{3\alpha,3\beta}$=14.0, $J_{3\alpha,3a}$=2.6, $J_{2\alpha,3\alpha}$=7.0, $J_{3\alpha,2\beta}$=8.8, $J_{3\beta,3a}$=9.6, $J_{2\beta,3\beta}$=10.2, $J_{4,8\alpha}$=1.5, $J_{4,8\beta}$=0.9, $J_{6\alpha,7}$=4.2, $J_{6\beta,8\beta}$=4.5, $J_{6\beta,7}$=0, $J_{7,7a}$=4.0, $J_{7,8\alpha}$=1.4, $J_{8\alpha,8\beta}$=10.0, $J_{3a,8\alpha}$=$J_{7a,8\alpha}$=0.

Table 4-20. ^{13}C NMR Data of **96a**, **96b**, **98a**, and **98d**.

Compound	δ (ppm) in C_6D_6.
96a	24.45(t), 33.58(t), 35.69(d), 38.85(t), 39.76(d), 43.22(t), 51.71(d), 54.16(d), 63.90(t), 64.60(t), 115.41(s), 218.26(s).
96b	21.50(C_3,t), 38.82(C_7,d), 39.56(C_6,t), 40.61(C_2,t), 41.47(C_{3a},d), 42.19(C_8,t), 48.52(C_4,d), 52.30(C_{7a},d), 62.87(C_9,t), 64.99(C_{10},t), 115.85(C_5,s), 220.64(C_1,s)
98a	23.92, 32.99, 37.40, 38.73, 39.16, 43.64, 53.43, 65.50, 212.55, 216.37.
98b[a]	21.45, 38.13, 38.89, 40.74, 41.53, 42.14, 51.34, 56.04.

a.Carbonyl carbons were missing due to too low concentration.

4-6-2. The Dimerization of 20 "Catalyzed" by *tris*(*p*-bromophenyl)Aminium Hexachloroantimonate (BAHA)

To a solution of **20** (35 mg, 0.28 mmol) in dry dichloromethane (10 ml) was added BAHA (163 mg, 0.20 mmol) under nitrogen atmosphere at 0°C. After 30 min of magnetic stirring the reaction mixture was taken out and passed through a short column the upper half of which was filled with silica gel (230-400 mesh, 10x50 mm) and the lower half with basic alumina (80-200 mesh, 10x50 mm). The eluent (50 ml, ethyl acetate and hexanes in 1:1 ratio) was collected and then the solvent was removed under reduced pressure to give a oily residue (19.7 mg, 56%) which consisted of **95**, **96a**, **96b**,

and trace of **98a, 98b** as confirmed by coinjection with the authentic samples obtained from $DBMBF_2$ "sensitized" photodimerization of **20**. The residue was treated with hydrochloric acid in methanol/H_2O (4:1 v/v) to give **98a** and **98b** as the sole products.

A controlled experiment, in which all conditions were the same as described above except 2,6-lutidine (54 mg, 0.5 mmol) was added prior to the reaction, was qualitatively examined. **No product was found in the GC traces checked in 10, 30, and 140 min after BAHA was added.**

4-6-3. The Photolysis of $DBMBF_2$-20 System in the Presence of Pyridine

Two Pyrex test tubes (100 X 13 mm) containing CH_3CN solutions (5 ml each) of $DBMBF_2$ (5 X 10^{-2} M) and **20** (5 X 10^{-1} M), in one of which was added pyridine (1 X 10^{-1} M), were irradiated for 90 min with a 350 nm light source in an identical condition according to **Method 3** described in 4-1-3. While the sample without pyridine produced at least 4 X 10^{-2} M of **95** as the major product estimated from the GC peak ratio against the internal standard (octadecane, 2.0 X 10^{-3} M), **the sample with pyridine added gave no product at all.** The pH values of the two sample were measured after the irradiation by mixing reaction solutions (0.2 ml) with equal amount of distilled water. The sample without pyridine added showed pH = 4, whereas the sample with pyridine added, pH = 6.5, as shown on a test paper (BDH).

4-6-4. Acid-Catalyzed Dimerization of 20

To two CH_3CN solutions (5 ml each) of **20** (5 X 10^{-1} M) were added one drop of BF_3-ether or sulfuric acid (98%) at room temperature respectively, and the reaction mixtures were checked by GC in 15 min. Both samples gave mixtures of **95**, **96a** **96b** and trace of **98a** and **98b** as well as 2-cyclopentenone, which was confirmed by coinjections with the authentic samples.

4-6-5. Dimerization of 20 by Direct Irradiation

A nitrogen-purged CH_3CN solution (5 ml) of **20** (5 x 10^{-1} M) in a Pyrex test tube (13 x 100 mm) was irradiated by a 350 nm light source for 1 h according to **Method 3** described in 4-1-3. The resulting reaction mixture was directly taken for GC analysis. As shown on the GC trace, two major products, **99a** and **99b**, were obtained in a ratio of 46:54. The MS data of **99a** [(m/e), CI: 209 (M^++1); EI: 208 (M^+,7), 126 (23), 99 (100), 86 (21), 55 (6)] and **99b** [(m/e), CI: 209 (M^++1); EI: 208 (M^+,11), 125 (23), 99(82), 86(100), 55(9)] suggested that they are the monoketal dimers. Upon adding a few drops of diluted hydrochloric acid, **99a** and **99b** were then readily converted to the *cis*-anti-*cis*, head-to-head cyclopentenone dimer **54**, and the *cis*-anti-*cis*, head-to-tail dimer, **53**, respectively. This was confirmed by coinjections with the authentic samples obtained by the photodimerization of 2-cyclopentenone in CH_3CN.[41,106]

4-7. Photodimerization of Acetylacetone

4-7-1. Photolysis of Acetylacetone in Hexanes

A solution of acetylacetone (1 g) in hexane (30 ml) was distributed in 6 Pyrex test tubes (100 X 10 mm) and sealed with a septum under nitrogen. These tubes were irradiated with a 300 nm light source for 36 h according to **Method 3** described in 4-1-3. The crude photolysate was evaporated and the residue was chromatographed (8% ethyl acetate in hexanes) on a silicic column. The major fraction (450 mg) was recrystallized from ethyl acetate-hexanes (1:6 v/v) binary solvent giving colorless parallelepiped crystals (compound **70**), m.p. 73-4°; GC-MS (CI mode): 183 (M^+-H_2O+1); (EI mode): 182 (M^+-H_2O, 0.5), 157 (9), 139 (18), 115(30), 97(52), 71(13), and 43(100); IR, (neat) 3450, 2988, 1710, 1358, 1177, and 1104 cm^{-1}; ^1H NMR (in C_6D_6), δ 3,89(dd, 1H, J = 10.6 and 7.5 Hz), 2.40(dd, 1H, J = 10.6 and 13.4 Hz), 1.78(dd, 1H, J = 7.5 and 13.4 Hz), 2.14(s, 3H), 2.07(s, 3H), 1.65(1H, D_2O exchangeable), 1.24(s, 3H), and 1.06(s, 3H); UV, 287.5 nm (ε 57). The ^1H NMR spectrum of **70** in C_6D_6 kept changing upon storage: the original signals decreased gradually while new signals appeared and increased to reach an equilibrium in about 12 hours. The major new peaks appeared at 1.06, 1.51, 1.55, 1.76, 2.03 and 2.25 ppm, respectively, all as singlet. The addition of trace of water accelerated the appearance of these new peaks. **70** dissolved readily in water and polar organic solvents.

4-7-2. X-ray Crystallographic Analysis*

The crystal structure of dimer **70** (Fig.4-8) was investigated with an ENRAF-NONIUS CAD diffractometer. A piece of the crystal (from CH_2Cl_2-hexane, m.p. 73-5° C) of dimensions 0.41 X 0.28 X 0.25 mm was examined. The crystal data are given as follows: $C_{10}H_{16}O_4$ mMτ = 200.2; monoclinic, $P2_1/C$; a = 16.766(2), b = 7.736(2), c = 11.024(1) Å , β = 130.44(2)°; V = 1088.2 $Å^3$; z = 4, Dx = 1.222 g/cm^3, μ(MoKα) =

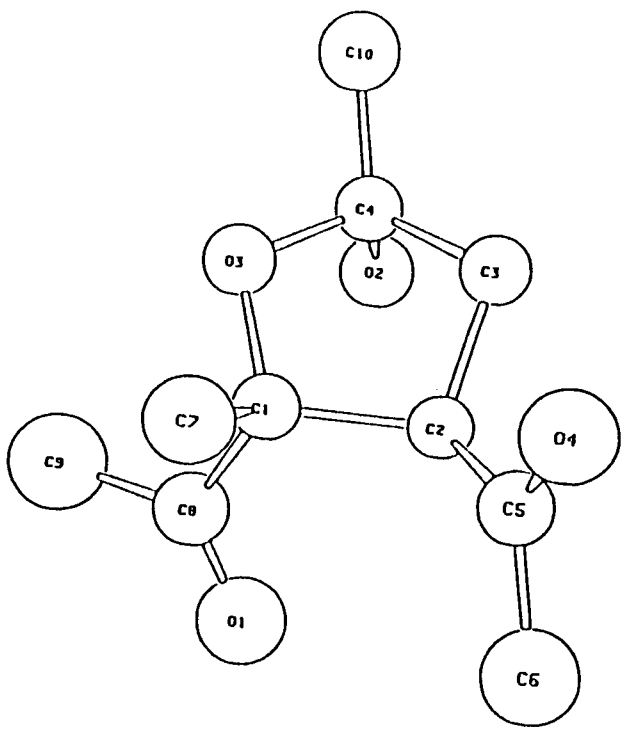

Figure 4-8. Perspective drawing of the molecular structure of **70**.

*The X-ray crystallographic analysis was carried out by Prof. Sheng-Zhi Hu at The Department of Chemistry, Xiamen University, Xiamen, P. R. China.

0.88 cm^{-1}, λ = 0.71013 Å. Of 2315 unique reflections collected to $2\theta_{max}$ = 52°, 1661 with I > 3σ(I) were considered observed and used for the refinement. LP corrections and PSI absorption correction were applied. The E map obtained from direct methods using MULTAN-82 programme gave all non-hydrogen atoms. After several cycles of full-matrix least-sqare anisotropic refinement, difference Fourier syntheses gave the hydrogen atoms. Convergence was reached at R_f = 0.040 and R_W = 0.051 with $\omega = [\sigma^2(F_o) + 0.0004|F|^2 + 1.0]^{-1}$. All residual peaks in the final difference map were under 0.33 $eÅ^{-3}$.

4-7-3. Preparation of the Methoxylated Dimer 71

A solution of **70** (180 mg, 0.9 mmol) in methanol (50 ml) containing 3 drops of concentrated hydrochloric acid was stirred at room temperature for 10 min. The starting material disappeared in 5 minutes and a new peak cleanly showed up on the GC traces. The solution was neutralized to PH = 6 with methanolic KOH solution and then evaporated. The residue was taken up in ether (30 ml) and washed with saturated $NaHCO_3$ solution and water. The residue from the ether solution was passed through a silicic acid column to afford **71** (109 mg) as a colorless oil; GC-MS: (CI mode) 183(M^+-OCH_3); (EI mode) 183(M^+-OCH_3, 10), 171(39), 139(55), 97(95) and 43(100); IR(neat) 2980, 2811, 1708, 1447, 1376, 1348, 1309, 1210, 1099, 1058 and 854 cm^{-1}; ^1H NMR (C_6D_6) 3.81(H_c, ddd, J=7.7,

0.4, and 11.4 Hz), 2.89(s, 3H), 2.37(H_a, dd, J=11.4 and 12 9 Hz), 2.04(s, 3H), 1.98(d, 3H, J=0.4 Hz), 1.87(H_b, dd, J=12.9 and 7.7 Hz), 1.20(s, 3H) and 1.01(s, 3H); ^{13}C NMR 205.18(CO), 209.99(CO), 107.72(s), 89.32(s), 53.82(d), 49.22(q), 40.72(t), 30.71(q), 24.05(q), 21.22(q), and 20.77(q). In ^1H NOE difference spectra, irradiation of the C_1-CH_3 protons caused enhancement of H_a and *vice versa*, and irradiation of H_c caused enhancement of H_b but not H_a. In selectively decoupled ^{13}C spectra, when a selective decoupling was applied to H_c, C_6-Me, C_1-Me, or C_4-Me, signal collapse or line sharpening were observed at 53.82 and 205.18 ppm, 30.71 and 209.99 ppm, 107.72 and 21.22 ppm, 20.77, 89.32 and 209.99 ppm, respectively.

4-7-4. Photolysis of Acetylacetone in Various Solvents

Nitrogen purged solutions of acetylacetone (400 mg in each solution, 0.8 M) in various solvents (hexane, benzene, CH_2Cl_2, CH_3CN, THF, and CH_3OH, 5 ml each) were put in Pyrex test tubes (100 X 13 mm) and irradiated by a 300 nm light source for 20 h according to **Method 3** described in 4-1-3. The photolysates were analyzed by GC, taking the amount of dimer **70** formed in hexane as the external standard. About 1/10 amount of **70** was formed in benzene; only trace amount of **70** was formed in CH_2Cl_2; no dimer was detected in either CH_3CN, THF, or CH_3OH.

4-7-5. Attempted Photolysis of Other β-Diketones in Hexane

2,4-hexanedione (**72**), 2,2,6,6-tetramethyl-3,5-heptanedione (**73**), 6-methyl-2,4-heptanedione (**74**), dibenzoylmethane (DBM), and benzoylacetone (BA) were examined. A solution of a ketone (5×10^{-1} M) in hexane (5 ml) were sealed in a Pyrex test tube under nitrogen and irradiated for 72 h by a 300 nm light source (for **72**, **73**, and **74**) or a 350 nm light source (for DBM and BA) according to **method 3** described in 4-1-3. For all runs, the diketone remained as the major peak (> 90% in area ratio) on GC traces after the irradiation. Two very small GC peaks were respectively found in the photolysates of **72** and **74**, showing parent peaks at m/e = 210 and 268, respectively, in the GC-MS spectra. No dimers were found for **73**, DBM, and BA by GC-MS analysis.

4-8. Photocycloaddition of Acetylacetone to Norbornene

4-8-1. Photolysis of Acetylacetone-Norbornene System in Hexane

A deaerated solution of acetylacetone (150 mg, 5×10^{-2} M) and norbornene (1.5 g, 5×10^{-1} M) in hexane (30 ml) was distributed in 6 Pyrex test tubes (100 X 13 mm) and irradiated by a 200 W Hanovia medium pressure mercury lamp

for 48 h according to **Method 2** described in 4-1-3. The photolysate contained, besides the excess norbornene, a major fraction (**75**) and other 10 minor fractions (**76-81** and **82a-82d**) but essentially no acetylacetone as seen from the GC analysis. The retention times, relative peak ratios on GC analysis, and the GC-MS data of each fractions are given in Tab 4-20 and 4-21, respectively. The photolysate was chromatographed (20% ethyl acetate in hexanes) giving **75** (144 mg, 49.5% based on acetylacetone) as a colorless oil;*

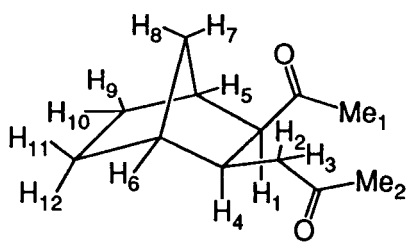

75

^{1}H NMR ($CDCl_3$): δ 2.86(H_3,dd,J=18.8, 9.8Hz), 2.81(H_1,bd,J=8.6, 1.1Hz), 2.40(H_2,dd,J=18.8, 5.4Hz), 2.20-2.27(H_4 and H_5,m), 2.11(Me_2,s,3H), 2.05(Me_1,s,3H), 1.89(H_6,s,J=2Hz), 1.79(H_7,dm, J=10.4,2.0,2.0Hz), 1.49-1.59(H_9 and H_{11},m,2H), 1.18-1.33(H_{10} and H_{12},m,2H), 1.08(H_8,dm,J=10.4,1.8,1.1Hz); ^{13}C NMR ($CDCl_3$) δ: 29.46, 29.60, 30.01, 32.27, 34.27, 41.40, 41.52, 41.76, 45.29, 56.39, 209.31, 211.93.

*The MS data are reported in Table 4-21.

Table 4-21. The Retention Time (RT) and Relative Area Ratio (AR) of the Products of Acetylacetone-Norbornene System.[a]

	product										
	76	**77**	**78**	**79**	**8**	**80**	**81**	**82a**	**82b**	**82c**	**82d**
RT(min)[b]	1.85	1.96	2.14	2.24	2.48	2.71	2.91	4.68	4.80	4.94	5.44
AR(%)[c]	6.8	8.6	4.6	2.6	45.6	5.1	9.1	5.2	1.9	1.0	4.1

a. In hexane, photolyzed for 72 h with a 200 W medium pressure mercury lamp through a Pyrex filter. The GC spectrum was taken after removal of hexane and unreacted norbornene by flash distillation.
b. OV-1 column (12 m X 0.20 mm), 180°.
c. The ratio of the GC peak area against the total area of all peaks appeared on the GC trace except the solvent peak. The sum of AR in this table is 94.6%.

Table 4-22. GC-MS Data of the Products of Acetylacetone-Norbornene System.

compd	m/e(CI,M^++1)	m/e(EI)
76	139	138(M^+,4), 120(5), 95(100), 80(19), 71(31), 67(49), 55(7), 43(24).
77	153	152(M^+,10), 134(26), 119(11), 109(38), 95(78), 94(81), 83(50), 79(46), 67(100), 66(90), 55(13), 43(16).

to be continued at next page

Table 4-22. (cont.)

78	181	180(M^+,17), 165(4), 151(9), 137(4), 123(20), 95(100), 81(27), 67(24), 55(8), 41(5).
79	179	178(M^+,52), 163(41), 149(12), 135(4), 121(6), 95(100), 81(72), 67(63), 55(20), 41(18).
75	195	194(M^+,96), 161(22), 151(91), 137(100), 109(34), 93(31), 79(20), 66(31), 43(73).
80	191	190(M^+,16), 159(20), 147(8), 134(8), 122(26), 108(18), 95(100), 80(47), 67(60), 55(7), 41(11).
81	189	188(M^+,4), 159(34), 145(6), 131(14), 117(21), 105(17), 91(100), 79(45), 66(33), 53(7), 41(16).
82a		232(M^+,7), 204(6), 174(100), 146(12), 123(36), 107(10), 95(22), 80(25), 67(24), 43(12).
82b		232(M^+,21), 214(9), 204(9), 189(50), 174(100), 165(49), 137(79), 123(24), 109(21), 95(31), 79(24), 67(29), 43(9).
82c		232(M^+,7), 204(8), 191(10), 174(100), 163(11), 146(12), 123(31), 107(12), 95(26), 80(22), 67(24), 43(12).
82d		232(M^+,5), 217(18), 204(10), 189(3), 174(100), 146(9), 137(8), 123(16), 109(7), 95(15), 80(10), 67(10), 43(4).

4-8-2. Quenching of the Cycloaddition by 1,3-Pentadiene

Solutions for the quenching experiment were prepared by pipetting appropriate amount of a stock solutions ([acetylacetone] = 5.47 X 10^{-2} M, [norbornene] = 5.00 X 10^{-1} M, [1,3-pentadiene] = 6.25 X 10^{-2} M, in hexane) into 5 ml volumetric flasks which were then filled up with another stock solution ([acetylacetone] = 5.47 X 10^{-2} M, [norbornene] = 5.00 X 10^{-1} M, [1,3-pentadiene] = 0, in hexane). Octadecane (2.53 X 10^{-3} M) was added to both stock solutions as the internal standard for GC analysis. The solutions containing various amounts of 1,3-pentadiene (0-6.25 X 10^{-2} M) were distributed in 6 septum-sealed Pyrex test tubes, purged with dry nitrogen for 5 min, and then irradiated with a 300 nm light source according to **Method 3** described in 4-1-3. The irradiation was stopped in 3.5 h for sampling then resumed for another 11 h by when the loss of acetylacetone was still less than 40% as shown by the GC analysis. The relative quantum yield of **75** as well as those of **80** and **82** were obtained from the GC peak ratios and plotted against concentration of 1,3-pentadiene as shown by Fig.2-38.

4-8-3. The Concentration Dependence

Deaerated hexane solutions (5 ml each) containing acetylacetone (5.21 X 10^{-2} M), octadecane (5.04 X 10^{-3} M,

internal standard), and various concentrations of norbornene (5.00×10^{-2} M - 6.24×10^{-1} M) were placed in Pyrex test tubes and irradiated for 6.5 h with a 300 nm light source according to **Method 3** described in 4-1-3. The photolysates were analyzed by GC, showing that the consumption of acetylacetone was less than 20%. The ratios of GC peak area of the products with respect to that of the internal standard were taken as the relative yields and the results are shown in Fig.2-40.

The dependence of the product yields on the concentration of acetylacetone was also determined by the same experimental procedure as described above, except the irradiation time was shortened to 5 h and the concentration of norbornene (5.03×10^{-1} M) was fixed, whereas that of acetylacetone varied from 5.1×10^{-2} M to 3.0×10^{-1} M. The results are shown in Fig.2-39.

4-8-4. Aldol Condensation of 75

(a). 75 in Acidic Methanol

Into a methanolic solution (20 ml) containing **75** (100 mg, 0.51 mmol) was added 2 drops of concentrated hydrochloric acid. The reaction mixture was stirred for 3.75 h at ambient temperature and then neutralized to PH = 6 by adding methanolic NaOH and then evaporated. The residue was taken up in ether (50 ml) which was washed with saturated aqueous $NaHCO_3$ followed by distilled water and then dried over magnesium sulfate. The GC analysis showed that the ether

solution contained unreacted **75** (5.5% relative yield according to the GC peak area), **83** (73.9%), **84a** (14.3%), **84b** (6.3%). The residue from the ether solution was chromatographed (20% ethyl acetate in hexanes) affording **83** (55 mg) and **84a** (12 mg) as colorless oils. 2-exo-acetonyl-3-endo-acetyl-norbornane (**83**); IR (neat) 2935(s), 2852(m), 1703(s), 1346(s, b), 1222(m), 1164(m, b), 944(w), cm^{-1}; GC-MS (m/e, CI mode) 195(M^++1); (m/e, EI mode) 194(M^+,10) 176(11), 138(57), 127(100), 109(50), 93(56), 43(40). ^1H NMR (C_6D_6), δ:

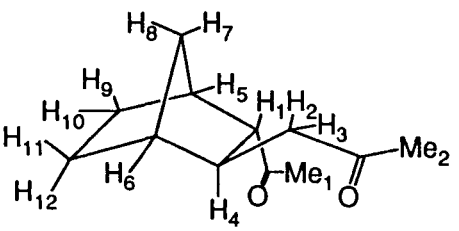

83

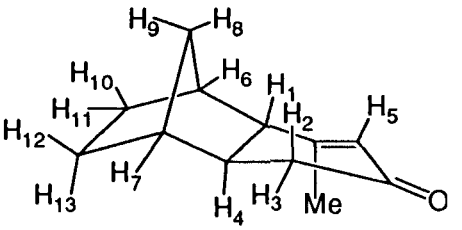

84a

1.02(H_8,dm,J=10.0,1.5,1.5,1.5Hz), 1.11-1.18(H_{10},H_{12},m,2H), 1.22(H_7,dm,J=10.0,1.8Hz), 1.31-1.44(H_9,H_{11},m,2H), 1.73(H_2, dd,J=14.9,8.8Hz), 1.77(Me,s,3H), 1.78(H_6,m,J=1.8,1.5Hz), 1.81(Me,s,3H), 1,98(H_3,dd,J=14.9,6.6Hz), 2.12(H_1,dd,J=7.2, 3.3Hz), 2.15(H_5,m,J=3.3,2.1,1.5Hz), 2.49(H_4, m,J=1.8,1.5Hz); ^{13}C NMR (C_6D_6), δ: 23.72, 28.95, 29.06, 29.38, 37.61, 38.16, 40.84, 42.39, 49.68, 61.51, 206.05, 206.63. **84a**, GC-FTIR 2961, 2881, 1684 cm^{-1}; GC-MS (m/e) 176(M^+,36), 161(6), 148(13), 109(12), 93(8), 82(100). ^1H NMR (C_6D_6), δ: 1.11(H_9,dm,

J=10.0,1.3,1.3,1.3Hz), 1.24-1.33(H_8,H_{13},m,2H), 1.38(H_{11},m,1H), 1.50-1.66(H_{10},H_{12},m,2H), 1.90(H_2,dd,J=18.7,4.4Hz), 1.90(Me,bs, 3H,J=1.2,1.2Hz), 2.05(H_7,bs,1H), 2.16-2.29(H_1,H_4,m,2H), 2.51 (H_3,dd,J=18.7,7.7Hz), 2.67(H_6,bs,1H), 5.88(H_5,m,J=1.2,1.0 Hz). **84b**, GC-FTIR 2963, 2883, 1695 cm^{-1}; GC-MS (m/e) 176(M^+,36), 161(6), 134(22), 109(100), 91(19), 80(30), 67(17).

(b). 83 in Acidic Methanol

A solution of **83** (300 mg, 0.15 mmol) in methanol (6 ml) with 1 drop of concentrated hydrochloric acid added was refluxed for 11.6 h. The reaction mixture was then cooled and diluted with 50 ml of methanol for GC analysis. The GC trace showed that the reaction mixture contained no trace of **75** but unreacted **83** (13.5%), **84a** (57.6%) and **84b** (28.9%).

(c). 75 in Acidic CH_3CN

A solution of **75** (5 mg, 0.025 mmol) in CH_3CN (5 ml) with 1 drop of concentrated hydrochloric acid added was stirred for 15 min at room temperature. The reaction solution was diluted with 15 ml of CH_3CN and then analyzed by GC. the GC trace showed that the resulting solution contained unreacted **75** (7%) and **83** (93%).

4-9. Sensitized Solvent Addition to Norbornene

4-9-1. Preparation of the Solvent Adducts

To nitrogen purged solutions of norbornene (1.0-1.9 X 10^{-1} M) in a solvent was added acetone (5-12.5% by volume) as the sensitizer except in the experiment where acetone itself was the solvent. The solutions were irradiated with a 200 W Hanovia medium pressure lamp through a Pyrex filter or with a 300 nm light source. The irradiation was applied until almost all norbornene disappeared on the GC trace. The photolysates were then evaporated and chromatographed (2-5% ethyl acetate in hexanes) to give the adducts all as colorless oil. Some of the adducts (**77**, **86**, **87**, **88**, and **89**) had very strong pleasant odor. The samples for microanalysis were further purified by preparative GC (OV-1, 4' X 0.25"). The experimental conditions and the yield of adducts are listed in Table 2-17 and the analytical data of the adducts are given in Table 4-23 - Table 4-26.

Table 4-23. IR Data of the Adducts of Norbornene to Various Solvents.[a]

compound	υ (cm^{-1})
77	2946(s), 2869(m), 1712(s), 1452(w), 1406(w), 1353(m), 1172(m).

to be continued at next page

Table 4-23. (cont.)

85	1968(s), 2888(s), 2260(m), 1464(m), 1431(m), 1366(w), 1327(w), 1318(w), 952(w), 930(w).
86a+86b (GC-FTIR)	2951(s), 2912(w), 2870(s), 1454(m), 1315(w), 1069(s), 1015(w), 945(w), 899(w).
87a+87b	2950(s), 2912(w), 2870(m), 2852(w), 1450(m), 1352(w), 1279(w), 1121(s), 1099(w), 1081(m), 903(m), 884(m).
88a	2940(s), 2861(s), 2759(w), 1470(w), 1449(w), 1391(b,m), 1206(w), 1176(m), 1158(m), 1123(m), 1080(s), 1030(m), 1020(m), 964(m), 941(m), 831(w).
88b(74%) +**88c**(26%)	2940(s), 2860(s), 2741(w), 1468(w), 1449(m), 1378(w), 1307(w), 1148(s), 1084(s), 1010(m), 937(s), 899(m), 829(w).
89	3400(b,s), 2945(s), 2864(m), 1457(m), 1371(s), 1297(m), 1211(m), 1160(s), 1146(w), 1124(m), 1110(w), 949(m), 924(m), 864(m).
90	2944(s), 2863(s), 1447(m), 1310(w,sh), 1300(m), 1217(m), 920(w), 741(s), 730(s,sh).
91a(70%) +**91b**(30%)	2972(s), 1891(s), 1463(m), 1440(m), 1310(m), 1240(w), 936(m), 739(m), 677(m).

a. Neat film unless otherwise specified.

Table 4-24. GC-MS Data of the Adducts of Norbornene to Various Solvents.

compd.	m/e(CI)	m/e(EI)
77	153(M^++1)	152(M^+,9), 134(28), 123(10), 109(34), 95(73), 94(91), 83(62), 79(49), 67(100), 66(88), 58(15), 43(88).
85	136(M^++1)	135(M^+,3), 134(10), 120(6), 107(12), 95(50), 79(21), 68(100), 67(98), 53(22), 41(55).
86a +**86b**	167(M^++1)	166(M^+,17), 123(10), 105(12), 79(18), 71(100), 55(11), 43(40), 41(43).
87a +**87b**		182(M^+,28), 153(12), 124(6), 95(80), 87(83), 86(100), 79(26), 67(70), 55(22), 43(29), 41(70).
88a	169(M^++1)	95(3), 73(100), 55(4), 45(30), 41(13).
88b	169(M^++1)	
89	137(M^++1-H_2O)	139(4), 121(3), 95(9), 81(12), 67(19), 59(100), 43(13), 41(10).
90	145(M^++1-Cl,9) 143(M^++1-Cl,23) 107(100)	143(M^++1,^{35}Cl)

to be continued at next page

Table 4-24. (cont.)

91a	193(M^++1,5,$^{35}Cl^{37}Cl$) 191(M^++1,6,$2^{35}Cl$) 159(7), 157(21), 121(100)	121(3), 95(100), 79(18), 67(45), 53(12), 41(18).
91b	159(6), 157(18) 121(100), 95(27)	121(6), 95(100), 79(18), 67(60), 53(14), 41(22).
92	159(10), 157(30)	121(4), 95(100), 79(4), 67(20).

Table 4-25. ^1H NMR Chemical Shift(δ) and Coupling Constants (J) of the Adducts of Norbornene to Various Solvents.

compound	δ(ppm) and J(Hz)
77(C_6D_6)	0.90(dm,1H), 1.00(dm, 1H), 1.09-1.23(m,3H), 1.37-1.53(m,3H), 1.68(s,3H), 1.79-1.90(m,3H), 1.98(dm,1H), 2.10(bs,1H).
85($CDCl_3$)	1.07-1.25(m,3H), 1.20(dm,1H,J=10.0), 1.30(dm,1H,J=10.0,2.0,2.0,1.8), 1.45-1.61(m,3H), 1.82(dddd,1H,J=8.0,7.5,7.4,4.8), 2.13(bs,1H), 2.15(dd,1H,J=16.2,7.4), 2.23(dd,1H,16.2,8.0), 2.28(m,1H).
86a($CDCl_3$)	0.99(dddd,1H,J=11.8,5.0,4.8,2.8), 1.09(dm,1H,J=10.1), 1.12-1.24(m,2H), 1.31-1.59(m,5H), 1.78-2.03(m,4H), 2.18(bs,1H), 2.33(bs,1H), 3.49(m,1H), 3.73(m,1H), 3.84(m,1H).

to be continued at next page

Table 4-25. (cont.)

	(C_6D_6)	0.92(dm,1H,J=12.0), 1.04-1.28(m,4H), 1.40(dm,1H,9.9), 1.43-1.77(m,7H), 2.15(bs,1H), 2.73(bs,1H), 3.42(ddd,1H,J=9.8,7.5,6.1), 3.57-3.66(m,1H), 3.77-3.83(m,1H).
86b	($CDCl_3$)	1.1-1.95(m,13H), 1.98(bs,1H), 2.23(bs,1H), ~3.50(m,1H), ~3.70(m,1H), ~3.80(m,1H).
	(C_6D_6)	1.04-1.77(m,13H), 1.97(bs,1H), 2.25(bs,1H), 3.50(m,1H), ~3.60(m,1H), ~3.70(m,1H).
87a	(C_6D_6)	0.81(m,1H), 0.97-1.15(m,4H), 1.22-1.52(m,4H), 2.07(bs,1H), 2.68(bs,1H), 3.05-3.26(m 2H), 3.33-3.55(m,4H), 3.72(m,1H).
87b	(C_6D_6)	0.97-1.70(m,9H), 1.82(bs,1H), 2.18(bs,1H), 3.05-3.26(m,2H),3.33-3.55(m,4H), 3.78(m,1H).
88a	(C_6D_6)	1.07(ddddd,1H,J=9.8,1.8,1.8,1.8,1.0), 1.09(m,1H),1.38-1.52(m,3H), 1.56(ddddd,1H,J=9.8,1.9,1.9,1.9,1.9), 1.65(dm,J=12.1,4.8,2.5,1.2), 1.86(dddd,1H,J=7.5,6.1,5.2,1.8), 2.17(bs,1H,J=4.8,4.0,1.9,1.8), 2.51(bs,1H,J=3.8,1.9,1.8), 3.40(m,2H), 3.56(m,2H),, 4.65(d,1H,J=6.1).
88b	(C_6D_6)	0.60(m,1H), 0.97-1.07(m,3H), 1.12(m,1H), 1.23(dm,1H), 1.30-1.50(m,3H), 2.04(bs,1H), 2.57(bs,1H), 3.27(dd,1H,J=7.5,6.3), 3.47(ddd,1H,J=9.8,6.3,6.3), 3.66(dd,1H,J=7.5,6.3), 4.82(s,1H), 5.01(s,1H).

to be continued at next page

Table 4-25. (cont.)

88c (C_6D_6)	0.97-1.63(m,9H), 1.65(bs,1H), 2.17(bs,1H), 3.29(dd,1H,J=7.2,7.2), 3.53(ddd,1H,J=7.2,6.8,6.8), 3.70(dd,1H,J=7.2,6.8), 4.78(s,1H), 4.99(s,1H).
89 (C_6D_6)	1.01(s,3H), 1.03(m,1H), 1.06(s,3H), 1.09-1.15(m,2H), 1.23-1.33(m,4H), 1.43-1.53(m,3H), 2.21(bs,2H).
90 (C_6D_6)	1.15(dm,1H), 1.20-1.38(m,3H), 1.47-1.63(m,3H), 2.15(dddd,1H,J=9.2,9.2,5.5,1.0), 2.32(bs,1H), 2.45(bd,1H,J=3.5), 5.36(d,1H,J=9.2).
91a (C_6D_6)	0.84(bdd,1H,J=10.0,1.1), 1.88-1.97(m,2H), 1.02(dm,1H,J=10.0,1.8,1.8,1.8), 1.22-1.37(m,4H), 1.68(bs,1H), 1.72(dddd,1H,J=9.3,7.5,6.0,1.8), 2.03(bs,1H), 3.28(dd,1H,J=11.9,3.3), 3.45(ddd,1H,J=9.3,5.5,3.3).
91b (C_6D_6)	0.52(dm,1H), 0.83-0.99(m,3H), 0.99-1.08(m,2H), 1.24-1.42(m,2H), 1.96(bs,1H), 2.49(bs,1H), 3.22(dd,1H,J=12.2,6.3), 3.27-3.38(m,2H).
92 (C_6D_6)	1.90-1.03(m,3H), 1.27-1.39(m,3H), 1.46(dddd,1H,J=12.2,6.8,4.0,2.5), 1.66(dm,1H,J=10.2), 1.71(s,3H), 2.02(dd,1H,J=7.1,8.1), 2.08(bs,1H), 2.37(bs,1H).

Table 4-26. Microanalysis Data of **85** and **89**.

85	Calcd.	C: 79.95,	H: 9.69,	N: 10.35.
	Found	79.66,	9.96	10.39.
89	Calcd.	C: 77.76,	H: 11.76.	
		78.12,	11.70	

4-9-2. Solvent Addition Reactions Sensitized by Acetylacetone

Solutions of norbornene (235 mg, 5 X 10^{-1} M) and acetylacetone (25 mg, 5 X 10^{-2} M) in various solvents (5 ml each) were placed in Pyrex test tubes (100 X 13 mm), purged with nitrogen for 5 min, and then irradiated with a 300 nm light source for 2.5 h according to **Method 3** described in 4-1-3. The reaction solutions were checked by GC immediately after the irradiation. The major products were identical with those obtained in acetone-sensitized solvent addition reactions (4-9-1) as proved by coinjections and their GC-MS spectra. As shown by the GC analysis, acetylacetone was only slightly consumed (< 10%). The GC yields of these major products, namely, the ratio of peak area of the product(s) over the sum of all peak areas appeared on the GC spectrum except the solvent and unreacted reactants, were: 63.1% (**85**,

in CH_3CN), 73.3% (**86a** + **86b**, in THF), 62.1% (**87a** + **87b**, in 1,4-dioxane), 58.6% (**89**, in isopropanol), 83.8% (**90**, in CH_2Cl_2), and 77.9% (**91a** + **91b**, in 1,2-dichloroethane). The minor products appeared also less than 15% in GC yield, having a similar composition as that found in acetone-sensitized reactions (4-9-1) though **77** showed up only in tiny amount (< 3%).

4-9-3. Quantum Yield measurements of Acetylacetone-Sensitized Solvent Addition Reactions of Norbornene.

The solutions for the quantum yield measurements were prepared by weighing norbornene (~95 mg), acetylacetone (~54 mg), and dodecane (~8 mg, internal standard for GC analysis) into 10 ml volumetric flasks which were then filled up with a solvent (CH_3CN, CH_2Cl_2, or THF). Each solution (4 ml) was pipetted into a Pyrex test tube (100 X 13 mm) and then purged with nitrogen for 5 min. The test tubes were sealed under nitrogen and put in a "merry-go-round" along with another test tube containing a deaerated benzophenone-benzhydrol actinometer (4 ml) as described in 4-3-5. These 4 test tubes were evenly placed and irradiated with a 300 nm light source according to **Method 3** described in 4-1-3. The actinometer was pulled out in 5 min and its place was immediately taken by another test tube loaded with a CH_3CN solution (4 ml) of acetylacetone (5×10^{-2} M) to keep the consistency of

irradiation. The photolysates were analyzed by GC after 35 min of irradiation by when the consumptions of norbornene were less than 5%. The quantum yields of the adducts were calculated according to the absorbed light intensity (1.205 X 10^{-5} Einstein/min) and the peak area ratios towards the internal standard. The results and experimental conditions are listed in Table 2-18.

4-9-4. The Photolysis of Norbornene-TCB System

Solutions of norbornene (1 X 10^{-1} M) and TCB (~2 X 10^{-2} M, except in hexane where ~2 X 10^{-3} M) in various solutions (5 ml of hexane, CH_2Cl_2, THF, CH_3CN, or benzene) each contained in a sealed Pyrex test tube (100 X 13 mm) were purged with nitrogen for 5 min and then irradiated with a 200 W Hanovia medium pressure mercury lamp for 4 h according to **Method 2** described in 2-1-3. The color of reaction solutions in hexane and THF did not change upon irradiation, whereas those in CH_2Cl_2, CH_3CN, and benzene had turned from light yellow to dark red at the end of reaction. The photolysates were checked by GC analysis which showed a main peak (compound **93**) at a retention time (RT) of 1.97 min (120°, OV-1, 12 M) with a high GC yield (70 - 90%) for all solvents except in THF. There were three minor peaks appeared on the GC traces at longer RT, 2.62, 2.72, and 3.12 min, respectively. The photolysates obtained from CH_3CN and CH_2Cl_2 were combined and

evaporated giving a dark red residue. The viscous oily residue was taken up in haxanes (10 ml) and passed through a short column (neutral alumina, 80-200 mesh, Fisher, 2 cm in length and 1 cm in diameter) which was then washed with another 10 ml of hexanes. The combined eluents were evaporated to give a yellow oil (49 mg) which contained **93** (~75%) and one of the three minor products (**94**, ~15%) as shown by the GC analysis. The pure samples of **93** and **94** for NMR studies were obtained from the preparative GC described in 2-1-2. **93**, GC-MS m/e (CI) 132(M^+,9,^{37}Cl), 130(M^+,27,^{35}Cl), 95(100); (EI) 132(M^+,1,^{37}Cl), 130(M^+,4,^{35}Cl), 95(9), 79(17), 67(100), 53(28), 41(48); ^1H NMR (C_6D_6) δ: 1.19(dm,1H,J=1.1,1.6,2.0,9.9Hz), 1.48(ddddd,1H,J=1.6,1.6,1.6, 2.2,10.1Hz), 1.54-1.68(m,2H), 1.72(dddd,1H,J=1.6,4.9,8.9, 12.0Hz), 2.03(ddd,1H,J=2.2,7.4,13.6Hz), 2.26(dddd,1H,J=2.0, 3.0,3.9,13.6Hz), 2.29(ddddd,1H,J=1.6,2.0,2.0,3.9,10.1Hz), 2.47(bs,1H,J=1.1,1.1,1.6,2.0,3.9Hz), 2.78(bd,1H,J=0.7,1.1, 1.6,1.6,4.9Hz), 3.11(ddd,1H,J=0.7,1.6,3.0,7.4Hz). **94**, GC-MS m/e (CI mode) 168((M^+,1,2^{37}Cl), 166((M^+,5,$^{35}Cl^{37}Cl$), 164(M^+,9,2 ^{35}Cl), 131(30), 129(100). ^1H NMR (C_6D_6) δ: 0.74(dddd,1H, J=2.5,4.6,9.1,12.5Hz), 0.90(dddd,1H,J=1.6,1.6,2.6,10.7Hz), 0.97(ddddd,1H,J=1.6,4.0,4.6,12.5,12.5Hz), 1.14(dddd,1H,J=4.2, 4.9,12.5,12.5Hz), 1.57(ddddd,1H,J=1.5,1.6,2.4,2.5,10.7Hz), 1.76(dddd,1H,J=2.4,4.2,9.1,12.5Hz), 1.98(bs,1H,J=1.5,1.6,4.0, 4.3Hz), 2.01(bd,1H,J=1.6,1.6,4.9Hz), 3.57(dd,1H,J=2.6,2.7Hz), 4.08(ddd,1H,J=1.6,2.7,4.3Hz).

4-9-5. The NMR Studies of Norbornene - TCB System under Irradiation

A deaerated CD_2Cl_2 solution (0.7 ml) of norbornene (~1 X 10^{-1} M) and TCB (~2 X 10^{-2} M) in an NMR tube was put into an EM360 NMR spectrometer and irradiated with a light beam through a Pyrex filter by the set up for the attempted CIDNP studies (4-5-1b). The ^1H spectra were consecutively (1 min each scan) recorded before, during, and after the irradiation. The signals of olefinic and bridgehead protons of norbornene showed up vividly in the spectrum taken before the irradiation (spectrum A in Fig.4-9), then started to broaden after the light was turned on and eventually lost in the baseline in 3 min (spectra B-D in Fig.4-9). However, they resumed immediately when the light was turned off (spectrum E in Fig.4-9). The disappearance and restoration of the proton signals could be repeated again and again by switching the light on and off alternatively.

4-9-6. ESR Studies on Norbornene - TCB System

(a). TCB in Benzene

A solution of TCB (2.0 X 10^{-2} M) in benzene (0.5 ml) was placed in a quartz ESR tube (5 mm in diameter) and deaerated by three frozen-thaw circles. The sample was put in the cavity of a Varian E-4 ESR spectrometer equipped with a

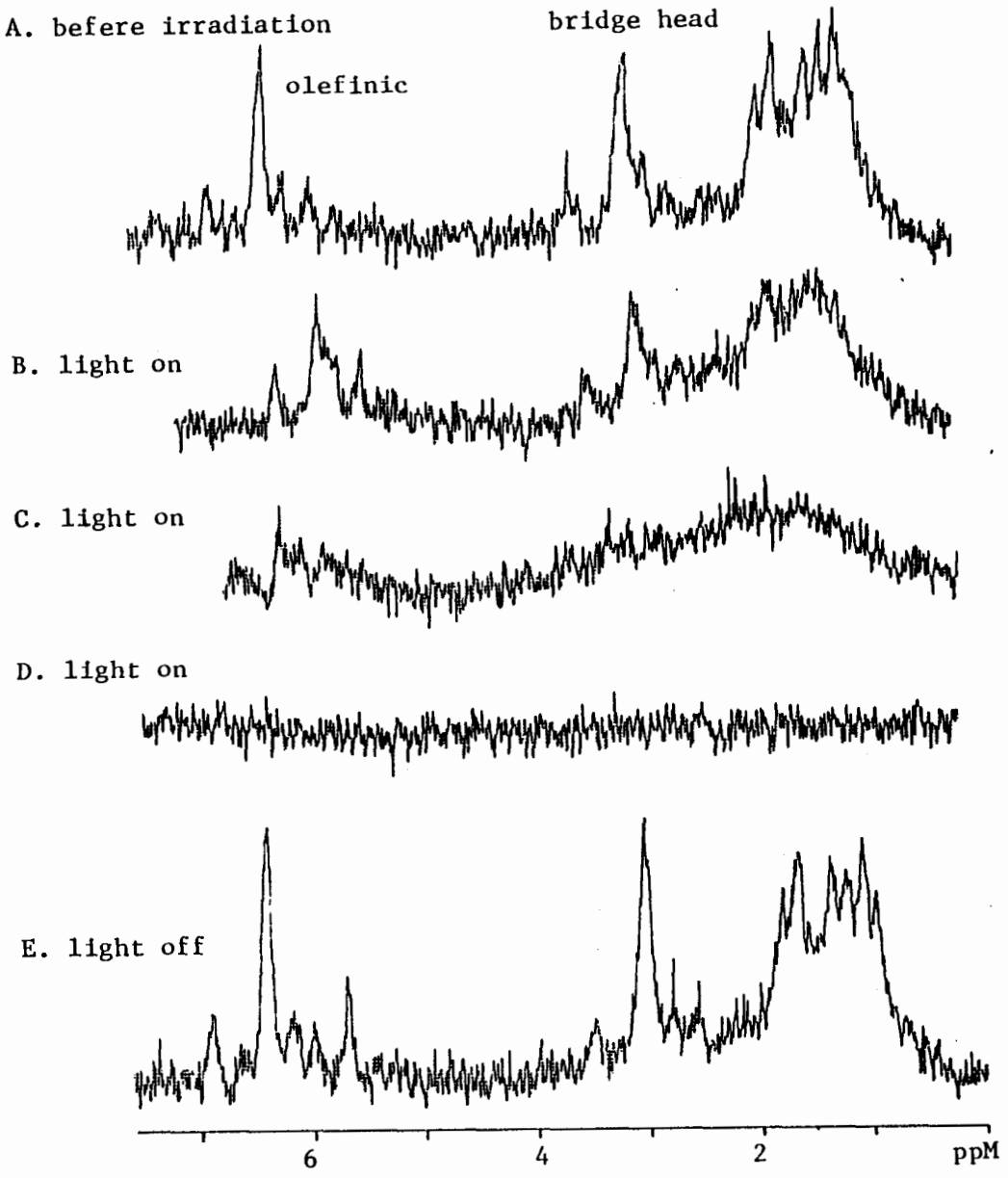

Figure 4-9. The ^{1}H NMR spectra (60 MHz, CD_2Cl_2) of norbornene (~1 X 10^{-1} M) in the presence of TCB (~2 X 10^{-2} M). The magnetic filed was calibrated by a external TMS sample in the same solution. The field was found drifting during the irradiation due to the change in temperature. The scan speed was 0.5 min.

window on the side of the cavity from where the light was introduced in. The light source was an 1000 W high pressure mercury lamp (Wild) through a Pyrex filter. The magnetic field was calibrated with a standard sample (g = 2.00260) supplied by Varian. It was checked that there was no signal detected from the sample before the irradiation. An ESR signal at g = 2.0061 with a peak-to-peak width of 6.5 G was detected when the light was turned on (spectrum A in Fig.2-41). A same sample with tiny amount of *tert*-nitrosobutane (~1 X 10^{-6} M) added was also examined (Fig.2-42).

(b). Norbornene - TCB System

A solution of norbornene (1.0 X 10^{-1} M) and TCB (2.0 X 10^{-2} M) in benzene (0.7 ml) was deaerated and then examined on the ESR spectrometer according to the procedure described above (4-9-6, a). A very strong signal at g = 2.0050 with no hyperfine structures was recorded after the light was turned on as shown in Fig.2-41. Consecutive scans were applied in order to follow the generation and decay of the signal. To a same sample was added CF_3COOH (~1 X 10^{-2} M) by injection through the rubber septum on the top of the ESR tube and the ESR spectrum was taken immediately with the light on. The addition of acid resulted in a sharp drop in intensity of the signal as shown in Fig.2-41. The spectra of another sample with *tert*-nitrosobutane (~1 X 10^{-6} M) added were also recorded (Fig.2-42).

REFERENCES

1. Lewis, F. D. In "*Photoinduced Electron Transfer*"; Fox, M. A.; Chanon, M., Ed.; Elsevier: New York, 1988; Part C, Chapter 4.1, p 1.

2. Chanon, M.; Eberson, L. In "*Photoinduced Electron Transfer*"; Fox, M. A.; Chanon, M., Ed.; Elsevier: New York, 1988; Part A, Chapter 1.11, p 409.

3. Klett, M.; Johnson, R. P. *J. Am. Chem. Soc.* **1985**, *107*, 6615.

4. Albini, A.; Arnold, D. R. *Can. J. Chem.* **1978**, *56*, 2985.

5. Roth, H. D. *Acc. Chem. Res.* **1987**, *20*, 343.

6. Arnold, D. R.; Borg, R. M.; Albini, A. *J. Chem. Soc., Chem. Commun.* **1981**, 138.

7. Lewis, F. D.; Kojima, M. *J. Am. Chem. Soc.* **1988**, *110*, 8660.

8. Lewis, F. D.; Kojima, M. *J. Am. Chem. Soc.* **1988**, *110*, 8664.

9. Jones, C. R.; Allman, B. J.; Mooring, A.; Spahic, B. *J. Am. Chem. Soc.* **1983**, *105*, 652.

10. Gassman, P. G.; Singleton, D. A. *J. Am. Chem. Soc.* **1984**, *106*, 7993.

11. Libman, J. *J. Chem. Soc., Chem. Commun.* **1976**, 361.

12. Gassman, P. G.; Olson, K. D. *Tetrahedron Lett.* **1983**, *24*, 19.

13. Mattes, S. L.; Farid, S. In "*Organic Photochemistry*"; Padwa, A.; Ed.; Marcel Dekker: New York, 1983; Vol.6, p 233.

14. Handman, J.; Harrison, A.; Porter, G. *Nature* **1984**, *307*, 534.

15. Ruggles, C. J.; Halpern, A. M. *J. Am. Chem. Soc.* **1988**, *110*, 5692.

16. Hub, W.; Schneider, S.; Dorr, F.; Oxman, J. D.; Lewis, F. D. *J. Am. Chem. Soc.* **1984**, *106*, 701.

17. Taylor, G. N. *Chem. Phys. Lett.* **1971**, *10*, 355.

18. Basu, S.; Nath, D.; Chowdhury, M. *J. Lumin.* **1988**, *40&41*, 252.

19. Creed, D.; Wine, P. H.; Caldwell, R. A.; Melton, L. A. *J. Am. Chem. Soc.* **1976**, *98*, 621.

20. Sakurai, H.; Pac, C. *Mem. Inst. Sci. Ind. Res. Osaka Univ.* **1980**, *37*, 59.

21. Caldwell, R. A.; Ghali, N. I.; Chien, C.-K.; DeMarco, D.; Smith, L. *J. Am. Chem. Soc.* **1978**, *100*, 2857.

22. Caldwell, R. A.; Creed, D. *J. Am. Chem. Soc.* **1978**, *100*, 2905.

23. Jones II, G.; Chiang, S.-H.; Becker, W. G.; Welch, J. A.; *J. Phys. Chem.* **1982**, *86*, 2805.

24. Kavarnos, G. J.; Turro, N. J. *Chem. Rev.* **1986**, *86*, 401.

25. Scaiano, J. C. *J. Phy. Chem.* **1981**, *85*, 2851.

26. Inber, S.; Linschitz, H.; Cohen, S. G. *J. Am. Chem. Soc.* **1980**, *102*, 1419.

27. Simon, J. D.; Peters, K. S. *J. Am. Chem. Soc.* **1982**, *104*, 6542.

28. Simon, J. D.; Peters, K. S. *J. Am. Chem. Soc.* **1983**, *105*, 4875.

29. Das, P. K.; Bobrowski, K. *J. Chem. Soc., Faraday Trans. 2.* **1981**, 77, 1009.

30. Freilich, S. C.; Peters, K. S. *J. Am. Chem. Soc.* **1985**, *107*, 3819.

31. Gersdorf, J.; Mattay, J.; Gornor, H. *J. Am. Chem. Soc.* **1987**, *109*, 1203.

32. Yang, N. C.; Hui, M. H.; Shold, D. M.; Turro, N. J.; Hautala, R. R.; Dawes, K.; Dalton. *J. Am. Chem. Soc.* **1977**, *99*, 3023.

33. Mattay, J.; Gersdrof, J.; Leismann, H.; Steenken, S. *Angew. Chem.,Int. Ed. Engl.* **1984**, *23*, 249.

34. Griller, D.; Howard, J. A.; Marriott, P. R.; Scaiano, J. C. *J. Am. Chem. Soc.* **1981**, *103*, 619.

35. Gersdorf, J.; Mattay, J. *J. Photochem.* **1985**, *28*, 405.

36. Mattay, J.; Gersdorf, J.; Mertes, J. *J. Chem. Soc., Chem. Commun.* **1985**, 1088.

37. Toporcer, L. H.; Dessy, R. E.; Green, I. E. *Inorg. Chem.* **1965**, *4*, 1649.

38. Houk, K. N.; Davis, L. P.; Newkome, G. R.; Duke, Jr., R. E.; Nauman, R. V. *J. Am. Chem. Soc.* **1973**, *95*, 8364.

39. Aue, D. H.; Webb, H. M.; Bowers, M. T. *J. Am. Chem. Soc.* **1975**, *97*, 4137.

40. Challand, B. D.; Kornis, G.; Lange, G.; de Mayo, P. *J. Org. Chem.* **1969**, *34*, 794.

41. Nozaki, H.; Kurita, M.; Mori, T.; Noyori, R. *Tetrahedron* **1968**, *24*, 1821.

42. Tada, M.; Harada, H.; Miura, K. *Bull. Chem. Soc. Jap.* **1978**, *51*, 839.

43. Barnum, D. W. *J. Inorg. Nucl. Chem.* **1961**, *21*, 221.

44. Fackler, J. P. *Progr. Inorg. Chem.* **1966**, 7, 361.

45. Kwan, C. L.; Kochi, J. K. *J. Am. Chem. Soc.* **1976**, *98*, 4903.

46. Chow, Y. L.; Buono-Core, G. E.; Marciniak, B.; Beddard, C. *Can. J. Chem.* **1983**, *61*, 801.

47. Vinogradov, M. G.; Fedorova, T. M.; Mikishin, G. I. *Russ. J. Org. Chem. (Engl. Transl.)* **1976**, *12*, 1183.

48. Heiba, E. I.; Dassau, R. M. *J. Org. Chem.* **1974**, *39*, 3456.

49. Russell, G. A.; Lokensgard, J. *J. Am. Chem. Soc.* **1967**, *89*, 3057.

50. Edwards, J. H.; McQuillin, F. J.; Wood, M. *J. Chem. Soc., Chem. Commun.* **1978**, 938.

51. Chow, Y. L.; Buono-Core, G. E. *J. Am. Chem. Soc.* **1982**, *104*, 3770.

52. Brown, N. M. D.; Bladon, P. *Chem. Commun.* **1966**, 304.

53. Burford, N.; Kennepohl, D.; Cowie, M.; Ball, R. G.; Cavell, R. G. *Inorg. Chem.* **1987**, *26*, 650.

54. Hester, R. E. *Chem. and Ind.* **1963**, 1397.

55. Pike, R. M.; Luongo, R. R. *J. Am. Chem. Soc.* **1965,** *87* , 1403.

56. Holloway, C. E.; Luongo, R. R.; Pike, R.M. *J. Am. Chem. Soc.* **1966,** *88* , 2060.

57. Taba, K.M.; Dalhoff, W. V. *J. Organometal. Chem.* **1985,** *280,* 27.

58. Pike, R. M.; Luongo, R. R. *J. Am. Chem. Soc.* **1966,** *88,* 2972.

59. Bally, I.; Balaban, A. T. *Studii Cercetari Chim.* **1969,** *17,* 431.

60. Mikhailov, B. M. *Pure & Appl. Chem.* **1977,** 749.

61. Morgan, G. T.; Tunstall, R. B. *J. Chem. Soc.* **1963,** *125,* 1924.

62. Brown, N. M. D.; Bladon, P. *J. Chem. Soc. (A)* **1969,** 526.

63. Hauser, C. R.; Frostick, F. C.; Mann, E. H. *J. Am. Chem. Soc.* **1952,** *74,* 3231.

64. Hauser, C. R.; Eby, C. J. *J. Am. Chem. Soc.* **1957,** *79,* 725.

65. House, H. O.; Reif, D. J. *J. Am. Chem. Soc.* **1955,** *77,* 6525.

66. Musso, H.; Figge, K. *Annalen* **1963,** 1.

67. Fischer, E. O.; Pleske, K. *Chem. Ber.* **1959,** *92,* 2841.

68. Umland, F.; Hohaus, E.; Brodte, K. *Chem. Ber.* **1973,** 2427.

69. Crimmins, T. F.; Hauser, C. R. *J. Org. Chem.* **1961,** 746.

70. Sone, K. *J. Am. Chem. Soc.* **1953,** *75,* 5207.

71. Jolm, R. H.; Cotton, F. A. *J. Am. Chem. Soc.* **1958,** *80,* 5658.

72. Darst, K. P.; Lukehart, C. M. *J. Organometall. Chem.* **1978,** *161,* 1.

73. Hanson, A. W.; Macauly, E. W. *Acta. Cryst.* **1972,** *B28,* 1961.

74. Halm, J. M. *Tappi* **1977,** *60,* 90.

75. Pross, A. *Acc. Chem. Res.* **1985**, *18*, 212.

76. El Shasly, M. F. Ph.D. Thesis, Virginia Polytechnic Institute and State University, (1972).

77. Halm, J. M. *U.S. US* **1982**, 4 360 584.

78. Karasev, V. E.; Korotkikh, O. A. *Russ. J. Inog. Chem. (Engl. Transl.)* **1986**, *31(4)*, 493.

79. Ilge, H.-D.; Faβler, D.; Hartmann, H. *Z. Chem.* **1984**, *24*, 218.

80. Ilge, H.-D.; Birckner, E.; Fassler, D.; Kozmenko, M. V.; Kuz'min, M. G.; Hartmann, H. *J. Photochem.* **1986**, *32*, 177.

81. Hawthorne, M. F.; Reintjes, M. *J. Org. Chem.* **1965**, *30*, 3851.

82. Utimoto, K.; Tanaka, T.; Nozaki, H. *Tetrahedron Lett.* **1972**, 1167.

83. Okada, K.; Hosoda, Y.; Oda, M. *J. Am. Chem. Soc.* **1986**, *108*, 321.

84. Reichardt, C. "*Solvent Effects in Organic Chemistry*" pp , Verlag Chemie: New York; 1979, 242-244.

85. Mulliken, R. S.; Person, W. B. "*Molecular complexes*" Wiley-Interscience, New York, 1969.

86. Yarwood, J. "*Spectroscopy and Structure of Molecular Complexes*"; Plenum Press: London, 1973.

87. Kim, E. K.; Kochi, J. K. *J. Org. Chem.* **1989**, *54*, 1692.

88. Murov, S. L. "*Handbook of Photochemistry*"; Marcel Dekker Inc.: New York 1973; p 4.

89. Rehm, D.; Weller, A. *Ber. Bunsenges. Phys. Chem.* **1969**, *73*, 834.

90. Rehm, D.; Weller, A. *Isr. J. Chem.* **1970**, *8*, 259.

91. Weller, A. *Z. Phys. Chem. NF* **1982**, *133*, 93.

92. Weller, A. *Z. Phys. Chem. NF* **1982**, *130*, 129.

93. Gassman, P. G.; Yamaguchi, R.; Koser, G. F. *J. Org. Chem.* **1978**, *43*, 4392, and reference cited therein.

94. "*Ionization Potential and Appearance Potential Measurements, 1971-1981*" Levin, R. D.; Lias, S. G., Ed., U. S. Government Printing Office: 1982.

95. Kubo, Y.; Suto, M.; Araki, T.; Mazzocchi, P. H.; Klingler, L.; Shook, D.; Somich, C. *J. Org. Chem.* **1986**, *51*, 4404.

96. Labianca, D. A.; Taylor, G. N.; Hammond, G. S. *J. Am. Chem. Soc.* **1972**, *94*, 3679.

97. McGullogh, J. *Chem. Rev.* **1987**, *87*, 811.

98. Bischof, P.; Heilbronnor. *Helv. Chem. Acta.* **1970**, *53*, 1677.

99. Masclet, P; Grosjean, D.; Mouvier, G.; Dubois, J. *J. Electron Spectro. Rela. Phenom.* **1973**, *2*, 225.

100. Lorenz, K. T.; Bauld, N. L. *J. Am. Chem. Soc.* **1987**,*109*, 1157.

101. Miller, L. L.; Nordblom, G. D.; Mayeda, E. A. *J. Org. Chem.* **1972**, *37*, 916.

102. Pouchert, C. J. "*The Aldrich Library of Infrsred Spectra*"; Aldrich Chem. Co: 1970, p 625.

103. Pasto, D. J.; Johnson, C. R. "*Laboratory Text for Organic Chemistry*"; Prentice-Hall, Inc.; New Jersey: 1979; p203.

104. de Mayo, P.; Takeshita, H.; Sattar, A. B. M. A. *Can. J. Chem.* **1963**, *41*, 440.

105. Budzikiewicz, H.; Djerassi, C.; Williams, D. H. *"Mass Spectrometry of Organic Compounds"*; Holden-Day. Inc: San Francisco. 1967; pp 155-157.

106. Wagner, P. J.; Bucheck, D. J. *J. Am. Chem. Soc.* **1969**, 5090.

107. Monroe, B. M.; Lee, C-G.; Turro, N. J. *Mol. Photochem.* **1974**, *6*, 271.

108. Roth, H. D.; Schilling, M. L. M.; Jones II, G. *J. Am. Chem. Soc.* **1981**, *103*, 1246.

109. Roth, H. D.; Schilling, M. L. M. *J. Am. Chem. Soc.* **1981**, *103*, 7210.

110. Valentine, D.; Turro, N. J.; Hammond, G. S. *J. Am. Chem. Soc.* **1964**, *86*, 5202.

111. Alder, K.; Stein, G. *Justus Liebigs Ann. Chem.* **1932**, *496*, 197.

112. Bellville, D. J.; Wirth, D. D.; Bauld, N. L. *J. Am. Chem. Soc.* **1981**, *103*, 718.

113. Engel, P. S.; Kitamura, A.; Keys, D. E. *J. Am. Chem. Soc.* **1987**, *52*, 5015.

114. Calhoun, G. C.; Schuster, G. B. *J. Am. Chem. Soc.* **1984**, *106*, 6870.

115. Reynolds, D. W.; Bauld, N. L. *Tetrahedron Lett.* **1985**, *26*, 2539.

116. Briegleb, P. G. *Angew. Chem. Internat.* Ed. **1964**, *3*, 617.

117. Majima, T.; Pac, C,; Sakurai, H. *Chem. Lett.* **1979**, 1133.

118. Pretsch, E.; Seibl, J.; Simon, W.; Clerc, T. "*Tables of Spectral Data for Structure Determination of Organic Compounds*"; Engl. Trnsl. by Birmann, K.; Springer-Verlag; Berlin: 1983; pp H185, 190.

119. Abraham, R. J.; Fisher, J. *Magn. Reson. Chem.* **1985**, *23*, 856.

120. DePuy, C. H.; Ponder, B. W.; Fitzpatrick, J. D. *J. Org. Chem.* **1964**, *29*, 3508.

121. Reusch, W. *J. Org. Chem.* **1962**, *27*, 1882.

122. Bruno, J. W.; Marks, T. J.; Lewis, F. D. *J. Am. Chem. Soc.* **1982**, *104*, 5580.

123. Yoshida, H.; Kambara, Y.; Ranby, B. *Bull. Chem. Soc. Jap.* **1974**, *47*, 2599.

124. Jones, II. G. In "*Photoinduced Electron Transfer*"; Fox, M. A.; Chanon, M., Ed.; Elsevier: New York, 1988; Part A, Chapter 1.7, p 245.

125. Mataga, N.; Ottolenghi, M. In "*Molecular Association*"; Foster, R. Ed.; Academic Press, Inc.: New York, 1979; Vol.2, p 1.

126. Davidson, R. S. *Adv. Phys. Org. Chem.* **1983**, *19*, 1.

127. Blann, W. G.; Fyfe, C. A.; Lyerla, J. R.; Yannoni, C. S. *J. Am. Chem. Soc.* **1981**, *103*, 2747.

128. Czekalla, J.; Schmillen, A.; Mager, K. J. *Electrochemie*, **1957**, *61*, 1053.

129. Mataga, N.; Murata, Y. *J. Am. Chem. Soc.* **1969**, *91*, 3144.

130. Kobayashi, T.; Yoshihara, K.; Nagakura, S. *Bull. Chem. Soc. Japn.* **1971**, 2603.

131. Jones, II. G.; Becker, W. G. *J. Am. Chem. Soc.* **1983**, *105*, 1276.

132. Prochorow, J. *Chem. Phys. Lett.* **1978**, *54*, 292.

133. Forster, T.; Kasper, K. *Z. Physik. Chem. NF* **1954**, *1*, 275.

134. Forster, T.; Kasper, K. *Z. Electrochem., Ber. Bunsenges. Physik. Chem.* **1955**, *59*, 976.

135. Forster, T. *Angew. Chem. Internat. Ed.* **1969**, *8*, 333.

136. Camerman, A.; Trotter, J. *Acta Crystallogr.* **1965**, *18*, 636.

137. Birks, J. B. "*Photophysics of Aromatic Molecules*"; Wiley-Interscience: London, 1970; p38.

138. Balzani, V.; Scandola, F. In "*Photochemical Conversion and Storage of Solar Energy*"; Connolly, J. S., Ed.; Academic: New York, 1981; Chapter 4.

139. Gassman, P. G.; Olson, K. D.; Walter, L.; Yamaguchi, R. *J. Am. Chem. Soc.* **1981**, *103*, 4977.

140. Baggott, J. E.; Pilling, M. J. *J. Chem. Soc. Faraday Trans.1*, **1983**, 79, 221.

141. Evans, T. R. *J. Am. Chem. Soc.* **1971**, *93*, 2081.

142. Corey, E. J.; Bass, J. D.; Le Mahieu, R.; Mitra, R. B. *J. Am. Chem. Soc.* **1964**, *86*, 5570.

143. Boerth, D. W. *J. Org. Chem.* **1982**, *47*, 4085.

144. Lam, E. Y. Y.; Valentine, D.; Hammond, G. S. *J. Am. Chem. Soc.* **1967**, *89*, 3482.

145. Casals, P.-F.; Ferard, J.; Ropert, R. *Tetrahedron Lett.* **1976**, *35*, 3077.

146. Rondan, N. G.; Paddon-Row, M. N.; Caramella, P.; Mareda, J.; Mueller, P. H.; Houk, K. N. *J. Am. Chem. Soc.* **1982**, *104*, 4974.

147. Lewis, F. D. *Acc. Chem. Res.* **1979**, *12*, 152.

148. Caldwell, R. A.; Creed, D. *Acc. Chem. Res.* **1980**, *13*, 45.

149. Mettes, S. L.; Farid, S. *Acc. Chem. Res.* **1982**, *15*, 80.

150. Yang, N. C. *Pure & Appl. Chem.* **1979**, *51*, 173.

151. Mimura, T.; Itoh, M. *J. Am. Chem. Soc.* **1976**, *98*, 1095.

152. Beens, H.; Weller, A. *Chem. Phys. Lett.* **1968**, *2*, 140.

153. Saltiel, J.; Townsend, D. E.; Waston, B. D.; Shannon, P. *J. Am. Chem. Soc.* **1975**, *97*, 5688.

154. Creed, D.; Caldwell, R. A. *J. Am. Chem. Soc.* **1974**, *96*, 7369.

155. Okajima, S.; Lim, B. T.; Lim, E. C. *Chem. Phys. Lett.* **1985**, *122*, 82.

156. Calhoun, G. C.; Schuster, G. B. *J. Am. Chem. Soc.* **1986**, *108*, 8021.

157. Lewis, F. D.; DeVoe, R. J. *Tetrhedron* **1982**, *38*, 1069.

158. Lewis, F. D.; DeVoe, R. J. *J. Org. Chem.* **1980**, *45*, 948.

159. Mettay, J. *Tetrhedron* **1985**, *41*, 2405.

160. Mazzocchi, P. H.; Minamikawa, S.; Bowen, M. J. *J. Org. Chem.* **1978**, *43*, 3079.

161. McGullough, J. J.; Miller, R. C.; Wu, W.-S. *Can. J. Chem.* **1977**, *55*, 2909.

162. Lewis, F. D.; Ho, T.-I.; DeVoe, R. J. *J. Org. Chem.* **1980**, *45*, 5283.

163. Albini, A.; Fasani, E.; Giavarini, F. *J. Org. Chem.* **1988**, *53*, 5601.

164. Smothers, W. K.; Meyer, M. C.; Saltiel, J. *J. Am. Chem. Soc.* **1983**, *105*, 545.

165. Hammond, G. S.; Turro, N. J.; Fisher, A. *J. Am. Chem. Soc.* **1961**, *83*, 4674.

166. Hammond, G. S.; Wyatt, P.; DeBoer, C. D.; Turro, N. J. *J. Am. Chem. Soc.* **1964**, *86*, 2532.

167. Murov, S.; Hammond, G. S. *J. Phys. Chem.* **1968**, *72*, 3797.

168. Turro, N. J.; Cherry, W. R.; Mirbach, M. F.; Mirbach, M. J. *J. Am. Chem. Soc.* **1977**, *99*, 7388.

169. Schwarz, W; Dangel, K.-M.; Jones II, G.; Bargon, J. *J. Am. Chem. Soc.* **1982**, *104*, 5686.

170. Jones II, G.; Chiang, S.-H.; Becker, W. G.; Greenberg, D. P. *J. Chem. Soc., Chem. Commun.* **1980**, 681.

171. Jones II, G.; Schwarz, W.; Malba, V. *J. Phys. Chem.* **1982**, *86*, 2286.

172. Jones II, G.; Becker, W. G.; *Chem. Phys. Lett.* **1982**, *85*, 271.

173. Jones II, G.; Xuan, P. T.; Schwarz, W. *Tetrahedron Lett.* **1982**, *23*, 5505.

174. Arnold, D. R.; Maroulis, A. J. *J. Am. Chem. Soc.* **1976**, *98*, 5931.

175. Graham-Bryce, J. J.; Corkill, J. M. *Nature (London)* **1960**, *186*, 965.

176. Bauld, N. L.; Bellville, D. J.; Harirchian, B.; Lorenz, K. T.; Pabon, Jr., R. A.; Reynolds, D. W.; Wirth, D. D.; Chiou, H.-S.; Marsh, B. K. *Acc. Chem. Res.* **1987**, *20*, 371.

177. Harirchian, B.; Bauld, N. J. *J. Am. Chem. Soc.* **1989**, *111*, 1826.

178. Bauld, N. L.; Harirchian, B.; Reynolds, D. W.; White, J. C. *J. Am. Chem. Soc.* **1988**, *110*, 8111.

179. Gassman, P. G.; Singleton, D. A. *J. Am. Chem. Soc.* **1984**, *106*, 6085.

180. Bellville, D. J.; Bauld, N. L. *J. Am. Chem. Soc.* **1982**, *104*, 2665.

181. Bellville, D. J.; Bauld, N. L.; Pabon, R.; Gardner, S. A. *J. Am. Chem. Soc.* **1983**, *105*, 3584.

182. H. Schomburg, H.; Staerk, H.; Weller, A. *Chem. Phys. Lett.* **1973**, *22*, 1.

183. Bauld, N. L.; Rabon, R. *J. Am. Chem. Soc.* **1983**, *105*, 633.

184. Weller, A. *Pure & Appl. Chem.* **1982**, *54*, 1885.

185. Goodman, J. L.; Peters, K. S. *J. Am. Chem. Soc.* **1986**, *108*, 1700. and reference cited therein.

186. Mataga, N.; Okata, T.; Kanda, Y.; Shioyama, H. *Tetrahedron* **1986**, *42*, 6143. and reference cited therein.

187. Masnovi, J. M.; Kochi, J. K.; Hilinshi, E. F.; Rentzepis, P. M. *J. Am. Chem. Soc.* **1986**, *108*, 1126. and reference cited therein.

188. Gould, I. R.; Moody, R.; Farid, S. *J. Am. Chem. Soc.* **1988**, *110*, 7242.

189. Miller, J. R.; Calcaterra, L. T.; Closs, G. L. *J. Am. Chem. Soc.* **1984**, *106*, 3047.

190. Oliver, A. M.; Paddon-Row, M. N. *J. Am. Chem. Soc.* **1989**, *111*, 7259.

191. Closs, G. L.; Johnson, M. D. Miller, J. R.; Piotrowiak, P. *J. Am. Chem. Soc.* **1989**, *111*, 3751. and reference cited therein.

192. McLendon, G. *Acc. Chem. Res.* **1988**, *21*, 160.

193. Gould, I. R.; Moser, J. E.; Armitage, B.; Farid, S.; Goodman, J. L.; Herman, M. S. *J. Am. Chem. Soc.* **1989**, *111*, 1917.

194. de Mayo, P. *Acc. Chem. Res.* **1970**, *4*, 41.

195. Eaton, P. E. *Acc. Chem. Res.* **1967**, *1*, 50.

196. Berenjian, N.; de Mayo, P.; Sturgeon, M. E.; Sydnes, L. K.; Weedon, A. C. *Can. J. Chem.* **1982**, *60*, 425.

197. Nakanish, H.; Morita, H.; Nagakura, S. *Bull. Chem. Soc. Jap.* **1977**, *50*, 2255.

198. Kropp, P. J. *J. Am. Chem. Soc.* **1969**, *91*, 5783. and reference cited therein.

199. Sandros, K. *Acta. Chem. Scand.* **1964**, *18*, 2355.

200. Huisgen, R.; Ooms, P. H. J.; Mingin, M.; Allinger, N. L. *J. Am. Chem. Soc.* **1981**, *53*, 171.

201. Schroeter, S. H. *Liebigs Ann. Chem.* **1974**, 1890.

202. McCloud, D. L.; Schleppnik, A. A. (Monsanto Co.) US 3,748,344, **1973**, CA., *79* ,78225C.

203. Jaouhari, R.; Maillard, B.; Filliatre, C.; Villenave, J. J. *Synthesis* **1982**, 760.

204. Jaouhari, R.; Filliatre, C.; Maillard, B.; Villenave, J. J. *Tetrahedron* **1982**, *38*, 3137.

205. Davies, D. I.; Parrot, M. J. *Tetrahedron Lett.* **1972**, 2719. and references cited therein.

206. Chen, C.-H.; Perlstein, J. H.; Reynolds, G. A.; **U.S. US** 4,496,730 (Cl. 546-23; C07F9/21), 29 Jan.1985. Appl. 420,461, 20 Sep.1982.

207. Hammond, G. S.; Leermarker, P. A. *J. Am. Chem. Soc.* **1962**, *84*, 1148.

208. Caldwell, R. A.; Creed, D.; Demarco, D. C.; Melton, L. A.; Ohta, H.; Wine, P. H. *J. Am. Chem. Soc.* **1980**, *102*, 2369.

209. Anorld, D. R.; Trecker, D. J.; Whipple, *J. Am. Chem. Soc.* **1965**, *87*, 2596 and references cited therein.

210. Kropp, P. J. *J. Am. Chem. Soc.* **1969**, *91*, 5783.

211. Still, C. "*MacroModel Molecular Modeling System, Version 2.0*" Department of Chemistry, Columbia University. New York 1988.

212. Haasnoot, C. A. G.; deLeeuw, F. A. A. M.; Altona, C. *Tetrahedron* **1980**, *36*, 2783.

APPENDICES

A-1. The False Quenching of $DBMBF_2$ Excimer Emission by Acrylonitrile

It has been reported that acrylonitrile could act as a specific quencher for certain exciplexes, e.g., the 9-cyanophenanthrene/diethylaniline exciplex.[208] In an attempt of using acrylonitrile to quench the $DBMBF_2$ excimer emission at 522 nm in CH_3CN, we observed that the addition of acrylonitrile did cause a decrease in the emission intensity as shown in Fig.A1 (spectrum A). As the quenching experiment was conducted by directly injecting fairly large amounts of the quencher into the fluorescence cell which contained a CH_3CN solution of $DBMBF_2$ (2 ml, 0.100 M), the concentration of $DBMBF_2$ was changed upon the addition of quencher. Considering that the intensity of the excimer emission was sensitive to the concentration of the fluorescer in the concentration range where the excimer and monomer emissions coexisted, we examined the dilution effect on the excimer emission as well. Adjusting the $DBMBF_2$ concentration from 0.100 M to 0.0816 M by injecting the blank solvent (CH_3CN) into the sample instead, we found the decrease in the emission intensity at 522 nm was just as much as that observed from the acrylonitrile "quenching" as shown by Fig.A1(spectrum B). Therefore, we concluded that acrylonitrile did not really quench the emission of $DBMBF_2$ excimer. This also alerted us to using acrylonitrile or other small polar molecule to

quench the emission of an excimer or exciplex emission where high concentration of the quencher usually had to be employed.

spectrum A

curve#	[$DBMBF_2$] (M)	[acrylonitrile] (M)
1	0.1000	0.00
2	0.0976	0.37
3	0.0943	0.86
4	0.0909	1.38
5	0.0879	1.98
6	0.0816	2.79

spectrum B

curve#	[$DBMBF_2$] (M)	[acrylonitrile] (M)
1	0.1000	0.00
2	0.0816	0.00

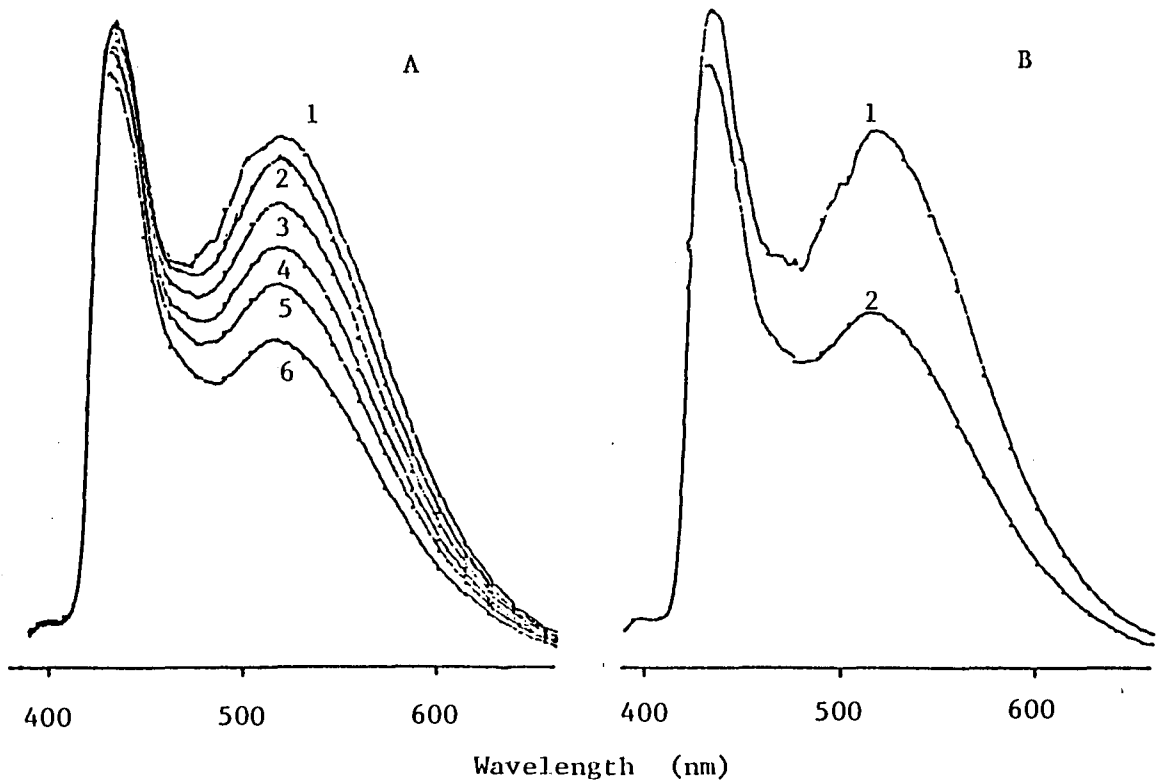

Figure A1. The false quenching of $DBMBF_2$ excimer emission by acrylonitrile in CH_3CN. λ_{ex} = 380 nm. Spectrum A: acrylonitrile "quenching". Spectrum B: the dilution effect.

A-2. The GSC of TCB and *trans*-Anethole

The light yellow color of a TCB solution (6 X 10^{-3} M) in CH_3CN changed to dark purple upon addition of *trans*-anethole (**3**, >10^{-2} M). The absorption spectra of TCB showed a new band with λ_{max} = 541.6 nm in the presence of **3** (Fig.A2). The absorbance of the new band increased with increasing [**3**]. The Benesi-Hildbrand plot (2-1-2) gave perfect straight lines (Fig.A3), indicating the formation of a GSC (K = 0.69 M^{-1}) of TCB with **3**.

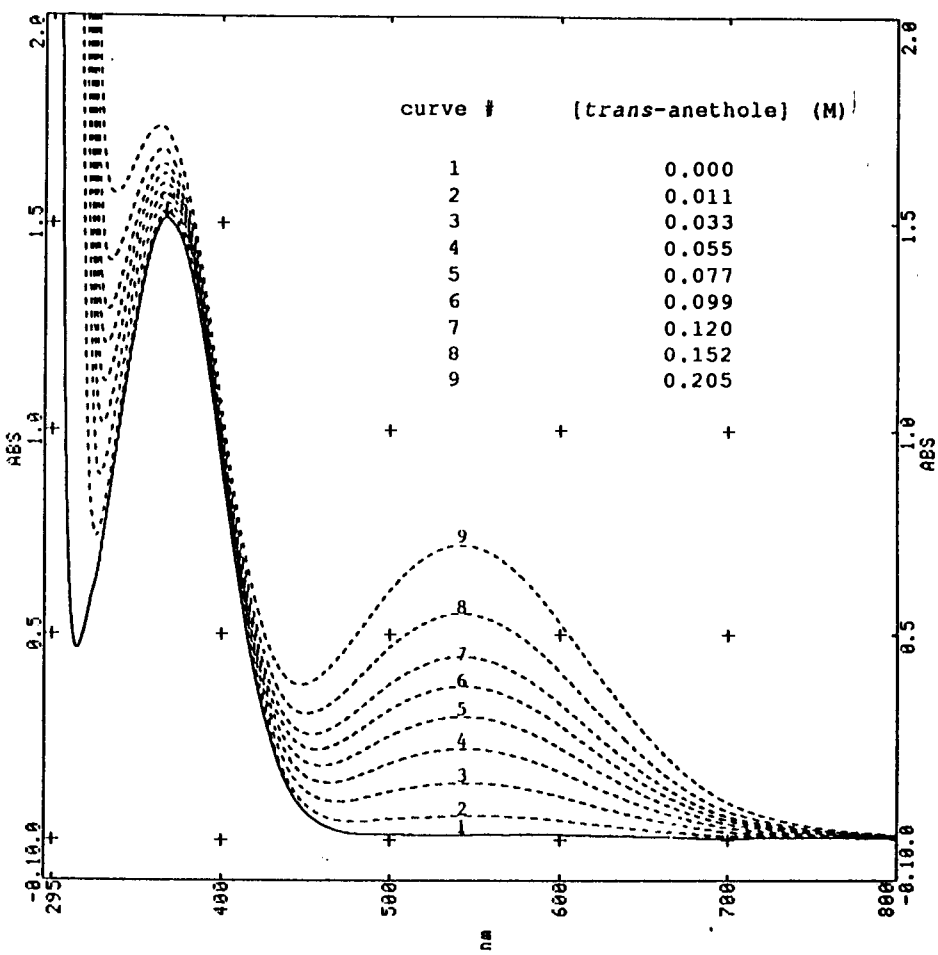

Figure A2. The absorption spectra of GSC of TCB and **3** in CH_3CN at 20°. [TCB] = 0.006 M.

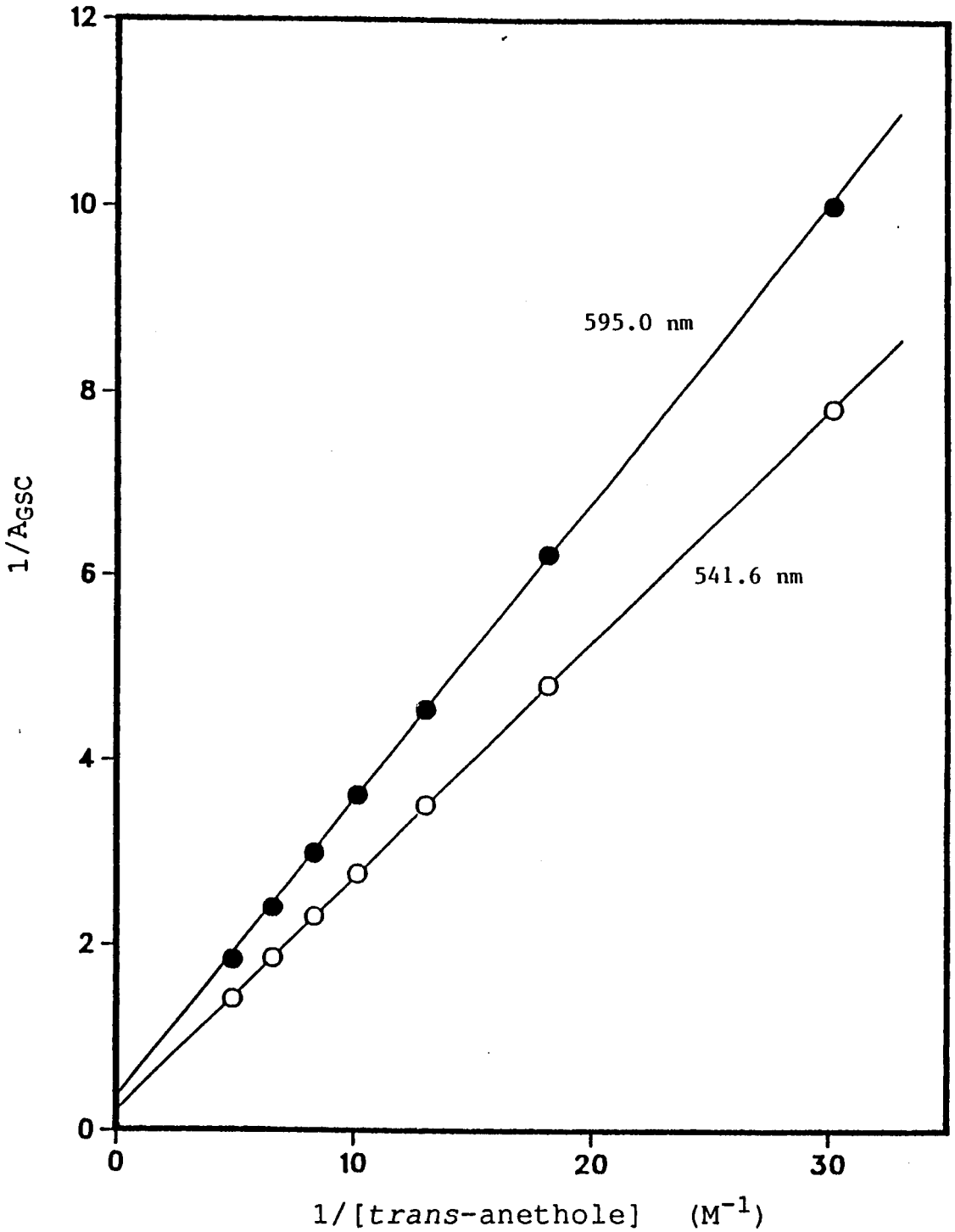

Figure A3. The Benesi-Hildbrand plot of TCB/**3** system in CH_3CN ([TCB] = 0.006 M). Data were adopted from Fig.A2 at 595.0 nm and 541.6 nm, respectively.

A-3. The Derivation of Eq.3-3

According to Scheme 3-4 and by assuming a quantum yield of unity for the singlet excited state $DBMBF_2$ (A^* in the Scheme), the quantum yields of the exciplex (Φ_{exp}) and the excimer (Φ_{exm}) can be written as Eq.A-1 and Eq.A-2,

$$\Phi_{exp} = \frac{k_{exp}[O]}{k_d^{mono} + k_{exp}[O] + k_{exm}[A]} \qquad (A-1)$$

$$\Phi_{exm} = \frac{k_{exm}[A]}{k_d^{mono} + k_{exp}[O] + k_{exm}[A]} \qquad (A-2)$$

where [O] and [A] denote the concentrations of olefin and $DBMBF_2$, respectively; and the rate constants are defined according to Scheme 3-4. Consequently, the quantum yield of the triplex (Φ_{trp}) can be obtained by Eq.A-3.

$$\Phi_{trp} = \frac{k_{trp}[O]}{k_{trp}[O] + k_d^{exm}} \Phi_{exm} \qquad (A-3)$$

Therefore, the quantum yield of the cycloadduct from the exciplex (Φ_p^{exp}) can be expressed by Eq.A-4;

$$\Phi_p^{exp} = \frac{k_p}{k_p + k_d^{exp}} \Phi_{exp}$$

$$= \frac{k_p}{k_p + k_d^{exp}} \cdot \frac{k_{exp}[O]}{k_d^{mono} + k_{exp}[O] + k_{exm}[A]} \qquad (A-4)$$

and that for the cycloadduct from the triplex (Φ_p^{trp}) by Eq.A-5.

$$\Phi_p^{trp} = \frac{k_p'}{k_p' + k_d^{trp}} \Phi_{trp}$$

$$= \frac{k_p'}{k_p' + k_d^{trp}} \cdot \frac{k_{trp}[O]}{k_{trp}[O] + k_d^{exm}} \cdot \frac{k_{exm}[A]}{k_d^{mono} + k_{exp}[O] + k_{exm}[A]} \qquad (A-5)$$

By defining constants M and N as follows,

$$M = \frac{k_p}{k_p + k_d^{exp}} \qquad (A-6)$$

$$N = \frac{k_p'}{k_p' + k_d^{trp}} \cdot \frac{k_{trp}[O]}{k_{trp}[O] + k_d^{exm}} \qquad (A-7)$$

Eq.A-4 and Eq.A-5 are then simplified to Eq.A-8 and Eq.A-9, respectively.

$$\Phi_p^{exp} = \frac{M\, k_{exp}[O]}{k_d^{mono} + k_{exp}[O] + k_{exm}[A]} \qquad (A-8)$$

$$\Phi_p^{trp} = \frac{N\, k_{exm}[A]}{k_d^{mono} + k_{exp}[O] + k_{exm}[A]} \qquad (A-9)$$

Obviously, the total quantum yield of the cycloadduct (Φ_p) is

$$\Phi_p = \Phi_p^{exp} + \Phi_p^{trp} \qquad (A-10)$$

Substituting Eq.A-8 and Eq.A-9 in to Eq.A-10, we obtain Eq.A-11 (Eq.3-3),

$$\Phi_p = \frac{M\ k_{exp}[O] + N\ k_{exm}[A]}{k_d^{mono} + k_{exp}[O] + k_{exm}[A]} \qquad \text{(A-11)}$$

the first derivative of which is:

$$\frac{d\Phi_p}{d[A]} = \frac{k_{exm}\{N(k_d^{mono} + k_{exp}[O]) - Mk_{exp}[O]\}}{(k_d^{mono} + k_{exp}[O] + k_{exm}[A])^2} \qquad \text{(A-12)}$$

Therefore, if

$$N > \frac{k_{exp}[O]}{k_d^{mono} + k_{exp}[O]}\ M$$

then

$$\frac{d\Phi_p}{d[A]} > 0$$

whereas if

$$N < \frac{k_{exp}[O]}{k_d^{mono} + k_{exp}[O]}\ M$$

then

$$\frac{d\Phi_p}{d[A]} < 0$$

A-4. The Derivation of Eq.3-9

Based on Scheme 3-13, one can directly write **Eq.A-13 to A-15,**

$$\frac{dP}{dt} = k_{add}[A^*][N] \qquad \text{(A-13)}$$

$$\frac{dD}{dt} = k_{dim}[N^*][N] \qquad \text{(A-14)}$$

$$\frac{d[N^*]}{dt} = k_1[A^*][N] - k_{-1}[N^*][A] - k_{dim}[N^*][N] \qquad \text{(A-15)}$$

where A, N, P, and D denote acetylacetone, norbornene, cycloadduct **86**, and dimers of norbornene, respectively. By applying steady state treatment to Eq.A-15, i.e. let

$$\frac{d[N^*]}{dt} = 0$$

Eq.A-16 is obtained.

$$[N^*] = \frac{k_1[A^*][N]}{k_{-1}[A] - k_{dim}[N]} \qquad \text{(A-16)}$$

Therefore, Eq.A-14 can be rewritten to Eq.A-17 by substituting Eq.A-16 into its right side.

$$\frac{dD}{dt} = \frac{k_1 k_{dim}[A^*][N]^2}{k_{-1}[A] + k_{dim}[N]} \qquad \text{(A-17)}$$

Then Eq.3-9 is obtained as Eq.A-18 here by dividing Eq.A-13 with Eq.A-17.

$$\frac{dP/dt}{dD/dt} = \frac{k_{add}[A^*][N](k_{-1}[A] + k_{dim}[N])}{k_1 k_{dim}[A^*][N]^2}$$

$$= \frac{k_{add}}{k_1} + \frac{k_{add}k_{-1}[A]}{k_{dim}k_1[N]} \qquad \text{(A-18)}$$

thank you.